Universidad Pública de Navarra
Nafarroako Unibertsitate Publikoa

Doctoral Thesis

ANALYSIS OF THE HYDROLOGICAL AND EROSIVE BEHAVIOR OF AGRARARIAN WATERSHEDS IN NAVARRE (SPAIN) BY EXPERIMENTATION AND MODELLING

Presented

By

YOUSSEF CHAHOR

Thesis advisors:

JAVIER CASALÍ SARASIBAR
RAFAEL GIMÉNEZ DÍAZ

Pamplona, 2017

upna
Universidad Pública de Navarra
Nafarroako Unibertsitate Publikoa

DÉDICACE

Je dédie cette thèse à
Ma chère femme FERDAOUS ZOUAGHI
Et à mes deux agréables enfants SARA et AMINE
À mes parents SAID CHAHOR et FATIMA HDIDOU
Pour leurs soutiens et amour
Et à mon frère et mes sœurs

AGRADECIMIENTOS

A Dr. Javier Casalí Sarasibar y Dr. Rafael Giménez Díaz, mis directores de tesis por su constante dedicación, apoyo y orientaciones para el desarrollo y culminación de esta tesis.

Gracias a todos los miembros del grupo de investigación THERRAE del Departamento de Proyectos e ingeniera rural de la UPNA por todo el apoyo que he recibo.

A mi familia, por todo el esfuerzo que han hecho sin el cual yo nunca hubiera llegado a esta instancia. A mi padre Said, a mi madre Fátima, a mis hermanos por mostrarme día a día que con esfuerzo y tenacidad nuestras metas pueden alcanzarse. Ellos siempre han confiado en mí. Estoy muy orgulloso de vosotros.

A mi querida esposa Ferdaous, por su apoyo incondicional, cariño, amor y paciencia tanto para soportar mi estado de ánimo como para apoyarme cuando tuve que decidir hacer mis estancias de investigación. Gracias cariño, esta también es tu tesis. A mis hijos Sara y Amine por comprender mi dedicación en el desarrollo del proyecto de tesis doctoral y por su amor infinito.

Un agradecimiento especial a la Dr. Ronald Bingner, Investigador en el "National Sedimentation Laboratory - United States Department of Agriculture, Agricultural Research Service, USDA-ARS", por darme la oportunidad de realizar mis estancias de investigación en su laboratorio, por haber compartido conmigo su gran experiencia, y por sus buenos consejos que me han ayudado a avanzar.

Esta investigación no habría sido posible sin la financiación recibida de los proyectos de investigación "CGL2007-63453/HID" y "CGL2011-24336" apoyados por el Ministerio de Ciencia e Innovación y por la ayuda pre-doctoral (FPI).

A mis estimados amigos y compañeros de doctorado, por su compañía y apoyo durante la realización del programa doctoral.

A todos, muchas gracias.

RESUMEN

Es de general conocimiento que la actividad agraria causa un importante efecto en el medio ambiente. Se hace por tanto necesario conocer este efecto así como proponer medidas para su control. Para ello, la información obtenida a partir de cuencas agrarias (experimentales) es de indudable valor. Por otro lado, los modelos de simulación permiten extender ese conocimiento a amplias zonas, una vez calibrados en zonas limitadas como pueden ser las citadas cuencas experimentales. Además, estas herramientas informáticas permiten analizar a largo y medio plazo las implicaciones de cambios en usos y manejos de las tierras, lo que resulta esencial para avanzar en el control de los problemas ambientales derivados de la actividad agraria.

De entre los problemas causados o incrementados por la actividad agraria destaca el de la erosión hídrica del suelo, objeto de atención preferente en esta tesis, en sus diferentes modalidades tradicionalmente reconocidas: laminar, en surcos y en cárcavas. Así, los principales objetivos planteados son: evaluar el modelo AnnAGNPS como herramienta para la estimación de escorrentía y exportación de sedimentos en una pequeña cuenca experimental (Latxaga, 207 ha) de uso homogéneo y representativa de amplias zonas de Navarra; realizar ese mismo ejercicio en una cuenca mayor (Cemborain, 50 km^2) y mucho más compleja en cuanto a relieve, clima, suelos, y uso y manejo de los mismos; explorar la capacidad del modelo para simular escenarios de cara a su utilización como herramienta de gestión; evaluar, en una zona extensa que muestra alto nivel de acarcavamiento, la capacidad del módulo APEGT, integrado en AnnAGNPS, para identificar los lugares de las cuencas hidrográficas en donde se espera la aparición de cárcavas efímeras (EGs); evaluar la capacidad de observaciones a partir de ortofotos para caracterizar la erosión EGs en amplias zonas y durante largos periodos de tiempo, aportando datos sobre las principales características del fenómeno en una zona de Navarra; evaluar el modelo TIEGEM, integrado en AnnAGNPS, para predecir la erosión por EGs en Navarra.

La evaluación AnnAGNPS para escorrentía y exportación de sedimentos se llevó a cabo, por un lado en la cuenca experimental de Latxaga, cultivada casi íntegramente con cereales de invierno; y por otro en la cuenca de Cemborain (en esta última el análisis de la evaluación se limita a la escorrentía), cultivada en un 24 %, siendo el resto mayoritariamente bosques y matorral (40% y 30% respectivamente). Los resultados indican que se ha podido llevar a cabo una muy buena calibración de la escorrentía en ambas cuencas, siendo el comportamiento del modelo en validación adecuado en el primer caso e insatisfactorio en el segundo. La calibración se ha llevado variando únicamente el CN y buscando la simulación adecuada a nivel mensual, posteriormente reescalada a nivel estacional y anual.

Calibration consisted of adjusting the initial CN values, as well as adding new CN values during winter and spring. Sin embargo, ha sido necesario utilizar valores de CN poco realistas en algunos casos, lo puede poner en duda la validez del método.

Por un lado, ello puede deberse a la necesidad de ajustar mediante el CN la elevada infiltración observada en las zonas en épocas secas, muy por encima de lo que cabría esperar de acuerdo con la textura del suelo. Ello puede a su vez deberse a la presencia de flujo preferente (preferential flow), constatado en la zona. Por otro lado, para ajustar la escorrentía simulada en invierno y primavera ha ocurrido en general lo contrario (aunque con mucha menor intensidad): ha sido necesario incrementar los valores de CN, como consecuencia tal vez del efecto transmitido del valor muy bajo del CN al principio del otoño y de la disminución de la infiltración por vías de flujo preferencial debido a la expansión del suelo como consecuencia del incremento de la humedad del mismo durante el invierno. Este comportamiento parece poner en evidencia las

limitaciones propias del método del CN para cuencas pequeñas o en las que fenómenos locales o peculiares pueden tener gran transcendencia y no ser adecuadamente simulados.

La evaluación del modelo para la simulación de la exportación de sedimentos dio lugar a resultados menos exitosos. Si bien la calibración, tras un novedoso análisis de sensibilidad en el que se identificaron 6 seis parámetros que finalmente intervinieron en el proceso, arrojó buenos resultados, persiguiendo, como objetivo la misma, optimizar las simulaciones anuales, la validación produjo pobres resultados. Se alude como explicación a la complejidad de los procesos erosivos en la cuenca a pesar de su pequeño tamaño, y a la necesidad de utilizar una información topográfica más detallada. Se sugiere así mismo el uso de modelos o submodelos más complejos y ya existentes en el entorno de AnnAGNPS, como CONCEPTS, que permiten una más detallada simulación de la dinámica de los sedimentos. Sin embargo, estas constataciones parecen disminuir la aplicabilidad de AnnAGNPS para nuestras condiciones, dadas las altas exigencias de información y cálculo detallado, poco adecuadas para un uso generalizado en la práctica. En todo caso, esta herramienta, y a falta de nuevas evaluaciones, puede ser de utilidad cuando se buscan no tanto valores absolutos como tendencias a largo plazo. En este sentido, cabe decir que los análisis de escenarios arrojan resultados muy realistas.

El módulo (APEGT) para la localización de cabeceras de EGs y basado en el denominado CTI (Compound Topographic Index), y más en concreto en su valor crítico CTIc, se ha evaluado en una zona homogénea en cuanto a clima, suelo y usos y manejos del mismo. Lejos de obtenerse un mismo valor para cada uno de los años analizados, se ha constatado una gran variabilidad. Ello indicaría que los procesos que controlan la formación de EGs son si cabe más complejos que lo generalmente admitido, tales como subsurface flow (exfiltration of seepage), preferential flow paths, condiciones del régimen de humedad del suelo, influidas a su vez por la posición en el paisaje, etc. Sin embargo, la variabilidad observada resulta similar de año a año, lo que permite sostener que CTIc puede ser representativo y por lo tanto de utilidad para estimar de media la localización de las EGs en una zona homogénea a largo plazo, lo que resulta coincidente y coherente con los objetivos planteados por los diseñadores de AnnAGNPS. Para un correcto análisis del método del CTI ha sido necesario identificar dos valores del mismo. CTIc1 se correspondería con las zonas de las cuencas donde se dan las condiciones para la formación de cabeceras nuevas. Mientras que CTIc2 permitiría identificar las zonas donde ya no es posible que la cabecera pueda continuar su proceso de migración. El análisis multitemporal de ortofotos a escala detallada y durante largos periodos de tiempo y obtenidas en los mismos momentos cada año, ha permitido una buena caracterización del fenómeno de la erosión por EGs en un área extensa y con un gran ahorro en recursos. En una reflexión similar a la anteriormente expuesta, cabe pensar que la baja repetitividad observada en la aparición de EGs (pocas veces ocurre que la cárcava se forme en una misma microcuenca) pone también de manifiesto la complejidad del fenómeno, controlado por muy diversos factores.

Se ha llevado a cabo la evaluación del modelo AnnAGNPS en cuatro pequeñas cuencas afectadas por EGs, siendo este estudio, aunque modesto, el más completo efectuado hasta el momento. Ello, dicho sea de paso, pone de manifiesto la escasez de datos existentes para proceder a estas evaluaciones, evidenciando la dificultad de su obtención, y poniendo en valor las aproximaciones metodológicas como las expuestas con anterioridad (ortofotos). La calibración se ha llevado a cabo únicamente modificando el parámetro τ_c (critical shear stress) y en ella se perseguía simular adecuadamente tanto el momento de aparición de las EGs, como la forma de las mismas y por tanto su volumen. Es destacable el hecho de que se consiga, en la fase de

calibración, una adecuada identificación por parte del modelo de los eventos causantes de la aparición de cada una de las EGs, Sin embargo, la estimación del volumen ha sido muy poco exitosa. Ello ha venido condicionado fundamentalmente por la muy mala predicción de la longitud de la cárcava.

ABSTRACT

It is general knowledge that agrarian activities causes important effects on the environment. It is therefore necessary to better understand these effects as well as propose controlling measures. To this end, the information obtained from agrarian watersheds (experimental) is very valuable. However, simulation models enable the extension of this knowledge to wider zones, once calibrated in limited zones such as the mentioned experimental watersheds. Computer tools allow for medium- and long-term analysis of the implications of changes in use and management of soil, which is essential to advance in the control of environmental problems derived from agrarian activities.

Among the issues caused or enhanced by agrarian activities, hydric erosion of the soil must be mentioned, which is the main focus of this thesis, in its traditionally recognized categories: sheet, rill, and gully erosion. The main objectives of this thesis are: evaluate the AnnAGNPS model as a tool to estimate runoff and sediment exports in a small experimental watershed (Latxaga, 207 ha), with homogeneous soil use and representative of wider zones of Navarre; carry out the same exercise in a larger watershed (Cemborain, 50 km2), much more complex regarding relief, climate, and soil use and management; explore the capacity of the model to simulate scenarios, aimed at its utilization as a management tool; evaluate, in an extensive zone with high gully activity, the capacity of the APEGT module, integrated within AnnAGNPS, to identify the locations of the hydrographic watersheds where the apparition of ephemeral gullies (EGs) are expected; evaluate the observation capacity of orthophotos to characterize EG erosion in wide zones and throughout long periods of time, providing data on the main characteristics of the phenomenon in a zone of Navarre, and evaluate the TIEGEM model, integrated within AnnAGNPS, to predict EG erosion in Navarre.

The evaluation of AnnAGNPS for runoff and sediment exports was carried out firstly in the experimental Latxaga watershed, almost entirely cultivated with winter cereal, and secondly in the Cemborain watershed (analysis limited to runoff), with 24% of its surface cultivated (the remaining 40% and 30% are respectively, forests and brushland). Results indicate that good calibration was performed for runoff for both watersheds, with satisfactory behavior of the model when validating the first case, but unsatisfactory for the second case. Calibration considered variation of CN only, searching for adequate simulation at monthly levels, then escalated to seasonal and annual scales.

Calibration consisted of adjusting the initial CN values, as well as adding new CN values during Winter and Spring. Nevertheless, it was necessary to utilize unrealistic CN values in some cases, with could raise questions on the validity of the model.

On one hand, this could be due to the necessity of adjusting the elevated infiltration observed in the zones during dry periods only by CN; infiltration was much higher than expected in accordance with soil texture. This could have happened due to the presence of preferential flows, verified in the zone. On the other hand, adjustment of simulated runoff in Winter and Spring presented the opposite effect (although less pronounced): it was necessary to increase CN values as a consequence of: i) very low CN values at the beginning of Autumn, and ii) decrease of infiltration by preferential flow paths due to the expansion of soil (consequence of elevated soil humidity during Winter). This behavior seems to evidence the own limitations of the CN method for small watersheds or in those where local or peculiar phenomena could have great transcendence and not be adequately simulated.

Evaluation of the model for the simulation of sediment exports resulted less satisfactory. Calibration, after an innovative sensibility analysis where six parameters that intervened in the process were identified, provided good results, aimed at the optimization of annual simulations. However, validation provided poor results. The complex erosion processes of the watershed, despite its reduced size, and the necessity of utilizing more detailed topographic information, could be the cause of such poor results in the validation stage. The use of more complex submodels or models is suggested, within the AnnAGNPS environment, such as CONCEPTS, which enables a more detailed simulation of sediment dynamics. Nevertheless, these verifications seem to decrease the applicability of AnnAGNPS for our conditions, given the high requirements for data and detailed calculations, inadequate for general use in practice. In any case, this tool can be very useful when long term trends are necessary, rather than absolute values. In this sense, it must be mentioned that scenario analysis provides very realistic results.

The APEGT module for the location of EG heads, based on the CTI (Compound Topographic Index), more specifically on its critical value, CTIc, has been evaluated for a homogeneous zone regarding climate, and soil use and management. Great variability has obtained throughout the years analyzed. This indicates that the processes that control the formation of EGs are much more complex than what is generally admitted, including subsurface flows (exfiltration of seepage), preferential flow paths, soil humidity regime conditions (influence in turn by its position within the environment), etc. The variability observed resulted similar across the years, which enables the affirmation that CTIc can be representative and therefore useful to estimate the average location of EGs in a homogeneous zone at the long term. This coincides and is coherent with the objectives established by the designers of AnnAGNPS. For the correct analysis of the CTI method, it was necessary to identify two values: CTIc1 corresponds to the watershed zones where special conditions are present that favor new heads, while CTIc2 enables identification of the zones where head migration is not possible anymore. Multitemporal analysis of orthophotos, at detailed scale and throughout long periods of time, obtained at the same moments each year, permitted a good characterization of the EG erosion phenomenon in an extensive area with significant savings in resources. In a similar reflection of what was previously exposed, the low repetitiveness in the apparition of EGs (it is rare that gullies form in the same microwathershed) also highlights the complexity of the phenomenon, controlled by very different factors.

The evaluation of the AnnAGNPS model was carried out in four small watersheds affected by EGs, and the study presented herein, although modest, is the most complete carried out up to date. This highlights the scarcity of existing data to proceed with these evaluations, evidencing the difficulties in data obtainment and providing value to methodological approaches such as those aforementioned (orthophotos). Calibration was carried out only by variation of the τ_c (critical shear stress) parameter, aimed at an adequate simulation of the moment of EG apparition as well as their shape and volume. It must be mentioned that, during the calibration phase, adequate identification of the events that caused the apparition of each EGs was accomplished by the model. However, estimation of volume has not been very successful. This has been fundamentally conditioned by the poor predictions of gully length.

Table of contents

List of figures

List of tables

Chapter 1: Introduction

1.1 Introduction

This chapter briefly addresses and describes some aspects of the thesis, with detailed introductions on each chapter.

Before the 20th century, changes in land use were generally slow, in response to demographic growth or market demands (García-Ruiz, 2010). However, the introduction of internal combustion engines along with requirements to increase food production (guaranteeing food supply for the growing world population) brought major changes to agriculture, leading to agricultural intensification (FAO, 2004). Intensive agriculture resulted in a remarkable demand for complementary inputs such as labor, irrigation, high-yielding crop varieties, and fertilizers and pesticides to achieve maximum yields at the lowest possible cost. There are several potential serious environmental burdens resulting from these practices. In fact, intensive agricultural activities are one of the main factors that cause soil and water degradation in agricultural areas (Matson et al., 1997, Mäder et al., 2002). Therefore the increasing demands for limited soil resources along with an on-going contraction of arable land area per capita, soil erosion has become a global issue (Lal et al., 2007).

Soil erosion is a global, serious and common issue (Lal, 2003). The European Commission's Soil Thematic Strategy has identified soil erosion as a relevant issue for the European Union, and proposed an approach to monitor soil erosion (Panagos et al., 2015). In Europe, approximately 12.7% of arable land is estimated to suffer from moderate to high erosion (EEA, 2003). Soil erosion is in fact a significant and common problem (Poesen et al., 2003, Auzet et al., 2004, Boardman and Poesen, 2006, García Ruiz and López Bermúdez, 2009). Eroded areas are frequently cultivated with crops of high social and economic importance. Conventional tillage is the main cropping system used, where the surface of the soil remains uncovered during long periods of time (soil preparation and crop establishment, frequently carried out during the wettest seasons). As a result, these croplands are highly susceptible to erosion because the soil was left without a protective vegetation cover (Pimentel et al., 1995, Quinton et al., 2010, Almagro et al., 2016).

In Navarre (Spain), soil erosion is also an important problem that is present in rain-fed arable agricultural lands (Casalí et al., 1999, De Santisteban et al., 2006, Casalí et al., 2008, García Ruiz and López Bermúdez, 2009, Casalí et al., 2010, Giménez et al., 2012).

In this context, the Navarre Government Department of Agriculture established a network of experimental agricultural watersheds with contrasting land uses to provide data for the assessment of the effect of agricultural activity on erosion and water quality (Donézar and Del Valle de Lersundi, J., 2001). The experimental watershed network consists of four watersheds: Latxaga, La Tejería, Oskotz and Landazuria.

The Latxaga watershed covers an area of 207 ha and is located in the central eastern part of Navarre (Spain). Climate is humid Sub-Mediterranean, with average annual precipitation of approximately 835mm, distributed over 95 - 100 days of rainfall (Casalí et al., 2008). The watershed is almost completely cultivated with winter grain (wheat and barley usually cover 80% or 90% of the total area). Average yields are approximately 3,500 – 4,000 kg ha^{-1}on the hillslopes and approximately 5,500 kg ha^{-1}, or even higher, in the swales. Tillage is conventional, and frequently parallel to contour lines. Tillage practices are performed in such a way that a vegetation strip

around the streams is maintained, thus allowing the growth of sometimes dense riparian vegetation (Casalí et al., 2008).

The La Tejería watershed covers an area of 169 ha and is located in the central western part of Navarre. Climate is also humid Sub-Mediterranean, with average annual precipitation of approximately 725 mm, distributed over 105 days of rainfall. Land use, crop productivity and soil management practices are very similar to those described for the Latxaga watershed, with cereal crops covering usually more than 90% of the total area with average yields of 3,500-4,000 kg ha^{-1} on the hillslopes and more that 5,500 kg ha^{-1} in the swales (Gastesi, 2014). However, the stream beds and banks within the La Tejería watershed are poorly vegetated, favoring the occurrence of bank erosion processes (Casalí et al., 2008). Both Latxaga and La Tejería watersheds are representative of wide areas of Navarre and Northern Spain in terms of morphology, climate, land use (winter grain crops) and management. Hydrological behavior and water quality data of these watersheds were analyzed in detail by Casalí et al. (2008) after almost a decade of data collection; findings identified clear differences in the behavior of both watersheds, especially in terms of sediment yield. La Tejería presented much higher sediment concentrations (383 mg l^{-1}) and sediment yield (1,979 kg $ha^{-1}year^{-1}$) than Latxaga (128 mg l^{-1} and 290 kg $ha^{-1}year^{-1}$, respectively). Those differences were unexpected, as both watersheds are similar regarding soil, land use and management practices. However, differences in watershed morphology, topography, and vegetation on stream channels were the main contributors to the discrepancy detected between both sites (Casalí et al., 2008).

The Oskotz experimental watershed comprises 1674 ha in the northeastern part of Navarre (Spain). Climate is sub-Atlantic, with average annual precipitation 1200mm, distributed over 130 days of rainfall, and average annual temperature 12 ºC (Casalí et al., 2010). Most of the watershed is covered with forest (1021 ha, 61%), with the remaining area devoted to pasture (653 ha, 39%), with cattle-breeding and a small part dedicated to cropping. Within the Oskotz watershed, an experimental 500 ha sub-watershed almost fully covered with forest (approximately 90%) is monitored. Data collection provides information on hydrological behavior and water quality for a typical forest watershed. Casalí et al. (2010) analyzed the behavior of forested/pastured experimental watersheds in terms of discharge and sediment yield, concluding that the same behavior as grain-sown watersheds was observed. Most runoff and sediment yield in Oskotz were generated during Winter, although most erosive rainfalls occurred during Summer. The average sediment yield for the forest sub-watershed and the entire watershed were 700 and 550 kg ha $year^{-1}$, respectively.

The experimental Landazuria watershed covers an area of 479.5 ha and is located in southern Navarre. Climate is dry Mediterranean, with average annual precipitation 426mm and average annual temperature 14 ºC. Approximately 88.3% of its area is cultivated land and 11.7% corresponds to streams, riparian vegetation, bare soils, ways and rock outcrops. 59.7 % (252.9 ha) of cultivated land was equipped for pressurized irrigation whereas the rest of the surface remained rainfed agriculture (170.5 ha). The main crops under irrigation where maize, winter cereal, tomatoes and onions. Rainfed surface was dominated by barley, and it must be mentioned that rainfed agriculture followed a rotation system where the land was left bare in one out of two years (INTIA, 2017).

Instrumentation in each watershed included a hydrological measuring station, where discharge, turbidity and water quality (nitrate, phosphate, sulphate, carbonate, potassium, calcium, magnesium and sodium) parameters were measured on a 10 min basis (Donézar and Del Valle de Lersundi, J., 2001, Casalí et al., 2008, Casalí et al.,

2010). The Oskotz watershed counted with two automatic hydrology stations: the first station monitors the entire watershed, and the second is located at the outlet of the forest sub-watershed. Automatic weather stations were installed except at Landazuria, where the nearest station is located approximately 5 km South (meteorological station of Bardenas-El Yugo).

These experimental watersheds provide extensive data, which are very useful to identify and evaluate environmentally-sound land management practices while building an invaluable database for the assessment of hydrological models (García Ruiz and López Bermúdez, 2009).

Data obtained by field monitoring are very useful for the estimation of water resources and hydrological characterization, in addition to the assessment of soil erosion and Non Point Source pollution (NPS pollution), which are considered important sources of sediment and nutrient loads. However, a high number of measurements are required to monitor the spatial and temporal changes in soil erosion and hydrological parameters within a watershed. Moreover, the labor and costs involved become limiting factors for large watersheds if monitoring continues for long periods of time. In these situations, watershed simulation models have arisen as a good alternative to overcome the aforementioned field monitoring limitations. Modelling can be considered a relatively low cost and time efficient solution (Shirmohammadi et al., 2006).

A computer model is a mathematical representation of the essential characteristics of natural systems or real situations. At a watershed scale, models have been developed to understand hydrological systems, sediment transport and water contamination. Referred to as watershed hydrologic and NPS pollution models, these simulate natural processes such as runoff, sediments, nutrients and chemicals within the watershed (Borah and Bera, 2003). Moreover, some models evaluate the impact of human activities under different conditions, by simulating different situations and alternative scenarios for agricultural practices. In fact, these models can help farmers and policy makers in selecting suitable land use and best management practices, to reduce the damaging effects of agricultural practices on the environment.

Numerous studies have utilized different watershed simulation models, from simple to complex, and from single rainfall event models to continuous simulation models. Some of these models are based on simple empirical relations and others use more complex, physics-based equations. A detailed review of several erosion and sediment transport models can be found in Borah and Bera (2003) and Merritt et al. (2003).

One of the most popular models is Areal Nonpoint Source Watershed Environment Response Simulation (ANSWERS) (Beasley et al., 1980). ANSWERS is a single event storm model, which reproduces spatially varying processes of runoff, infiltration, subsurface drainage, and erosion. Within ANSWERS, the description of runoff processes is empirical, while erosion and sediment transport processes are based on physics-based continuity equations. The MIKE SHE (Christiaens and Feyen, 2002) is based on the SHE model (European Hydrological System), and contains physics-based processes that simulate runoff, sediment and water quality parameters. MIKE she also counts with continuous long term and single event simulation abilities. The European Soil Erosion Model (EUROSEM) (Morgan et al., 1998) is an event-based model developed to compute sediment transport, erosion and deposition over the land surface during a storm. The Limburg Soil Erosion Model (LISEM, (De Roo et al., 1996) is a spatially distributed, physics-based hydrological and soil erosion model, developed by the Department of Physical Geography at Utrecht University and the Soil Physics Division at the Winard Staring Centre in Waneningen, the Netherlands, for planning

and conservation purposes. The LISEM model is based on EUROSEM (Morgan et al., 1998). LISEM incorporates a number of different processes, including rainfall interception, surface storage in microdepressions, infiltration, vertical water movement through the soil, overland flow, channel flow, detachment by rainfall and throughfall, detachment by overland flow and transport capacity of flow (Merritt et al., 2003).

The Soil and Water Assessment Tools (SWAT) (Arnold et al., 1996) is another physically-based, continuous time model that operates on a daily time step to estimate the impact of management on water, sediment and agricultural chemical yield in large watersheds over long periods of time. The Chemical Runoff and Erosion from Agricultural Management Systems model (CREAMS) (Knisel, 1980) was developed to evaluate the relative effects of agricultural practices on pollutants in surface runoff and in soil water below the root zone (Knisel, 1980, Lane et al., 1992). The Hydrologic Simulation Program, Fortran (HSPF) was developed based on the 1960s Stanford Watershed Model, for the simulation of watershed hydrology and water quality (nitrogen, phosphorus, suspended sediment and other toxic organic or inorganic pollutants) (Walton and Hunter, 1996). The Watershed Erosion Prediction Project (WEPP) is a physics-based model developed in the United States in an initiative between the Agricultural Research Service, the Soil Conservation Service, the Forest Service in the Department of Agriculture and the Bureau of Land Management in the US Department of the Interior (Laflen et al., 1991). The kinematic runoff and erosion model, KINEROS, is an event-oriented, physics-based model describing the processes of interception, infiltration, surface runoff, and erosion from small agricultural and urban watersheds (Woolhiser et al., 1990). The TOPMODEL-based Land–Atmosphere Transfer Scheme (TOPLATS) simulates water and energy balances at different time steps, in both lumped and distributed modes. TOPLATS was developed based on the TOPMODEL framework, by the implementation of simple soil–vegetation–atmosphere transfer schemes (SVAT) (Famiglietti and Wood, 1994). TOPLATS incorporates SVAT to represent local scale vertical water fluxes within the catchment scale TOPMODEL approach.

Finally, one of the most important models is the Annualized Agricultural Non Point (AnnAGNPS) (Bingner et al., 2012). AnnAGNPS is a distributed parameter, physics-based, continuous simulation watershed scale program based on the single-event model AGNPS. AnnAGNPS was developed by the USDA Agricultural Research Service (ARS) and the Natural Resources Conservation Service (NRCS) to evaluate the impacts of agricultural NPS pollution on water quality and environment (Young et al., 1989). AnnAGNPS simulates surface water, sediment, nutrient and pesticides exiting agricultural areas through drainage streams. AnnAGNPS uses the SCS Curve Number (CN) technique (USDA, 1972), which is in fact the same technique implemented in the SWRRB and EPIC models (Williams et al., 1985). SCS CN determines surface runoff on the basis of a continuous soil moisture balance. The Revised Universal Soil Loss Equation (RUSLE) (Renard et al., 1997) is used to estimate the daily sheet and rill erosion of the area whenever a runoff event occurs (e.g., rainfall, irrigation, snowmelt). The Hydro-geomorphic Universal Soil Loss Equation (HUSLE) is used to simulate sediment delivery to streams (Theurer and Clarke, 1991). Several studies have evaluated AnnAGNPS's ability to predict runoff and sediment load worldwide, under different climatic conditions and land uses. Studies have also evaluated the model's capability of predicting erosion in ephemeral gullies.

In scientific literature, most water soil erosion studies focused on sheet, interrill and rill erosion processes. Several methodologies and models have been developed to

evaluate these particular types of water erosion within agricultural fields (Wischmeier and Smith, 1978, Knisel, 1980). However, few approaches and process-based watershed scale soil erosion models have been established to assess processes within ephemeral gullies. Ephemeral gully erosion has been recognized as an important source of sediment from cropland, in comparison with sheet and rill erosion (Poesen et al., 2003). There is a recent, growing interest in ephemeral gully erosion, verified through the number of studies established under different climatic conditions, aimed at the quantification of soil loss rates due to this type of erosion.

Ephemeral gullies EGs are small channels caused by concentrated surface runoff flowing on erodible agricultural soils during rain events. Since the scoured soil volume is not significant, EGs can be easily refilled by farmers, but reappear in the same locations (Foster, 1986, Thorne et al., 1986, Casalí et al., 1999). While rills are more common on planar elements of watersheds, EGs appear on valley bottoms or within swales. Linear features of the landscape, such as plot borders, lanes, tractor ruts or furrows, can promote the development of EGs (Casalí et al., 1999).

Permanent gullies, on the other hand, are often associated with agricultural land and are caused by concentrated, intermittent flow of water. Permanent gullies usually appear during and immediately after heavy rain, with the flow being deep enough to interfere with, and not to be obliterated by, normal tillage operations. These gullies typically range from 0.5m to as much as 25 to 30m in depth. Permanent gullies are typically found in abandoned agricultural fields, rangelands, or shrubland (Campo-Bescõs et al., 2013).

Gully erosion causes important on-site and off-site damages in agricultural soils. Soil losses due to EG erosion can contribute to reductions in crop productivity due to the removal of top soil and nutrients. Channels can also be formed in the middle of cultivated plots, entailing additional management efforts and costs to the farmers.

Soil losses will be significantly higher over long time periods of routinely adding topsoil to eroded areas, through tillage activities and repair of ephemeral gullies. Poesen et al. (2003) reported that ephemeral gully erosion is an important soil degradation process, affecting several environments worldwide. Bernard et al. (2010) reported that in the USA, EG erosion contributed with 18%-73% of the total erosion in 17 states, according to USDA-NRCS. Poesen et al. (1996) noted that the mean contribution of EG erosion to sediment production in southeast Portugal and southeast Spain could be over 80%, whereas in European areas this contribution ranges from 10% to 46%. Casalí et al. (1999) and De Santisteban et al. (2006) reported that EG erosion could range from 30% to 100% of total soil losses in actively eroding areas in southern Navarre (Spain).

Concerning the modelling of EG erosion processes in agricultural fields, there has been limited recent development of physics-based EG erosion models. Among the existing models, the Chemicals, Runoff and Erosion from Agricultural Management Systems (CREAMS) (Knisel, 1980) simulates ephemeral gully erosion through a procedure that takes into account detachment of soil due to shear of flowing water, sediment transport capacity and changing channel dimensions. The equations that describe change in channel dimensions were developed by Foster and Lane (Foster and Lane, 1983). Watson et al., (1986) developed a method for the estimation of ephemeral gully erosion, based on the regression equations to predict outputs of the CREAMS model. The computer program developed was named Ephemeral Gully Erosion Estimator (EGEE), which estimates the quantity of soil eroded from a single ephemeral gully. The Ephemeral Gully Erosion Model (EGEM) (Woodward, 1999)

was based on the erosion component of EGEE. EGEM predicts soil losses by ephemeral gully erosion for a single storm or for average annual conditions.

Souchere et al. (2003) developed the STREAM ephemeral gully model to predict the location and volume of ephemeral gullies by combining field measurements with knowledge on erosion processes. STREAM is based on the excess shear stress concept, where erosion occurs when the overland flow discharge produces a shear stress that exceeds the critical soil shear stress.

Vieira et al. (2014) developed a physics-based EG model, the Ephemeral Gully Erosion Estimator (EphGEE). EphGEE simulates ephemeral gully erosion through a procedure that takes into account detachment of soil through the shear force of flowing water, sediment transport capacity, and changing channel dimensions due to erosion and deposition. EphGEE computes ephemeral gully evolution for a series of storm events over a network of potential gully channels, which are either generated through terrain analysis algorithms based on high-resolution elevation data, or using a channel configuration specified by the model user.

Gordon et al. (2007) extended the capabilities of EGEM through the Revised EGEM (REGEM) by adding a new algorithm that estimates the migration rate of the headcut (Alonso et al., 2002), as well as incorporating analytic formulations for plunge pool erosion and headcut retreat within single or multiple storm events in unsteady, spatially varied flow at a sub-cell scale. REGEM was enhanced to a new version, the Tillage-Induced Ephemeral Gully Erosion Model (TIEGEM) (Bingner et al., 2012). TIEGEM incorporated several algorithms to determine the minimum gully width for each event. The ephemeral gully components within AnnAGNPS were based on TIEGEM. A new approach was integrated into the AnnAGNPS/ GIS interface, enabling the identification of the mouth of a gully headcutm based on topographic analyses (Parker et al., 2010).

In Spain, few efforts have been made to evaluate AnnAGNPS model and only in small watersheds under agricultural monoculture (Taguas et al., 2009, Gastesi, 2014). This justifies the needs for continuing evaluating the model not only in different small watersheds but also and mainly in large and complex ones. To this end, two Navarrese watershed Latxaga and (see above) and Cemborain were selected to evaluate the model

The Cemborain watershed covers an area of 5,000 ha and is located in Central Navarre. Climate is Sub-Mediterranean, with average annual precipitation ranging from 400 to 800 mm, and average annual temperature 12.4ºC. Watershed land use is characterized by its variation, with 40% of area covered by natural forest, 24% by agricultural fields, 31% by shrubs, 4% by rangeland and 1% by urban areas.

The Cemborain watershed outlet is equipped with a hydrological station, which provides daily discharge data since 1955. However, from September 2005 onwards, discharge has also been recorded every fifteen minutes. Three meteorological stations have been implemented around the watershed.

1.2 Objectives

In response to the needs discussed in the previous section, the overarching aim of this thesis was to carry out modelling and experimentation to deepen knowledge and improve management of some agricultural systems in Navarre, in terms of runoff and erosion. The objectives of the work herein presented are:

Evaluate the AnnAGNPS model as a tool for the estimation of runoff and sediment load in a small experimental agricultural watershed, representative of large areas of Navarre, with homogeneous land use and management;

Evaluate the AnnAGNPS model as a tool for the estimation of runoff and sediment load in a larger (more than two orders of magnitude larger then the previous), more complex watershed in terms of topography, climate, soils, land use and management;

Explore the ability of the model to simulate scenarios, aimed at its application as a management tool;

Evaluate the ability of the module integrated within AnnAGNPS to identify sites prone to EG formation in an extensive area with high levels of gulling;

Evaluate the ability of orthophoto observations to characterize EG erosion in large areas for long periods of time, providing data on the main characteristics of this phenomenon in areas of Navarre;

Evaluate the TIEGEM model, integrated within AnnAGNPS, to predict EG erosion in Navarre.

1.3 Thesis structure

This thesis was organized in seven chapters, as follows:

Chapter 1: General Introduction, where aspects of the thesis were presented along with the main objectives.

Chapter 2: AnnAGNPS model description, which contains a brief description of the model and the main components used to simulate runoff, sediment and EG erosion.

Chapter 3: Evaluation of the AnnAGNPS model for the prediction of runoff and sediment yield in the Latxaga watershed, where the AnnAGNPS model was evaluated regarding the simulation of surface runoff and sediment yield at the Latxaga watershed, for period of nine years. The model's response to different scenarios regarding land use and management were also analyzed.

Chapter 4: Evaluation of the AnnAGNPS model for the prediction of surface runoff at the Cemborain watershed. This chapter evaluates the AnnAGNPS model, within a large watershed with varied land use, including natural crop and non-crop lands, in terms of surface runoff.

Chapter 5: Evaluation of EG location prediction with the AnnAGNPS PEG tool by Compound Topographic Index (CTI) and critical Compound Topographic Index CTIc

Chapter 6: Evaluation of the AnnAGNPS model for the prediction of ephemeral gully erosion

Chapter 7: General conclusions

Chapter 2: AnnAGNPS model description

2.1 Introduction

First of all it should be noted that a very detailed description of the model can be found in Bingner et al.(2012) and Gastesi(2014). The latter is a recently published thesis in our research group. Thus, in this chapter, we have limited ourselves to a general description of the model and, instead, we have gone further into the aspects of special incidence in this thesis.

Annualized **AG**ricultural**N**on-**P**oint **S**ource Pollution Model (AnnAGNPS) (Bingner et al., 2012) is a distributed-parameter, continuous simulation, watershed scale model based originally on the single-event model AGNPS (Young et al., 1989). The USDA Agricultural Research Service (ARS) and the Natural Resources Conservation Service (NRCS) developed AnnAGNPS to evaluate the impacts of agricultural non-point source pollution on water quality and the environment (Young et al., 1989).

AnnAGNPS is a computer model written in standard ANSI_FORTRAN 90, designed to predict the origin and movement of water, sediment, and chemicals at any location in primarily agricultural watersheds. It distinguishes between erosion caused by sheet and rill, tillage-induced ephemeral gullies, other gully processes, and streambed and bank erosion sources.

In AnnAGNPS, the analysed watershed can be divided into many small drainage areas called cells. Each cell homogeneously represents the landscape in terms of soil type, land use and land management within its respective land area boundary. They are connected to each other by defining a network of channels or reaches, in which water, sediment and nutrients are transported (figure 2.1).

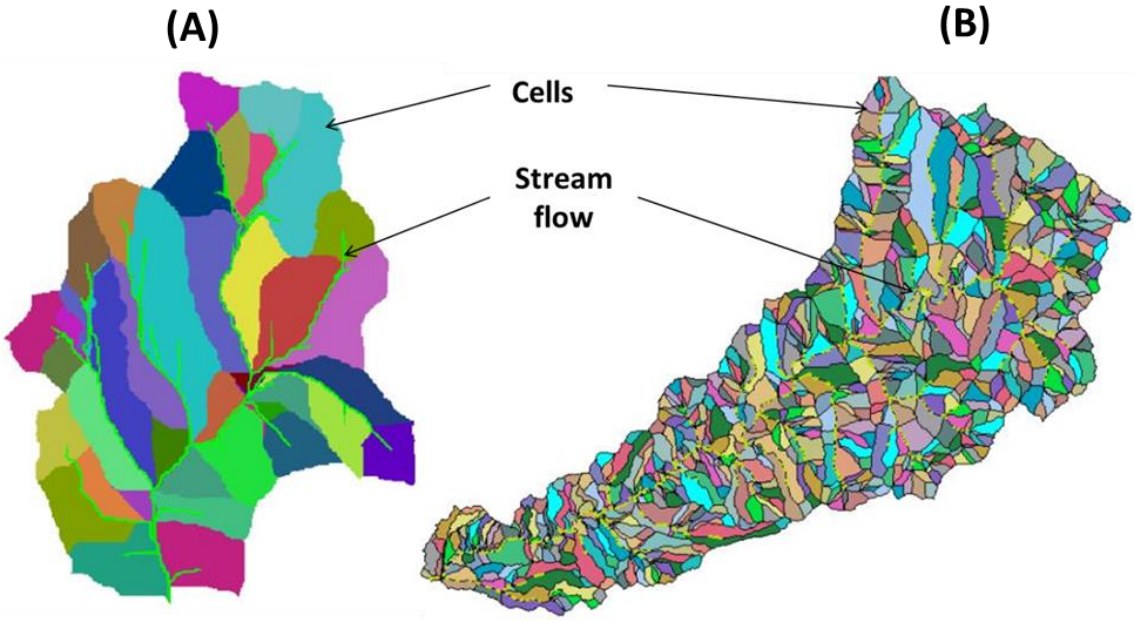

Figure 2. 1: Example of watershed division into homogeneous cells and stream networks within AnnAGNPS: (A) Latxaga watershed (205 ha) and (B) Cemborain watershed (5000 ha)

The main components of AnnAGNPS are now described. The SCS curve number technique (SCS, 1986) is used to generate daily runoff. It is in fact the same technique

utilized in many other hydrologic models such as SWRRB and EPIC models (Williams et al., 1985). The RUSLE technology (Renard et al., 1997) is used to predict daily sheet and rill erosion from fields. The parameters that are used for RUSLE are also used in AnnAGNPS. Each cell within AnnAGNPS can have different RUSLE parameters associated with describing the farm operations. This can provide a suitable characterization of the spatial and temporal variation of the management practices associated with a watershed system. Sheet and rill erosion is calculated for each runoff event during a user-defined simulation period and averaged for this same time period. However the Hydro-geomorphic Universal Soil Loss Equation (HUSLE) is used to predict field deposition and delivery ratio of the sediment yield from sheet & rill erosion to sediment delivery to the stream (Theurer and Clarke, 1991). More recently, Tillage-Induced Ephemeral Gully Erosion Model (TIEGEM) was incorporated into AnnAGNPS to provide a watershed-scale assessment of management practice effects on sediment production from ephemeral gully erosion within croplands (Gordon *et al.*, 2007). The sediment determined for the land areas and gullies is subdivided into particle size classes (clay, silt, sand, small aggregate, and large aggregate) before being added to the stream system. Particle sizes are routed separately in the stream reaches. Some of the specific approaches used in the most important components of the model are outlined in table 2.1. Additional detailed information can be found in (Bingner et al., 2012).

The input data required by the AnnAGNPS model are of two major types. The first one is a daily climate record. The second one includes the physical characteristics and management of a watershed such as morphological parameters, soil, crops and agricultural practices. Cell and reach topographic properties can be estimated using additional modeling components supporting the development of AnnAGNPS input parameters, such as the TOPAGNPS and AGFLOW programs(Bingner et al., 1997, Bingner and Theurer, 2001), which are incorporated into AnnAGNPS Arc view interface. These programs can be used through AnnAGNPS/Arcview interface when employing a DEM to generate the management field and soil identifiers used in the cell data section of the AnnAGNPS Input Editor. Moreover, the output parameters are available at daily, monthly and annual scales. In this chapter, a brief description of AnnAGNPS model algorithms and equations used for surface runoff and sediment yield computing is given based on technical model process documentation (Bingner *et al.*, 2012).The diagram in Figure 2.2summarizes clearly the operating model inputs and outputs.

2.2 Simulation of hydrological processes by AnnAGNPS

Within AnnAGNPS rainfall/runoff relationship runoff is based upon the (U.S. Soil Conservation Service) SCS runoff curve number (CN) procedure. The curve number method was developed by the USDA Natural Resources Conservation Service from an empirical analysis of runoff to determinate direct runoff from a rainfall event in a particular area. Also called a curve number (or simply CN) is an empirical parameter used in hydrology for predicting direct runoff or infiltration from rainfall excess. This section describes the calculation of direct runoff using CN (Mockus, 1972), modified to adjust CN in function of the soil humidity content. CN adjustments require calculation of continuous soil humidity content for definition of previous humidity conditions. This section also describes calculation of different components of the hydric balance. Generation of hydrographs require a storm definition model based rainfall distribution type (SCS, 1986). Circulation of effective precipitation through the watershed is based on the triangular unit hydrograph of SCS, and hydrograph propagation is achieved

through a simple translation, calculating the travel time by applying Manning's equation to the riverbed section.

Table 2. 1. Summary of some AnnAGNPS model characteristics

Model characteristics, approaches and processes	**Comments**
Spatial scale (watershed)	Limited by data availability and computer memory, drainage areas up to 300,000 ha
Subdivision (cells)	Square grid or hydrologic boundaries
Temporal scale (daily time step)	Unlimited number of years
Water	
Surface runoff	SCS curve number and extended TR55
Irrigation	Water with dissolved chemicals and sediment with attached chemicals
Sediment	
Sheet and rill erosion	RUSLE technology
Ephemeral Gully erosion	Tillage-Induced Ephemeral Gully Erosion Model
Stream-bed and bank erosion	Transport capacity
Transport	Einstein deposition equation with Bagnold transport capacity equation
Impoundments	Settling time and dilution due to permanent storage
Particle size classes	Five (clay, silt, sand, small aggregate, and large aggregate)
Nutrients	
Nitrogen	Dissolved and attached
Phosphorous	Dissolved and attached
Organic carbon	Dissolved and attached
Pesticides	Dissolved and attached
Feedlots	Dissolved nutrients only
Point sources	Water and dissolved nutrients

The soil humidity content is the result of different water inputs to the system (rain, snowmelt, irrigation) as well as outputs such as direct runoff, evapotranspiration, percolation and subsurface flow. Real evapotranspiration is a function of the potential evapotranspiration calculated by Penman's equation (Penman, 1948) and of soil humidity content.

The daily surface runoff volume Q, generated by each cell, is calculated by the Curve Number (CN) SCS (Mockus, 1972). This procedure, developed in 1960 taking the data of numerous experimental catchments, permits the estimation of catchment water losses from the characteristics of the vegetation and the existing soil. In AnnAGNPS the CN is modified daily with the soil moisture content, and, if it exists, with the presence of a shallow layer of frozen soil. The curve number associated with mean moisture conditions (CN2) may vary due to any agricultural operation that produces a significant change in the soil surface (e.g. harvesting), and also may slowly change after sowing in the active growth phase of the crop as its leaves open and cover the earth. A daily value is recalculated for CN2, interpolating linearly between the CN2 value of the recently sown crop and the CN value of the ripe crop.

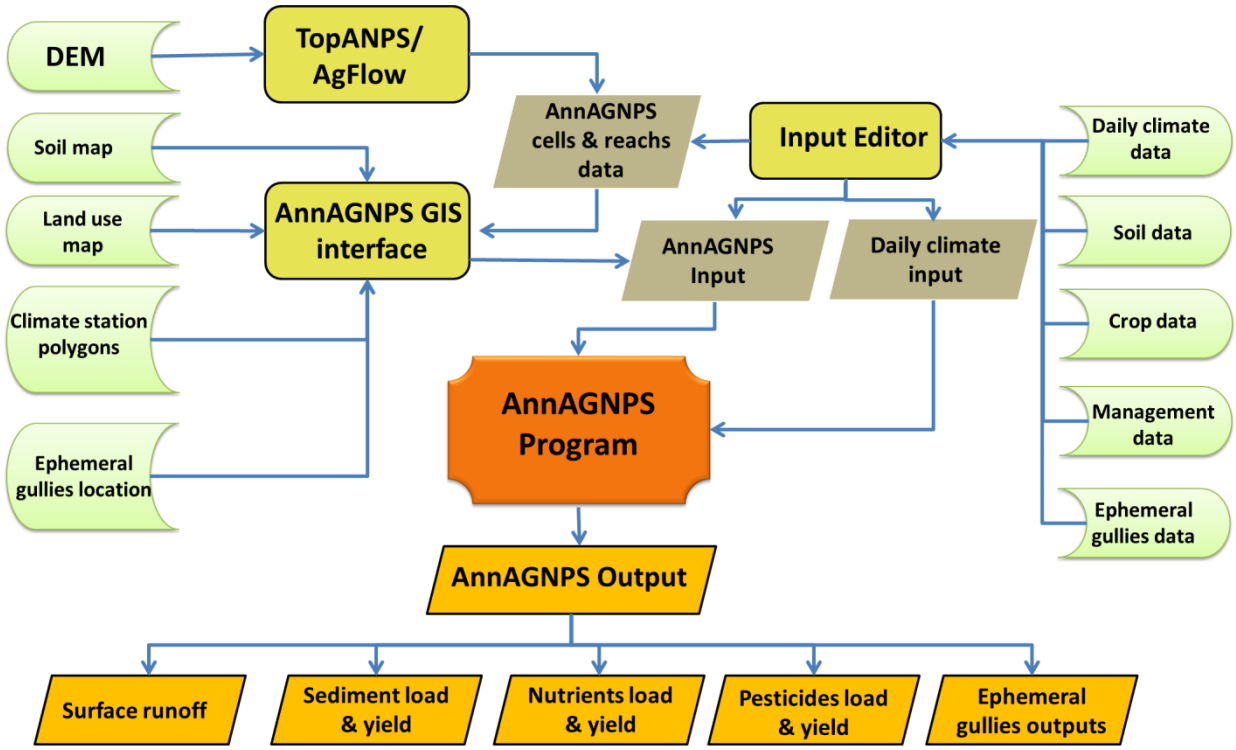

Figure 2. 2: Flowchart showing the AnnAGNPS basic inputs and outputs

The equation (2.1) for the calculation of the runoff or effective precipitation is proposed by materializing the hypothesis that, after the soil has retained a certain amount, I", the soil's infiltration capacity goes on diminishing over the time; i.e. runoff is generated in a growing proportion. The proportion of the growth of the direct runoff with time is obtained by establishing that the real retention ($P_d - l_a - Q$), and the maximum potential retention (S) which is equal to the ratio between the real runoff (Q and the maximum potential runoff ($P_d - l_a$).

$$Q = P_e = \frac{(P_d - I_a)^2}{P_d - I_a + S} \quad (2.1)$$

$$I_a = 0.2\,S \quad (2.2)$$

$$S = 254\left(\frac{100}{CN} - 1\right) \quad (2.3)$$

Where:

Q: volume of direct runoff (mm)

P_e: effective precipitation (mm)

P_d: total daily precipitation (mm)

l_a: initial abstraction (mm)

S: coefficient of storage (mm)

CN: curve number

The parameter CN permits the calculation of loss or initial abstraction, la, This value represents the volume of precipitation retained in the catchment as a result of interception (part of the rainfall is trapped by the vegetation before reaching the soil), and of the surface storage produced at the beginning of the rain event. Once that is

satisfied and the runoff begins, the amount of additional rain retained in the soil stored in the catchment, F_a, is lesser or the same as a retention capacity, or maximum potential retention in the catchment *(S)* and, in the same proportion, the abstraction produced is lower than the maximum abstraction. Although the CN theoretically varies from 0 to 100 (from nil to totally impermeable), in practice the values validated by the experiment vary from 40 to 98 (Van Mullem, 1989).

2.2.1 Calculation of the soil moisture content

The AnnAGNPS model updates the soil's moisture content daily, in terms of its content on the previous day and of the hydric balance that it makes, the result of adding contributions of water and subtracting the losses for that same day. In that balance, all the hydrologic processes simulated by the model intervene, which permits it to be distinguished as a continuous model. The event models calculate the hydrograph generated by a specific rain event represented by its hyetograph and by its antecedent moisture state. That state depends on the circumstances undergone by the catchments days before the event simulated (rainfall, temperature, wind, sunshine, relative moisture) therefore, it is, in principle, different for each simulated event. There is great uncertainty in the determination of previous moisture conditions and no consensus in their calculation, in spite of their importance. The employment of a continuous model like AnnAGNPS overcomes this difficulty as it presents an exhaustive resource for calculating the storage of the water in the soil continuously.

The phenomenon of the water's movement in the soil is highly non linear due to its heavy dependence on hydraulic conductivity and the potential matrix of the moisture content in the soil. Both parameters control the percolation process, so that the variation in the soil moisture has a direct repercussion. In another direction, evapotranspiration has a very marked daily variation, closely linked to the variation in air temperature. It is considered appropriate to simulate these hydrologic processes with shorter time spans of under one day and using a simple constant time span procedure. The day is divided into several intervals of equal duration and the hyetograph (daily rainfall as per type of rain distribution) is considered to be uniform in the course of each interval; namely, it adopts the form of a hydrograph with those intervals. The number of intervals into which the day is split up is specified by the user. By default it takes a value of 8, so that each interval lasts three hours. The value of all the elements implicated in the hydric balance is updated for each interval by default of 3 hours.

The soil moisture is simulated for two layers of soil. Each of these is composed of the different horizons defined by the edaphologic study. The top one, 20 cm thick, called tilling layer, whose properties (e.g bulk density) are susceptible to changes, will be identified with the suffix 1, and the second layer, that is constituted by the profile of the remaining soil, whose properties remain invariable, goes from the deepest part of the tilling layer down to either an impermeable layer or the total depth of the soil (by default it is of 2 m), is identified with the suffix 2 (Figure 2.3). The properties (i.e. texture, porosity, etc.) of each layer or stratum are calculated as the arithmetic mean of the properties of the different horizons proceeding from the edaphologic study, that make up each of the two layers.

The hydric balance for each period of time is calculated for the first soil layer:

$$SM_{t+1} = SM_t + \frac{WI_t - Q_t - PERC_t - ET_t + Q_{lat} - Q_{tile}}{D_{SL1}} \quad (2.4)$$

Where:

SM_t = moisture content for each soil layer at beginning of time period (fraction),

SM_{t+1} = moisture content for each soil layer at end of time period (fraction),

WI_t = water input, consisting of precipitation or snowmelt plus irrigation water (mm),

Q_t = surface runoff (mm),

$PERC_t$ = percolation of water out of each soil layer (mm),

ET_t = potential evapotranspiration (mm),

Q_{lat} = subsurface lateral flow (mm)

Q_{tile} = tile drainage flow (mm)

D_{SL} = thickness for soil layer (mm)

t = the time period.

For the second soil layer, surface runoff $Q_{t,2}$=0:

$$WI_{t,2} = PERC_{t,1} + Inf_{t,2}$$

$$SM_{(t+1),2} = SM_{t,2} + \frac{PERC_{t,1} + Inf_{t,2} - PERC_{t,2} - ET_{t,2} + Q_{lat,2} - Q_{tile,2}}{D_{SL2}} \quad (2.5)$$

Where:

$PERC_{t,1}$: percolation from the top layer (mm)

$Inf_{t,2}$: direct infiltration from the surface to the lower layer (mm)

The remaining variables that appear in Equation 3.2 are described within Equation 2.5, with the only difference being the second layer that divides the soil profile.

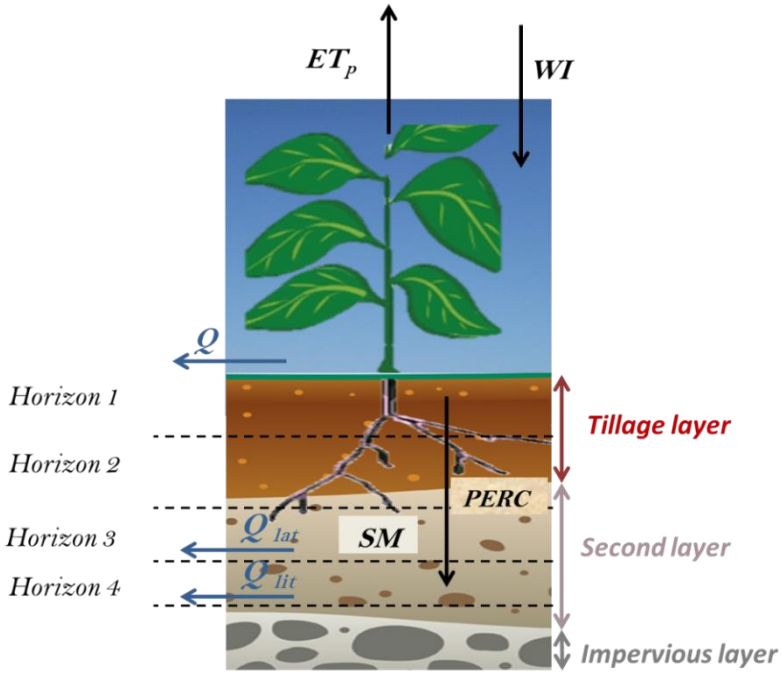

Figure 2. 3: Representation of soil profile division, and hydrological process scheme simulated by AnnGNPS.

2.2.2 Adjustment of CN to the soil moisture content

The tabulated values of the CN reflect mean moisture conditions of the soil. If there is abundant rainfall on previous days, the soil's moisture content will be elevated, the

CN higher and more runoff will be generated. Analogically, and on the contrary, if the soil is dry the losses are greater, the CN lower and less runoff is generated. It is necessary to determine the fraction of the soil's saturation (2.14.) in order to fit the curve number every day (2.18.). The degree or fraction of soil saturation varies conceptually from between O and 1 and is defined as:

$$FS_t = \frac{SM}{f} = \frac{V_w}{V_v} \tag{2.6}$$

Where:

FS_t: fraction of soil saturation (fraction)

SM: soil moisture content (volume of water over the total volume), (fraction)

f: soil porosity (volume of voids over the total volume), (fraction)

V_w: volume of water in the soil) (m 3

V_v: total volume of pores (the sum of the volume of water and the volume of air) (m 3)

The depth of the soil used to calculate this fraction of soil saturation is variable and depends on the hydraulic conductivity. Under the most favorable percolation conditions, namely, when the soil is saturated, there is a maximum depth down to which the water can percolate in a day. The soil found below that depth cannot affect the curve number because its moisture content does not vary, so that it is not necessary to fit it. This maximum depth is calculated, for the first stratum of soil, with the following expression indicated:

$$D_{FS1} = \frac{K_{SAT1}}{f_{v1}} \tag{2.7}$$

Where

D_{FS} : the thickness of the soil that affects the saturation fraction for the calculation of the curve number (mm)

K_{SAT}: the hydraulic conductivity in the saturation for each soil layer (mm/h)

If $D_{FS1} > D_{SL1}$:

$$D_{FS1} = D_{SL1} \tag{2.8}$$

$$FR = \left(1 - \frac{D_{FS1}}{D_{SL1}}\right).\frac{24h}{1day} \tag{2.9}$$

Where:

D_{SL1}: thickness of the first soil layer (mm)

D_{FS1}: thickness of the first soil layer affecting the saturation fraction for the calculation of the curve number (mm)

FR: fraction of the remaining day, as from the percolation through the thickness of the first stratum (h)

For the second soil layer, this is multiplied by the FR factor because part of the day has been occupied by the water percolating through the first layer

$$D_{FS2} = \frac{K_{SAT2}}{f_{v2}}.FR \tag{2.10}$$

If $D_{FS2} > D_{SL2}$

$$D_{FS2} = D_{SL2} \tag{2.11}$$

$$D_{FStot} = D_{FS1} + D_{FS2} \quad (2.12)$$

Where:

D_{FStot}: total depth of soil that affects the curve number (mm)

$$S_{max} = D_{FS1}(FC_1 - WP_1) + D_{FS2}(FC_2 - WP_2) \quad (2.13)$$

S_{max}: maximum content of moisture in the soil (mm)

(FC-WP) (i): the field capacity minus the wilting point for each soil layer (fraction)

$$FS_t = \frac{D_{FS1}(SM-WP)_{(1,t)} + D_{FS2}(M-WP)_{2,t}}{S_{max}} \quad (2.14)$$

Where:

FS_t: soil saturation fraction (fraction)

(SM-WP) (i): soil moisture content minus wilting point for each soil layer (fraction)

The daily ajustment of the curve number CN in terms of the moisture content in the soil requires some additional parameters. The moisture content at the beginning of each day determines the antecedent moisture condition AMC, that is used to adjust the CN each day and that varies between the Curve Number associated with dry conditions (CN1) and the curve number associated with wet conditions (CN3) according to the moisture reserves in the soil.

The dispersion of these rain-runoff points from one storm to another shows the variation in S (figure 2. 4) and therefore that in the CN. Most of this difference in the inter-event CN lies in the variation in the moisture preceding each storm. Mockus (1949) divided antecedent moisture into three ranks by observing the amount of rain falling in the five days prior to the storm.

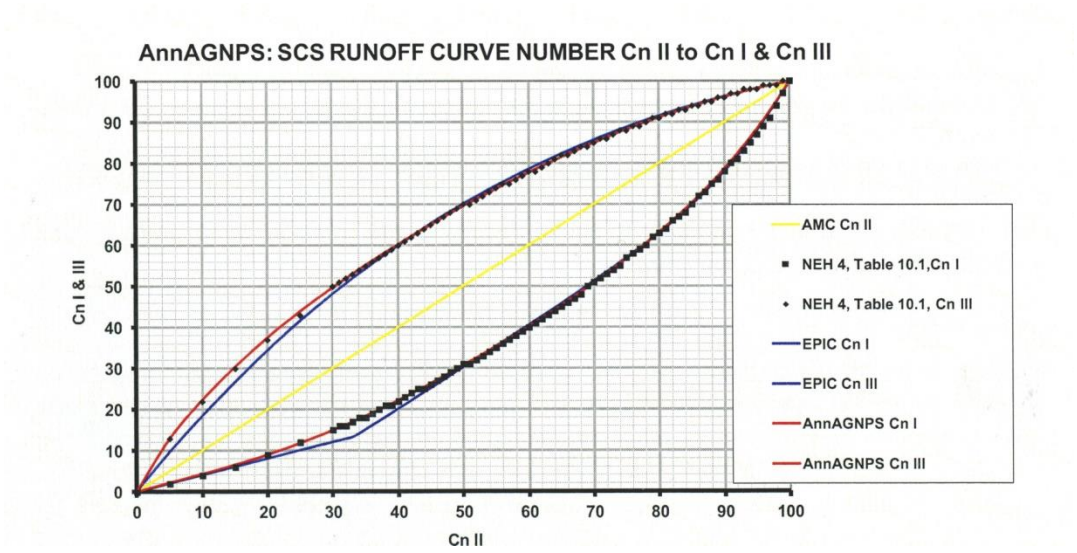

Figure 2. 4: Comparison of the fit of the CN to the soil moisture content of EPIC, NEH 4 and AnnAGNPS. Depiction of CN I, CN II and CN III. (Source: (Gastesi, 2014)

The Curve Numbers CN1 and CN3 are calculated in terms of CN2 by a adjust (Figure 3.2). their corresponding retention factors S1 and S3 are calculated by applying the equation (III.3.), as a function of which the weights used in the daily fit to the storage coefficient S are obtained (W1 and W2).

$$CN_1 = CN_2 - \frac{20(100-CN_2)}{100-CN_2+\exp(2533-0.0636\,(100-CN_2)} \quad (2.15)$$

And

$$CN_3 = CN_2 \exp(0.00673(100 - CN_2)$$

$$W_2 = 2\left[\ln\left(\frac{0.5}{1-\frac{S_2}{S_1}} - 0.5\right) - \ln\left(\frac{1}{1-\frac{S_3}{S_1}} - 1\right)\right] \quad (2.16)$$

$$W_1 = \ln\left(\frac{0.5}{1-\frac{S_2}{S_1}} - 0.5\right) + W_2 \quad (2.17)$$

The real value of S used in the calculation of the surface runoff for a specific day *t*, is subject to a dynamic change due to fluctuations in the soil's moisture content. *S* is a state variable with a single relationship with the soil moisture content SM, described by the following expression:

$$S_t = S_1\left(1 - \frac{FS_t}{FS_t+exp(W_1-W_2FS_t)}\right) \quad (2.18)$$

Where:

S_1 : daily storage coefficient adjusted to the soil moisture content (mm)

FS_t: soil saturation fraction (equation (2.14)) (fraction)

S_1: maximum storage coefficient associated by (equation (2.3.) with the minimum curve number CN1 (mm)

W_1, W_2: weights used in the fit to the daily storage coefficient (fraction)

This algorithm permits a gentle and curvilinear variation in the storage coefficient *S*, from a maximum value of S_1, passing through the value S_2 (associated with the curve number of the mean condition CN_2), to the minimum value of S_3 (associated with the maximum curve number CN_3), when $SM = FC$. The result of these calculations is simply to establish at a new scale the soil moisture content SM, at values that can be used in the curve number equation to calculate the surface runoff.

AnnAGNPS in turn permits the fit of the curve number in situations in which the soil is frozen, which is not habitual in the study catchment, and this characteristic is only cited without entering into any detailed formulation of it.

InAnnAGNPS CN2 may change due to the following two situations

(1) When an agricultural operation is performed for the current day in the simulation, then a new CN is assigned. For example, at crop harvesting, when significant changes in the land cover occur.
(2) When a newly planted crop is in the active growth phase.

When a new CN is specified for a new planting operation, the model then sets up the information needed to transition the CN from its current value to the value applicable to when the crop is fully developed. Information on time fraction of crop

planting to crop harvesting as well as plant growth stages (initial, development, maturity, and senescence) is given by the user. The actual curve number used for calculating runoff varies depending on soil moisture content.

2.2.3 Peak flow

AnnAGNPS utilizes an extended, modified version of TR55, the extended TR55, for the generation of the required peak flow to define the direct runoff hydrograph (Theurer and Comer, 1992). TR55 is based on the graphic TR55 method (Technical release 55) of the U.S. Soil Conservation Service (SCS, 1986). Extended TR55 not only widens the application range regarding the combination of I_0/I (from 0 to 1) and T_c (from 0 to 48h), but also integrates an important conceptual contribution in comparison with TR55, which is the utilization of precipitation as a normalization factor instead of runoff. This is based on the unit hydrograph theory, and is a function of the amount of rainfall (I_0/P) and its distribution (RDT), of the SCS curve number $(I_0/P)_f$ and of concentration time (T_c). As the watershed under study is located in Navarre, the corresponding rainfall distribution must be calculated as well as the unit peak flow for the entire parametrical space, according to the NEH-4 method. Finally, a continuous function is created by non linear regression for the NEH-4 points, with a second degree rational polynomial equation in the numerator and a third degree equation in the denominator. These equations only depend on concentration time T_c, and six coefficients are obtained from the regression equation for each I_0/P and for each rainfall distribution type (RDT). From the regression curve, AnnAGNPS calculates the unit peak flow.

The unit peak flow is multiplied by the drainage area (A_d), providing synthetic adjustment curves. Then peak flow for the convoluted hydrograph is calculated for each cell. The triangular SCS hydrograph is generated for direct runoff at any node of the drainage network, by introducing real watershed and climatic data.

Calculation of concentration time in any node of the drainage network requires combined calculations of concentration time in each cell and of travel time in the riverbed section channels. Of all possible combinations of concentration times, the one that maximizes the value of concentration time at the outlet of the watershed is selected.

The time of concentration in each cell is calculated by the model from the sum of the travel times from the hydraulically most distant point to reach the channel for the three flow types within the cell (sheet flow, shallow concentrated flow, and concentrated flow). Calculations for the three flow types are based on the NRCS TR-55 methodology (SCS, 1986) procedures, modified by Cronshey and Theure, (1998). The first 50 m of flow length are treated as overland flow. The next 50 m are treated as shallow concentrated flow, while the length beyond this is treated as concentrated flow.

Additional parameters are calculated associated with runoff, the potential evapotranspiration is a function of potential evapotranspiration calculated using the Penman equation (Penman, 1948) and soil moisture content. An enhancement for computing the evapotranspiration were made by incorporating the FAO dual crop coefficient procedure for determining the daily impact of vegetation transpiration (K_{cb}) and soil evaporation (Ke) on evapotranspiration (ETc)(Allen et al., 1998). These coefficients provide better transpiration and soil moisture losses account by taking in account the changes in the variation of evapotranspiration during the growth stages (initial, development, mature and Senescence growth stages)

2.3. Sediment

2.3.1. Sheet and rill erosion

RUSLE is an erosion model that predicts longtime average annual loss resulting from raindrop splash and runoff from specific field slopes in specified cropping and management systems and from rangeland. RUSLE is the update of the Universal Soil Loss Equation (USLE) (Wischmeier and Smith, 1978), including improvements in determining certain factors. These include a revised time-varying approach for soil erodibility factor; a subfactor approach for evaluating the cover-management factor; a new equation to reflect slope length and steepness; and new conservation-practice values (Renard et al., 1997). Currently, RUSLE is considered to be the best sheet and rill technology for continuous simulation of watershed sediment yield. Hence, AnnAGNPS uses the Revised Universal Soil Loss Equation (RUSLE) technology (Renard et al., 1997) to predict daily sheet and rill erosion of a watershed's landscape.

RUSLE is essentially expressed in equation 2.10 as:

$$A = R.K.LS.C.P \tag{2.19}$$

Where

A: Temporal average soil loss per unit of area and (t/ ha/yr)

R: Rainfall erosivity factor (MJ/. ha. mm/hr)

K: Soil erodibility(t/ha/(MJ.ha/mm.hr)

L: Slope length factor

S: Slope steepness factor

C: Cover management factor

P: Support practice factor

2.3.1.1. Estimation of RUSLE factors

During the data preparation the RUSLE components within AnnAGNPS are calculated for each cell, and a K factor for each soil, in the watershed. The R factor of rainfall erosivity product is the sum of kinetic energy for high intensity in 30 minutes of each of the n storms in a year.

RUSLE R factor; The rainfall erosivity factor is the erosion potential of the rain that affects the process of soil erosion. Erosion by rain drops increases with the intensity of the rain. The R factor is directly proportional to the product of the total kinetic energy of the storm (E) times its maximum 30-minute intensity (I). Thus R factor is the average annual summation of (EI) values in a normal year's rain.

The EI30 values are determined for each event were summed every 15 days (24 values annually).Then, the average of these values was calculated with the total simulated years. The sum of these 15 day periods average values give us the annual value of RUSLE R factor.

RUSLE K factor: This represents the susceptibility of soil to erosion from rain drops and surface runoff. Soil texture and structure affect both susceptibility to detachment and infiltration. In addition, organic matter decreases erodibility by reducing the susceptibility of the soil to detachment, and it increases infiltration, which reduces soil erosion due to runoff. For each soil in the watershed, K factor is calculated or provided through user input. For this study, the K factor was calculated following Wischmeier and Smith (1978), which includes soil texture, structure and organic matter content.

InAnnAGNPS the K factor is considered as a variable depending on the soil moisture content. So 24 K factors (two per month) are calculated.

RUSLE LS factor, or topographic factor. This is derived from the slope-length and slope-steepness along a flow profile. An automated procedure to determine the average LS factor for each cell in AnnAGNPS using digital elevation maps (DEMs) has been included in AnnAGNPS(Bingner and Theurer, 2001). More precisely, from the DEM (at any resolution), a raster-weighted LS-factor for each cell is determined by AGFLOW model using the slope length and steepness factor algorithms for irregular and segmented slopes (Renard et al., 1997). The accuracy of the resulting LS-factors is a function of the horizontal and, in particular, the vertical raster resolution of the DEM.

RUSLE C factor, or cover-management factor. This is used to indicate the effect of cropping and management practices on erosion rates. It represents the effects of plants, soil cover, soil biomass, and soil disturbance activities on erosion.

The computation of C factors inAnnAGNPS for a single cell is identical to that of the original model, with one exception. The original RUSLE model only allowed one contour practice to be applied to a noncropland cell. AnnAGNPS allows multiple contour practices to be applied in rotation on a non-cropland land use. In the original RUSLE model, when a contour is specified on a non-cropland land use, the average annual C factors degrade over a period of time. The length of time is equal to the number of years it takes the soil to consolidate as specified in the soil data. For example, if it takes seven years for the soil to consolidate, the original RUSLE model would calculate seven average annual C factors, with the C factor decreasing each successive year until it reached its minimum value in the seventh year.

RUSLE P factor, or support practice factor.This factor reflects the impact of support practices on the average annual erosion rate. These practices affect soil erosion by modifying the flow pattern grade of surface runoff inducing a reduction in its amount and rate (Renard et al., 1997). For cultivated land, the support practices considered include contouring tillage and planting, stripcropping, terracing and subsurface drainage. In this study, RUSLE P factor ranges between 0.4 and 0.6 in watersheds under different slope percentages with contour tillage and where gullies or rills do not occur. The P factor has a value of 1 in the case of tillage parallel to main slope gradient.

2.3.1.2 AnnAGNPS delivery ratio

Sediment delivery to the edge of the field is calculated whenever a runoff event occurs from rainfall, irrigation, or snowmelt in the Simulation Processing phase of the AnnAGNPS model run. Each of the RUSLE parameters is either calculated or retrieved from previously calculated data. Since RUSLE is used only to predict sheet and rill erosion and not field deposition, a delivery ratio of the sediment yield from this erosion to sediment delivery to the stream is needed. The Hydro-geomorphic Universal Soil Loss Equation (HUSLE) is used for this procedure (Theurer and Clarke, 1991). HUSLE calculates the total sediment yield for a given storm event to any point in the watershed when it is given the upstream (Eq 2.20, (Theurer and Clarke, 1991)using: average RUSLE parameters, drainage area, volume of water runoff, peak discharge and RUSLE regression coefficients for the applicable hydro-geomorphic area.

$$S_y = 0.22 * Q^{0.68} * q_p^{0.95} * KLSCP \qquad (2.20)$$

Where:

S_y: sediment yield (T/ha)

Q: surface runoff volume (mm)

q_p: peak rate of surface runoff (mm/s)

And K, LS, C, P are the RUSLE factors

Applying the equation 2. 20 (S_y) for two different points in the same cell where point "B" is located downstream of the point "A" and with the same runoff volume at all locations within the homogeneous area, the delivery ratio from location "A" to "B" is :

$$D_r = S_{yB}/S_{yA} = \left(q_{pB}/q_{pA}\right)^{0.95} \quad (2.\,21)$$

Where:

S_{yA}: sediment yield at location "1" (T/ha)

S_{yB}: sediment yield at location "2" (T/ha)

q_{pA}: peak rate of surface runoff at location "1" (mm/s)

q_{pB}: peak rate of surface runoff at location "2" (mm/s)

Dr: delivery ratio from location *"A"* to *"B"*

The delivery ratio is assumed to be proportional to the mass fall velocity of the individual particle-size classes. The particle-size sediment deposition within the field also called the deposition mass rate was normalized with respect to the smallest value, which is clay.

2.3.2. Tillage Induced Ephemeral Gully Erosion

In addition to the prediction of sheet and rill erosion, AnnAGNPS model developers (NRCS and USDA –ARS) were interested in incorporating new technologies to predict ephemeral gully erosion, which includes the technology to identify where ephemeral gullies may form using GIS (Bingner et al., 2012). Therefore, AnnAGNPS integrated Tillage-Induced Ephemeral Gully Erosion Model (TIEGEM) technology to provide a watershed-scale assessment of management practice effects on sediment production from ephemeral gully erosion within croplands.

TIEGEM is an enhanced version of Revised EGEM (REGEM). Gordon et al. (2007) extending the capabilities of EGEM (Woodward, 1999) to REGEM by adding a new algorithm which estimates the migration rate of the headcut, and an algorithm which creates the initial headcut's knickpoint, refining some of the existing EGEM components and developing additional components into a revised and further enhanced algorithm. The sediment delivered to the mouth of the gully is estimated using the HUSLE procedure (Theurer and Clarke, 1991). Moreover, AnnAGNPS model developers incorporated a new tool into AGNPS GIS components for identifying where the mouth of the ephemeral gully headcut can form based on topographic analysis (Parker et al., 2010).

2.3.2.1 Theoretical basis for estimating ephemeral gully erosion in AnnAGNPS

EG erosion simulation in AnnAGNPS is based on the technology used in EGEM, but adapted for being used at cell level. As already mentioned, each cell is uniform in a number of parameters (soil, land use, etc.) and these parameters will be invariant in space and time during each runoff event when EG simulation processes occur.

2.3.2.2 Hydrology

The calculation of EG erosion requires the peak discharge and total runoff volume for each simulated storm so that an event hydrograph can be constructed. These parameters may be supplied by the user or calculated based on TR-55 methods (SCS, 1986) using drainage area, rainfall, curve number, and storm type (Gordon et al., 2007).Given the event peak discharge at the mouth of the gully (Qp) and runoff volume (V_b), a triangular hydrograph is constructed using an even number of timesteps(ti) representing each one. At the gullymouth, this hydrograph has a time to base (tb) (figure 2.5 and Eq. 2.13).

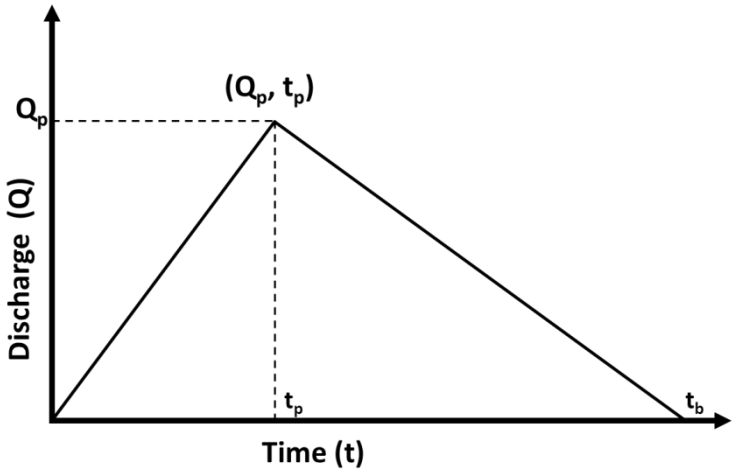

Figure 2. 5: Triangular hydrograph used in AnnAGNPS

$$t_b = \frac{2V_b}{Q_p} \qquad (2.13)$$

And discharge at the mouth of the gully (Q_{mi}) during each time step ti can be determined from:

$$Q_{mi} = \left(\frac{t_i}{t_p}\right) Q_p \qquad \text{when } 0 < ti < tp \qquad (2.22).$$

And

$$Q_{mi} = \left(\frac{(t_b - t_i)}{(t_b - t_p)}\right) Q_p \qquad \text{When } tp < ti < tb \qquad (2.23)$$

Thus the total flow is

$$Q_m = \sum_{i=1}^{t} Q_{mi} = \frac{V_b}{t_b} \qquad (2.24)$$

2.3.2.3 Ephemeral gully initiation

EG mouth is initially located in the landscape and is referred to the point furthest downstream of an EG. For a given runoff event, a hydrograph can be constructed at the mouth, and the flow rate at a given location within the cell will be proportional to the upstream drainage area, depending on the length of the gully; thus, flow is unsteady and spatially varied (Gordon et al., 2007).This concentrated flow generates a *"Shear stress"* τ (N m^{-2}) expressed according to Chow et al, (1988)in Eq.2.25. Once this shear stress exceeds a certain critical value τ_c, which is the soil resistance to erosion by flowing water, detachment of soil particles by concentrated flow may occur (Léonard and Richard, 2004) indicating the EG initiation. Subsequently, a relatively small length of the ephemeral gully channel is incised until the tillage depth is reached, thus

creating a scour hole (plunge pool) at the gully mouth also called nickpoint(Gordon et al., 2007).

$$\tau = \rho\ g\ d\ S \quad (2.25)$$

Where:

ρ: Water mass density (kg/ m^3)

g: Gravity constant (m/s^2)

d: hydraulic depth (m)

S: friction slope

The detachment capacity of the flow is defined as:

$$DC = k_d\ (\tau - \tau_c) \quad (2.26)$$

$$K_d = 2910^{-6} e^{(-0.224\tau_c)} \quad (2.27)$$

Where:

DC: the detachment capacity (g/ m^2. s)

K: soil erodibility coefficient (g/N.s)

In the AnnAGNPS model the τ_c value can either be defined by the user or be estimated by the model (by default) using an empirical expression based on soil texture. The soil material detached after the nickpoint formation is not considered in the total EG erosion calculation due to the small volume it produced.

2.3.2.4 Headcut migration

Once the EG channel reaches the tillage depth, the EG headcut is then formed. The impinging jet that drives the concentrated flow in the plunge pool exercises the force that overcomes the resistance presented by the soil. Consequently, the headcut propagates upstream (figure 2. 6) (Alonso et al., 2002). To describe headcut migration AnnAGNPS uses the equations developed by Alonso et al. (2002). Headcut migration rate, and thus the length of ephemeral gully, is calculated as follows:

$$M = V\sqrt{\frac{\mu q}{S_D - h}} \quad (2.28)$$

being

$$\mu = \frac{1}{2}\rho_w k sin^2\left(\frac{\theta}{2}\right) \quad (2.29)$$

Where:

M: headcut migration rate (m/s)

V: jet entry velocity(m/ s)

q: unit discharge (m^2/s)

S_D: scour depth (equal to the tillage depth, m)

h: vertical distance from the brink to the pool surface (m)

θ: jet entry angle (radians)

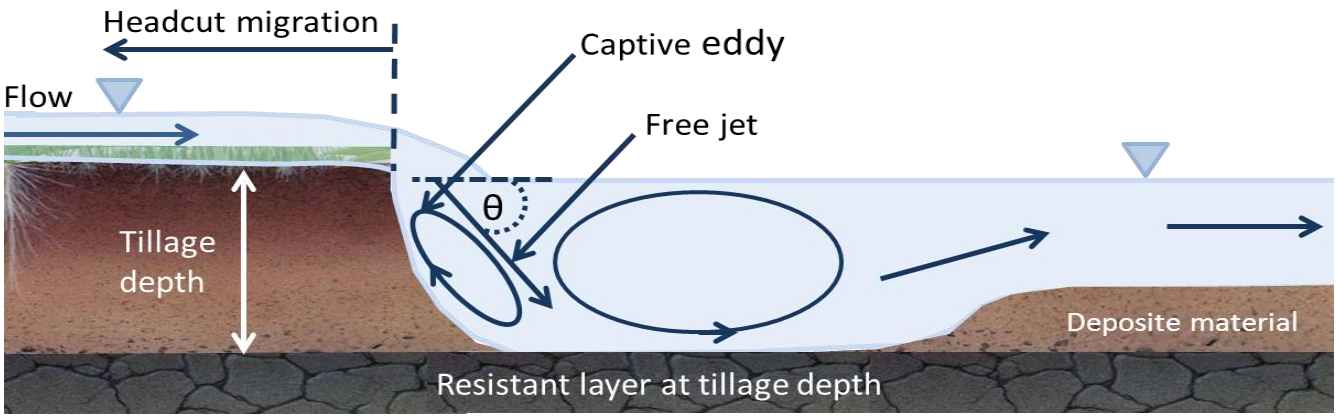

Figure 2. 6 : Illustration of headcut migration and their related parameters (Gordon et al., 2007).

2.3.2.5 Ephemeral gully length

The EG reaches its maximum length in one or various events in a long continuous simulation. As shown before, the EG headcut migrates upstream, which means that the EG headcut contributing to the drainage area decreases with its increase in length , so the discharge at the head of the gully also decreases. For this reason, in AnnAGNPS the maximum EG length (L_{max}) for a given drainage area (A_d) is calculated based on Leopold et al. (1964) equation:

$$L_{max} = 80.3\, A_d^{0.6} \tag{2.30}$$

Where:

L_{max}: maximum EG length (m);

A_d: EG drainage area (ha).

2.3.2.6 Ephemeral gully width

According to Smith (1993), EG are widest at their mouths and narrowest at the locations of the headcut, due to the decrease in discharge in the upstream of the EG. The same observations can be attributed to the monitored EG by Casalí (1997) and De Santisteban (2003) in Navarre region. Therefore,AnnAGNPS developers consider that of the three space dimensions that define an ephemeral gully, the most sensitive one is its width (Bingner et al., 2012). The ephemeral gully width is a function of the maximum discharge that occurs at some time during its development (Nachtergaele et al., 2001). Several different gully width relationships have been offered, with the AnnAGNPS model proposing that users by default select between six empirical algorithms to determine the minimum gully width at EG mouth for each event. The six algorithms are:

(a) Nachtergaele et al's (2002) equation

In this equation, the relationship between channel width and flow discharge for ephemeral gullies formed on cropland was established by Nachtergaele et al. (2002) using six experimental data sets from south-east Portugal and central Belgium

$$W_n = 2.51\ Q_p^{0.412} \tag{2.31}$$

Where: Q_p: peak discharge at gully station (cm)

W_n: minimum width (m)

(b) Gully-Located Hydraulic Geometry equation

The hydraulic geometry for concentrated flow can be related to each cell in which the EG mouth is located.

$$W_h = \left\{ \left(\frac{a^{(d/b)}}{c} \right)^{5/3} \left(\frac{n \cdot Q}{\sqrt{S_0}} \right) \right\}^{\left(\frac{1}{1+[(5/3)(d/b)]} \right)} \quad (2.32)$$

Where:

W_h: hydraulic geometry's minimum gully width (m)

a, *b*, *c* and d: hydraulic geometry's width regression coefficients

n: Manning's roughness coefficient

S_0: gully bed slope (m/m)

Q: discharge (m^3/sec)

(c) Non-submerging Tailwater equation

$$W_s = Q_p / \left[\left(d_t^{5/3} * \sqrt{S_0} \right) / n \right] \quad (2.33)$$

Where

W_s: incipient submerged flow's minimum width (m)

Q_p: peak discharge at gully station (cm)

d_t: tailwater depth

n: Manning's roughness coefficient

S_0: average bed slope above the knickpoint (m/m)

(d) Woodward's (1999) Equilibrium Gully Width equation

Used in EGEM, the equilibrium width is the gully width while the headcut is deepening to its non-erosive layer.

$$W_e = 2.66 * Q_p^{0.396} * n^{0.387} S_0^{-0.160} * \tau_c^{-0.240} \quad (2.34)$$

Where:

W_e: equilibrium minimum gully width (m)

Q_p: peak discharge at gully station (cm)

τ_c: critical shear (N/m^2)

n: Manning's roughness coefficient

S_0: average bed slope above the knickpoint (m/m)

(e) Woodward's (1999) Ultimate Gully Width

Used also in EGEM, the ultimate width is the width at which the shear stress is equal to the critical shear stress

$$W_u = 179.0 * Q_p^{0.552} * n^{0.556} S_0^{0.199} * \tau_c^{-0.476} \quad (2.35)$$

W_u is the ultimate minimum gully width (m)

(f) Well's 2011 equation

This empirical equation was established based on nine experiments conducted in the laboratory hydraulic flume to examine gully expansion as a function of channel slope and overland flow discharge (Wells et al., 2013). The founded relationship is as follows:

$$W_f = \sqrt{\left[\frac{1}{0.002985 - 0.002917 exp^{-S}}\right]} QS + 46.07S^3 + 0.0104 \quad (2.36)$$

Where

W_f: channel width (m)

Q: Discharge on channel

S: channel slope

2.3.2.7 Sediment erosion, transport and deposition

In the case of EG erosion three possible sources of sediment can be distinguished: 1) sediments received from upstream; 2) internal sediments generated by headcut migration and channel widening 3) previously deposited sediment on the EG bed. Five classes of sediments (sand, large aggregates, small aggregates, silt, and clay) are considered and routed separately.

2.3.2.8 Sediment transport

For each runoff event, sediment routing is computed according to these schemes:

- If the incoming suspended sediment is less than the sediment transport capacity for that timestep, all available sediment will be moved to the next downstream section.
- If the amount of suspended sediment is larger than its sediment transport capacity, then the excess amount is deposited in a layer on the channel bed, and the deposition algorithm is used.
- If the available sediment is less than transport capacity, previously deposited sediment will be entrained and eroded until transport capacity is reached.

2.3.2.9 Sediment transport capacity algorithm

According to each particle size and its physical properties, the sediment transport capacity is calculated with:

$$q_{sc} = \frac{\eta * K * \tau * V_m^2}{V_f} \quad (2.37)$$

Where:

q_{sc}: unit-width sediment transport capacity(t/sm)

η: effective transport factor (non-dimensional)

k: transport capacity factor (non-dimensional)

τ: bed shear stress (t/m^2)

v_w: flow velocity of water (m/s)

v_f: particle fall velocity (m/s)

3.3.2.10 Sediment deposition algorithm

The sediment routing within each reach will be computed using the unit-width, steady-state, uniform, spatially-varied sediment discharge model (Bingner and Theurer, 2002).

All upstream sediment discharges (q_{s1}) will be the sum of all incoming sediment from upstream plus the local sediment associated with the immediate upstream reach.

$$q_{s2} = q_{sc} + (q_{s1} - q_{sc}) * \exp(-N_d) \quad (2.38)$$

Where:

q_{s2}: downstream unit-width sediment discharge (t/sm)

q_{sc}: unit-width sediment transport capacity (t/sm)

q_{s1}: upstream unit-width sediment discharge (t/sm)

N_d: deposition number (non-dimensional)

2.4 AnnAGNPS GIS interface

2.4.1. Topography

AnnAGNPS pack integrated ArcView Geographic Information System (GIS) interface to simplify the use of TOPAGNPS and AGFLOW models (Bingner et al., 1997). TOPAGNPS or TOPAZ (TOpographicPArameteriZation) is a digital landscape analysis designed to assist with topographic evaluation and watershed parameterization in support of hydrologic modeling and analysis. TOPAZ includes three subprograms Digital Elevation Drainage Network Model (DEDNM), RASterPROperties (RASPRO) and RASterFORmatting (RASFOR). These subprograms process the digital elevation model (DEM) to identify and measure topographic features; define surface drainage, flow direction and flow paths; subdivide watersheds along drainage divides into subcatchments; quantify the drainage network and calculate channel parameters; and estimate representative subcatchment parameters.

The AGricultural watershed FLOWnet generation program (AGFLOW) is used to determine the topographic related input parameters needed by AnnAGNPS. Both AGFLOW and TOPAGNPS provide information on cell area, slope perimeter, channel segment length and slopes, the RUSLE LS-factor and the topology of the cell network.

2.4.2. Soil and field data assignation

The ArcView interface allows users to assign to each cell soil type and specific land use using, respectively, soil and land-use maps. Basically, the soil and land-use maps are laid over the generated cell map. As each cell has homogeneous soil and land use, if the cell normally has more than one soil and land-use type. (figure 2.7).

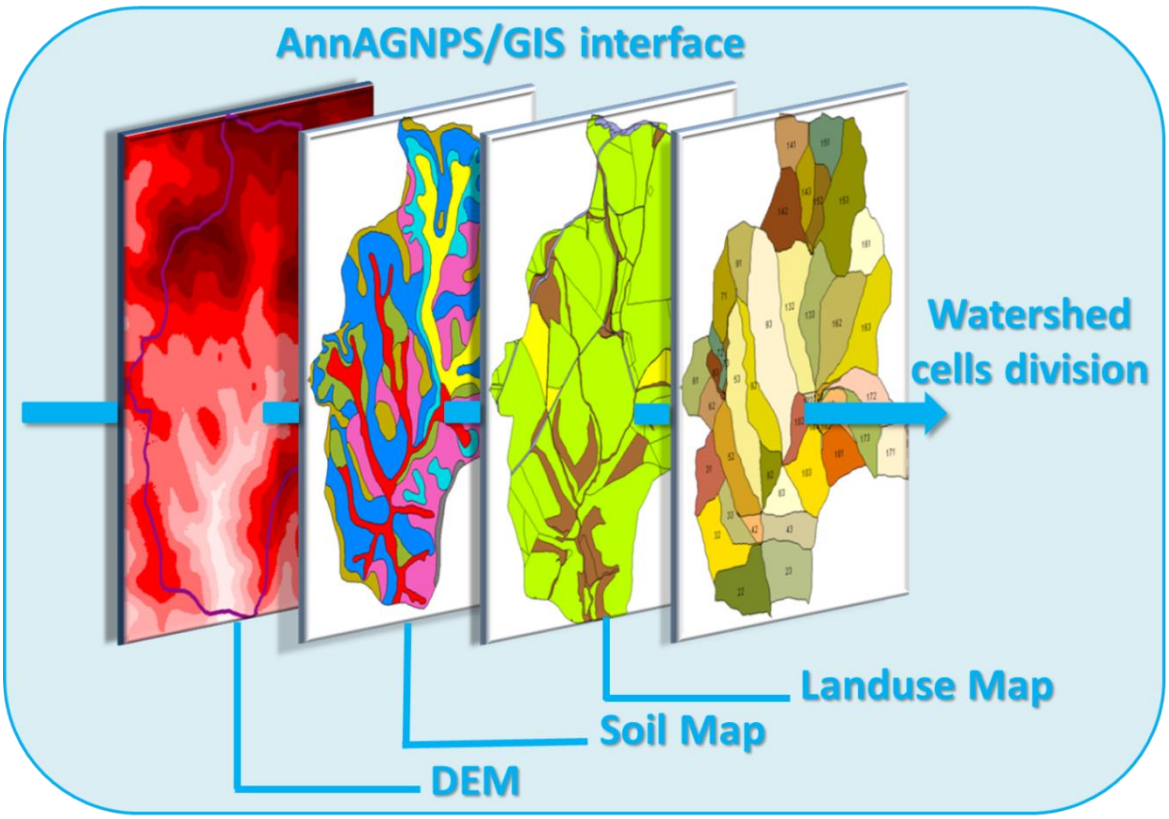

Figure 2. 7: GIS AnnAGNPS interface process for watershed cells division and soil and land-use assignation

After soil and land-use are assigned to the cells, the chemical and physical properties of the soils and the required land-use data, etc needed to run the model are introduced by the AnnAGNPS Input Editor.

2.4.3 AnnAGNPS Potential Ephemeral Gully Tool (APEGT) procedures

Recently AnnAGNPS developers have integrated into the existing AGNPS GIS interface a new GIS-based graphical interface tool to identify the potential ephemeral gully (PEGs) location on a watershed. The automated identification of PEG mouth is based on the Compound Topographic Index (CTI) (Thorne and Zevenbergen, 1990). Several studies have investigated the relationship between ephemeral gully initiation and land topography considered as one of the most important factors controlling EGs formation. Most of these indexes are based on runoff contributing to area and soil surface slope. Thorne (1986) used these parameters to calculate CTI (Eq. 2.38) for each grid cell to identify potential locations for ephemeral gullies based on land topography. The CTI is defined as follow:

$$CTI = A * S * PLANC \qquad (2.39)$$

Where:

A: upstream drainage area (ha);

S: local slope (m/ m);

PLANC: planform curvature (1/m).

To use the APEGT within AnnAGNPS/ArcView interface requires a DEM in raster grid format to identify and measure the slope and accumulated upstream area

draining in each raster grid through TOPAGNPS components. Then the planform curvature is computed with ArcView internal curvature function by using a moving 3×3 raster grid to determine the curvature of the terrain at individual raster grid cells.

The CTI values for each raster grid cell are obtained by multiplying upstream area, local slope, and planform curvature. After computing the CTI and eliminating negative CTI values, two new datasets are added to the project: a table document and a raster grid. CTI values are then graphically represented by categories of cumulative percentage values. Raster grid cells,whose CTI values are less than the 90% category, are not displayed (figure 2.8). The table document contains unique CTI values, the number of raster grid cells with that value, and the cumulative count and percent associated with each CTI value.

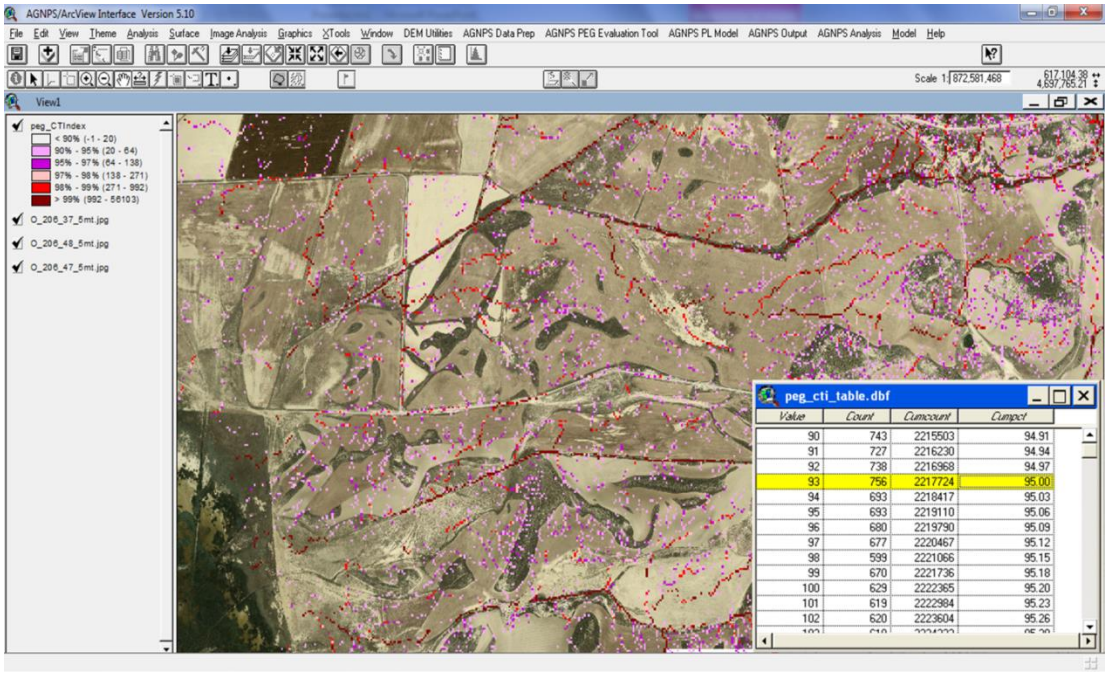

Figure 2. 8: Screen capture example of raster grid of CTI values and table summarizing CTI values generated using the AGNPS PEG Evaluation Tool used in the identification of PEG locations in Pittilas region.

2.4.4 Identification of PEGmouths through CTI

The APEGT permits the user to identify the PEG mouths location where headcuts begin to migrate upstream (Parker et al., 2010). The user can select the CTI threshold value to identify PEG mouths using either a percent value or a single CTI value.Utilization of the APEGT provides the ability to iteratively adjust (through a trial-and-error process) threshold values until a satisfactory CTI value is found that best represents the location of potential EGs within the watershed. This can be based on comparison of CTI values of locations with an active gully observed in the field.

Once the appropriate threshold has been selected for the study area, the process starts by identifying all the raster grid cells with CTI values above the user-provided threshold. The PEG mouths generated were represented graphically in the AGNPS–ArcView interface and classified into two groups: AnnAGNPS cell located and AnnAGNPS reach located. In addition, a table containing completed PEG dataset is generated, in which each PEG is defined by a single identifier. The topographic parameters required by AnnAGNPS model for EG erosion simulations are also incorporated (table 2.2).These features are then exported by the user for their

inclusion in theAnnAGNPS watershed input file. When the most appropriate threshold has been selected for the area of interest, procedures to manually add or remove PEG points can be performed.More information on CTI approach and AnnAGNPS/ ArcView interface processes is detailed in Parker et al, (2007)and Momm et al, (2012).

Table 2. 2. AnnAGNPS EG parameters generated with the AGNPS/PEG interface.

Parameters	Description
Ephemeral gully ID	Alphanumeric string identifying the ephemeral gully
Gully location	"T" for AnnAGNPS cell-located and "F" for AnnAGNPS reach located
Cell ID*	AnnAGNPS Cell ID whose gully's drainage area is wholly contained within this cell
Reach ID**	AnnAGNPS cell ID of the reach whose thalweg contains the gully mouth
Drainage area to mouth*	Total drainage area contributing to the mouth of the gully
Cell's drainage subcell*	Total drainage area of the cell before the reach receiving the flow from the mouth.
Local drainage area**	Total drainage area contributing to the mouth of the gully
Soil ID	Assigned soil ID found in the soil database
Gully slope	Land slope immediately upstream from the mouth
Management ID	Assigned management ID found in the management database
Headcut migration barrier	Sum of drainage areas of all upstream ephemeral gullies

* AnnAGNPS cell-located only.

**AnnAGNPS reach-located only.

Chapter 3: Evaluation of the AnnAGNPS model in the prediction of runoff and sediment yield at the Latxaga watershed

3.1 Introduction

Agricultural activities are some of the main factors causing soil and water degradation in agricultural areas. Excessive loads of nutrients (e.g. nitrate, phosphorus) and sediments from non-point source pollution and soil erosion recorded at the outlet of agricultural watersheds have been reported (Schaffner et al., 2011). Additionally, excessive amounts of sediment in runoff water cause degradation of drinking water quality, siltation of reservoirs and pollution of aquatic ecosystems. Soil erosion is a common phenomenon in Navarre's agricultural lands, where sheet and rill (Casalí et al., 2008, Casalí et al., 2009, Casalí et al., 2010), gully (Casalí et al., 1999, De Santisteban et al., 2006, Casali et al., 2015) and channel erosion (Casalí et al., 1999, Campo et al., 2007) are frequently observed (Donézar et al., 1990). For that reason, four experimental watersheds with contrasting land uses located in the region of Navarre, and maintained by the local government, have been monitored and studied since 1996 or 2001 onwards in order to assess the environmental impact of agrarian activities and to identify and implement environmentally sound land management practices (see Chapter 1).

An adequate management of agrarian land must contemplate the possibility of changing land use, either to search for improvements in the management of the affected zones or for adequacy to new socio-political policies. In fact, the existence of vegetation cover natural or cultivated- is frequently the main determinant of hydrological-erosive processes (García Ruiz and López Bermúdez, 2009). The type of land use and management is therefore a decisive factor when explaining these processes.

Usually, the main Spanish crop lands present important erosion problems when the slope increases, as the soils remain more or less unprotected during most of the year (García Ruiz and López Bermúdez, 2009). More concretely, cereal agriculture - especially on steep slopes - produces very high erosion rates (e.g., (Casalí et al., 2008); especially when alternated with fallow conditions. However when considering forest environments, runoff is usually reduced as a consequence of rain interception and high consumption of water by the trees (García Ruiz and López Bermúdez, 2009). This is why sediment loads at forest basins are relatively low and limited to reduced spaces. Pasture and even dense bushes can be as effective to reduce erosion rates as the forest. However, inadequate forest management can give place to elevated soil losses - even superior to those registered at cereal cultivated lands (Casalí et al., 2010).

The Mediterranean environmental characteristics - e.g., irregularity and intensity of precipitations, steep slopes, vulnerable soils - create adequate conditions for the occurrence of intense erosion processes, with consequent damage to the environment. It must be highlighted that the environmental impact associated with the erosion phenomenon is not limited to the reduction of the soil's productive capacity and transitability in affected terrain, but also includes remote effects caused by the deposition of the eroded material. Therefore, the economic losses caused by the clogging and/or pollution of lakes, rivers and reservoirs can be many times superior to those produced in the terrain.

Various studies worldwide have evaluated the ability of AnnAGNPS model (Bingner et al., 2012) to predict runoff and sediment loads under different climate conditions and land uses (Chapter 2). These studies have utilized watershed with areas

ranging from 0.1 to 130 km2 and for short time periods (24 months on average) except Das et al. (2008), who assessed the AnnAGNPS model for 120 months. However, few efforts have been made hitherto to evaluate AnnAGNPS under Mediterranean conditions (Licciardello et al., 2007, Taguas et al., 2009, Gastesi, 2014, Abdelwahab et al., 2016).

The purpose of this study is twofold, (i) to test the suitability of the AnnAGNPS model for simulating direct runoff and sediment loads in a small Mediterranean, grain-sown watershed for a long term time period (9 years) and (ii) to highlight the potential of the model as a management tool for agricultural land by creating fictitious agrarian scenarios in Navarre and evaluating their potential environmental effects.

3.2 Study area

3. 2.1 Location

The Latxaga watershed covers an area of 207 ha (UTM zone 30N coordinate limits, North: 4,740,385; South: 4,738,208; East: 628,834 and West: 627,241) and is located in the central eastern part of Navarre (Spain), between the municipalities of Lizoiain and Urrotz, 22 km from Pamplona (capital of Navarre) (Figure. 3.1). The watershed elevation is between 504 m to 639 m, with slopes from 7% to 30%. The watershed is drained by a 5.38 km stream characterized by dense riparian vegetation. The outlet is located at UTM coordinates North 4,738,254 and West: 627,886.

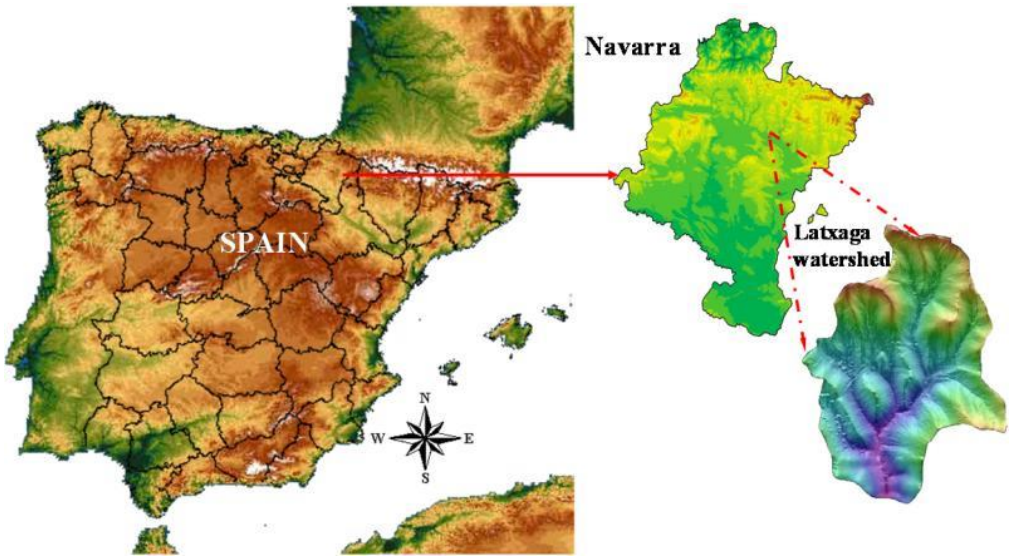

Figure 3. 1: Latxaga watershed location

Table 3. 1. Different studies where the AnnAGNPS model was evaluated

Authors	Location	Climate	Area (km^2)	Land use	Analyzed variables	Study Period (months)	Calibrated parameters	Time Scale of evaluation	Observations
(Yuan et al., 2001)	Mississippi Delta (The Deep Hollow lake watershed)	Humid subtropical	0.1	Cotton and soybeans	Runoff and sediments	36	None	Event and monthly	AnnAGNPS predicted adequately long-term monthly runoff and sediment yield (R^2 = 0.7). On an individual event basis, sediment prediction was less satisfactory (R^2= 0.5).
(Baginska et al., 2003)	90 km Northwest of Sydney Australia (Currency Creek watershed)	Temperate	2.5	Crop land and pasture	Runoff and nutrients (N, P)	21	CN (Curve number)	Event	AnnAGNPS simulated satisfactory flow events (E= 0.82)
(Shrestha et al., 2006)	Siwalik Hills of Nepal (Masrang Khola watershed)	Subtropical	1.3	Forest, maize, rice, bush forest and grazing land	Runoff and sediments	15	CN, Manning's *n*, values of sheet and concentrated flows	Event	AnnANGPS predicted runoff volume with acceptable accuracy (R^2= 0.93 for calibration and R^2= 0.91 validation) and sediment yield with moderate accuracy (R^2= 0.63 for calibration and R^2= 0.59 for validation)
(Licciardello et al., 2007)	East of Sicily Italy (Cannata watershed)	Mediterranean	1.3	Pasture and cropland	Runoff and sediments	84	CN, surface Long term random roughness and Manning's *n*	Event, monthly, yearly	AnnAGNPS showed satisfactory capability in simulating surface runoff on an event (R^2 = 0.72, E= 0.70) ,

									monthly (R^2 = 0.78, E= 0.77) and annual (R^2 = 0.85, E= 0.84) basis. For sediment yield high values of R^2 = 0.84, E= 0.79 and model efficiency were found for 24 events
(Polyakov et al., 2007)	Kauai Island Hawaii (Hanalei River basin)	Tropical	48	Shrub and evergreen forest	Runoff and sediments	24	CN	Daily and monthly	Monthly runoff volumes predicted by AnnAGNPS compared well with measured data (R^2 = 0.90). Prediction of daily runoff was less accurate (R^2 = 0.55). Predicted and observed sediment yield on a daily basis was poorly correlated (R^2 = 0.5).
(Sarangi et al., 2007)	British West Indies (St. Lucia Watershed)	Tropical	0.12	Cropland	Runoff and sediment	19	CN, root mass and crop residue	Event	The model estimated runoff reasonably well for days with high precipitation ($-0.5<C_{P'A}<14.8$)* and less accurate estimations for low precipitation events.
(Shamshad et al., 2008)	Malaysia (River Kuala Tasik Watershed)	Tropical	125	Cropland and forest	Runoff, sediment and nutrients (N, P)	25	CN, root mass and canopy cover	Event	Runoff was predicted "well" (R^2 = 0.9 and E= 0.70), sediment prediction was "reasonable" (R^2 = 0.53 and E= 0.49).

(Das et al., 2008)	Canada – Ontario (Canagagigue Creek)	Humid continental	53	Cropland	Runoff and sediment	120	None	Event, monthly and yearly	AnnAGNPS performed very well in predicting runoff during calibration (E = 0.79 and validation E= 0.69). Sediment yield was overestimated by 28%, with E= 0.53 and 0.35 for calibration and validation, respectively.
(Yuan et al., 2008)	Mississippi Delta (Beasley Lake watershed)	Humid subtropical	0.07	Cotton, soybean and corn	Runoff and sediment	60	None	Event	The model demonstrated satisfactory capability in simulating runoff (E= 0.89) and sediment yield (E= 0.54) at an event scale.
(Parajuli et al., 2009)	South central Kansas (Red Rock creek and Goose creek watersheds)	Humid subtropical	136	Cropland	Runoff and sediment and total phosphorus	45	CN, RUSLE C factor	Monthly	The model simulated surface runoff with fair to very good model efficiency (R^2 = 0.8 and E= 0.69) and sediment yield (R^2 = 0.83 and E= 0.60)
(Taguas et al., 2009)	Cadiz – Spain (Setenil watershed)	Mediterranean	0.07	Olive orchard	Runoff and sediment	24	CN, RUSLE C factor	Event, monthly	The results confirmed the applicability of AnnAGNPS to predict runoff E= 0.66 , E= 0.95 and sediment yield E=0.61, E= 0.61 respectively at event and monthly scales
(Abdelwahab et al., 2014)	Apulia region (Southern Italy -	Mediterranean	506.2	winter wheat,	Runoff and sediment	48	CN and Manning's n	Event	Obtained model performances were:

	Carapelle watershed)			olive-groves rangeland, forest, urban, fallow and pasture					E=0.76, E= 0.67 in calibration, and E=0.81 and E=0.86 in validation, for runoff and sediment loads.
(Gastesi, 2014)	Navarre Spain (La Tejeria watershed)	Mediterranean	1,6	winter wheat	Runoff and sediment	108	CN, RUSLE C factor	Event, monthly, annual	Monthly performances were: E=0.82 and E=0.66 for runoff calibration and validation, respectively. Unsatisfactory results were obtained for sediment yield predictions

* $C_{P'A}$: Coefficient of prediction

3.2.2 Soil

Geologically, the Latxaga watershed area is underlined by clay marls and Pamplona grey marls. The soil map (Figure 3.2) and detailed soil characteristics were provided by the Department of Rural Development, Environment and Local Administration of the Government of Navarre.

The prevailing soil class is Paralitic Xerorthent covering 43% of the watershed, and located on eroded hill slopes. These soils are shallow (less than 0.5m deep) and the upper horizon is silty-clay-loam. Fluventic Haploxerept soils cover 36% of the watershed area, and are located on swales and hill slopes where eroded soil accumulates. These soils are deeper (over 1m deep) and the upper horizon is also silty-clay-loam. Xerorthent Typhic cover approximately 21% of the Latxaga surface. These soils are deep (over 1 m). The texture of its upper horizon is loam-clay-silty.

The estimated average soil bulk density and porosity of the top horizon are approximately 1.26 $Mg.m^{-3}$ and 0.52 $Mg.m^{-3}$, respectively (Rawls and Brakensiek, 1989). The soil erodibility factor of the Universal Soil Loss Equation (Wischmeier and Smith, 1978) KUSLE for the top horizon is approximately 0.48 (t. m^2 h) / (ha hJ cm), and the area-weighted average soil depth is 1.03m. The estimated watershed hydraulic conductivity at saturation (Rawls and Brakensiek, 1989) is approximately 2.01mm h^{-1}(Casalí et al., 2008).

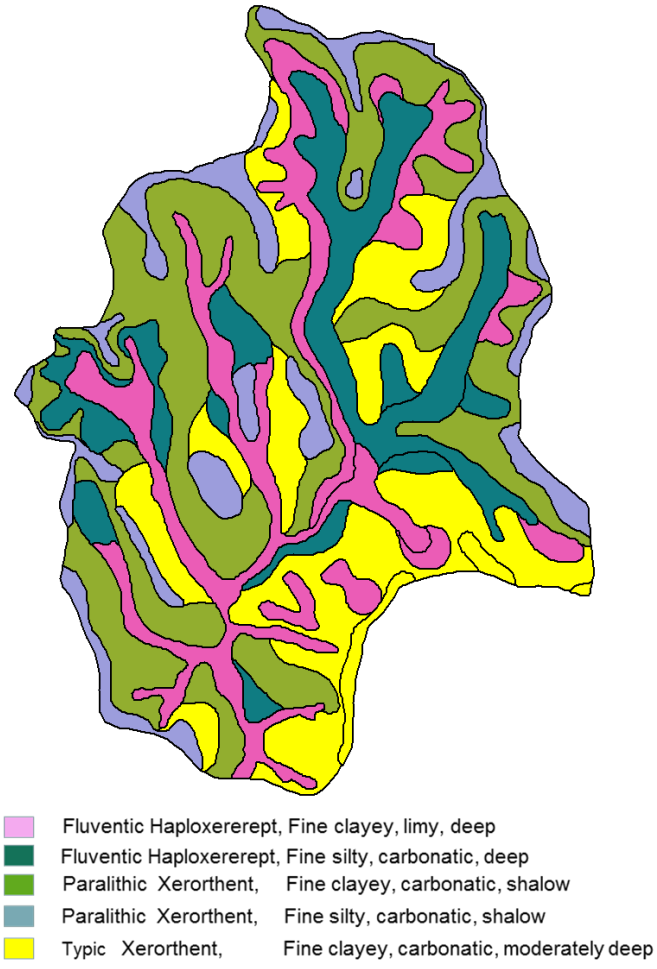

Figure 3. 2: Latxaga soil map

3.2.3 Climate

The climate at the Latxaga watershed is humid submediterranean, with an average annual precipitation of 835mm, distributed over 95–100 days of rainfall, and an average annual temperature of 12.8ºC (Gobierno de Navarra, 2001). Watershed climate data was provided by a *Beortegi GN* automatic meteorological station located within the watershed, at 580m altitude at UTM coordinates North: 4739541 and West: 627997. The station was installed in 1998 and is managed by Navarre government, providing daily and 10-min meteorological records.

The maximum precipitation occurs in Autumn, and November presents the highest average rainfall (more than 90 mm). March, April, October and December are also wet, with exceeding 80 mm .month^{-1}. The driest months are July and August, with less than 40 mm/month. The potential evapotranspiration was estimated by the Penman-Monteith method (Allen et al., 1998). The mean annual evapotranspiration is approximately 1010 mm, with the most important records during Summer. Comparing rainfall amounts with potential evapotranspiration, the months from May to September presented negative water balances (Figure 3.3-A).

Regarding temperatures, the coldest period of the year corresponds to the Winter months, with average temperature between 4.5 and 5.5°C. The hottest months are July and August, which reach 21ºC average temperature (Figure 3.3-B).

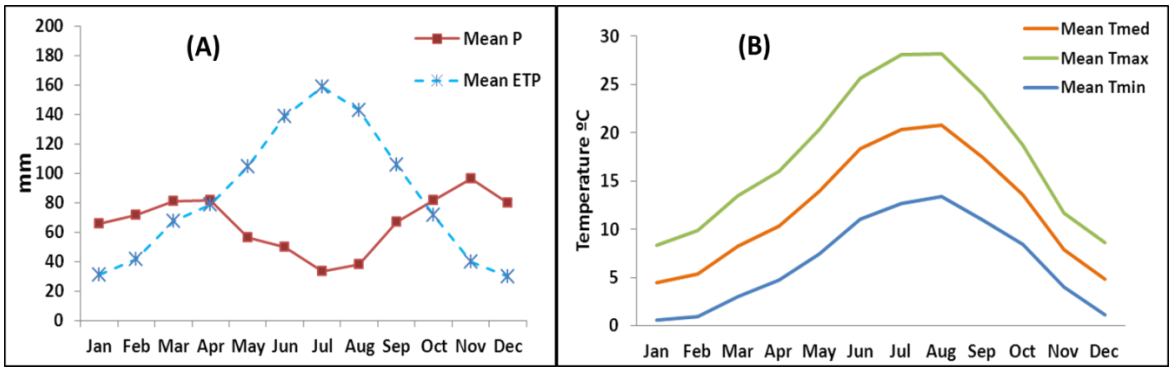

Figure 3. 3: Monthly water balance (rainfall vs. potential evapotranspiration) (A) and monthly temperature averages at the Latxaga watershed (B)

3.2.4 Land use

Most of the watershed (approximately 90% of the total area) is occupied by croplands, while the remaining area is devoted to natural bushes and the main stream network. The watershed is crossed by a 2 km road that reaches the Beortegui village, which is also within the watershed and covers approximately 0.7 ha (Figure 3.4).

The main crop at the watershed is cereal (wheat and barley), with average yields of 3500 - 4000 kg.ha^{-1}. However some farmers cultivate legumes, sunflower or leave the land fallow (three-year rotation).

Conventional tillage is the main practice of farmers in this area. For cereal crops, firstly the farmers execute primary tillage by moldboard at the end of summer. Tillage depth generally exceeds 25 cm and it is frequently parallel to the contour lines. In this operation, the crop residue (from harvest) is mixed with soil. Harrow is then used for land smoothing, followed by crop seeding (secondary tillage) using combined seeding machine. Tillage depth can reach up to 5 cm. During this operation, farmers apply the first fertilization, mixing cereal seed and phosphate manure (90-100 kg .ha^{-1} and 200 kg, .ha^{-1} respectively). During Winter and Spring, crops are fertilized twice with urea:

210 kg .ha^{-1} and 250 kg .ha^{-1}, respectively. Weeding occurs in February. Finally, harvesting takes place in the end of June or beginning of July. In the following plots, the primary tillage is performed in the end of Spring (May-June).

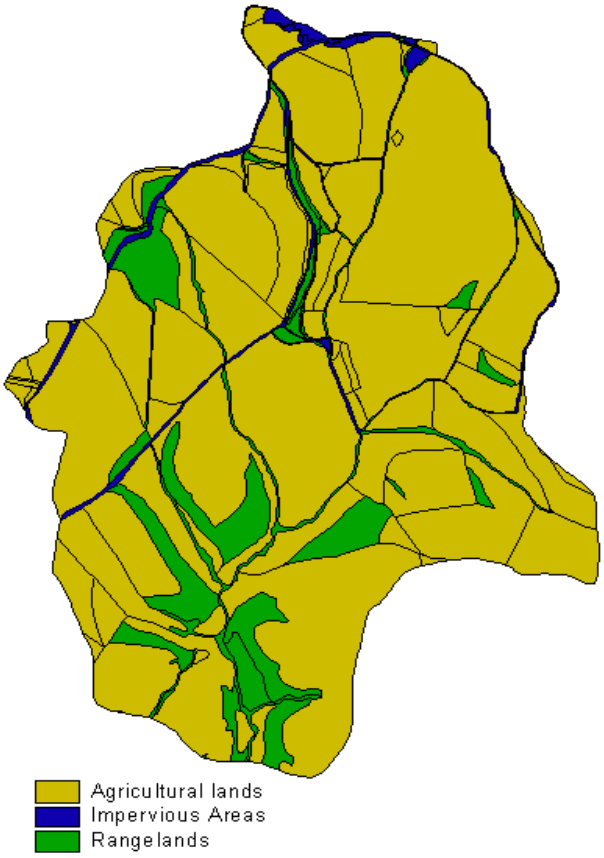

Figure 3. 4: Latxaga land use map

3.2.5 Watershed instrumentation

3.2.5.1 Gauging station

Since 1993, the watershed has been monitored and data collected on discharge, sediment yield and solutes within the watershed, where a meteorological station is also present (Donézar and Del Valle de Lersundi, J., 2001).

For the measurement of discharge, the watershed outlet was equipped with a triangular profile flat-V Crump type"weir, according to the model developed by the Hydraulics Research Station of Wallingford (United Kingdom) (Bos, 1989).

The first part of the structure is triangular, from 0 to 0.24m, and rectangular from 0.24 m to 1.2 m (Figure 3.5-A). This hydraulic structure was selected, among other reasons, because its design permitted the sediment to pass the control section. Discharge (Q, $L \cdot s^{-1}$) was calculated from the water level (h, m) using the following rating curves:

$$Q = 16.866\ h^3 + 4.0544\ h^2 - 0.0925\ h + 0.0005 \quad \text{for} \quad 0<h<0.24\ \text{m} \qquad \text{(Eq 3.1)}$$

$$Q = 0.1282\ h^3 + 8.2083\ h^2 + 1.6091\ h - 0.4407 \quad \text{for} \quad 0.24<h<1.2\ \text{m} \qquad \text{(Eq 3.2)}$$

Water discharge was also directly measured using a propeller-type current meter and triangular and rectangular sharp-crested weirs (Bos, 1989), for verification purposes. For the determination of water quality, water samples were collected every 6

hours from a hemispheric hole (0.66m diameter) made in the downstream face of the triangular profile flat-V weir. An automatic programmable sampler was used, consisting of 54 (500 ml) bottles. The four samples collected each day were mixed before analysis to provide a representative daily average sample for the determination of sediment and nutrient concentrations, according to Isidoro et al. (2003). A turbidity meter was installed to measure water turbidity every 10 minutes. Records on water level, accumulated discharge and turbidity, on a daily and 10-min basis are available at the Government web site (http://cuencasagrarias.navarra.es/datos/).

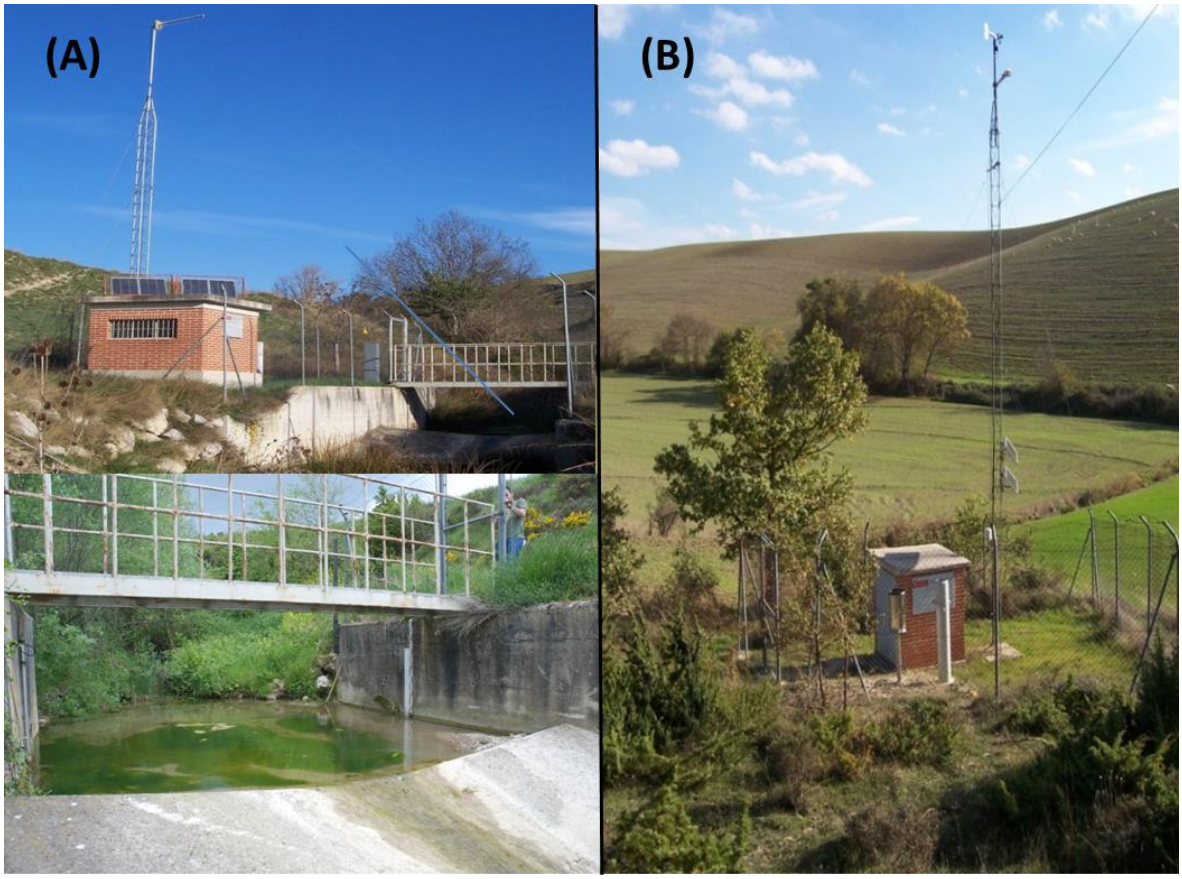

Figure 3. 5: Photos of the Latxaga gauging station (A) and automatic meteorological station (B)

3.2.5.2 Meteorological station

An automatic meteorological station was installed at the watershed, called the Beortegi station (Figure 3.5-B), located at UTM zone 30N coordinates North: 4,739,750 and West: 628,103, at 580 m height. The station was installed in 1998 and is supervised by the local Government. The meteorological station presents several sensors to measure different climate parameters on a daily and 10-min basis. These meteorological data can be consulted at the Government web site (http://meteo.navarra.es/estaciones/mapadeestaciones.cfm#).

The Beortegui station instrumentation includes: wind monitor to measure wind speed and direction at 2 m height; relative humidity sensor; temperature sensor; solar radiation sensor; soil temperature sensor at 20, 40 and 80 cm deep; tipping bucket rain gauge with heating system (to melt any ice and snow that is caught in its funnel). The meteorological station is equipped with a datalogger, modem and phone line, which enables electronic registry and data transference. The energy consumed by these devices is provided by solar panels and batteries.

3.2.6 Hydrological and erosive behavior of the Latxaga watershed

3.2.6.1 Rainfall

Hydrological and erosive behaviors are strongly influenced by climatic conditions, geomorphologic parameters and soil characteristics and conditions within the watersheds. In the Latxaga watershed, rainfall pattern is typical for humid Mediterranean climate. The inter-annual variability of the precipitation is quite high with maximum variability observed in winter, and minimum in Spring (Casalí et al., 2008) (figure 3.6). From 1999 to 2011, the accumulated annual rainfall ranged from 548 mm in 2011to 994 mm in 2008 (maximum), with an average of 803 mm .year^{-1}. At a seasonal level, Autumn was the wettest period, whereas Summer was the driest season, accounting for only 15% of annual precipitation. Autumn, Winter and Spring presented 32%, 26% and 27% of precipitation, respectively (Figure 3.6). The wettest and the driest months of the year were November and July, respectively.

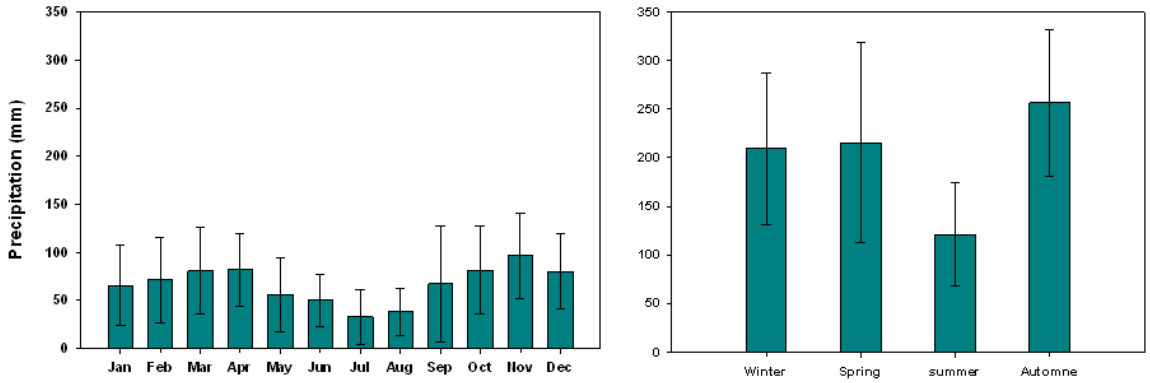

Figure 3. 6: Monthly and seasonal rainfall average in the Latxaga Watershed

Casali et al. (2008) analyzed more than 1100 rainfall events at the Latxaga watershed to characterize rainfall event intensity and erosivity, through the determination of the rainfall erosivity index EI_{30}, in accordance with Brown and Foster (1987). EI30 is a compound index of kinetic energy of rain "E", and its maximum intensity "I_{30}". Table 3.2 shows rainfall characteristics for selected events within the Latxaga watershed.

Table 3. 2. Rainfall characteristics for categorized precipitation events at the Latxaga watershed (Source: (Casalí et al., 2008)

	Rainfall event category (mm)						
Rainfall variables	0-10	10-20	20-30	30-40	40-50	50-60	>60
Number of events	928	138	40	19	7	3	5
Average rainfall depth (mm)	2.5	14.4	24.5	35.2	43.5	55.5	75.3
Average storm duration	7.1	20.3	26.6	36.3	30.8	43.9	58.8
Average rainfall erosivity (EI_{30})	108	1837	2646	6847	4702	36,675	32,154

Table 3.2 shows that that more than 80% of the registered rain events along the year presented very low erosivity with EI30 < 100 Jmmm^{-2} h^{-1}. Few rain events presented very high erosivity, which occurred mainly during Autumn and Spring.

3.2.6.2 Runoff

Regarding runoff discharges within the Latxaga watershed, a different pattern was obtained in comparison to precipitation. High inter-annual and annual variability of

runoff discharges were observed. Between 2003 and 2011, the accumulated annual discharge ranged between 123 and 520 mm for 2011 and 2008 respectively, with an average of 256 mm.

Like precipitation, runoff depth presented a seasonal pattern. Most of the runoff, 59.5%, is recorded in Winter, especially in January and February, although winter did not present the highest precipitation (26%). The runoff coefficient was calculated as described by Chow et al. (1988). For Winter, it was approximately 0.73. However, during Spring, when total precipitation amounts are almost equal to Winter, there was less runoff discharge recorded by the gauging station, representing only 19.8% of total runoff and a runoff coefficient of 0.23%. Despite Autumn being the wettest season regarding precipitation (32% of annual precipitation), the runoff discharge represented only 20.3 % of annual runoff with runoff coefficient 0.20. The highest runoff occurred in November. Finally, Summer presented the smallest runoff (0.4% of annual runoff), despite the fact that, during this season precipitation was 15% of total annual rainfall (Figure 3.7).

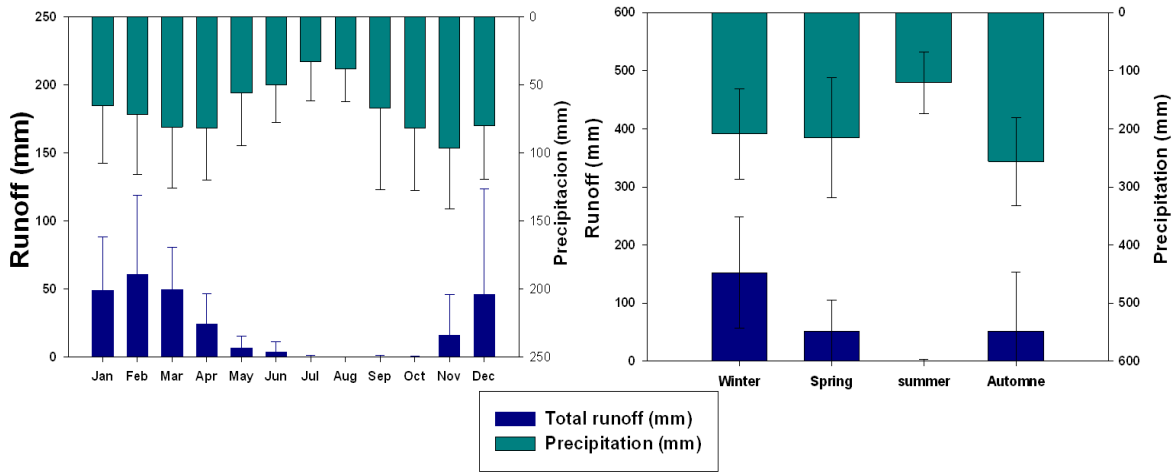

Figure 3. 7: Monthly (left) and seasonal (right) average runoff and rainfall at Latxaga

During Summer, precipitations are very low and ETP is very high, thus soils are dry. In Autumn and early Winter, the precipitation amounts are important, sometimes increasing soil moisture until saturation. Consequently, runoff starts even with low rainfall amounts. Despite the significant amounts of rainfall in Autumn, runoff was low due to the previous soil conditions. During Spring, although precipitation quantities are similar to those recorded in Winter, runoff is lower. This occurs due to the dense vegetation cover ,which increases canopy interception and evapotranspiration - this leads, to some extent, to an important decrease in runoff (Casalí et al., 2008). Similarly to runoff, sediment yield presented inter-annual variability and seasonal patterns. Figure 3. 8 shows the accumulative sediment yield annually recorded in the gauging station, which ranged from 53 kg ha^{-1} $year^{-1}$ (minimum, in 2003) to 741.6 kg ha^{-1} $year^{-1}$ (maximum sediment yield, recorded in 2007), with an average of 330 kg ha^{-1} $year^{-1}$ for the period 2003-2011.

Sediment yield in the Latxaga watershed presented a typical seasonal behavior. Most of sediment yield (64.8% of the annual sediment load) occurred during Winter. 30% of the annual sediment yield was produced in Spring and 15.8% during Autumn. Summer presented the lowest quantities, approximately 0.35% of the sediment yield recorded by the gauging station.

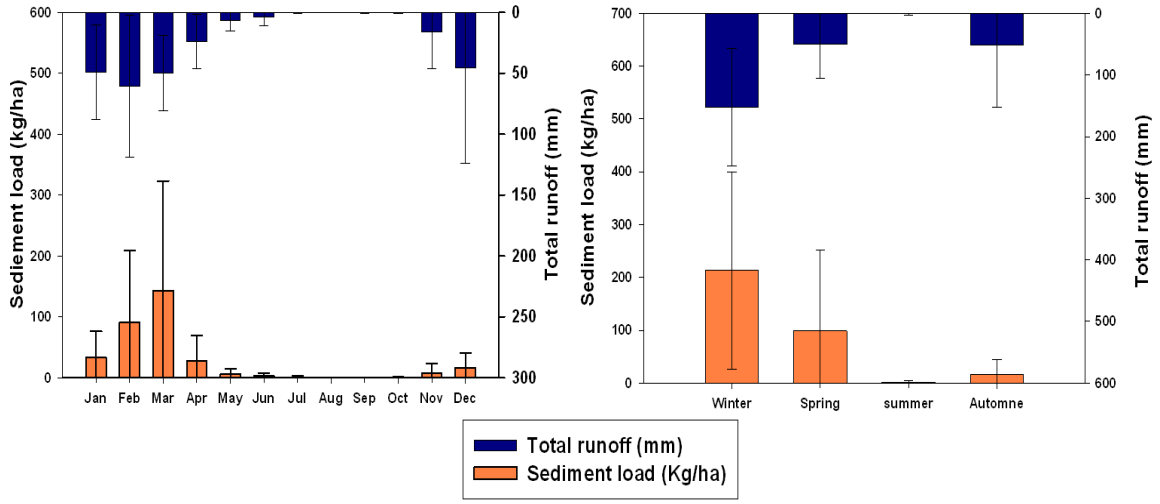

Figure 3. 8: Monthly (left) and seasonal (right) average sediment yield and runoff at the Latxaga watershed

Sediment yield occurred mainly during Winter and the beginning of Spring, when most rainfall events presented low erosivity, but highest runoff amounts (Casalí et al., 2008). At the beginning of Winter, crops are still in the first growing stage, and soil can be considered poorly protected, with high moisture content as previously explained. These conditions lead to large runoff rates flowing over unprotected and then vulnerable soils, in addition to the raindrop erosive effect on the bare soil surface. During Spring, sediment yield represented half of amount recorded in Winter. This can be explained by the effect of canopy cover in this period, which is very important, especially in April and May. Vegetation intercepts a significant part of rain. In this period, most of soil erosion results from overland flow (Morgan, 1995). Sediment load was recorded only during November and the beginning of December. In September and October, it was almost nonexistent. This is explained by the small runoff amounts during these months, which are not sufficient to transport detached sediments to the outlet. In addition, the stream network within the Latxaga watershed is characterized by very dense riparian vegetation during the entire year, promoting sedimentation. These sediments can be transported more easily during the end of Autumn and beginning of Winter, when runoff amounts are important although precipitation events are not significant. Finally, during Summer the sediment load is almost zero. 85% of sediment loads occurred in the Summer of 2008, especially in July after two important events of 22mm and 18.4mm (June, 26 and July, 1, respectively).

3.3 Procedure for AnnAGNPS model evaluation

3.3.1 Data acquisition

Input data required by AnnAGNPS model can be classified into two types. The first type is daily climate records. The second type includes watershed physical characteristics (i.e., morphologic parameters, soil data, crops data, agricultural practice, etc.). The most important input data required is detailed in Table 3.3. Output parameters are available on a daily, monthly and annual basis.

Table 3. 3. Most important input data used in AnnAGNPS model simulations

CLIMATE DATA	WATERSHED DATA		
Climate station description	**Soil Data**	**Crop data**	**Management Field**
Station Latitude	Hydrologic Soil Group	Crop ID	Field Land use Type
Station Longitude	RUSLE K factor	Units Harvested	1st Year of Rotation
Station Elevation	Albedo	Residue Weight Ratio	Random Roughness
Global Storm Type ID	Depth to impervious layer	Crop Residue	**Operation Field**
	Soil Name	Yield Unit Weight	Residue Cover Remaining
Daily weather parameters	Soil Texture	Harvest C-N Ratio	Area Disturbed
2 Yr 24 Hr Precipitation	Layer Depth	Harvest Water	Initial Random Roughness
Daily Max Temperature	Bulk Density	Growth Time	Final Random Roughness
Daily Min Temperature	Clay Ratio	Growth N Uptake	Surface Residue
Daily Precipitation	Silt Ratio	Growth P Uptake	**Fertilizer Application**
Daily Dew Point Temperature	Sand Ratio	Root Mass	Fertilizer Name ID
Daily Sky Cover	Rock Ratio	Canopy Cover	Fertilizer Rate
Daily Wind Speed	Very Fine Sand Ratio	Rain Fall Height	Fertilizer Depth
Daily Wind Direction	CaCO3 content	**Non-Crop Land uses**	Fertilizer Nitrate
Daily Solar Radiation at Ground Level	Saturated Conductivity	Annual Root Mass	Fertilizer Inorganic N
Potential ET	Field Capacity	Annual Cover Ratio	Fertilizer Inorganic
Actual ET	Wilting Point	Surface Residue Cover	**Pesticide Application**
RUSLE rainfall factor R	pH	**Management schedule**	Pesticide Rate
Energy Intensity distribution (EI)	Organic Matter Ratio	Event Date	Pesticide Depth
	Inorganic N Ratio	Event New Crop ID	Pesticide Foliage Fraction
	Organic P Ratio	Curve Number ID	Pesticide Soil Fraction
	Inorganic P Ratio	Event Fertilizer Application	Pesticide Solubility
	Soil Structure code	Event Fertilizer Application	Pesticide Soil Half-life

3.3.1.1 Climate data

The AnnAGNPS model requires a climate file describing daily climate data. The time span of data acquisition was nine years, from January 2003 to the end of 2011. Most of climate data have been recorded by the Beortegi climate station (UTM zone 30N coordinates, North: 4,739,750; West: 628,103; at 580 m height). Additional inputs are calculated separately, including dew point temperature, maximum 24-hour precipitation with a two year return period, and global storm type.

The dew point temperature (T_d) was calculated from the relative humidity and the mean air temperature using the inverse of Tetens's equation (Chow et al., 1988), optimised for dew points in the range -35 to 50 °C :

$$T_d = \frac{C_3 \cdot \ln(\frac{e}{C_1})}{C_2 - \ln(\frac{e}{C_1})} \quad (3.3)$$

$$e = \frac{e_s \cdot HR}{100} \quad (3.4)$$

$$e_s = C_1 \cdot exp^{(\frac{T \cdot C_2}{C_3 + T})} \quad (3.5)$$

e: is the the saturation vapour pressure (kPa), e_s is the vapour pressure (kPa), RH refers to the relative humidity (%), T is the air temperature (°C), and constants C_1, C_2, and C_3 are, respectively, 0.61078, 17.558, and 241.88.

Due to the lack of sufficiently long precipitation records from the Beortegi station, the maximum 24-hour precipitation with a two-year return period was estimated as the average value of other two stations (Pamplona-Observatorio and Ustés stations), which are situated roughly under the same climate type (humid Sub-Mediterranean). Thus, the maximum 24 hour precipitation with a two year return period value was 54.7 mm (Ministerio de Agricultura Pesca y Alimentación, 1986).

The global storm type was determined by comparing the rainfall distribution of Beortegi to the rainfall distribution of USA, as included in AnnAGNPS. The USA region that most closely resembled the local annual rainfall distribution pattern corresponded to the West Coast, for Seattle (Washington) and San Francisco (California). The global storm type selected was "Ia".

3.3.1.2 Topography data

A Digital Elevation Model (DEM) (5m x 5m) of the watershed was acquired from the Department of Rural Development, Environment and Local Administration of the Government of Navarre. DEM was used to obtain the necessary input data for running the TopAGNPS program. More precisely, DEM was used to (i) identify and measure topographic features, (ii) define surface drainage channels, (iii) subdivide watersheds in cells along drainage divides and (iv) calculate representative cell parameters, including cell area, slope and length. The size of the cells depended on the values of the critical source area (CSA) and minimum source channel length (MSCL). CSA is defined as the minimum upstream drainage area above which a source channel is initiated and maintained. MSCL is the minimum acceptable length of the cell swale for the source channel to exist. Different combinations of CSA/MSCL values were tested until obtaining a realistic representation of the main drainage system and of the land use of the Laxtaga watershed. Visual comparisons between a real land use map and the watershed division were made by using the TopAGNPS program. Finally, values of 4 ha and 100 m were defined for CSA and MSCL, respectively. These values led to a division of the watershed into 43 cells and 17 reaches (Figure 3.9).

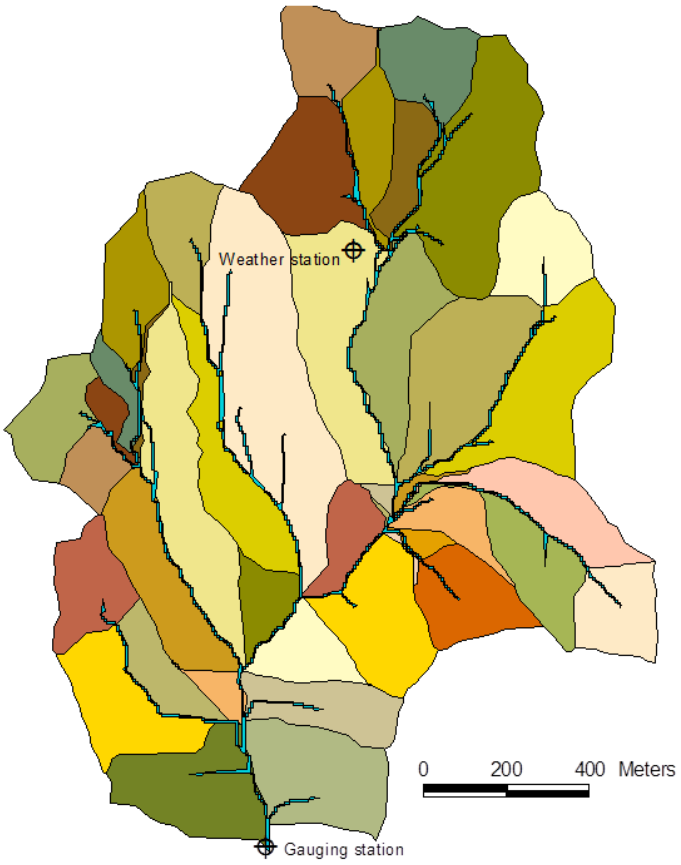

Figure 3. 9: Latxaga watershed with subwatershed (cells) division and stream channels

3.3.1.3. Soil data

For each soil type, the model requires specific data on all the different soil layers up to the impervious layer (i.e., for the entire solum). However, for the sake of simplicity, only the dataset regarding top soils is shown (Table 3.4), although the model was also provided with similar information on the different soil sublayers.

Soil maps (Figure 3.2) and physical and chemical soil characteristics contents of clay, silt, sand, nitrogen, phosphorous, potassium, organic matter and calcium carbonate were obtained from the Department of Rural Development, Environment and Local Administration of the Government of Navarre. The soil erodibility factor (K) was determined following Wischmeier and Smith (1978) (Eq 3.6, table 3.4). The wilting point, field capacity, saturated hydraulic conductivity and bulk density of the different soil layers were computed by the Soil Water Characteristics Hydraulic Properties Calculator, developed by USDA-ARS and Washington State University (Saxton and Rawls, 2006).

$$K = [2.1.10^{-4}(12 - OM)M^{1.14} + 2.25(s - 2) + 2.5\,(p - 3)]/100 \qquad (3.6)$$

K is the soil erodibility factor (t ha h ha^{-1} MJ^{-1} mm^{-1}), M is the particle size parameter = [(%silt + % Very fine sand) (100 - %clay)], OM refers to organic matter %, s is the soil structure code (very fine granular = 1; fine granular = 2; medium or coarse granular = 3; blocky, platy or massive = 4), and p refers to the profile permeability class (rapid = 1; moderate to rapid = 2; moderate = 3; slow to moderate = 4; slow = 5 and very slow = 6).

Table 3. 4. Classification of the main soils at the Laxtaga watershed as well as information required by AnnAGNPS for each soil layer. Only data of the upper horizons (10-20 cm depth) are shown

Classification (USDA SOIL Taxonomy, 1998)	Geomorphology	Upper horizon texture (USDA)	Sand %	Silt %	Clay %	Organic Matter %	*Wilting Point % Vol	**Field Capacity % Vol	Saturation % Vol	Sat hydraulic conductivity $mm.hr^{-1}$	Bulk Density g/cm^3	K-factor (t ha h ha^{-1} MJ^{-1} mm^{-1})	Hydrologic soil Group
FLUVENTIC XEROCHREPT	Swales	Loam-clay-silty	16.8	47.2	36.0	1.9	22.0	34.7	48.9	3.8	1.35	0.035	C
FLUVENTIC XEROCHREPT	Accumulation hilloslopes	Loam-clay-silty	20.7	42.0	37.2	1.8	22.6	37.4	48.4	3.4	1.37	0.033	C
FLUVENTIC XEROCHREPT	Swales	Loam-silty	24.8	46.8	28.4	1.8	17.7	33.5	46.6	6.1	1.42	0.038	B
FLUVENTIC XEROCHREPT	Accumulation hilloslopes	Loam-clay-silty	23.4	41.3	35.3	1.4	21.4	36.2	47.1	3.4	1.40	0.034	C
PARALITHIC XERORTHENT	Erosion hilloslopes	Loam-clay-silty	22.9	42.6	34.4	1.3	20.8	35.8	46.7	3.4	1.41	0.036	C
PARALITHIC XERORTHENT	Erosion hilloslopes	Loam-clay-silty	19.3	46.6	34.0	1.1	20.7	36.1	46.7	3.2	1.41	0.037	C
TYPIC XERORTHENT	Erosion hilloslopes	Loam-clay-silty	22.7	42.9	34.3	1.7	20.9	36	47.5	3.9	1.39	0.038	C
TYPIC XERORTHENT	Erosion hilloslopes (gentele)	Loam-clay-silty	22.6	42.3	35.1	1.8	21.5	36.4	47.8	3.8	1.38	0.036	C

*Wilting Point: water content at 1500 kPa.
**Field Capacity: water content at 33 kPa.

3.3.1.4 Land use data

Most of the watershed (more than 90% of the total area) is occupied by cereals (wheat and barley), while the remaining area is devoted to legumes (*Viciafaba* and *Pisumsativum*), sunflower, and, finally, a minimum part of the land lies fallow. It should be noted that plots given over to the minor uses aforementioned may change from year to year, without following a strict crop rotation. Information on the management schedule (Table 3.5) was obtained by interviewing local farmers.

A land use map containing plot delimitations was provided by the Department of Agriculture, Livestock and Food of the Government of Navarre (figure 3.4). Although in figure 3.4 the different crops (and fallow land) are merged into a single class "agricultural lands", these were distinguished and taken into account separately when running the model.

The Curve Number values proposed by the SCS (1986) were initially assigned to each land use (Table 3.6). The CN for bare soil was used for crop land after tillage, the CN for small grain and row crop were used, respectively, for cereal (wheat and barley) and legumes, when the crops were growing. The CN for fallow land with crop residue cover was used after grain harvesting, while crop residues remained on the soil.

3.3.2 Hydrology and sediment load data

The watershed outlet was equipped with a hydrology station that contained a water level sensor model 6531 (UNIDATA, Australia, Willetton), which measured total discharge calculated from water level. An automatic sampler ISCO 6712 (Teledyne Isco, Lincoln, Nebraska, USA) collected samples every 6 hours to determine sediment yield and water quality. Water samples (sediment concentration and dissolved nitrate and phosphate, sulphate, carbonate, potassium, calcium, magnesium and sodium) were analyzed following the standard methods for water quality parameters proposed by the Department of Rural Development and Environment and Local Administration of the Government of Navarre. Chemical analysis was performed using UV-Visible spectrometry and liquid chromatography coupled with a conductivity detector. The four samples collected each day were mixed before analysis to provide a representative daily average sample, for determination of sediment and nutrient concentrations according to Isidoro et al. (2003). The base flow was previously separated from measured runoff using digital filtering of hydrographs as proposed by Eckhardt (2005), for posterior comparison between predicted and measured runoffs. Following the same criteria and procedure described by Gastesi (2014) the digital filter was applied to the measured total runoff within the Latxaga watershed. The average annual base flow rate was 70% (Figure 3.10). Gastesi (2014) found the average annual base flow rate to be 65% at the La Tejeria watershed. Arnold et al. (1995) compared results of several studies that used digital filtering for automated base flow separation at an Eastern USA watershed, finding that the ratio between base flow and total runoff ranged from 32% to 72%.

Table 3. 5. Schedule of annual cultivation and agricultural practices usually followed by farmers at the Latxaga watershed

Land use	Date	Operation	Observation
Wheat and barley	September, 15	Tillage	Moldboard (25 cm)
	September, 20	Smoothing	Harrow
	October, 10	Fertilization	Phosphate (200 kg . ha^{-1})
	October, 15	Seeding	Combined seeding machine (90-100 kg.ha^{-1})
	January, 15	Fertilization	Urea 210 kg. ha^{-1}
	February, 15	Weeding	Mesosulfuron-methyl *Atlantis*® (400g.ha^{-1})
	March, 15	Fertilization	Urea 250 kg . ha^{-1}
	July, 1	Grain harvesting	4500-5000 kg . ha^{-1}
	July, 2	Straw packaging	
Bean (*Viciafaba)*	September, 15	Tillage	Moldboard (25 cm)
	September, 20	Smoothing	Harrow
	September, 21	Seeding	Combined Seeding machine (220 kg . ha^{-1})
	February, 15	Weeding	Fluazifop-p-butil *Fosilade*® (1L. ha^{-1})
	July, 1	Grain harvesting	2000-2500 kg . ha^{-1}
Pea (*Pisumsativum)*	September, 15	Tillage	Moldboard (25 cm)
	September, 20	Smoothing	Harrow
	December, 1	Seeding	Combined seeding machine 220 kg.ha^{-1}
	December, 3	Weeding	Imazethapyr, ammonium salt *Poursuit*® (1.5 L . ha^{-1})
	July, 1	Grain harvesting	2000 kg.ha^{-1}
Sunflower	September, 20	Tillage	Moldboard (25 cm)
	March, 15	Smoothing	Harrow
	May, 1	Seeding	Precision seeder (300 g . ha^{-1})
	May, 3	Weeding	Fluorocloridona*Racer 25*®(2 L. ha^{-1})
	May, 15	Fertilization	15% N, 15% P_2O_5, 15% K_2O (270 kg.ha^{-1})
	July, 15	Grain harvesting	2500 kg. ha^{-1}
	July, 17	Straw packaging	
Fallow	May, 15	Tillage	Moldboard (25 cm)

Table 3. 6. Initial (SCS, 1986) and final CNs applied to each land use at the Latxaga watershed

Cover descriptions	Curve Numbers for hydrologic soil groups			
	Initial values		Final values	
	B	C	B	C
Bare soil	86	91	43	45
Small grain	75	83	60	66
Fallow (with crop residue cover)	83	88	33	35
Row crop	78	83	62	66
Grassland	67	77	No change	
Residential districts	75	83	No change	

3.4. AnnAGNPS model evaluation

It is recommended that calibration and validation are carried out in two separated periods of time (not necessarily covering the same number of years). Gan et al. (1997), Kim et al. (2007) and Vázquez et al. (2008) state that selected calibration and

validation periods should be representative of a wide range of precipitations. Such variability is considered necessary for a rigorous and comprehensive evaluation of the model.

Herein the model was calibrated for runoff volume and sediment load using five years of observed data, from 2003 to 2007. The period between 2008 and 2011 was used for validation. Years 2006-2007 and 2008-2009 were relatively wet, while 2004-2005 and 2010-2011 were relatively dry years. Three consecutive years of climate data were used as "warm-up" period.

According to Donigian (2002), hydrological model calibration is a hierarchical process that begins with calibration of runoff and stream flow, followed by calibration of sediment yield. This order was followed herein. Calibration was carried out at monthly, seasonal and annual scales.

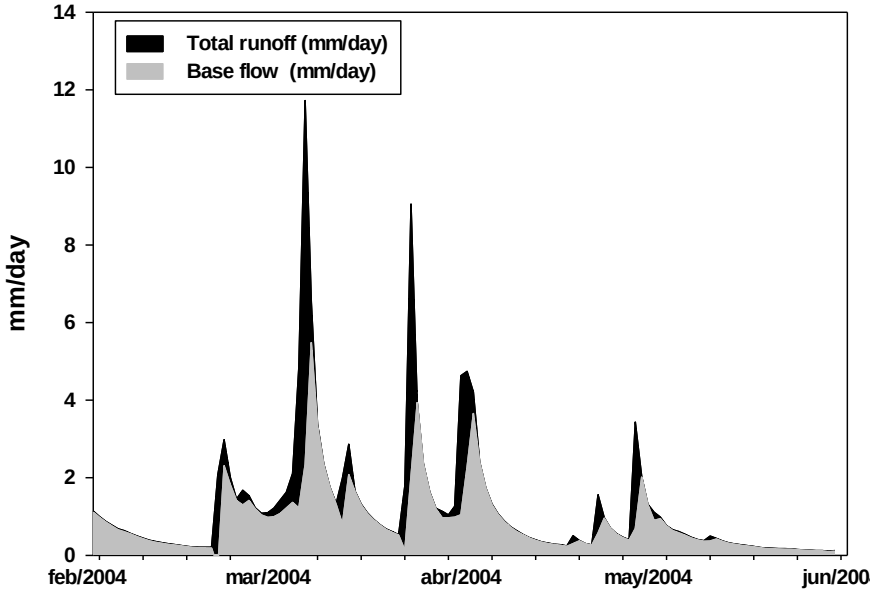

Figure 3. 10: Example of daily measured total runoff and calculated base flow for the Latxaga watershed (February, 2004-May, 2004)

3.4.1. Runoff evaluation

Most of the worldwide studies that evaluated AnnAGNPS (Baginska et al., 2003, Shrestha et al., 2006, Licciardello et al., 2007, Polyakov et al., 2007, Yuan et al., 2008, Shamshad et al., 2008, Das et al., 2008, Parajuli et al., 2009, Taguas et al., 2009) indicated CN as the most sensitive input parameter for the prediction of surface runoff. Corroborating these indications, Table 3.1 shows that in most of the cited studies AnnAGNPS was successfully calibrated for surface runoff simulation due to precise adjustment of CN values. Therefore herein the runoff calibration process was also carried out by modifying CN values. A sensitivity analysis is an instrument that assesses the impact of input parameters on the model's output, which was only considered necessary for the following sediment calibration.

3.4.2. Sediment yield. Sensitivity analysis

Most authors who studied prediction of sediment load with AnnAGNPS (Tsou and Zhan, 2004, Shrestha et al., 2006, Licciardello et al., 2007, Sarangi et al., 2007, Shamshad et al., 2008, Parajuli et al., 2009) calibrated the model by adjusting different input parameters without previous sensitivity analysis. Licciardello et al. (2007)

carried out calibration by modifying surface random roughness and sheet and concentrated flow Manning's roughness coefficients, concluding that the model's response was remarkably more sensitive to random roughness than to Manning's coefficients. Similarly, Shrestha et al. (2006) calibrated the model by modifying surface roughness. Parajuli et al. (2009) calibrated AnnAGNPS for sediment yield by adjusting the crop cover management factor (RUSLE-C) as well as the support practice factor RUSLE-P. Shamshad et al. (2008) and Sarangi et al. (2007) carried out calibration by adjusting root mass, crop residue and canopy cover.

In a different direction, Das et al. (2008) carried out a sensitive analysis before calibration, including various input parameters. Das et al. (2008) results showed that the sediment yield generated was sensitive to soil erodibility factor (K), RUSLE-C and RUSLE-P (crop management and erosion-control practice factors of the RUSLE equation, respectively). Das et al. (2008) also concluded that Manning's roughness factor had significant impacts on runoff peaks and sediment loads. Gastesi (2014) also carried out a sensitivity analysis including several AnnAGNPS inputs that affect sediment load prediction, concluding that sediment load was more sensitive to the RUSLE C factor.

Herein a sensitivity analysis was considered necessary before calibration for the prediction of sediment load. Among the different sensitivity analysis methods, the Differential Sensitivity Analysis (DSA) was used (Hamby, 1994, Lenhart et al., 2002, Frey et al., 2003, Das et al., 2008). The DSA method was selected due to its simplicity and low computational time in comparison to other statistical sensitivity analysis methods. The DSA is calculated at one or more points in the parameter space of an input, maintaining the other inputs fixed.

Based on the aforementioned studies, eight input parameters were selected to assess the model's sensitivity when predicting sediment load: random roughness, Manning's sheet and reach coefficients, remaining residue cover, canopy cover, root mass, rainfall height and the RUSLE-P factor.

The DSA sensitivity analysis was applied to the eight parameters through variation of the initial value (Δx) by a fixed percentage $\Delta x = \pm 10\%$ (Lenhart et al., 2002), whereas the other parameters remained constant. The model was then run for the five calibration years (2003-2007). The annual average sediment yield at the outlet of the watershed was used to quantify the degree of sensitivity regarding the variations of input parameters.

The sensitivity index, I (Lenhart et al., 2002) classified input parameters according to their sensitivity:

$$I = \frac{(y_2 - y_1)/y_0}{2\Delta x / x_0} \tag{3.7}$$

The model output y_0 is calculated with an initial value x_0 for parameter x. This initial parameter value is varied by $\pm\Delta x$, yielding $x_1 = x_0 - \Delta x$ and $x_2 = x_0 + \Delta x$ with corresponding values y_1 and y_2. x_0 is either a default value provided by the model or obtained from USDA's handbooks.

The sign of the index shows if the model reacts co-directionally (+) or counter-directionally (-) to input parameter changes. An I value near zero indicates that the output is not sensitive to the studied parameter, whereas a value of I significantly different from zero shows a high degree of sensitivity. The Sensitivity Index is ranked into four values (Lenhart et al., 2002): i) less than 0.05: small to negligible sensitivity;

ii) 0.05–0.2: medium sensitivity; iii) 0.2–1.0: high sensitivity, and iv) over 1: very high sensitivity.

Sediment load calibration was carried out using alternate input parameters in a decreasing order of sensitivity. Each input parameter was alternately changed –within realistic values– by 5% of its original value, until reaching the best possible match between observed and predicted sediment load values. Observed and simulated sediment yield were compared at monthly, seasonal and annual time scales.

3.4.3 Model performance assessment

Qualitative and quantitative approaches were used to assess the model's performance in predicting runoff and sediment load during calibration and validation phases. This evaluation was carried out at monthly, seasonal and annual time scales. The qualitative approach consisted of a visual graphic comparison of observed and predicted values. For the quantitative procedure, statistical criteria were used: Nash-Sutcliffe efficiency coefficient E (Eq. 3.8), modified Nash-Sutcliffe efficiency coefficient E_1 (Eq. 3.9) and percent bias PBIAS (Eq. 3.10).

Nash-Sutcliffe efficiency E. The coefficient of efficiency, proposed by Nash and Sutcliffe (1970), is calculated as:

$$E = 1 - \frac{\sum_{i=1}^{n} (O_i - S_i)^2}{\sum_{i=1}^{n} (O_i - O)^2} \qquad (3.8)$$

n refers to the number of observations, O_i is the observed data, S_i is the simulated data, O refers to the mean of observed data, and S is the mean of simulated data.

The Nash-Sutcliffe efficiency is a normalized statistical parameter that determines the relative magnitude of residual variance ("noise") compared to measured data variance ("information") (Nash and Sutcliffe, 1970). The coefficient E indicates how well the plotting of observed versus simulated data fits the 1:1 line. E is dimensionless and ranges from minus infinity to 1; E= 1 is considered a perfect fit and E< 0 indicates that the mean value of the observed data is a better predictor than the model.

The Nash-Sutcliffe efficiency coefficient has been widely used to evaluate the performance of hydrological models in simulating flow and sediments (Moriasi et al., 2007). Van Liew et al. (2003) proposed that results were highly satisfactory when E was at least 0.75, satisfactory for $0.36 \leq E \leq 0.75$ and unsatisfactory for E under 0.36.

It should be noted that E is very sensitive to extreme values (Legates and McCabe Jr., 1999) as the difference between observed and simulated data values is raised to the second power. To avoid this, Legates and McCabee (1999) and Krause et al. (2005) suggested adjusting E to reduce the effect of squared terms by rewriting the coefficient of efficiency in a more generic form, as follows:

$$E_1 = 1 - \frac{\sum_{i=1}^{n} |O_i - S|}{\sum_{i=1}^{n} |O_i - O|} \qquad (3.9)$$

The adjusted E with the desired properties (not inflated by squared values) is E_1.

Krause et al. (2005) reported that, in general, E1 is lower than E. In addition, Licciardello et al. (2007) considered values of E1 between 0.51 and 0.71 to demonstrate satisfactory model efficiency.

Percent bias PBIAS: (Eq. 3.8) is a measure of the average trend of simulated values to be higher or lower than observed values. The optimal PBIAS value is 0. Moreover, a positive value indicates model bias towards underestimation, whereas a negative value indicates bias towards overestimation (Gupta et al., 1999). Model efficiencies were classified by Moriasi et al. (2007) and Parajuli et al. (2009) as being very good for ±11 ≤PBIAS ≤ ±15% for runoff prediction, and ±16%≤PBIAS ≤ ±30% for sediment prediction.

$$\text{PBIAS} = \frac{\sum_{i=1}^{n} (O_i - S_i) \times 100}{\sum_{i=1}^{n} O_i} \qquad (3.10)$$

3.5 Runoff evaluation

3.5.1 Runoff Calibration

Application of the AnnAGNPS model at the Latxaga watershed conditions requires data collection and model input preparation (Table 3.3). This was carried out by calculating or searching for information in scientific literature and at local agriculture agencies. Then, the model was run using five curve number categories proposed by SCS (1986) (Table 3.6), with "CN-grassland" representing grassland and shrubs within the watershed and the "CN residential districts" illustrating the CN values of the area occupied by the Beortegui village. For the crops, three types of CN were used throughout each crop cycle year: CN "bare soil" was used for crop land after tillage; CN "small grain" was used when the crops (cereal and legumes) were installed. The CN for fallow with crop residue cover was used after grain harvesting, because crop residues remained on the soil (Table 3.6). As a result, the model generated an annual average runoff of 158 mm. year^{-1}, which was nearly three times higher than the observed value (58.2 mm). At a monthly time step, runoff overestimation was observed throughout the entire period with Nash coefficient and PBIAS presenting a poor result (E= -1.52 and PBIAS= -164%). A similar overestimation trend was reported by Polyakov et al. (2007) in a 4,800ha watershed located on the island of Kauai, Hawaii. Polyakov et al. (2007) observed that, during the preliminary model simulations, the model over-predicted runoff amounts and runoff event frequencies (Table 3.1).

The CN values related to the crop cycle were reduced to improve the match between the observed and the simulated surface runoff amounts. AnnAGNPS was run several times using progressively decreasing values of CN each time, and statistical analysis was carried out again focusing mainly on monthly results (although seasonal and annual results were the sum of monthly records). The best results were obtained when decreasing the CN values of bare soil, small grain and fallow by 20%, 20% and 50%, respectively. The coefficient of efficiency obtained on monthly and seasonal basis were E = 0.54 and E = 0.49, respectively, considered as satisfactory and unsatisfactory performances (Moriasi et al., 2007). Annual average simulated runoff was 62.5 mm.year^{-1}. It should be mentioned that "CN-grassland" and "CN residential districts" were decreased during calibration but no clear effects were detected on the simulated

surface runoff. This is probably due to their small corresponding areas within the catchment, not producing significant amounts of runoff compared to the remaining area. This first calibration clearly improved the model response. However, the model's trend was still to overestimate surface runoff during Summer and Autumn, while in Winter and Spring , runoff was underestimated. This could have occurred because SCS CN's were not seasonally described in the input parameters. A new calibration phase was performed.

New CN values for Winter were introduced to adjust the underestimation of surface runoff during this season. The initial CN value chosen for this period was "row crop" (Table 3.6), representing the crop stage throughout Winter. The results obtained after the introduction of new CN values were acceptable in terms of surface runoff prediction in Winter. However, during Spring, runoff was overestimated by 37%, which led to the introduction of another CN value for Spring, to correct this overestimation.

The spring CN value was determined by decreasing the "row crop" CN value by 20%. An even better performance was obtained by also decreasing the CN values of "bare soil" and "fallow CN", by 50% and 60%, respectively (Table 3.6).

A noticeable improvement in model prediction was obtained, with less than 1% of difference between simulated and observed average annual runoffs. Model performance indicators were E_m= 0.75 and E_s= 0.79 for monthly (m) and seasonal (s) time scales, respectively, as well as E_{1m}= 0.58, E_{1s}= 0.60 and $PBIAS_m$= -2.65% $PBIAS_s$= -2.38% (Table 3.7). According to Moriasi et al. (2007) and Parajuli et al. (2009) the results obtained after calibrating the AnnAGNPS model can be considered satisfactory (Figure 3.11).

A slight over-prediction of runoff still persisted, especially in Summer and for the beginning of Autumn (Figure 3.12). Despite of the low values attributed to CN, the model predicted some runoff –especially for major precipitation events– although no runoff was recorded by the outlet gauging station. This over-prediction can be due to soil conditions (very dry) in this period, with macropores promoting water incorporation to the soil, instead of runoff. This over-prediction can be observed, for example, in September, 2006 and June, 2007 (data not shown), when precipitation was, respectively, 234 mm and 93 mm, which generated simulated surface runoff 79% and 89% higher than measured values, respectively. Rainfall was 53 % and 58% higher than the average precipitation for the same months. At an annual scale, the average simulated and observed surface runoff amounts were 61.4 mm and 59.8mm, respectively with a difference of approximately 2.5%.

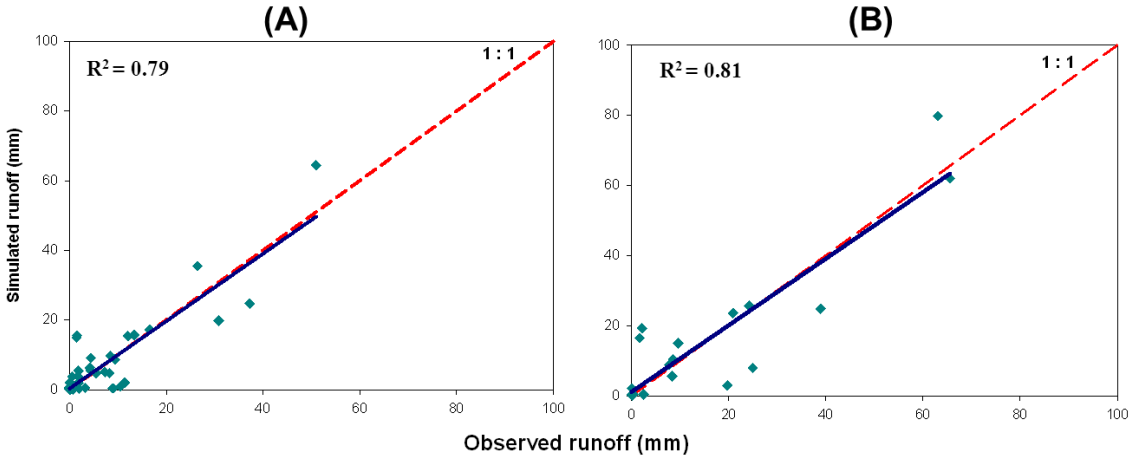

Figure 3. 11: Comparison between observed and simulated surface runoffs at monthly (A) and seasonal (B) scales, for the calibration process

Table 3. 7. Model performance indicators for calibration and validation of runoff and sediment yield

		Calibration				Validation			
		E	**E1**	**PBIAS %**	**R²**	**E**	**E1**	**PBIAS %**	**R²**
Monthly scale	**Runoff**	0.75	0.58	-2.65	0.79	0.69	0.58	-11.75	0.82
	Sediment	0.13	0.2	-0.06	0.20	-0.05	0.14	-2.3	0.13
		E	**E1**	**PBIAS %**	**R²**	**E**	**E1**	**PBIAS %**	**R²**
Seasonal scale	**Runoff**	0.79	0.6	-2.38	0.81	0.94	0.75	-11.01	0.81
	Sediment	0.26	0.23	7.4	0.30	-0.04	0.21	-7.1	0.11
		E	**E1**	**PBIAS %**	**R²**	**E**	**E1**	**PBIAS %**	**R²**
Annual Scale	**Runoff**	0.63	0.4	-2.65	0.78	0.37	0.35	-11.75	0.69
	Sediment	0.46	0.3	-0.06	0.46	-0.73	0.34	-7.16	0.03

3.5.2 Runoff validation

Like calibration, results for validation at monthly and seasonal time scales can be considered satisfactory (Table 3.7) (Figure. 3.13, Figure 3.14). On an annual basis, the difference between simulated and observed surface runoffs was only approximately 10.5%m with an average of 51.7 mm and 46.3 mm, respectively. These results confirm the ability of the model to predict surface runoff after calibration.

The accuracy of the simulations presented herein was similar to that found in scientific literature for watersheds of approximately the same size (e.g., (Licciardello et al., 2007); Table 1). Moreover, there appears to be an inverse correlation between watershed size and the success of the simulation; that is, the smaller the watershed the more satisfactory the model prediction seemed to be (cf. (Taguas et al., 2009, Parajuli et al., 2009); Table 1). This could be partly explained by the homogeneous hydrological and climate conditions expected in a small watershed, which simplify model simulation.

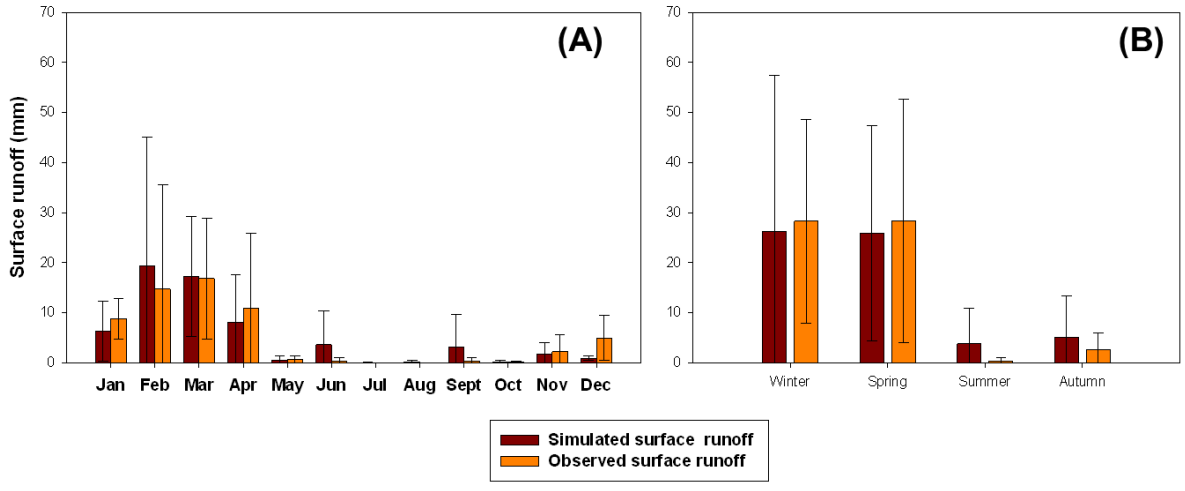

Figure 3. 12: Comparison between simulated and observed monthly (A) and seasonal (B) average surface runoffs, for the calibration phase

Thorough, detailed evaluations of AnnAGNPS at an annual scale are scarce in scientific literature, e.g. Licciardello et al. (2007), who obtained –at an annual scale– a more successful simulation in a similar (Mediterranean), but smaller watershed (Table 1). This corroborates the behavior observed between watershed size and simulation accuracy.

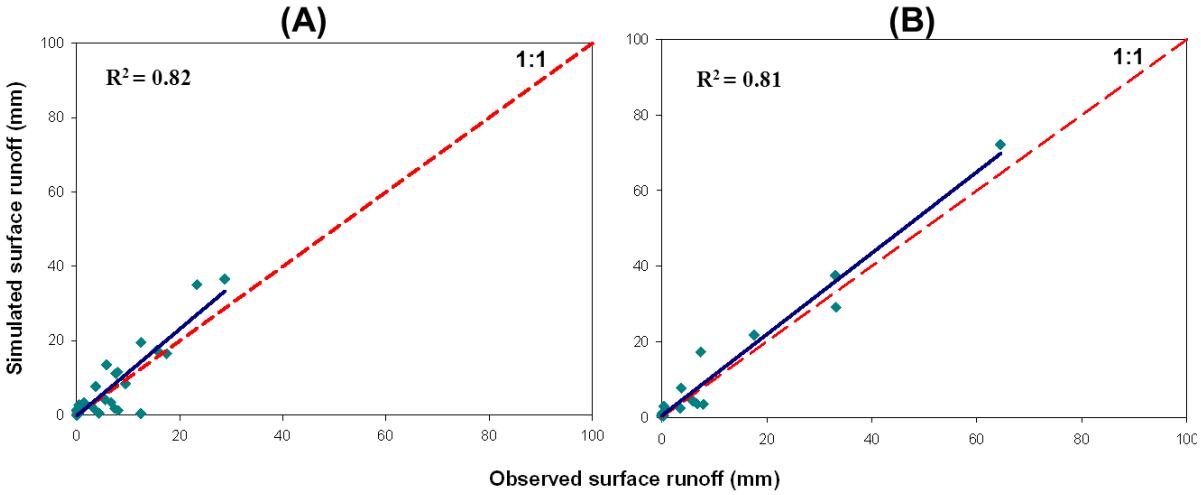

Figure 3. 13: Comparison between observed and simulated surface runoffs at monthly (A) and seasonal (B) scales, for the validation phase

3.6. Sediment Yield evaluation

3.6.1 Sensitivity analysis

Most input parameters had a linear effect on sediment yield prediction, except for Manning's sheet and reach coefficients (Figure 3.15). The model's output for sediment load presented a negative correlation with most of the input parameters selected, while RUSLE-P factor was positively correlated. The RUSLE-P factor is the relationship between soil loss with contouring and/or strip-cropping and the corresponding soil loss with straight row farming up-and-down slope.

According to Lenhart et al. (2002), only the RUSLE-P factor and canopy cover can be classified as high sensitivity parameters. The remaining six parameters are classified as intermediate sensitivity parameters. However, within the intermediate category, there was a wide range of variation in the sensitivity index, with I= 1 for canopy cover, which is three times higher than that for Manning's sheet coefficient (Table 3.8).

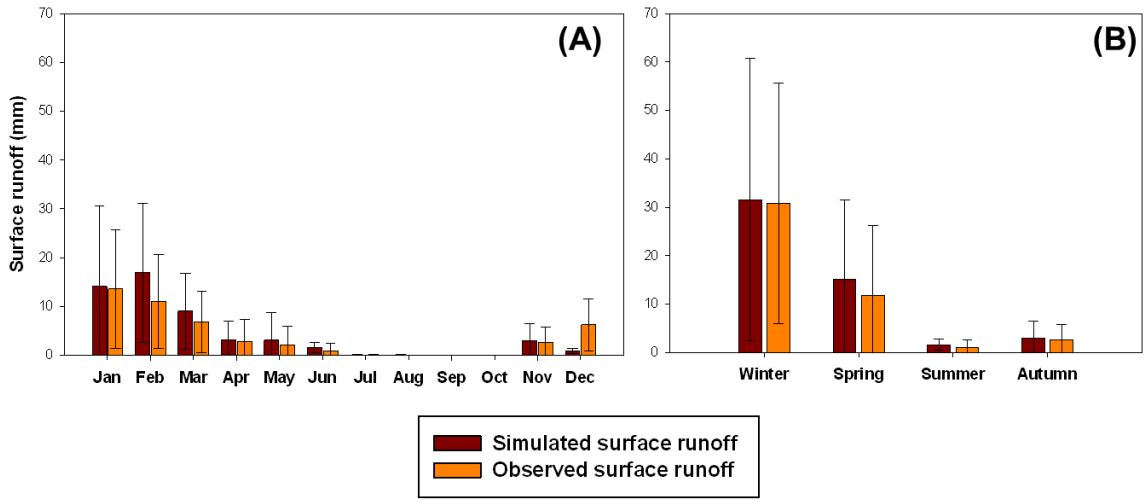

Figure 3. 14: Comparison between simulated and observed monthly (A) and seasonal (B) average surface runoffs, for the validation phase

3.6.2 Sediment yield calibration

Calibration was carried out by adjusting the RUSLE-P factor, which is the most sensitive input parameter. Wischmeier and Smith (1978) and Renard et al.(1997) reported that the contour RUSLE-P factor can have a value between 0.4 and 0.6 in watershed conditions, under different slope percentages with contour tillage and nonexistence of gullies or rills. As reported by Casalí et al. (2008) from field observations at the Latxaga watershed, no gullies/rills were observed. This led to the assignment of a P factor value within the interval 0.4-0.6; the best results were obtained for 0.5. As a result, sediment yield was reduced by 58%, although some overestimation still persisted at 30%, for the annual average. Parajuli et al. (2009) fixed P factor=0.5 to calibrate the model for sediment yield prediction, obtaining good correlation and good agreements between observed and simulated monthly sediment yields after calibration.

Random roughness was varied, followed by canopy cover, root mass, rainfall height, remaining residue cover, Manning's sheet coefficient and finally, reach coefficient.

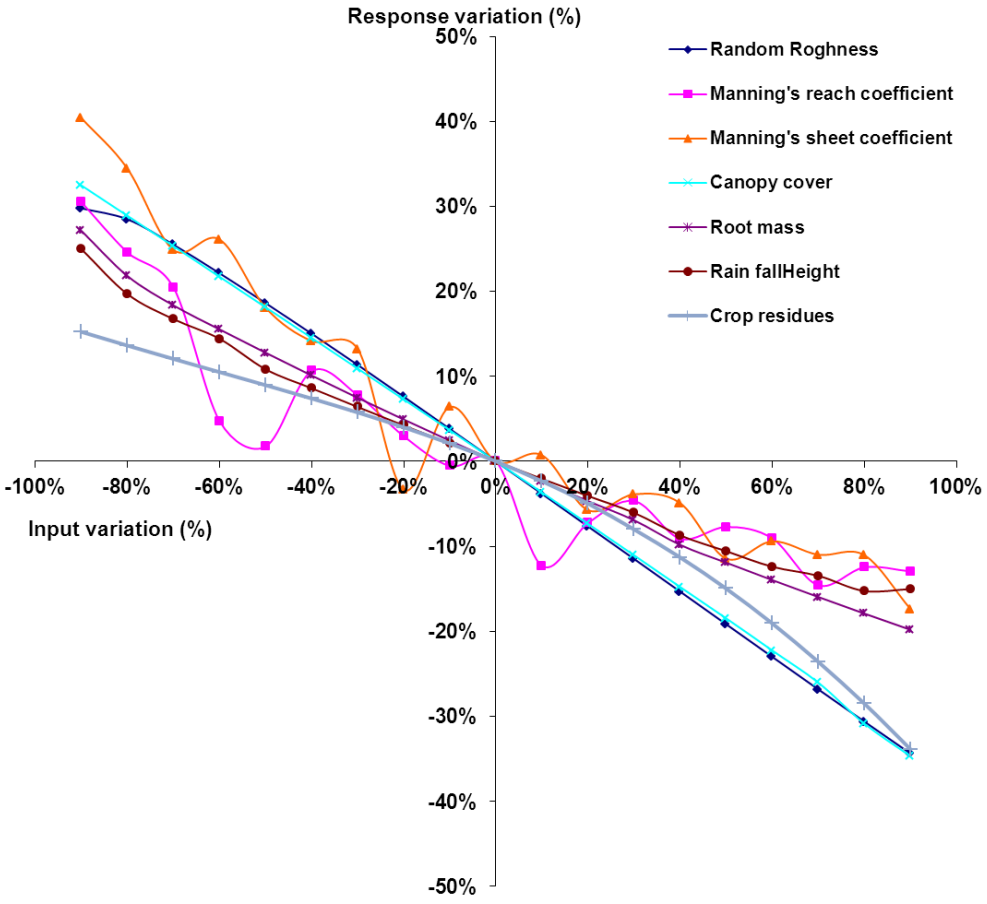

Figure 3. 15: Sensitivity of AnnAGNPS sediment yield predictions to the seven selected input parameters, expressed as percentage of output variation as consequence of percentage input variation

Table 3. 8. Sensitivity index of AnnAGNPS sediment yield predictions to selected input parameter variations.

Input parameters	Sensitivity index (I)
Manning's reach coefficient	-0.07
Rainfall height (annual average)	-0.10
Manning's sheet coefficient	-0.11
Root mass	-0.12
Random roughness	-0.18
Crop residues	-0.19
Canopy cover	-0.22

During sediment yield calibration, the performance indicators obtained on monthly and seasonal basis were almost unsatisfactory, leading to a comparison between observed and simulated annual average sediment yields to evaluate the model's performance. The best results were obtained by increasing the input data as follows: random roughness coefficient by 10%, canopy cover, root mass and rainfall height by 20%, remaining residue cover by 20%, Manning's sheet by 25% and reach coefficient by 30% (Table 3.6).

The increment in random roughness and in Manning's sheet and reach coefficients led to a decrease in transport capacity and runoff detachment. A high value was attributed to Manning's reach coefficient due to the nature of the stream network within the Latxaga watershed, characterized by very dense riparian vegetation during the entire year, especially towards the outlet, where sedimentation is frequent.

Increasing canopy cover and rainfall height increase the effectiveness of vegetation in reducing the energy of rainfall striking the soil's surface. In addition, vegetation affects erosion by reducing the transport capacity of runoff (Foster, 1982).

Sediment load prediction was improved mainly at annual scale. The annual average sediment yields were 341.5 kg .ha^{-1} .year^{-1} and 341.3 kg .ha^{-1} .year^{-1} for simulated and measured sediment loads, respectively (0.06% difference between observed and simulated sediment loads). However, comparisons between predicted and observed sediment loads on a monthly and seasonal basis presented low correlations (Table 3.7, Figure. 3.16 and Figure. 3.17). The results obtained after calibration for efficiency coefficients (E, E1) can be considered unsatisfactory on monthly and seasonal basis, while the PBIAS values obtained were classified as very good, according to the performance ranting (PBIAS $\leq \pm 15$) proposed by Moriasi et al. (2007) and Parajuli et al.(2009). The model tends to overestimate sediment yields during Autumn and underestimate during Winter and Spring. Gastesi (2014) found almost the same results with unsatisfactory performance in the prediction of annual sediment yield (E=0.47), but very good performance concerning PBIAS(=9.61%).

The use of stream networks and corridors models (CCHE1D and CONCEPTS), already embedded within AnnAGNPS, include more details on channel hydraulics, morphology, and transport of sediments. These models are required for a more precise explanation of sediment yields at event, seasonal and monthly scales, even for small watersheds. To this end, a more detailed topographic representation of the watershed, and mainly of channel slopes, would be required. Moreover, a thorough field inspection and survey within the watershed would help better understand the processes behind sediment generation and, hence, lead to the correct selection of auxiliary models.

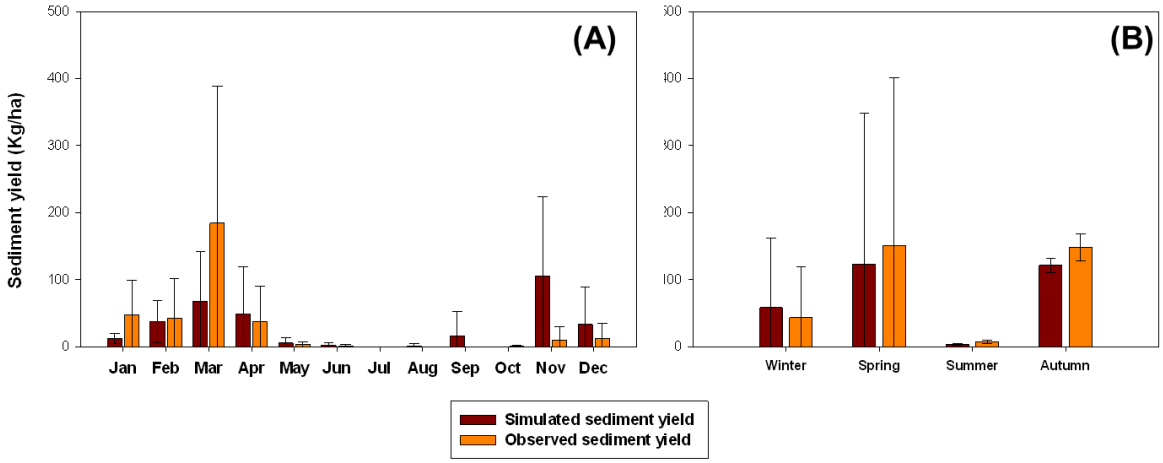

Figure 3. 16: Comparison between simulated and observed monthly (A) and seasonal (B) average sediment yield, for the calibration phase

3.6.3 Sediment load validation

The model was not able to satisfactorily reproduce observed records at monthly and seasonal time scales (Table 3.7, Figure 3.18 and Figure 3.19). At an annual scale, the model performed much better with only 7.1% of difference between observed and simulated sediment loads. The annual averages were 338.4 kg. ha^{-1}. $year^{-1}$ and 315.8 kg. ha^{-1}. $year^{-1}$ for simulated and observed sediment loads, respectively. These considerable discrepancies in the model's performance, depending on the time scale considered, might be explained by the noticeable mismatch frequently observed between the amounts of sediment reaching the outlet with the corresponding runoff, on a monthly basis. This occurs because of the relatively easy re-entry of previously deposited sediment into streams. This would obviously lead to some failure in the model's simulation, when considering short time scales. But, sooner or later, sediment reaches the watershed outlet so that in annual balance context, sediment and runoff values finally roughly matched. However, this better performance of the model at an annual scale is not reflected on the corresponding statistical indexes (Table 5) possibly because of the limited number of years used in the analysis. In fact, existing evaluations of the model's prediction of annual sediment production are even fewer than those regarding annual runoff prediction (e.g., Das et al., 2008; Table 1). Furthermore these works are normally limited to showing proportional –numerical or graphical– differences between observed and simulated values without statistical analyses (e.g., Das et al., 2008).

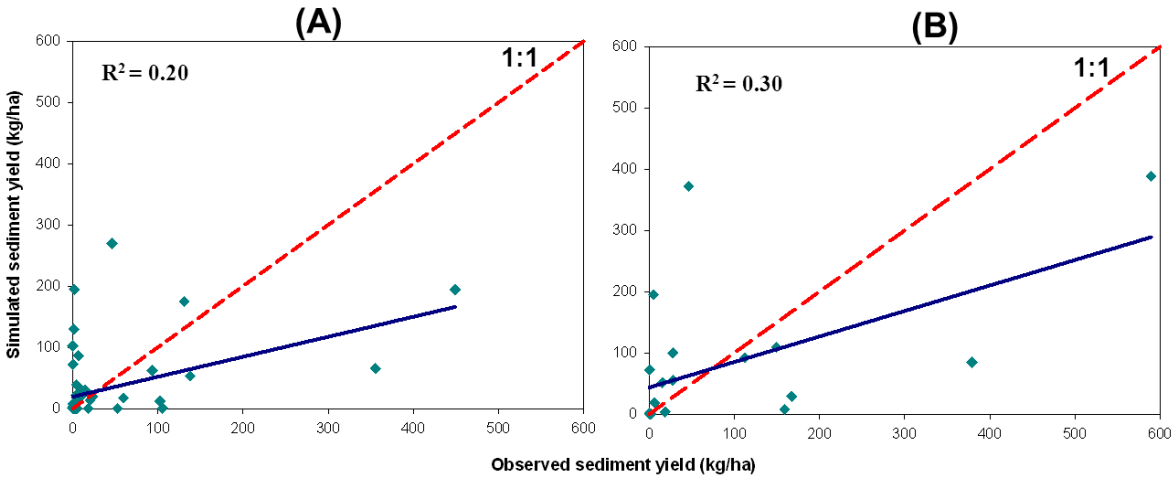

Figure 3. 17: Comparison between observed and simulated sediment loads at monthly (A) and seasonal (B) scales, for the calibration phase

Regarding the evaluation of sediment simulation at a monthly scale, the results shown in scientific literature are varied but, in general, better than those obtained herein (Table 1) perhaps because the model overlooked some important (in-stream) processes that occurred in the watershed. This reinforces the former hypothesis established herein on the necessity to use stream network and corridor models.

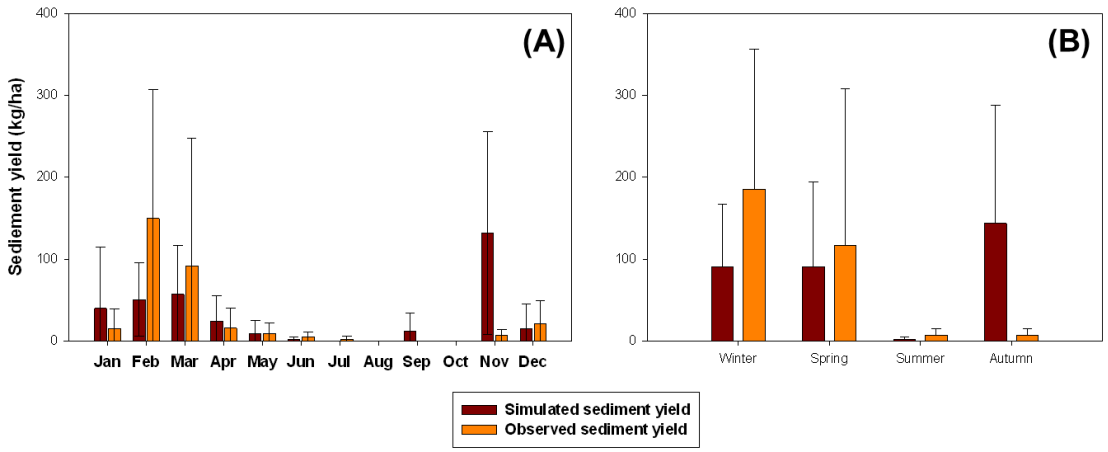

Figure 3. 18: Comparison between simulated and observed monthly (A) and seasonal (B) average sediment yields, for the validation phase

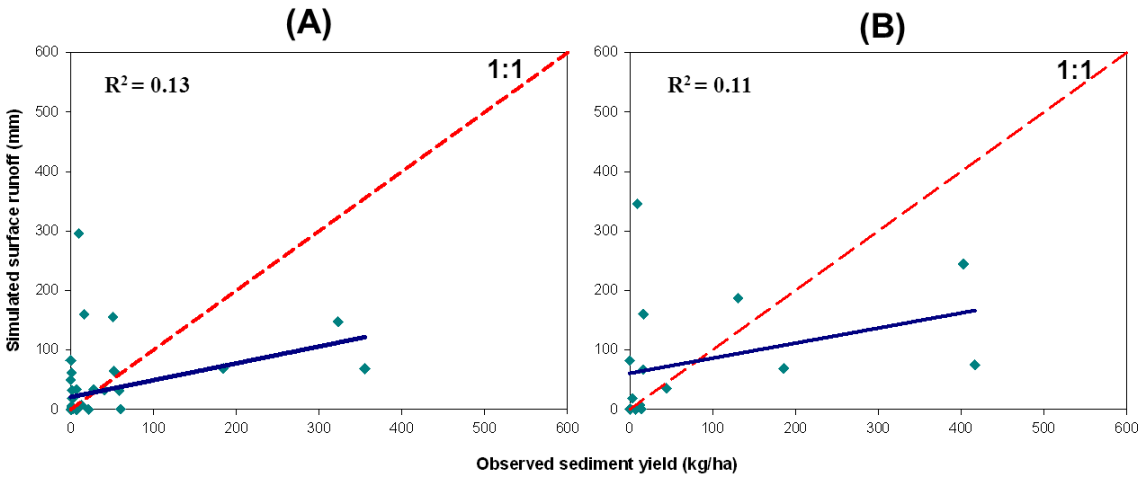

Figure 3. 19: Comparison between observed and simulated sediment loads at monthly (A) and seasonal (B) scales, for the validation phase

3.7 Potential agricultural scenarios

Throughout Spain's history, the type of exploitation of a specific territory has suffered changes - usually slow - induced by cultural, demographic or even economic phenomena. In recent decades, these changes - which now are accelerated - were induced by the market and/or Common Agricultural Policy (CAP). This is how the global market has favored (mainly though subsidies) the fast expansion of specific exploitation and crop systems, in detriment to other land uses. There has even been incentives to the abandonment of land (set-aside) to favor soil conservation and improvement of hydric balances (García Ruiz and López Bermúdez, 2009).

In Navarre, cereals (mainly barley and wheat) have represented, for a long time, approximately 80% of arable crops, with a special presence in the dry lands of the central zone of the territory, due to optimal ecological conditions. Nevertheless, the main land uses of the Navarre region have also suffered changes in recent decades. For example, the surface cultivated with rape in the beginning of the 1990's was five times the area cultivated in the 1980's. However, rape cultivation suffered a drastic drop in the following years. Rape cultivation nowadays is barely existent, despite the recent arrival of the biodiesel industry (Goñi et al., 2008). Equally, the cultivation of sunflower experienced a sudden increment during the first half of the 1990's, also followed by a sharp decrease. Nowadays, sunflower cultivation oscillates but is still strongly present (Lezaun et al., 2004). Sunflower is actually a traditional alternative to cereal cultivation in the regions of Baja Montaña and Zona Media. The surface occupied by protein pea has experienced a pronounced increase after 1995, especially during the first years of the XXI century, thanks to economic incentives of the CAP.

Based what has been stated in the paragraphs above, the following scenarios are proposed as potential agricultural uses for the study basin (Laxtaga):

a) Scenario 1: 60% cereals, 25% sunflower
b) Scenario 2: 60% cereals, 25% rape
c) Scenario 3: 60% cereals, 25% legumes
d) Scenario 4: 60% cereals, 25% (sunflower + rape+ legumes, in equal parts)
e) Scenario 5: 60% cereals and alternatively, 20%, 30%, 40% and 50% brushland.

The percentage values refer to the total surface of the basin. Approximately 12% of the basin is, as mentioned before, unproductive (shallow soil, rocky outcrops, constructions). The presence of brushland reflects the situation of abandoned land (not

cultivated), as the Mediterranean brushland (thyme, gorse, rosemary, etc.) is the main natural vegetation of the zone (Departamento de Agricultura. Ganadería y Alimentación del Gobierno de Navarra).

It must be highlighted that any predictions made with simulation tools, especially in complex environments, such as the one considered herein, is certainly tentative. Therefore, to reduce such uncertainties to the minimum, it is important that the scenarios considered are similar to those in which the model was validated. The proposed scenarios are plausible and close to the real conditions in which AnnAGNPS was evaluated.

3.7.1 Simulation with AnnAGNPS. Analysis of results

The average production of runoff and sediment load at the output of the basin, in different scenarios, were estimated with the application of the AnnAGNPS model based on meteorological and hydrological data registered at the Laxtaga watershed in the period 2003-2008 (Chahor et al., 2014). Table 3.9 shows management data, for each crop, utilized in the simulations.

Previous work (Chahor et al., 2014) has evaluated the model through a simulation - carried out in the same time period - of runoff and sediment exports in the actual land use conditions. This evaluation was supported by an extensive database. By adjusting the initial, default values of the Curve Number (CN) for different stages of the crop, an adequate simulation of annual scale runoff was obtained. Overestimation was present in the dry period. Sediment load was also adequately simulated, on an annual basis, after adjustment of Manning's roughness and surface long-term random roughness coefficients (Chahor et al., 2014).

Given the fact that there are no pronounced differences in physical (e.g., texture, depth) and chemical fertility in the dominant soils of the area, the different crops that make up each scenario were randomly distributed in the basin, until occupying the total pre-established area. Under other circumstances, sunflower could have been allocated to deeper, more fertile soils, and rape to loamy texture soils, which would allow for rapid emergence (Alberto Lafarga, personal communication).

It must be mentioned that if sediment load is directly related to the intensity of soil losses, some under-estimation is embedded as part of the eroded soil could have been deposited before reaching the output of the watershed. However, in small basins - such as the one considered herein - the aforementioned deposition can be considered minimal.

Table 3. 9. Chronogram of agricultural activities applied to simulation. Information collected from interviews with local farmers

Crop	Date	Activity	Observation
Cereal/rape	September, 15	Tillage	Moldboard (25 cm)
	September, 20	Smoothing	Harrow
	October, 10	Fertilization	
	October, 15	Seeding	Combined seeding machine
	January, 15	Fertilization	
	February, 15	Weeding	
	March, 15	Fertilization	
	July, 1	Grain harvesting	
Legumes	September, 15	Tillage	Moldboard (25 cm)
	September, 20	Smoothing	Harrow
	September, 21	Seeding	Combined seeding machine
	February, 15	Weeding	

	July, 1	Grain harvesting	
Sunflower	September, 20	Tillage	Moldboard (25 cm)
	March, 15	Smoothing	Harrow
	May, 1	Seeding	Precision seeder
	May, 3	Weeding	
	May, 15	Fertilization	
	July, 15	Grain harvesting	

The "brush land" condition has been recreated in the model by assuming an annual root rate of 5000kg/ha, cover percentage 90%, and annual rainfall height 0.2m.
Analysis of the actual/real conditions of the watershed (Esc_Real., figure 3.20), the average values of direct runoff (after elimination of flow base) and sediment loads simulated by the model (61 mm and 316 kg.ha^{-1}, figure 3. 20) are very close to the real registered values of the period (Chahor et al., 2014): 57mm and 309 kg.ha^{-1}, respectively. This excellent simulation suggests that the results to be estimated in the potential scenarios considered herein are not too far from reality.
Regarding the fictitious scenarios, there were no significant differences regarding runoff generation, except for a slight increase when the alternative crop is legumes. Nevertheless, there are greater contrasts when analyzing the average sediment loads at the output of the basin. Cultivation of sunflower would generate similar soil losses to these actually suffered (figure 3. 21), and the remaining alternative crops generate more pronounced changes. Rape would generate an increase of 30% in the sediment load (figure 3. 20). Evidently, reduction of the area occupied by rape (Esc_ 4) results in sediment exports closer to the actual conditions (figure 3. 20).
All simulations were carried out under similar conditions (for rape, Esc. 2, even identical farming methods to the real conditions - Esc Real. - were considered) (Table 3.9). These differences are mainly due to the different coverage degrees of the soil and characteristics and permanence of stubble (e.g., relationship between the weight of plant residue and weight of grains) for each crop.

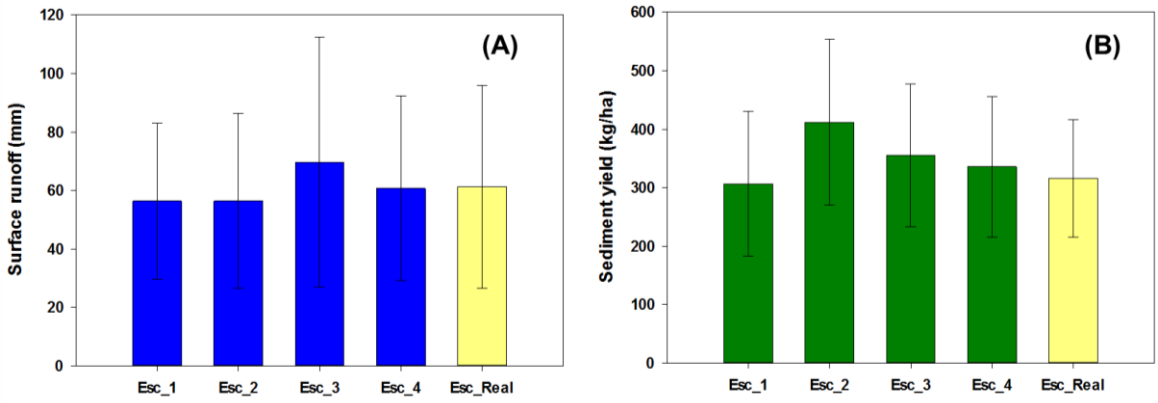

Figure 3. 20: Annual average volume of surface runoff (A) and sediment yield (B) simulated by AnnAGNPS for the different scenarios considered. Esc_Real. refers to simulation under the real/actual conditions of land use

The percentage increments predicted for soil erosion for each fictitious scenario were not preoccupying as, actually, these values are far from the tolerance limits at the Laxtaga watershed (1,12 kg m^{-2} year^{-1}; (Hall et al., 1985)). However, if the scenarios were shifted to cereal-cultivated watersheds similar to Laxtaga the estimations would raise concerns due to higher vulnerability to erosion and much higher average sediment exports than Laxtaga.

Regarding the situation of land abandonment (presence of brushland), a clear decreasing trend was observed in runoff and the production of sediments as the brushland area increased (figure 3. 21). After 40% soil losses (figure 3. 21), an upturn in runoff is predicted, but does not affect the decreasing sediment load trend. In general, it is accepted that the condition of soil abandonment favors reductions in erosion and runoff (García Ruiz and López Bermúdez, 2009), as experimentally verified (Lasanta et al., 2006). However, this occurs in advanced states of brushland colonization, from which there is an effective reduction in the generation of runoff and erosion. After the first abandonment months, however, when brushland is still developing, high erosion rates can be achieved. This explains the paradoxical presence of deteriorated soil under dense brushland.

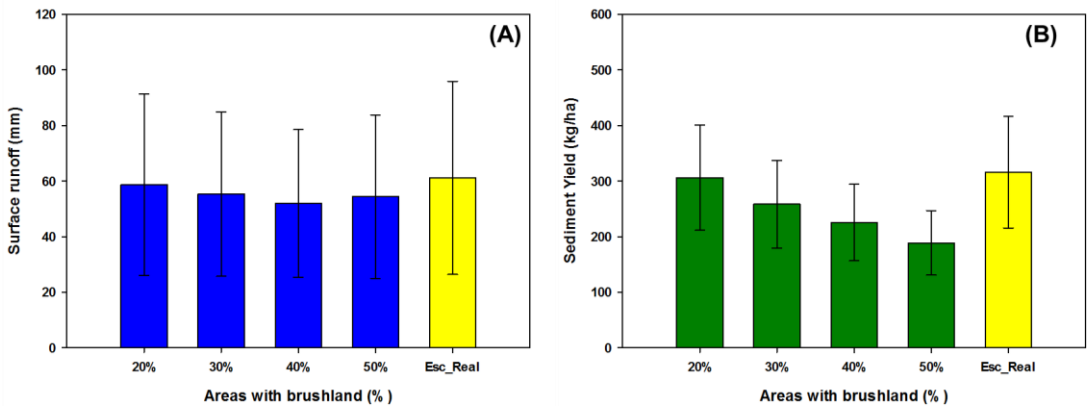

Figure 3. 21: Annual average sediment load simulated by AnnAGNPS for the different scenarios considered. Real Sc. refers to simulation under the real/actual conditions of land use

Chapter 4: Evaluation of the AnnAGNPS model evaluation to predict surface runoff at the Cemborain watershed

4.1 Introduction

The AnnAGNPS model has been evaluated worldwide, at different watershed superficies scales and land uses. In general, in Spain and particularly in Navarre, the AnnAGNPS model has been mainly evaluated at small watersheds areas under monoculture agricultural practices. Taguas et al. (2009) evaluated AnnAGNPS in a microcatchment of 6.7 ha, cultivated with olive trees, in the province of Cádiz. In Navarra, Gastesi (2014) evaluated the AnnAGNPS model at the LaTejería watershed, with 170 ha of surface area completely cultivated with winter grain crops. With almost the same crop conditions, the model was also applied to predict surface runoff and sediment loads at the Latxaga watershed (see Chapter 3) (Chahor et al., 2014). However, the AnnAGNPS model has not yet been evaluated in Navarre at a large catchment with varied land use. In other sites of the world, few studies have included varied land use when assessing the AnnAGNPS model. For instance, Shrestha et al. (2006), Polyakov et al. (2007) and Shamshad et al. (2008) evaluated the capability of AnnAGNPS to predict runoff and sediments in watersheds with mixed land use crops, including forest. Therefore, the Cemborain watershed, where different and representative land uses can be found, was selected to evaluate the AnnAGNPS model herein (Chahor et al., 2011). Land uses include forest, shrubs, rangelands, agricultural fields and urban area. The significant surface area of the Cemborain watershed (5000 ha) is also a differencing factor, compared to the small dimensions of other watersheds previously used to evaluate the model in Spain and Navarre.

The Cemborain watershed watershed was also selected because a long series of runoff records is available from the existing gauging station. The objective of this study was to evaluate the capability of the AnnAGNPS model to predict surface runoff at the Cemborain watershed.

4.2 Study area: Cemborain Watershed

4.2.1 Location

Covering an area of 50 km^2, the Cemborain watershed is located in the central part of Navarra, approximately 30 km away from Pamplona. The watershed area extends across four municipalities; most of the watershed is located in the Leoz municipality, meanwhile the downstream part is divided between three municipalities (Orísoain, oloriz anb Garinoain).

The Cemborain watershed is drained by the Cemborain River, which is more than 18 km long and crosses the watershed from Northeast to Southwest. The UTM outlet coordinates are North: 4,717,013 and West: 611,419. The Cemborain River is an affluent of the Cidacos River, and both watersheds are within the Aragón river watershed (Figure 4.1).

4.2.2 Soil

In the Cemborain watershed, the geologic material belongs to the continental Tertiary period. Conglomerate strata dominate the Northeast part of the watershed. Descending to the Barasoain village, the dominant strata is sandstone with sludge paleochannels also from the continental Tertiary period. In the valley, bottoming materials from sedimentation accumulate, forming fluvial deposits. The Cemborain watershed soil map was obtained from the Navarre soil map 1:50.000 (Iñiguez et al.,

1982 - 1992), while the specific soil texture characteristics of the different soil layers were obtained from trial pits executed by the Department of Agriculture of the Government of Navarre in adjacent watersheds with the same type of soils.

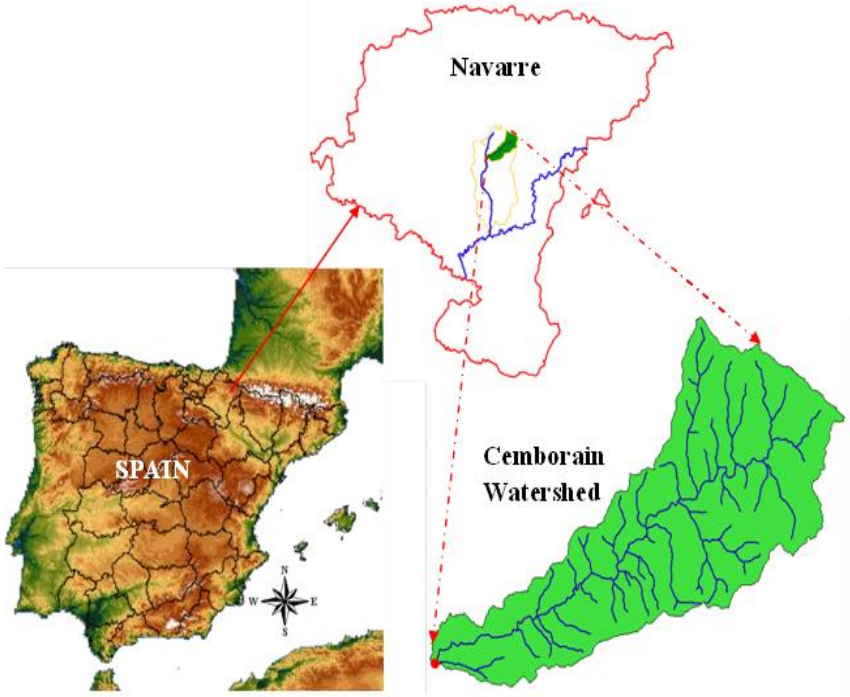

Figure 4. 1: Location of the Cemborain watershed

According to USDA Soil Taxonomy Classification (1998), six soil types cover the Cemborain watershed (Figure 4.2). The dominant soils are Calcicxerollic Xerochrepts, covering 56% of the watershed (2800 ha) with silty loam texture, located on steep hillslopes (slope gradient 10 - 20%). These soils are shallow and developed over conglomerate and sandstone. Typic Xerorthent soils cover 18% of the watershed area (917 ha), and are located on eroded hillslopes (up to 20%). These soils are relatively shallow and usually have a lithic or paralithic contact at an approximate 50 cm depth, usually not cultivated. These are loamy in texture and silty clay loamy in the superficial horizon. Lithic Xerorthent soils are formed over sandstone, being silty loam in texture in the upper horizon (Table 4.1); these are essentially present in areas within the watershed with slopes ranging from 10% to 20 % and covering approximately 11% of the watershed surfaces. Typic Xerofluvent soils cover 8% of the watershed area and are silty loamy in texture. These soils are deep, covering the Cemborain River bottom valley (Figure 4.2). Typic Calciustepts soils are principally present in the central part of the watershed, covering an area of 250 ha (5%). These soils are silty clay loamy in texture in the superficial layer, with moderate depth. Finally, Typic Hapludalf soils cover 2% of the watershed surface, in the extreme North part, with silty clay loamy texture.

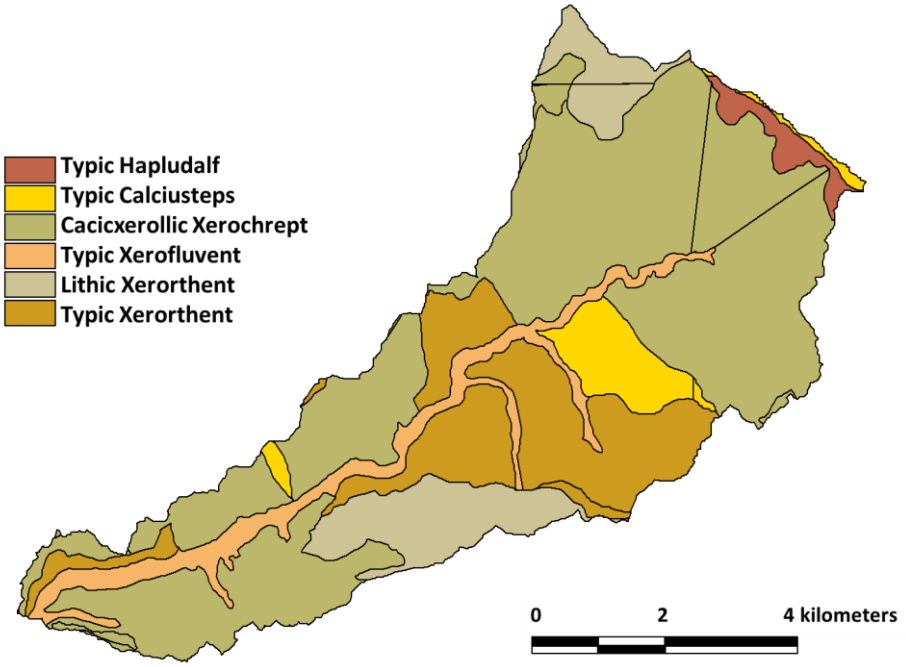

Figure 4. 2: Cemborain soil map

Table 4. 1. Soil properties for each textural class

Soil Types	Layer depth (cm)	Sand (%)	Loam (%)	Clay (%)	Texture
Xerochrept Calcicxerollic	0-40	55.6	31.7	12.7	Silty loam
Typic Xerorthent	0-30	10.8	61.5	27.8	Silty clayl oam
	30-50	22.1	47.9	30	
Lithic Xerorthent	0-40	55.6	31.7	12.7	Silty loam
Typic Xerofluvent	0-35	74.7	15.9	9.4	Silty loam
	35-150	77.2	14.9	7.9	
	150-200	45.2	33.9	20.9	
Typic Caciustepts	0-40	26.3	45.8	28	Silty clay loam
	40-70	18.8	51.3	29.9	
Typic Hapludalf	0-30	10.8	61.5	27.8	Silty clay loam
	30-50	22.1	47.9	30	

4.2.3 Climate

Climate at the Cemborain watershed is Sub-Mediterranean, with cold winters and hot summers. Temperature and precipitation vary considerably from North to South, due to the significant difference of altitude between upstream and downstream areas (1000m to 500 m, respectively). Annual average precipitation is approximately 800 mm in the North and 520mm in the South part of the watershed. Annual average temperatures range from 11.8ºC in the North to 12.7ºC in the South parts of the watershed, even if altitude differences are important. Figure 4.3 shows the monthly average temperature of the three meteorological stations within the study area.

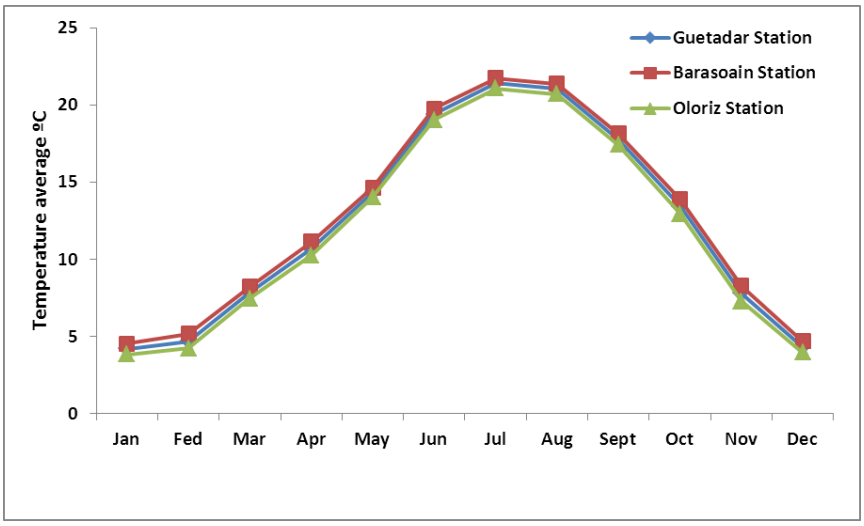

Figure 4. 3: Monthly temperature average

4.2.4 Land use

Land use within the Cemborain watershed is characterized by its diversity, where forest and Mediterranean shrubland are dominant, generally covering steep hill slopes within the watershed. Most of the cultivated crops are located in the flat areas of the watershed, bordering the river bed.

However, for this study different land uses were grouped in a global category (Table 4.2) utilized to evaluate the model. Crop variations (*e.g.*, crop rotation) and corresponding management practices were respected. Land use was classified into five categories with different percentages: natural forest (40%), agricultural fields (24%), shrubs (31%), rangeland (4%) and urban areas (1%) (Figure 4.4 and Table 4.2). The crops are mainly herbaceous, with a three-year rotation period. Cereal (wheat and barley) alternate with legumes, sunflower and rapeseed. Olive cultivation areas are scattered across the watershed.

Table 4. 2. Different land uses within the Cemborain watershed

Land use categories	Specific land use	Area (%)
1. Agricultural fields	Herbaceous crops with fallow (cereals, legumes etc.)	24
	Market garden	
	Olive and vineyard	
2. Forest	Common box (*Buxussempervirens*)	40
	Avergreenoak (Quercusilex)	
	Kermes oak (*Quercuscoccifera*)	
	Common juniper (*Juniperuscommunis*)	
	Ribera soto	
	European beech (*Fagus sylvatica*)	
	Aleppo pine (*Pinushalepensis*)	
	Black pine (*Pinusnigra*)	
	Scots pine (*Pinussylvestris L*)	
	Portuguese oak (*Quercusfaginea*)	
3. Shrubs	Mediterranean Shrubland	31
4. Range land	Grassland	4
5. Urban lands	10. Villages	1

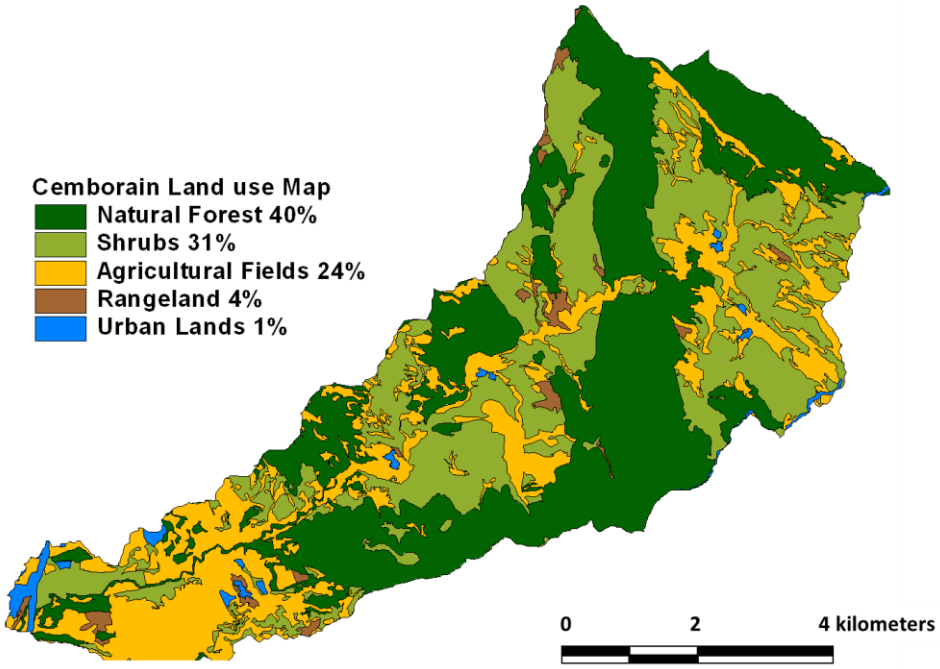

Figure 4. 4: Cemborain land use map

.4.2.5 Watershed instrumentation

4.2.5.1 Gauge station

The Cemborain watershed is part of the Ebro watershed. The Ebro Hydrographic Confederation (CHE) is responsible for monitoring runoff depth. To this end CHE installed a gauging station at the Cemborain River. The station is part of an automatic station network installed throughout the Ebro River basin.

The Cemborain station was built in the Garinoain municipality, at UTM coordinates North: 4,717,013 and West: 611,419. The gauging station provides runoff data on a daily basis, since 1955. After September 2005, runoff is also recorded in fifteen-minute intervals. The gauging station was designed with a rectangular structure to measure discharge, with two different sections as shown in figure 4.5. The small section is used to measure small discharges. Water level measurements are accomplished with a buoy connected to a pulley by a flexible cable, which is connected to a counterweight, according to buoyancy principles. Level measurements are recorded by a data logger and discharge is calculated by applying the corresponding ranting curve. All recorded data are transmitted at real time to CHE by a radio frequency transmitter.

5.2.5.2 Meteorological station

Despite the number of meteorological station scatted across the Navarre area, the Cemborain watershed does not count with any meteorological station of its own, although three stations are located around the watershed. Figure 2.13 shows the location of the three stations. Getadar is an automatic station located at UTM coordinates North 4,719,604 and West: 625,357, at 710 m altitude and installed July 22nd, 2000. Getadar provides daily meteorological data and at 10 minute intervals, consisting of: 1) wind monitor to measure wind speed and direction at 2 m height; 2) relative humidity sensor; 3) temperature sensor; 4) solar radiation sensor; 5) soil temperature sensors at 20, 40 and 80 cm deep, and 6) tipping bucket rain gauge with heating system.

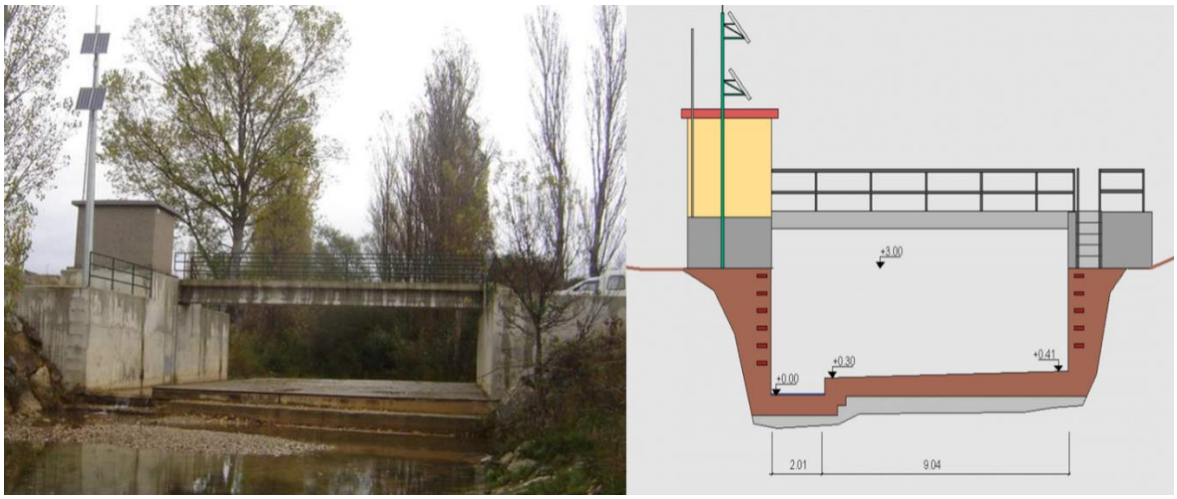

Figure 4. 5: Outlet of gauging station (left) and a scheme of the gauging station sections (Measurements are in meters)

The Oloriz and Barasoain stations are both manual stations, providing daily maximum and minimum temperatures as well as accumulated daily precipitations, installed on January 1st, 1982 and July 1st, 1975, respectively. Oloriz is situated at the North part of the watershed (UTM coordinates North 4,722,753, West: 616,757 and 706 m altitude). Barasoain is situated at UTM coordinates North 4,717,772 and West: 611,068 and 524m altitude.

4.2.6 Hydrological behavior of the Cemborain watershed

In this study, rainfall and runoff datasets were analyzed to characterize the hydrological behavior of the Cemborain watershed. The Lataxaga watershed was analyzed in details in other works (Casalí et al., 2008).

4.2.6.1 Rainfall

Temporal and spatial rainfall characteristics were studied by analyzing rainfall data recorded by three climates stations. As aforementioned, the stations Getadar, Oloriz and Barasoin are located outside the watershed. Figure 4.6 shows the influence area for each station, determined by Thiessen polygons. Figure 4.6 reveals that the Oloriz station has the greatest influence area, with 62.6% of the total area, including the central part of the watershed. The influence areas of the Getadar and Barasoain stations represent, respectively, 19.7% and 17.7% of the watershed area. The influence area of Getadar includes the Western part of the upstream area, meanwhile Barasoain influences the entire downstream area.

Dataset from 2003 to 2012 were obtained from the three selected stations and utilized to analyze rainfall distribution - same data were used to evaluate the AnnAGNPS model. The variation of precipitation within the watershed, from upstream to downstream, was clearly observed when comparing rainfall data from the Barasoain, Oloriz and Getadar stations, where the annual average rainfalls were 540, 783 and 805 mm, respectively. Despite the precipitation differences, the three stations present the same behavior. The wettest season is Spring, with 30% of recorded precipitation, whereas Summer is the driest season, with 12% of recorded precipitation. Autumn and Winter presented 29% and 28%, respectively, of recorded precipitation. April and July were, respectively, the wettest and the driest months (Figure 4.7).

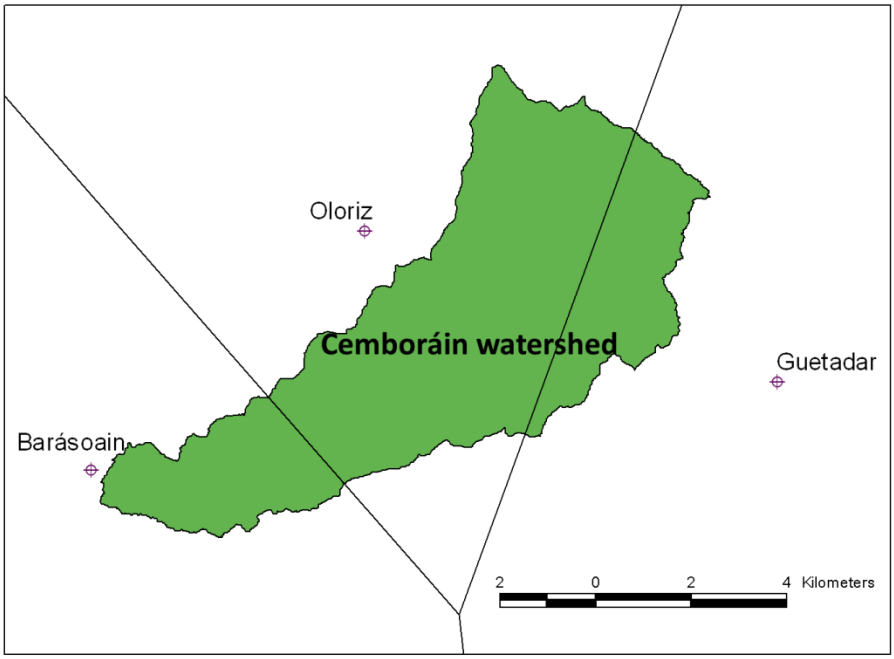

Figure 4. 6: Meteorological station location and Thiessen polygons

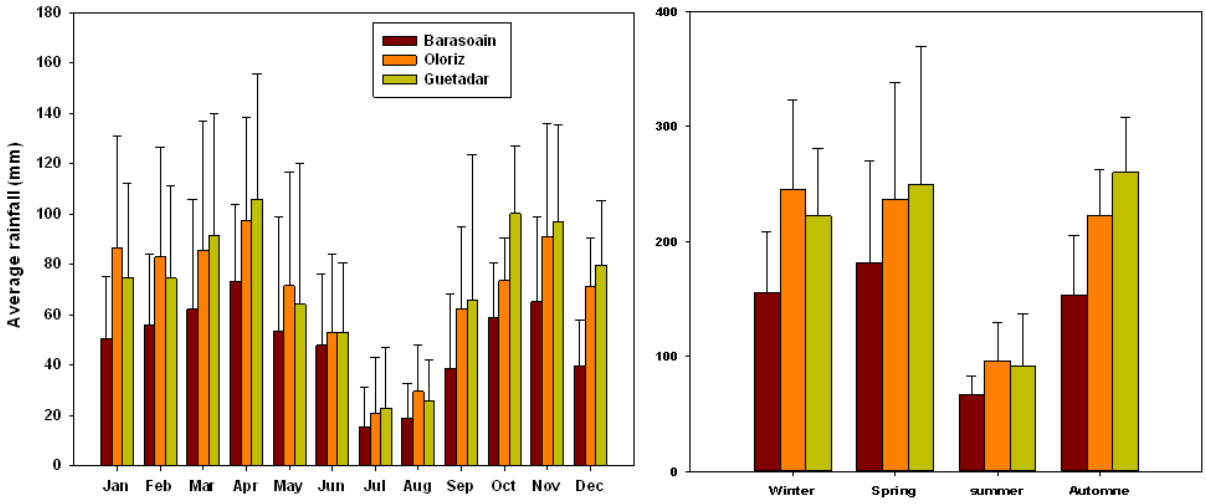

Figure 4. 7: Monthly (left) and seasonal (right) average rainfalls at the Barasoain, Oloriz and Getadar meteorological stations

Rainfall intensity I_{30} and erosivity EI_{30} (Eq. 4.1) were determined for the Cemborain catchment using 10-minute rainfall records to explore the influence of rainfall intensity and kinetic energy on water erosion and runoff contribution:

$$EI_{30} = (\sum_{r=1}^{0} e_m v_m) I_{30} \quad (4.1)$$

Where e_m is the unit rainfall energy (MJ ha^{-1} mm^{-1}) and v_m is the rainfall volume (mm) during a time period m. I_{30} is the maximum rainfall intensity during a period of 30min during the event (mm h^{-1}). The unit rainfall energy is calculated for each time interval as follows:

$$e_m = 0.29\left[1 - 0.72\, e^{(-0.05\, i_m)}\right] \quad (4.2)$$

Where i_m is the rainfall intensity during the specific time interval (mm h^{-1}).

Therefore, rainfall events recorded at the Getadar station (January 2002-December 2012) were analyzed by determining the corresponding erosivity EI_{30}.

Firstly, events with more than 1mm were analyzed: 928 events were registered, and Table 4.3 shows the distribution according to rainfall amounts. The greatest rainfall events (>40mm), with greatest erosivity values, comprised only 2% of all events, but accounted for more than 15 % of total rainfall.

With an exception for Summer, when the lowest number of rainfall events occurred (12%), the other seasons presented almost the same number of events. Regarding event durations and intensities, events during Winter and Spring were typically long but with low intensities. Summer and Autumn were characterized by shorter, more intense events (Figure 4.8).

Regarding erosive events, these were selected according to the criteria proposed by Renard *et al.* (1997): (i) the cumulative rainfall of an event should be greater than 12.7 mm, or (ii) the event has at least one peak that is greater than 6.35 mm in 15 min and (iii) a rainfall-period of less than 1.27 mm in 6 h is used to divide a long storm period into two shorter storms.

A total of 101 rainfall events fulfilled these criteria, and most events occurred in Spring (35.6%) and Autumn (36.6%), followed by Winter (14.9%) and Summer (12.9%).

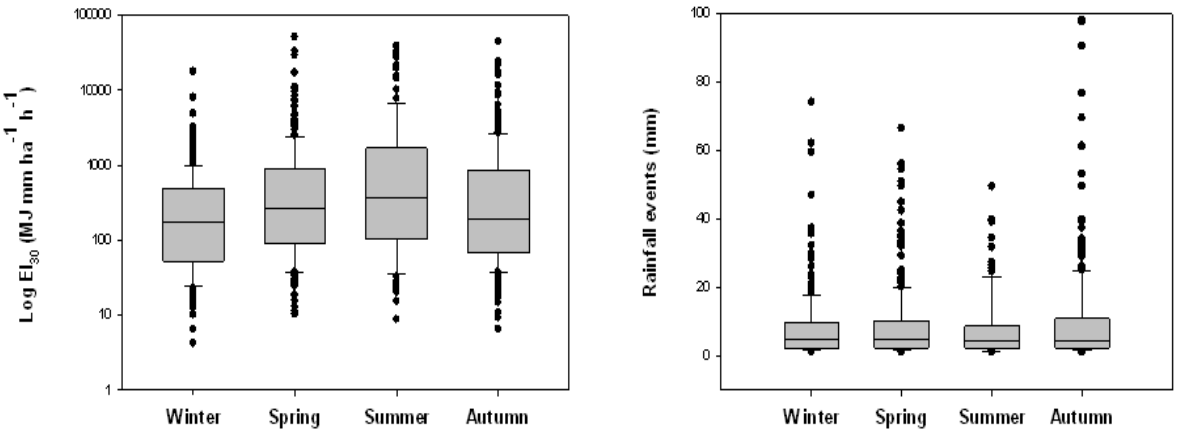

Figure 4. 8: Seasonal erosivity and rainfall amounts of recorded events at the Getadar station

Table 4. 3. Rainfall characteristics for categorized precipitation events at the Getadar station, from 2003 to 2012

	Rainfall event category (mm)						
Rainfall variables	0-10	10-20	20-30	30-40	40-50	50-60	>60
Number of events	691	138	45	33	6	5	9
Average rainfall depth (mm)	4	13.9	23.7	34.3	47	54.7	77.2
Percentage of total rainfall amount (%)	33.8	23.65	13.17	13.96	3.48	3.34	8.57

Winter events were characterized by lower amounts of rainfall (less than 36 mm) and lower erosivity values, with average EI_{30} = 19.12 MJ mm ha^{-1} h^{-1}. Despite the high number of events that occurred in Spring, only 12 % of them presented rainfall over 40 mm, with average EI_{30}= 62.6 MJ mm ha^{-1} h^{-1}. The highest number of significant events was recorded in Autumn, which were also the most erosive events. Summer

presented the lowest number of events; however, these events presented the highest erosivity values with average EI30= 146.1 MJ mm ha^{-1} h^{-1} (Figure 4.9).

4.2.6.2 Runoff

In this study, runoff datasets were analyzed to characterize the hydrological behavior of the Cemborain watershed on event-based, monthly, seasonal and annual time basis. Water levels were recorded every fifteen minutes at the gauging station, between September, 2005 and December, 2012.

Figure 4.10 shows the total annual runoff recorded at the outlet from 2006 to 2012. Annual runoff ranged from 73.4 mm. $year^{-1}$ in 2012 to 367 mm. $year^{-1}$ in 2007. Inter-annual variation is observed, mainly due to the inter-annual variation of precipitation amounts. High discharge values are usually related to high precipitations amounts.

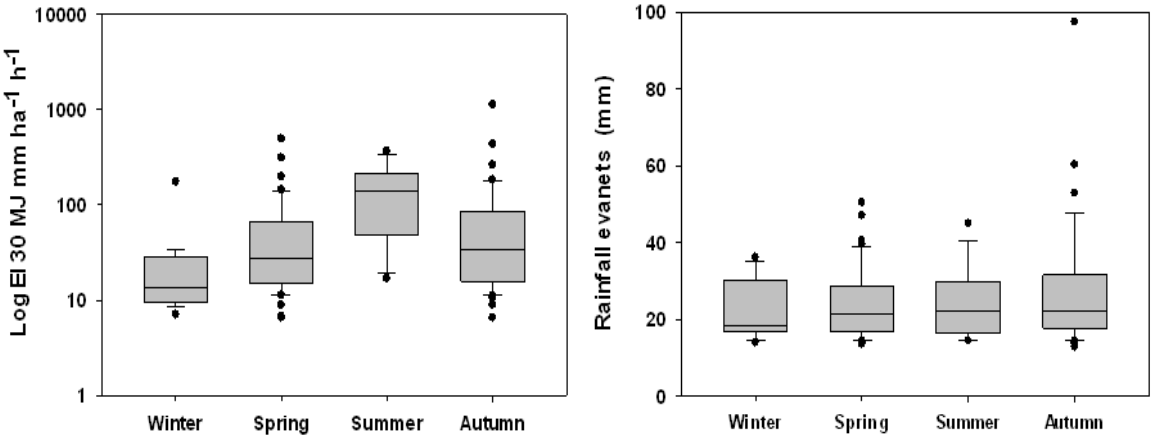

Figure 4. 9: Seasonal erosivity and rainfall amounts of erosive events

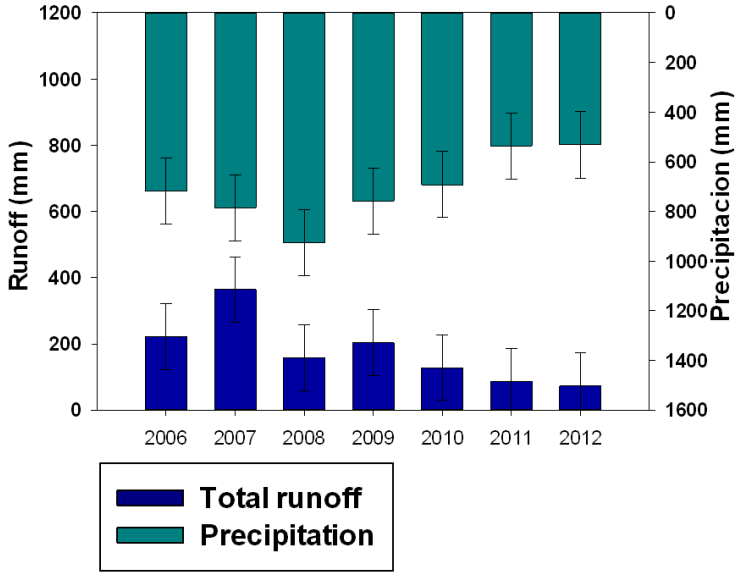

Figure 4. 10: Annual average runoff and rainfall at Cemborain.

Runoff discharge within the Cemborain watershed follows a seasonal pattern, with more than 90% of total runoff recorded during Winter (42%) and Spring (48%)(Right side of Figure 4.11). However Winter and Spring have the same runoff coefficient (0.4). Regarding Autumn, despite the precipitation amount being approximately the

same of Winter and Spring, runoff amounts were very low: 6.5 % of total runoff with a 0.06runoff coefficient. Summer is characterized by the lowest runoff discharge (3.5% of total runoff), which is directly linked to climatic characteristics (low precipitation amounts and high temperature and evaporation rates).

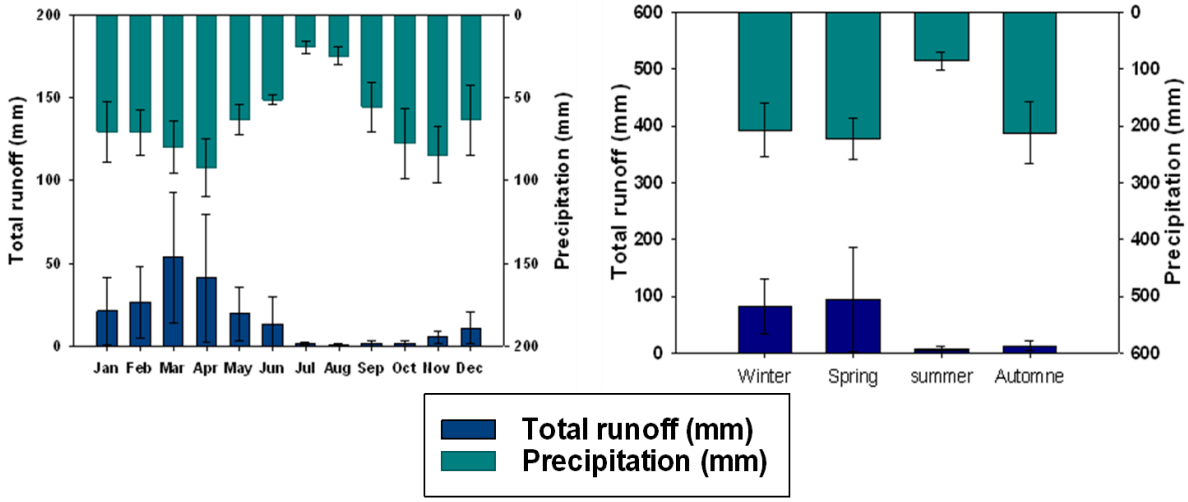

Figure 4. 11: Monthly (left) and seasonal (right) average runoff and rainfall at Cemborain

The left side of Figure 4.11 shows that, throughout January and March, runoff increased, reaching its maximum in March, with more than 53 mm .month^{-1}. Then, runoff declined reaching its minimum in August, with 0.9 mm .month^{-1}. From September to November, small amounts of discharge were recorded although significant precipitation events occurred. Thus, the runoff coefficient was very low in these months (0.03, 0.02 and 0.06 respectively). The depletion of soil water reserves during the previous dry and hot period (July and August), could be the cause for such low runoff coefficients. For instance, September, October and November received, on average, 55.6, 77.5 and 84.5mm, respectively, which represented 28% of annual precipitation. However, for the same months, average runoffs recorded were 1.62, 1.62 and 5.55 mm, respectively, which represented 4.5% of annual runoff. The high flow period from January to April coincided with a long rainy period, with continuous rainfall storms. Comparing monthly runoff coefficients, March and October presented the highest and lowest values (0.7 and 0.02, respectively). Similar conclusions were found by Serrano-Muela et al. (2008) for the San Salvador catchment (central-western Spanish Pyrenees), which presents similar climate conditions to the Cemborain watershed.

A hydrograph analysis was carried out to study the hydrological response of Cemborain watershed to rainfall events. To this end, hydrographs were drawn for four seasons, including storms of different intensities. Hydrographs were elaborated from 30 minute accumulated runoffs (Figure 4.12).

Long, low-intensity rainstorms characterize Winter and Spring, and hydrographs have a long duration in comparison with rainfall events, with slow reactions when runoff increases or decreases, and absence of clear peak flows. However, during Summer and Autumn, the hydrographs plotted were different, with a relatively acute peak flow and fast runoff increasing phase, followed by a fast flow decrease after the storm event ended. Hydrographs with intense peak flows were associated with high intensity rainstorms, where the amount of rainfall presented less importance.

During Winter and Spring, high runoff volumes were generated despite the small rainfall amounts recorded. However, Summer and Autumn presented low runoff amounts after big storm events. This could be attributed to previous soil moisture conditions, as soils are generally saturated during Winter and Spring and dry during Summer and Autumn.

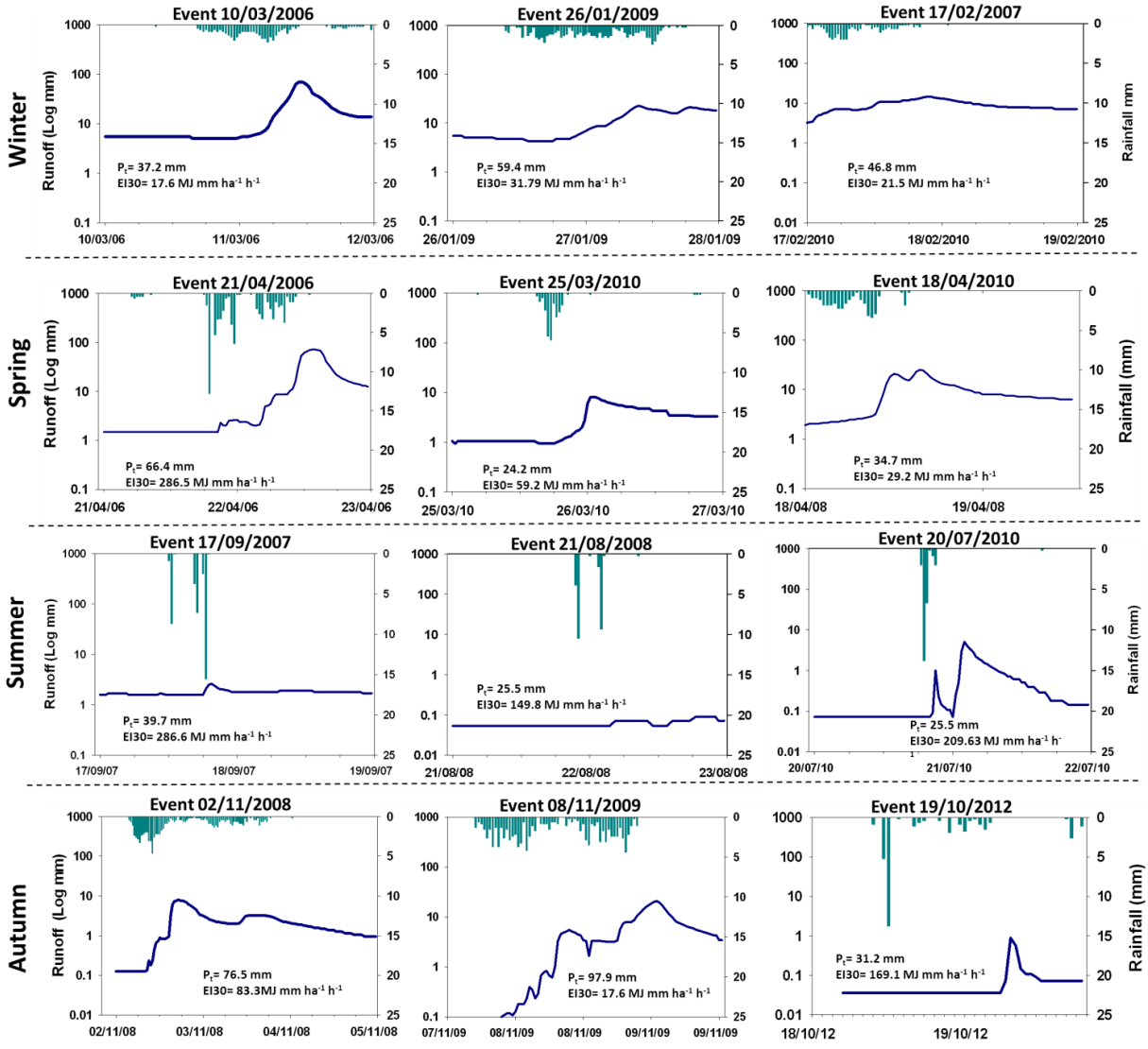

Figure 4. 12: Examples of hydrographs plotted for the Cemborain watershed, per seasons

4.3 Procedure for AnnAGNPS model evaluation

AnnAGNPS version 5.30 was used for the Cemborain watershed, to test the model's capabilities when simulating surface runoff. To this end, the general approach previously used at the Latxaga watershed (Chapter 3) was followed. Simulated sediment yield records were used as reference due to the absence of reliable, measured data.

4.3.1 Data acquisition

Basic data required for the assessment of AnnAGNPS were acquired from different sources (*e.g.*, total runoff data were acquired from the gauging station

installed at the watershed outlet). Observed data were compared to the outputs of the model to evaluate its prediction.

4.3.1.1 Climate data

As reported by Bingner et al. (2012), climate data required by AnnAGNPS can be provided by one main actual weather station or from a combination of weather station data. Herein, combined data from the three meteorological stations surrounding the watershed were used. The Barasoain and Oloriz stations provided only rainfall and daily temperatures, while the Getadar station provided complete climate inputs. The Oloriz station was considered as the main weather station as it presented the greatest influence area on the watershed, as previously shown after the application of the Thiessen polygon division method, while Barasoian and Getadar were secondary stations (Figure 4.6).

Therefore three climate input files "DayClim.inp" were created, with values of daily precipitation and minimum and maximum temperatures corresponding to the three station records, for the period 2003-2012. The remaining records (wind velocity, dew point and solar radiation) were acquired from the Getadar automatic station.

An improvement in climate input files has been incorporated herein with respect to the previous chapter when AnnAGNPS was evaluated at the Latxaga watershed: application of the RIST program to 10-minute rainfall records. RIST is a Windows-based program developed by the National Sedimentation Laboratory - USDA to facilitate analysis of time-and-date stamp tipping-bucket precipitation records (http://www.ars.usda.gov/Research/docs.htm?docid=3254). In fact, the Getadar meteorological station provides daily rainfall calculated by adding the 10-minute rainfall records throughout 24h, starting from midnight. These records do not consider the rainfall amounts of events occurred throughout two days or more; when this happens, the available daily records divide the event amounts in different events, according to the duration (number of days). A Rainfall Intensity Summarization Tool (RIST) was applied to the 10-minute rainfall records of the Getadar weather station, for appropriate reporting of rainfall condition to the daily climate inputs of AnnAGNPS and to avoid the division of events amounts. The RIST output consisted of daily rainfall records where events amounts were regrouped in one daily register. Within AnnAGNPS, daily precipitation is considered to be the prime driver of the hydrologic cycle.

Dew point temperature was calculated from the relative humidity recorded at the Getadar station, using the inverse of Tetens's equation (Chow et al., 1988), optimized for dew points in the range -35-50 °C.

Maximum 24-hour precipitation with a two-year return period was estimated from the Tafalla station, located approximately 10 km from the Cemborain watershed, with a value of 40.9mm (Ministerio de Agricultura Pesca y Alimentación, 1986). The global storm type for the three stations was determined by comparing rainfall distributions of the selected stations with American stations included in AnnAGNPS. The USA region that most closely resembled the local annual rainfall distribution pattern corresponded to the West Coast, and the global storm type selected for the three stations was "Ia".

4.3.1.2 Soil data

Required soil data for model simulation included soil types and texture, which were obtained from the soil map (Figure 4.2) and Table 4.1. The soil erodibility factor (K) was determined following Wischmeier and Smith (1978). Wilting point (Wp), field

capacity (Fc), saturated hydraulic conductivity and bulk density (Ks) of the different soil layers were computed by the Soil Water Characteristics Hydraulic Properties Calculator, developed by USDA-ARS and the Washington State University (Saxton and Rawls, 2006), based on the sand and clay percentages (Table 4.4).

Table 4. 4. Soil parameters required for model operation

Soil Types	K factor (T. h. MJ^{-1}. mm^{-1})	Wp (%)	Fc (%)	Ks ($mm.h^{-1}$)hr
Xerochrept Calcicxerollic	0.045	18.7	36.7	5.7
	0.045	18.7	36.7	5.7
Typic Xerorthent	0.042	19.3	36.6	5.7
	0.036	20.9	36	3.9
Lithic Xerorthent	0.037	23.4	39.2	2.9
Typic Xerofluvent	0.049	14.8	32.5	7.2
	0.035	21.4	36.2	3.4
	0.038	20.7	35.5	2.9
Typic Caciustepts	0.036	21.5	36.4	3.8
	0.039	22.8	38.3	2.1
Typic Hapludalf	0.045	18.7	36.7	5.7
	0.035	22	34.7	3.8

As showed in the soil map (Figure 4.2), six soil types were identified. Hapludalf Typic and Xerorthent Typic presented the same soil characteristics of Xerorthent Lithic and Xerochrept Calcicxerollic soils. This reduced the number of soil types considered to four (instead of six).

4.3.1.3 Land use and management

The Department of Agriculture, Livestock and Food of the Government of Navarre provided a land use map containing plot delimitations (Figure 4.4). Analyses were carried out on crop data within cultivated area as well as on rotation crop data provided from optical image classification (Landsat 5 TM and SPOT5). In fact, land use and cover maps were obtained by merging data from MCA ancillary information (common agricultural maps), annual crop statistics from SIGPAC (Geographic Information System of the EU Common Agricultural Policy in Navarre) and optical image classifications (Landsat and SPOT5) for the analysed years (Figure 4.13). this analysis was performed by other members of our research group.

4.3.1.4 Topography data

Within the AnnAGNPS model, the watershed is subdivided into different land areas with homogenous soil types, land uses, and land managements, referred to as "cells". Herein a 5m x 5m resolution DEM was used by the TopAGNPS program (Garbrecht and Martz, 2004) to divide the watershed into 1106 cells and 460 reaches using values from the critical source area (CSA= 4ha) and minimum source channel length (MSCL=100m). TopAGNPS also provided the subwatershed topographic parameters required by AnnAGNPS including slopes and lengths of cell areas and reaches. The combination of CSA/MSCL values enables the obtainment of a realistic representation

of the main drainage system. For a good land use representation, the ArcView interface enables the utilization of new CSA/MSCL values to reduce or increase cell areas. With the objective of highlighting the presence of small cultivated plots and urban areas within the Cemborain watershed, new CSA/MSCL values of 2ha and 50m, respectively, were applied to rural areas where small plots were located. 1138 cells were created, which were used as cell data input, as required by AnnAGNPS (Figure 4.14).

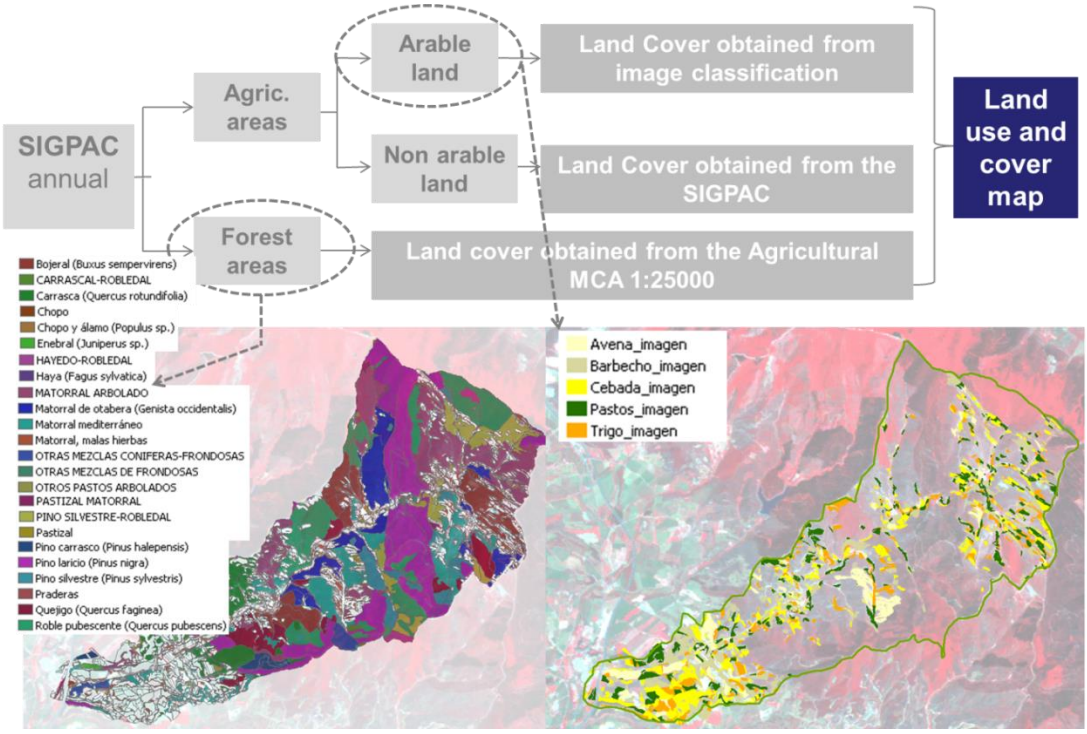

Figure 4. 13: Simplified procedure used to determine annual land use and cover for the Cemborain watershed

4.3.1.5 Hydrology

As aforedescribed, the Cemborain watershed was equipped with a gauging station that measured the total runoff at the outlet. The water level was measured every 15 minutes, enabling calculation of total runoff. As AnnAGNPS simulates only surface, automated recursive digital filtering of hydrographs (Eckhardt, 2005) was utilized to separate base flows from total runoffs (Figure 4.15), for comparison of predicted and measured surface runoffs.

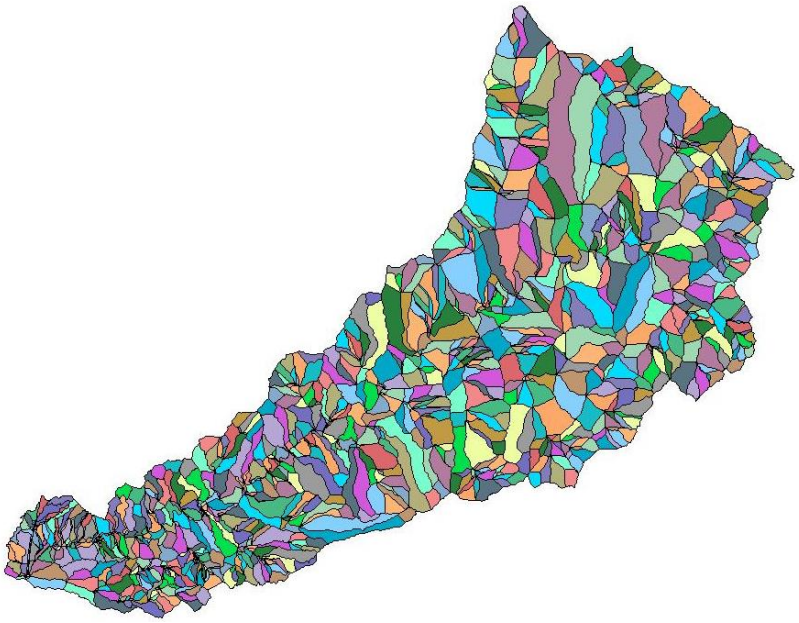

Figure 4. 14: Cemborain subwatersheds/ cell divisions

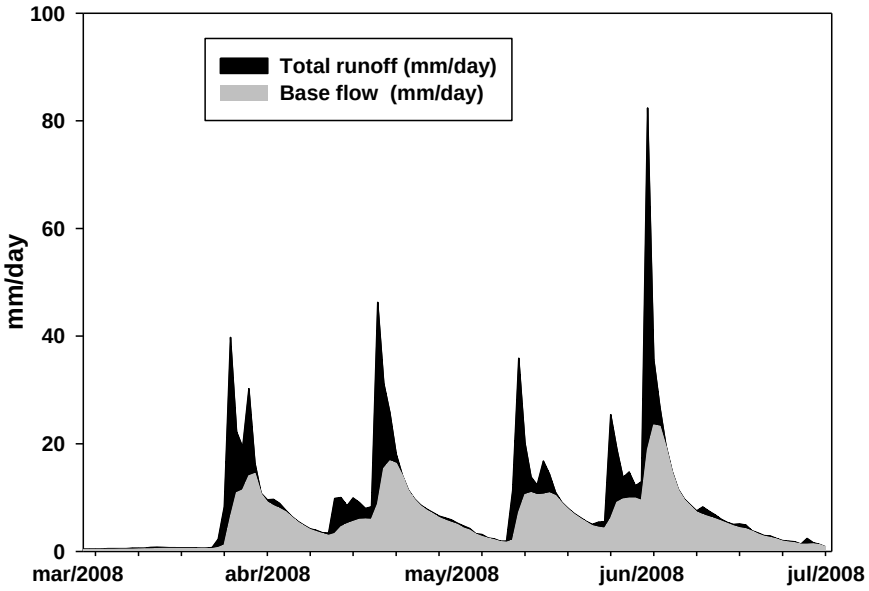

Figure 4. 15: Example of daily measured total runoff and calculated baseflow for the Cemboràin watershed (March 2008 - July 2008) (Eckhardt, 2005).

4.4 Model evaluation

4.4.1 Model calibration and validation

In general, model evaluation is carried out throughout a specific time period, during which calibration and validation periods are chosen on the basis of availability of measured dataset. Only surface runoff was considered due to the lack of reliable observed sediment load data.

Herein the AnnAGNPS model was evaluated using daily measured surface runoff data from September, 2005 to December, 2012. The starting date was selected due to the availability of 15-minute runoff records, which were not available prior to 2005. These records were used to separate surface runoff from total runoff. Model calibration

and validation were carried for two separate periods (Van Liew et al., 2003, Kim et al., 2007, Vázquez et al., 2008). The model was calibrated using 52 months of observed data, from September, 2005 to December, 2009. The period between 2010 and 2012 was used for validation. Sediment load data after runoff calibration were presented to provide a perspective on the watershed erosion behavior. A two-year (2003 and 2004) warm-up period was considered to reduce the influence of initial condition errors on model prediction. During this period, climate data of 2003 and 2004 were used to run the model and then discarded. Only the results of predicted daily surface runoff were used for calibration and validation.

4.4.2 Model performance assessment

During calibration and validation processes, model performance was evaluated by statistical and graphical analyses. Graphical analysis consisted of graphic presentation of the relationship between measured and predicted values (Legates and McCabe Jr., 1999), enabling an initial visual inspection of model performance (*e.g.*, scatterplot). Statistical analysis involved goodness-of-fit statistic indicators. The same indicators utilized at the Latxaga watershed (Chapter 3) were considered herein: Nash-Sutcliffe efficiency coefficient E (Eq. 3.8), modified Nash-Sutcliffe efficiency coefficient E1 (Eq. 3.9) and the percent bias PBIAS (Eq. 3.10) (Krause et al., 2005, Moriasi et al., 2007) at monthly, seasonal and annual time steps. Seasonal data was formed by grouping monthly data as follows: Winter (December, January and February), Spring (March, April and May), Summer (June, July and August), and Autumn (September, October and November). Another statistical method, a bootstrap method, was added with the objective of improving model performance assessment. In fact, Ritter and Muñoz-Carpena (2013) revealed that the interpretation of goodness-of-fit indicators can always be considered subjective. Thus, in order to reduce this subjectivity, the same authors integrated goodness-of-fit indicators (*i.e.*, Nash-Sutcliffe efficiency coefficient E) and its probability distribution using a bootstrap method. This methodology consisted of creating random sub-samples of observed data and corresponding simulated values, then calculating performance indicators for each bootstrap re-sample, enabling the construction of an empirical probability distribution of the E coefficient.

The bootstrap is a computer-based method introduced by Efron (1979) as a universal tool to obtain an approximation of the distribution of statistics. The general principle of the bootstrap process begins by generating a large number of bootstrap samples or re-samples that have the same number (n) of elements as the original dataset. Each re-sample is generated by sampling with replacement n times from the original dataset (Efron and Tibshirani, 1993). A MATLAB algorithm developed by Ritter and Muñoz-Carpena (2013) was used herein. Thus, monthly, seasonal and annual observed surface runoff and corresponding model predicted values were considered for the generation of 2000 bootstrap re-samples, using Politis and Romano (1994) block bootstrap method for stationary dependent data. Therefore, E was calculated for each re-sample to construct an empirical probability distribution of this statistical indicator. From the created probability distribution, a statistical test was carried out by considering a null hypothesis (H0). H0 represents the fact that if the median E value is lower than the E threshold value ($E < E$ threshold) then the goodness-of-fit is not acceptable. The alternative hypothesis (H1) considers it to be acceptable ($E > E$ threshold). Herein the E threshold = 0.50 was considered as the lower limit of a valid goodness-of-fit, as reported by Moriasi *et al.* (2007). If the p-value (representing the probability of obtaining $E< 0.5$) is lower than significance level $\alpha= 0.1$, then statistically significant goodness-of-fit results are acceptable, as suggested by

Ritter and Muñoz-Carpena (2013). For instance, when p-value > α= 0.1, H0 cannot be rejected and model fit is not considered acceptable. The algorithm also provides classification of the E coefficient within performance classes, as proposed by Moriasi *et al.* (2007): for 0.75 < E ≤1.00 very good, 0.65 < E ≤ 0.75 good, 0.50 < E ≤0.65 satisfactory and E ≤0.50 unsatisfactory.

4.4.3 Runoff calibration

According to previous studies that evaluated the capability of AnnAGNPS to predict surface runoff (Yuan et al., 2001, Shrestha et al., 2006, Licciardello et al., 2007, Shamshad et al., 2008, Das et al., 2008, Taguas et al., 2009) and also to the model assessment performed previously (Chapter 3) for the Latxaga watershed, the SCS curve number (CN) was the key factor in obtaining accurate predictions of surface runoff.

The AnnAGNPS model was executed for the period September, 2005-December, 2009, using different initial CN values (Table 4.4) corresponding to existing land use and crops as reported in SCS (1986). "CN-Wood", "CN-Grassland", "CN-Bush" and "CN-Residential districts" curve numbers (CN) represented Non-Crop land use for the forest, rangeland, shrubs and rural villages within the watershed, respectively. CN for "Row Crops (Poor)" and "Row Crops (Good)" was used for sunflower seeded in mid-April and leguminous seeded in December; CN for fallow land with residue was used when crop was harvested in Summer; CN for bare soil and orchard was used for seeded crop land in Autumn after tillage (winter cereal and rapeseed) and olive orchard land use (table 4.5).

Comparisons between observed and simulated surface runoffs revealed an underestimation of approximately 27.6% (PBIAS = 27.6). Results obtained for the first model simulation, considering only the Nash coefficient, yielded good performance according to Moriasi *et al.* (2007) for monthly, seasonal and annual predictions with E_m=0.71, E_s= 0.76 and E_a= 0.65, respectively (Figure 4.16). These results were beter than those obtained for the Latxaga watershed when surface runoff was underestimated, with E=-1.52negative Nash coefficient.

Table 4. 5. Initial CNs (SCS, 1986) and final CNs used for each land uses in Cemboràin watershed

Curve Number ID	Curve Numbers for hydrologic soil groups					
	Initial values			Final values		
	A	B	D	A	B	D
CN-Fallow	74	83	90	74	83	90
CN-Bare Soil	58	72	85	42	50	57
CN-Row crops(Poor)	72	81	91	89	92	99
CN-Row crops (Good)	67	78	89	85	95	99
CN-Grassland	49	69	84	No change		
CN-Residential districts	57	72	86	No change		
CN-Wood	36	60	79	No change		
CN-Brush	48	67	83	No change		
CN- Orchard	57	73	86	No change		

However, based on the boostrapping approach, surface runoff prediction varied from unsatisfactory to very good for the three analyzed time scales. Despite the satisfactory E values obtained, the statistical significance tests indicated that the fit

between observed and simulated surface runoffs before calibration were not statistically valid at monthly, seasonal and annual scales, with p-values equal to 0.162, 0.185, and 0.238, all above 0.1 (Figure 4.17).

Poor fit between observed and simulated surface runoffs was observed throughout the entire year. The highest overestimation of surface runoff was observed in November, September and October. The depletion of soil water reserves by the preceding dry period (July and August) due to absence of precipitation could be the probable cause, in addition to high water consumption by vegetation (more than 50 % of the area is covered by forest and shrubs). The same conclusions were drawn by Serrano-Muela *et al.* (2008) at the San Salvador catchment (central-western Spanish Pyrenees), which presents the same climate conditions of the Cemborain watershed. However, the model simulated that precipitation events at the watershed were sufficient to reach soil moisture saturation, and generated more surface runoff than what was observed. The highest underestimation of the model was recorded in April and March (Figure 4.17-A), despite the fact that these months are characterized by significant precipitation depth records. The model was not able to accurately predict surface runoff, displaying almost the same behavior at the Latxaga watershed (chapter 3), by overestimating surface runoff during Summer and Autumn and underestimating runoff during Winter and Spring (Chahor et al., 2014). Gastesi (2014) found that the model overestimated surface runoff in Autumn, while underestimation occurred in Winter at the La Tejería watershed.

When comparing seasonal time steps, the model underestimated surface runoff by 139%, 59% and 94% during Winter, Spring and Summer, respectively. Overestimation was observed in Autumn (54%) (Figure 4.17-B). The main differences were observed in Spring. In general, the trends towards underestimation or overestimation were present in all studied years, from 2005 to 2009.

These first results highlight the difficulties that the model experimented while predicting runoff within a totally cultivated watershed (such as the Latxaga watershed, with more than 90% of its area cultivated) in comparison with an area with a high noncrop percentage (such as Cemborain). Certainly, within cultivated areas the variation of canopy and residue covers from crop seeding to crop harvesting is significant, resulting in variations of crop evapotranspiration (ET) that affect moisture losses (Bingner et al., 2012) and runoff amounts. In addition, during tillage operation, soil transformations can affect the hydraulic properties of the soil by increasing percolation and decreasing runoff. For these reasons, CN adjustment during the calibration phase was focused only on CN values related to cultivated area.

A calibration process was required to approximate the observed and simulated surface runoffs. The model was calibrated by a trial-and-error process in which crop initial curve number (CN) values were adjusted until achieving the best fit between observed and simulated runoff volumes. Graphical comparison and statistical analysis were compared at monthly, seasonal and annual time scales (Shrestha et al., 2006, Licciardello et al., 2007, Shamshad et al., 2008, Das et al., 2008, Parajuli et al., 2009).

Model behavior was not uniform throughout the year in the prediction of surface runoff, with overestimation in Autumn and underestimation in Winter and Summer. A systemic increase or decrease in all initial CN values would affect the predictions made for the entire simulation period, without considering seasonal variation. The same approach utilized for model calibration within the Latxaga watershed was followed (introduction of new CN values when the model was not able to accurately predict surface runoff). It was tested whether adjustments of cultivated CN values improved model prediction results.

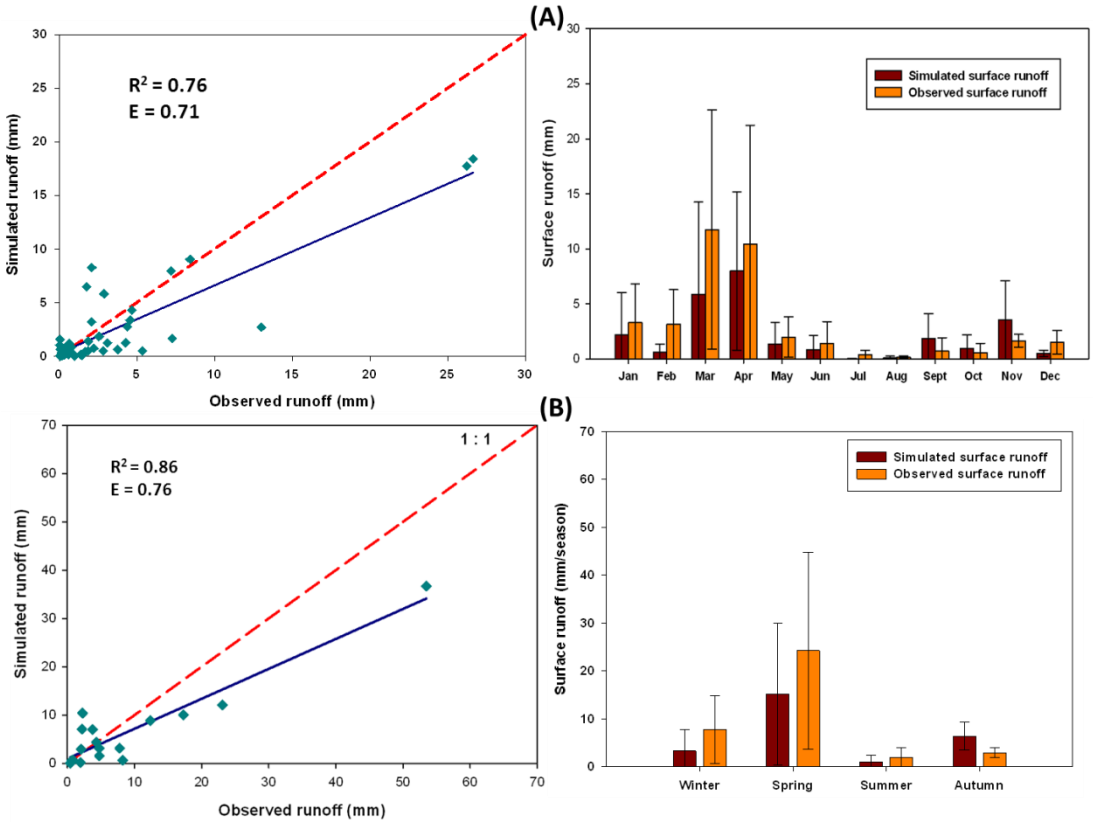

Figure 4. 16: Comparison between observed and simulated surface runoffs at monthly (A) and seasonal (B) scales before calibration

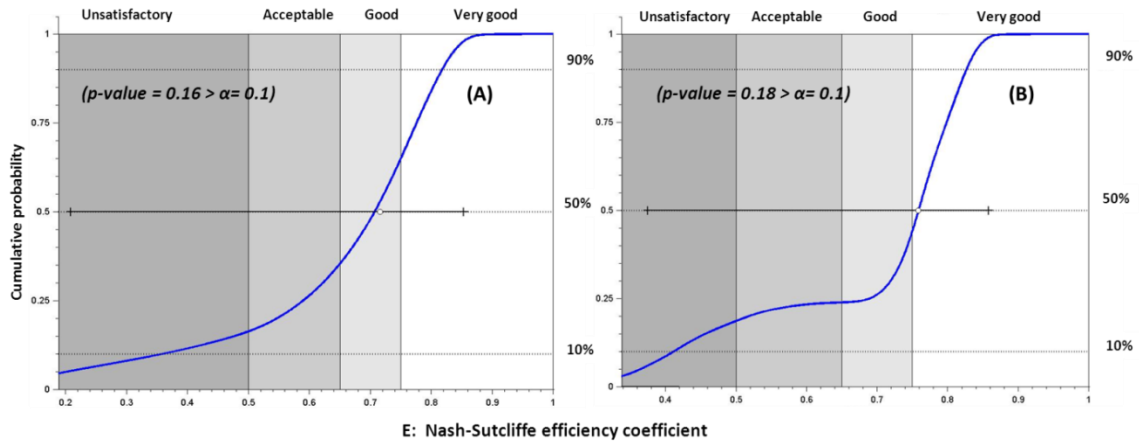

Figure 4. 17: Nash efficiency coefficient probability distribution obtained by bootstrapping and its corresponding statistical significance for monthly (A) and seasonal (B) surface runoff comparison before calibration.

As the majority of crops were seeded in Autumn, the initial "CN-Bare Soil" corresponding to soil preparation was decreased by 30%, to enable a reduction in the overestimation of runoff observed in this period. Such a decrease reduces the runoff predicted for Winter and Spring, further decreasing runoff underestimation in comparison with the actual situation. According to Bingner *et al.* (2012), within AnnAGNPS the average CN value changes slowly after planting and during the active growth phase, as the plant foliage develops and covers the ground. Therefore,

following the same procedure as for the Latxaga watershed, new CN values were introduced in the middle of December and end of March, for Winter and Spring. The objective was to adjust the underestimation of surface runoff during these seasons. Thus CN values for Winter and Spring were determined by increasing "CN-Row crops (Poor)" and "Row crops (Good)" by 20% and 15%, respectively (table 4.5). Increased CN for were used also for the crops seeded in Winter and Spring such as legumes and sunflower respectively. A noticeable improvement in model prediction was obtained after calibration at monthly, seasonal and annual time scales.

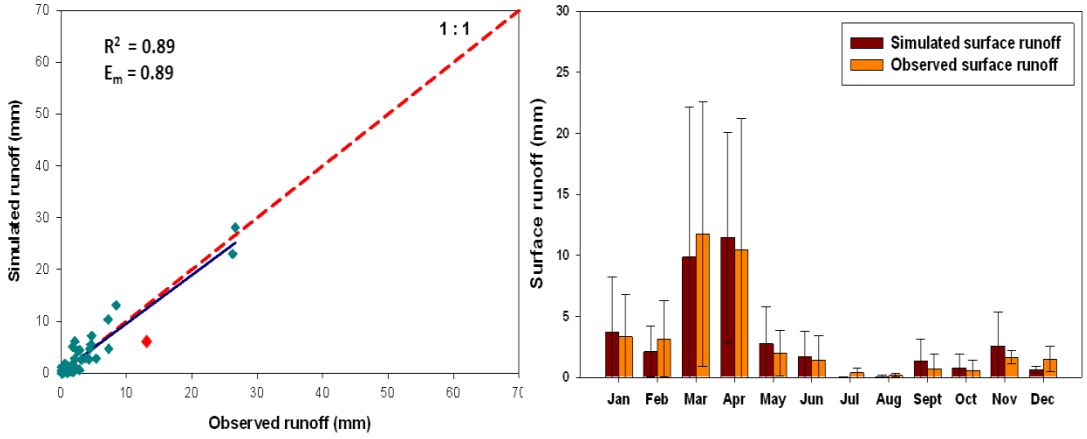

Figure 4. 18: Comparison between observed and simulated monthly surface runoffs after calibration

Figure 4.18 shows a very good prediction performance, with E ranging from acceptable to very good [0.57 – 0.97], with E_m= 0.89 (table 4.6) and 84% of fit probability categorized as very good. In this case (p-value = 0.017< α = 0.10), the null hypothesis H_0 can be rejected and the goodness-of-fit of the model at a monthly time scale is considered statistically valid (Figure 4.19). In addition, the value $PBIAS_m$=-6.3 indicates a slight overestimation bias of the model, but still within very good performance according to Moriasi *et al.* (2007). According to the "Q-test" statistical analysis (Rorabacher, 1991), monthly comparison revealed the presence of outliers that could affect the E coefficient. Other studies that evaluated AnnAGNPS for monthly runoff predictions obtained Nash efficiency coefficient between 0.55 and 0.95 (Licciardello et al., 2007, Das et al., 2008, Taguas et al., 2009, Parajuli et al., 2009, Abdelwahab et al., 2016).

Table 4. 6. Model performance indicators for calibration and validation of runoff in Cemborain

		Calibration				Validation			
		E	**E1**	**PBIAS**	**R^2**	**E**	**E1**	**PBIAS**	**R^2**
Monthly scale	**Runoff**	0.89	0.63	-0.61	0.89	0.43	0.38	-30.65	0.73
		E	**E1**	**PBIAS**	**R^2**	**E**	**E1**	**PBIAS**	**R^2**
Seasonal scale	**Runoff**	0.97	0.81	-1.39	0.97	0.71	0.47	-30.65	0.86
		E	**E1**	**PBIAS**	**R^2**	**E**	**E1**	**PBIAS**	**R^2**
Annual Scale	**Runoff**	0.97	0.79	-2.11	0.97	-2.09	-0.39	-30.65	0.99

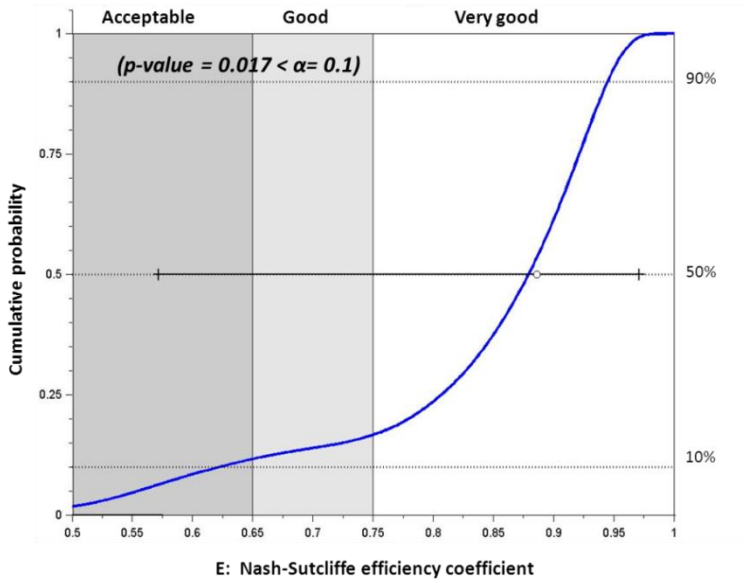

Figure 4. 19: Probability distribution of the Nash efficiency coefficient, obtained by the bootstrap method, and its corresponding statistical significance for monthly surface runoff comparison after calibration

The graphical comparison between observed and predicted monthly values shows an outlier corresponding to the value of March 2006 (red point on the left side of Figure 4.18), when the model underestimates surface runoff. During this month, especially between March 5th and 10th, 2006, precipitation amounts of 80mm and 100.6mm were registered by Getadar and Oloriz meteorological stations, respectively, with event amounts reaching 55mm. According to Yuan *et al.* (2001), AnnAGNPS is more inclined to underestimate runoff prediction, especially for large rainfall events. This can explain runoff surface underestimation during March 2006. Elimination of this outlier from the monthly data series did not affect the goodness-of fit indicator (E_m= 0. 90) (table 4.6).

Comparison between observed and predicted seasonal surface runoffs showed a very good model performance, with E_s ranging from acceptable to very good, E_s= 0.97 with 99.9% of probability of fit categorized as very good and p-value = 0, thus rejecting H_0. The negative $PBIAS_s$= -7 value indicates the model overestimated surface runoff, mainly during Autumn (Figure 4.20). CN Values corresponding to this period were decreased, taking into account realistic values. However, despite the low values attributed to CN, the model overestimated runoff especially for high precipitation records, such as in November 2008 and 2009, when 121 mm and 136 mm were registered, respectively.

The dry soil conditions of the soil, after a long dry period during summer (very scarce precipitations), promoted water infiltration instead of runoff. For instance, during Autumn, despite the significant precipitation amounts registered (almost equal to those recorded in Winter and Spring) the generated runoff was only 6.5% of total runoff amounts. This indicates a difficulty of the model to predict surface runoff in these conditions. Gastesi (2014) obtained the worst efficiency results after calibration in Autumn months.

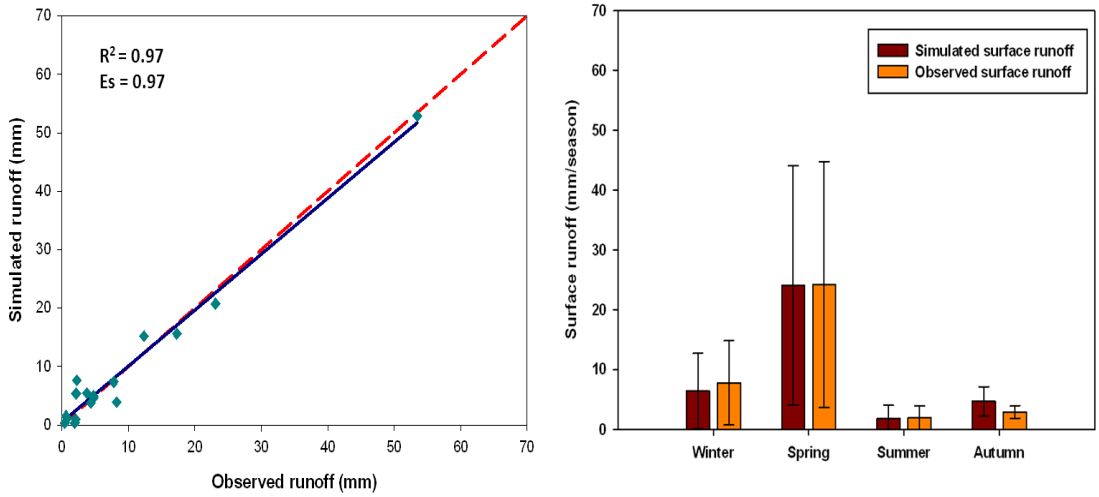

Figure 4. 20: Comparison between observed and simulated seasonal surface runoffs after calibration

Statistical significance tests indicate that annual model prediction performance can be considered very good, with E_A=0.93 (p-value = 0.037< α = 0.10) and $PBIAS_A$= -7.2 as result of surface runoff overestimation for years 2008 and 2009 (Figure 4.21). Annual results obtained at Cemborain were much better than those obtained at the Latxaga watershed.

Overall, the CN values utilized within the Cemborain watershed after calibration improved model performance with the highest efficiency coefficient values. The CN values after calibration were not very different from those found by Gastesi (2014), after model calibration in LaTejería watershed.

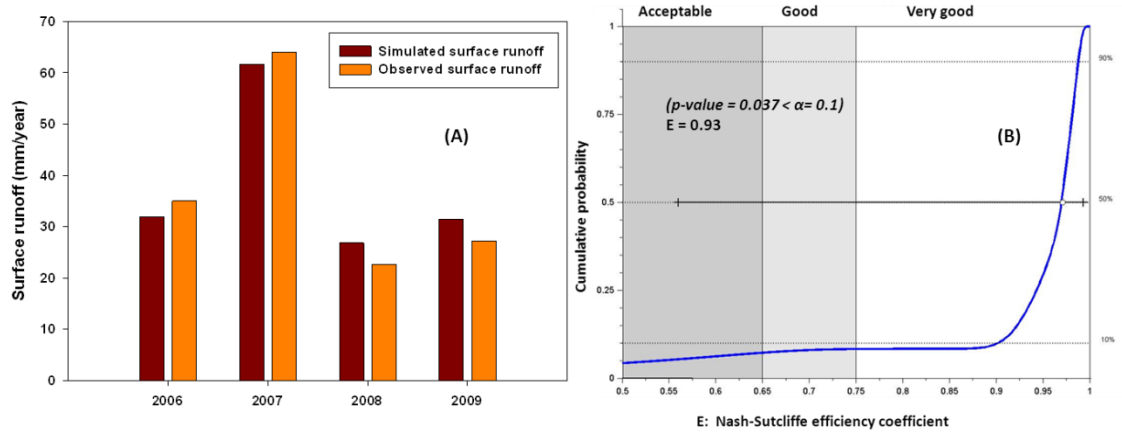

Figure 4. 21: Comparison between observed and simulated surface runoffs (A) and (B) probability distributions of the Nash efficiency coefficient at annual scale after calibration

4.4.4. Runoff validation

For the validation process, simulated and observed surface runoffs were compared throughout three years (from 2010 to 2012) using the same statistical assessment conditions.

Model performance on a monthly time basis was not satisfactory as in the calibration process, according to Moriasi et al. (2007), with E_m=0.43 (table 4.6), 65.2% of probability of fit is categorized as unsatisfactory and p-value = 0.65> α = 0.10

indicating that H_0 cannot be rejected, highlighting the poor fit between observed and simulated surface runoffs for the validation phase.

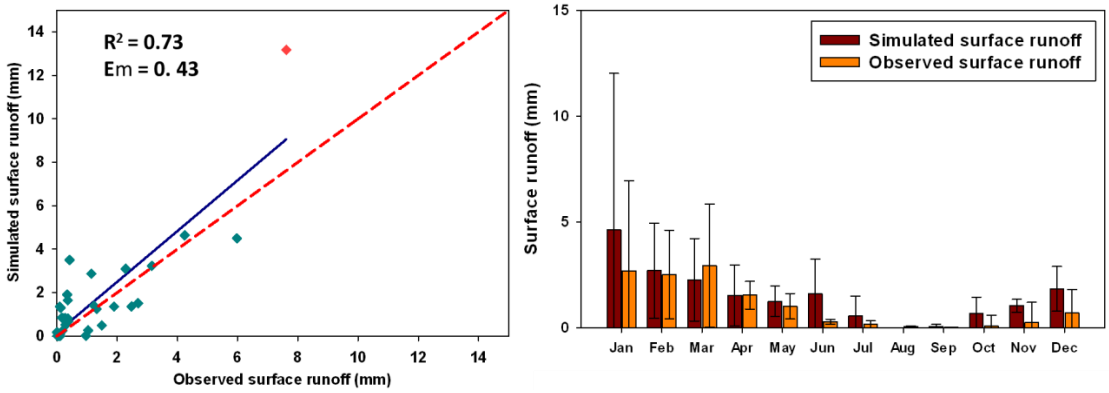

Figure 4. 22: Comparison between observed and simulated surface runoff at monthly scale for the validation phase

Graphical comparison between observed and simulated values revealed the presence of outliers (red point on the left side of Figure 4.22), corresponding to January, 2010, when the simulated surface runoff was overestimated by 73%. This overestimation could have been caused by snowmelt after an important event recorded on January 13th, 2010 with 63 mm of snow precipitation. Within AnnAGNPS, snowmelt is simulated using the daily temperature estimated from maximum and minimum temperatures, which might not correspond to the real temperature. This disparity in temperatures could result in incorrect estimation of snowmelt. Das *et al.* (2008) reported the same limitations when considering snowmelt in the Canagagigue watershed (Grand River basin in southern Ontario, Canada). Therefore an improvement in the snowmelt routine is suggested.

Elimination of these points from data series improves goodness-of-fit, with E=0.68 (table 4.6) but still not sufficient to reject the H_0 hypothesis (p-value = 0.17> α = 0.10). However, Parajuli *et al.* (2009) concluded that the performance of the AnnAGNPS model in the prediction of surface runoff on a monthly time basis ranged from fair to good, comparing model predictions with measured data during the validation phase in Goose Creek watersheds, with E= 0.69 and E=0.47 respectively.

Overall, the AnnAGNPS model tends to overestimate surface runoff with PBIAS=-30.7 mainly in June and July, where differences reached -435% and -233%, respectively. In terms of runoff amounts, January presented the highest recorded difference.

Better performance was obtained on a seasonal basis, varying from unsatisfactory to very good, with E_s=0.71 (table 4.6) being a statistically valid fit with p-value = 0.062 < α = 0.10 (Figure 4.23) and the 93.8% of probability of feet ranges between acceptable and very good. The most important differences were observed in Winter and Summer as a consequence of the differences revealed on a monthly basis.

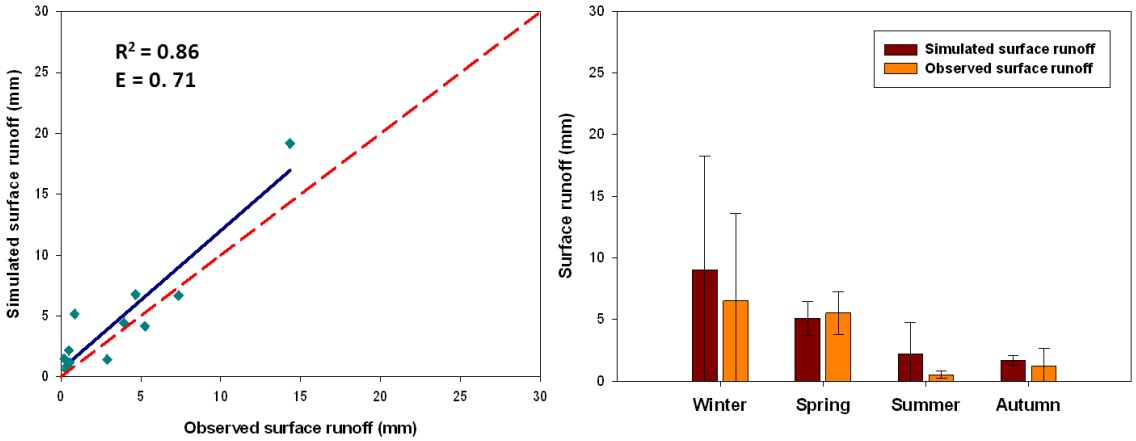

Figure 4. 23: Comparison between observed and simulated surface runoffs at seasonal scale for the validation phase

Finally, a poor correlation was observed between simulated and observed annual surface runoff with E=-2.09 due principally to the clear overestimation registered during 2010 reaching 63%. Existence of outlier at monthly basis was identified during 2010 (figure 4.24) which can explain the low quality of the simulations. In addition, the number of years for the analysis only three can make the analysis statistically no significant.

In general model shows low performance in validation phase comparing to the calibration at all time basis. Moriasi et al. (2007) reported that stricter performance ratings should generally be required during model calibration than during validation. This difference is recommended because parameter values are optimized during model calibration, but parameters are not adjusted in validation, which is possibly conducted under different conditions than those occurring during calibration. In addition, in this study the simplicity of the calibration procedure by varying only CN and considering only the cultivated area can explain the poor results in validation.

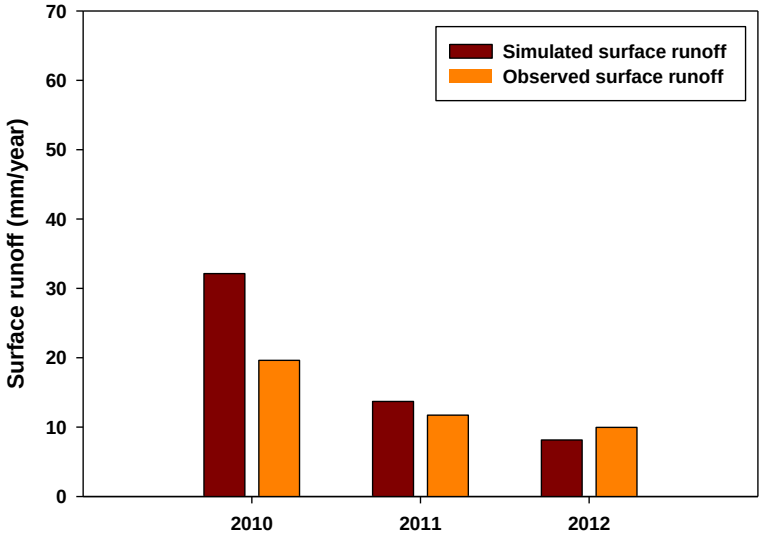

Figure 4. 24: Comparison between observed and simulated surface runoff at seasonally scale for validation phase

4.4.5 Sediment yield prediction

During the period when the model was evaluated for runoff prediction at the Cemborain watershed, unfortunately the lack of data sediment yield dataset was available. Therefore, only simulated sediment loads at the watershed outlet were presented herein. Input data after runoff calibration were utilized to simulate the sediment loads generated by sheet and inter-rill erosion for the entire studied period (2005-2012). The results obtained showed that the predicted annual average sediment load, 50.2 kg. ha^{-1}. $year^{-1}$, was very low in comparison to Latxaga watershed (341.5 kg. ha^{-1}. $year^{-1}$) even very low than the entire forestal watershed of Oskotz 706 kg. ha^{-1}. $year^{-1}$ (Casalí et al., 2010). The presence of a large area of forest and shrubs within Cemborain has a clear effect on the erosion process, providing continuous soil protection. On a seasonal time basis, it was observed that Spring is characterized by the highest sediment load amounts (Figure 4.25-A), although usually soil surface is at its maximum protection against erosion in Spring. This could be due to the high runoff amounts recorded in Spring. In Autumn and Winter, however, the erosion process can really affect soil surface because of the absence of soil protection (bare soil after tillage and low forest canopy cover), causing sediment loads. The low runoff amounts during these seasons did not have sufficient force to transport all the produced sediments to the watershed outlet. The sedimentation processes therefore take place within watershed cells and reaches. However, during Spring, runoff amounts were important and presented sufficient force to transport previously deposited sediments to the outlet of the watershed.

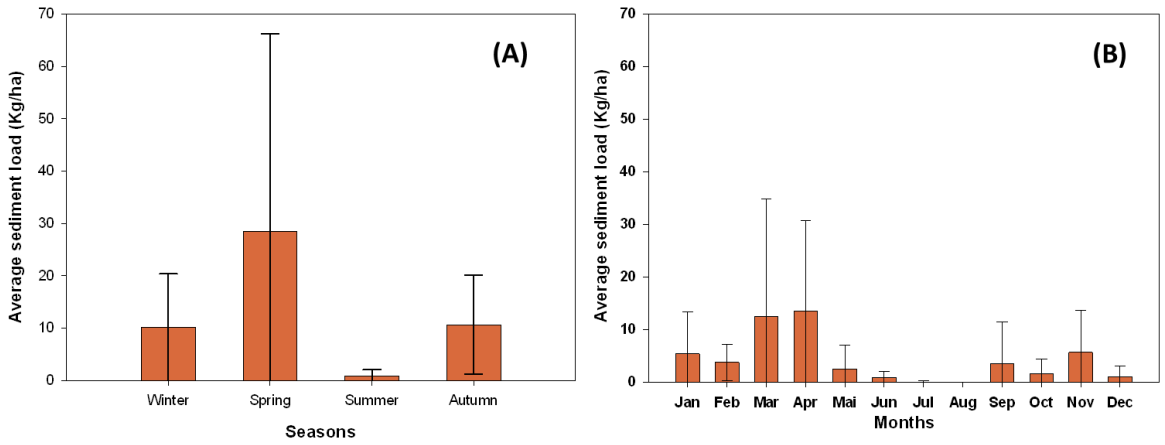

Figure 4. 25: Seasonal (A) and monthly (B) simulated sediment loads for the Cemborain watershed, from 2005 to 2012

On a monthly time basis, results show that March and April (Figure 4.25-B) presented the highest sediment load amounts, coinciding with the months with highest runoff amounts. A high correlation was observed between sediment loads and runoff amounts on a monthly time basis, with R^2=0.90 (Figure 4.26).

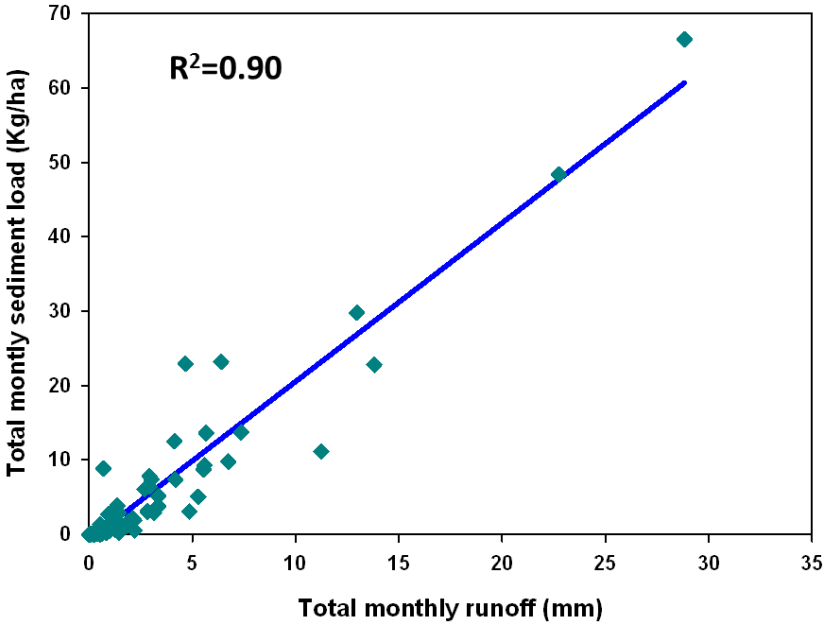

Figure 4. 26: Simulated total monthly sediment load vs. total monthly runoff for the Cemborain watershed, from 2005 to 2012

Chapter5: Evaluation of EG location prediction with AnnAGNPS PEG tool by Compound Topographic Index (CTI) and critical Compound Topographic Index CTIc

5.1 Introduction and objectives

The TIEGEM model (Gordon et al., 2007) has been incorporated into the AnnAGNPS model to predict EG erosion and to evaluate the effect of agricultural conservation practices on EG erosion within agricultural watersheds. As mentioned in Chapter 3, within TIEGEM, EG starts at the location referred to as *mouth* and then travels upstream.

Therefore the precise location of the gully's mouth is critical when defining the associated parameters utilized in the simulation of EG dynamics. Definition of the location of EGs in a watershed is a key issue and remains a challenge, and is also a preliminary step for other estimations such as headcut migration, gully length and eroded volume. When analyzing agricultural watersheds, many potential EG locations are possible, and modeling can be utilized to automatically identify EG locations. However, AnnAGNPS requires the location of ephemeral gullies to be manually defined throughout the watershed. This task is time consuming and users might not be able to locate and describe all EG locations accurately (Momm et al., 2012).

An automated GIS-based graphical interface tool to identify the location of areas prone to ephemeral gulling (Parker et al., 2007) was created when AnnAGNPS modules were integrated within the existing AGNPS GIS interface.

The automated Potential EG (PEG) identification is based on the Compound Topographic Index (CTI) (Thorne and Zevenbergen, 1990), which utilizes field topography. Generally, EGs are formed along swales, where surface and subsurface runoff converge to produce concentrated overland flow. (Thorne and Zevenbergen, 1990) verified that EGs form where there is sufficient magnitude and duration of concentrated surface flow to initiate and maintain erosion, leading to channelization. According to Thorne et al. (1984), the concentration of surface runoff can be physically represented by the specific stream power, which is commonly utilized to represent flow intensity and predict sediment carrying capacity. The stream power is a function of discharge, slope and width (Parker et al., 2010) Drainage area is often used in geomorphic analysis instead of discharge - therefore, multiplication of drainage area by the slope yields a parameter that represents total stream power (Desmet et al., 1999, Parker et al., 2007).

Thorne et al. (1986) introduced a third topographic factor to stream power function: the Planform curvature (degree of flow convergence that determines the concentration of stream power on the soil surface). The level of convergence on the land surface controls the initial flow path geometry, and therefore also controls the initial channel location. More details on the mathematical calculation of the Planform curvature are provided by Zevenbergen and Thorne (1987).

The Compound Topographic Index (CTI) (Eq. 2.38) was developed to substitute concentrated surface runoff stream power at any point of the swale, and is the result of multiplying the three aforementioned parameters (Thorne et al., 1986).

The CTI approach was used in studies aimed at establishing a critical CTI (CTIc) value or CTI threshold value for a specific area (Parker et al., 2007, Taguas et al., 2010, Momm et al., 2012, Daggupati et al., 2013). The concept of a topographic threshold was widely used to predict the location of gullies (Moore et al., 1988,

Vandaele et al., 1996, Desmet et al., 1999, Poesen et al., 2011, Daggupati et al., 2013). Knapen et al. (2007) reported that concentrated flow erosion is generally considered to be a threshold phenomenon, similar to the threshold concept introduced by Horton (1945) and Patton and Schumm (1975). This concept states that incision only occurs where a threshold of soil resistance is exceeded. This critical value represents the intensity of concentrated overland flow necessary to initiate erosion and channelized flow within a specific set of circumstances (Parker et al., 2007). The formation of an EG occurs when CTI exceeds the critical value. CTIc designates the possible location of EG initiation or nickpoint where headcuts begin traveling upstream until reaching the EG's end. CTIc represents therefore the combination of drainage area, slope and land curvature at a specific point that originates a flow with stream power (A x S x Planc) that exceeds soil resistance, leading to EG initiation.

Existing studies consider only a *single* CTIc value, usually obtained by adjusting the CTI threshold until a value is found that fits the present EG mouth, which is then set as CTIc (Taguas et al., 2010, Momm et al., 2011, Daggupati et al., 2013). Parker and Bingner (2007) used the same method to find CTI values for grid cells at the start and end points of each EG in a field, and then averaging these values across the field and considering it CTIc. Parker and Bingner (2007) also found the CTI values for each pixel of a grid that contained the known location of an EG, then plotting these CTI values to find a base value that would result in the formation of a gully.

However, at this point it is necessary to distinguish between two different CTIc as the downstream and upstream ends cannot utilize the same CTIc value, as different processes are involved (Chahor et al., 2016). CTIc1 represents the minimum intensity of concentrated overland flow necessary to initiate an EG nickpoint, corresponding to the location of headcuts whose migrations originate EGs (figure 5.1). CTIc2 represents the minimum energy of concentrated overland flow necessary for a headcut to migrate once it is created. CTIc1 could be related to the primary downstream headcut, whereas CTIc2 could be related to the end or actual position of the migrating headcut. CTIc1 would be useful for locating original headcuts, while CTIc2 would be useful for locating gully channels. This requires the acceptance of the fact that creating the incision head and enlarging the gully mouth requires more overland flow intensity than headcut migration itself because mainly different drainage area are involved in both situations (Figure 5.1).

This study considered two hypotheses to analyze the CTI-based method utilized to locate EGs. Firstly, it is only reliable to use CTI values as an index to quantify the susceptibility of a given area to EG provided homogeneous conditions of soil, land use, management and rainfall. However, since the latter is subjected in Mediterranean condition to important interannual variability, CYI is expected to be different along the time. Secondly, it is however feasible to determine a typical CTI for a homogeneous area as a result of averaging several years of measurement.

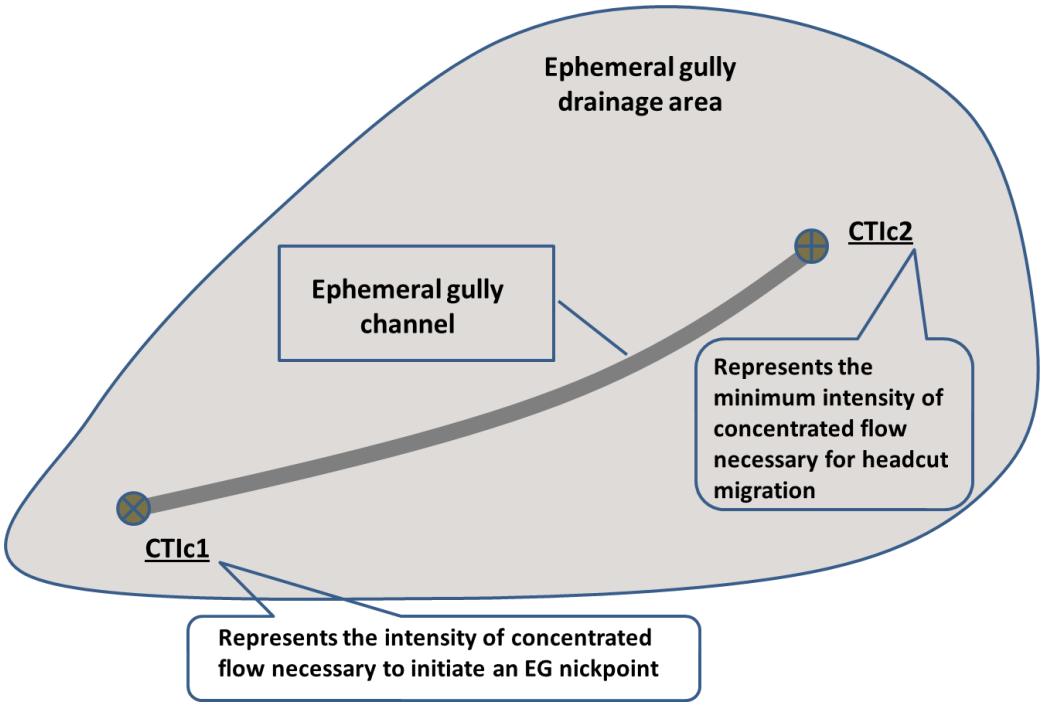

Figure 5. 1: CTIc1 and CTI2 within a classical EG channel

Some studies have evaluated the applicability of the CTI method for predicting the location of EGs; however these studies do not distinguish between CTIc1 and CTIc2.

CTIc applicability will be analyzed by reversing the habitual process, to test the two hypotheses aforementioned and verify the suitability and validity of the definitions of CTIc1 and CTIc2 (i.e., CTIc values corresponding to observed and existing EGs are obtained).

The existence of representative CTI1 and CTI2 values for large areas would fit well with the purpose and objectives of AnnAGNPS, which simulates the long term effects of management decisions.

The study presented herein is the first evaluation of the applicability of CTI to predict EG locations in Navarre (Spain), considering a homogeneous area in terms of soil, climate and land use. Thus the main objectives of this study are:

i) To verify whether the two aforementioned hypotheses hold true for a specific location in Navarre (Pitillas);
ii) To evaluate the possibility of a better EG characterization by introducing a new CTI critical value ($CTIc_2$)
iii) To analyze the applicability of the current CTI approach within the study area conditions.

To this end, an extensive area of 570 ha in the Pitillas region was considered; 310 ha of which were agricultural fields with homogeneous soil type, land use and management. Areas affected by EGs erosion were analyzed through orthophotos taken throughout eight years. Various EGs were identified and corresponding CTIc1 and CTIc2 values were calculated using LIDAR DEM 2mx2m and 5mx5m resolutions by AnnAGNPS/PEG interface.

5.2 Study area

The study area is located in the Pittilas district, in the central region of Navarre, approximately 50 km from Pamplona. The study area comprises 570 ha being 310 of them agricultural fields frequently affected by EGs and it is situated 5 km from the Pittilas village (Figure 5.2). Land-surface elevations vary between 346 m and 540 m above sea level, with different slope gradients. Cultivated lands are generally located in flat zones with variable slope gradients, however no cultivated areas are situated on hill slopes where slopes can reach 40%. Drains and channels were built to evacuate excess water runoff throughout the study area. Many of these drains were affected by erosion due to design problems or inappropriate location (Casalí et al., 1999). Natural and artificial stream networks flow to the Pitillas Lagoon, an endorheic basin. Studies carried out at the same area have detected soil erosion caused by concentrated flows in agricultural areas (Casalí et al., 1999, De Santisteban et al., 2006).

The capability of the AnnAGNPS model to predict the location and erosion of ephemeral gullies will be evaluated at the study area, which was selected due to the repetitive and continuous formation of EG in the area and the conventional agricultural activities carried out at this location. Also, previous studies were carried out by our research team on the analysis of EG erosion processes at Pitillas. According to De Santisteban (2003), Pitillas was classified as an experimental laboratory, in natural settings, for the study of EG erosion. A description of the study area is presented next.

5.2.1 Soil

Consultation of a geological map of Navarra, at 1/25000 scale, provided a simple description of geological materials. The central part of the study area is constituted essentially of a Quaternary period Glacis that extends over most of the flat land adjacent to the Pitillas Lagoon, with a small outcrop of continental Tertiary sandstone and siltstone. From North to South, siltstone and clay substrate (continental Tertiary) dominate until reaching the Lagoon substrate in the South. The occidental part of the Lagoon is covered by intercalations of Quaternary Glacis and strip of continental Tertiary siltstone. The soil texture is loamy and clay loamy in the lower layers, and in the topsoil, loam is the most abundant fraction, which reaches 42-62 %. These soils are particularly rich in sodium salts that promote the formation of surface crust. Increases in soil water include dissolved salts from the groundwater level, causing the dispersion of clay in the soil, increasing vulnerability to water erosion.

Soil samples from the study area were analyzed by Casalí (1997) and De Santisteban et al. (2003); the K factor for RUSLE ranged between 0.28 and 0.49, bulk density varied from 0.28 to 0.49, and saturated hydraulic conductivity reached 54 dS/m.

5.2.2 Climate

The climate of the Pitillas region is continental Mediterranean, moderately wet in spring and dry in summer. According to the nearest meteorological station, "Olite-INTIA", the mean annual temperature is approximately 13.6 ºC, with maximum temperature recorded in July (31ºC) and minimum temperatures during December and January (1.3ºC) (Figure 5.3- A).

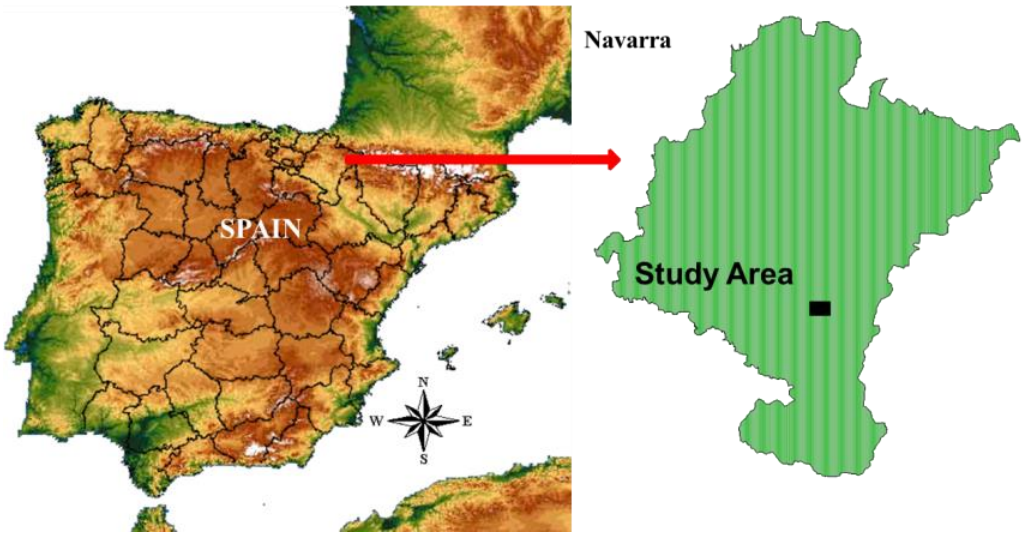

Figure 5. 2: Approximate location of the study area within Navarre

The Olite-INTIA station is 5 km from the study area, which presents mean multi-annual precipitation of approximately 512 mm. The annual mean potential evapotranspiration was estimated at 2448 mm/year, with 50% recorded during summer. Water balance has been in deficit throughout the entire year, which is a characteristic of the dry continental climate (Figure 5.3- B). Rainfall erosivity factor (RUSLE *R-factor)* (Wischmeier and Smith, 1978) and 24 h rainfall for a 10-year return period are, respectively, 50 hJ cm.m^{-2} h^{-1} year^{-1} and ≥ 90 mm (De Santisteban et al., 2006).

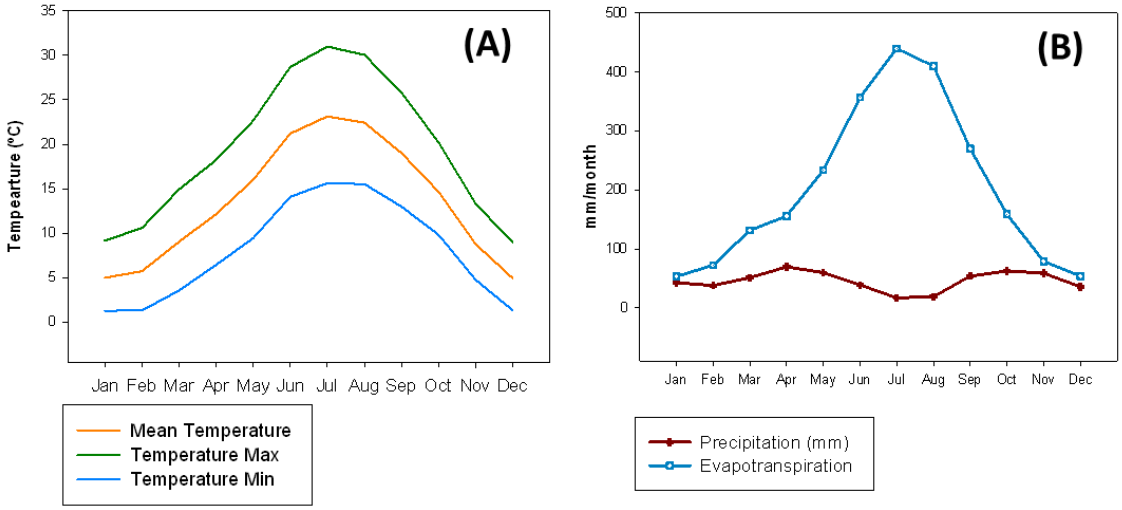

Figure 5. 3: Monthly temperature averages (A) and water balance (rainfall vs. potential evapotranspiration) (B) at the Pitillas zone

Data provided from *Olite-INTIA* metrological station were used to analyze rainfall behavior in the study area. Daily precipitations for the period 2003-2012 were used to study the monthly and seasonal rainfall distribution. Figure 5.4 depicts seasonal and monthly rainfall distribution at the study area throughout ten years. Spring is the wettest season with 33.9 % of annual precipitation, meanwhile summer is the driest season with 15.7% of precipitation. Autumn and winter presented, respectively, 28.2% and 22.2 % of total annual precipitation

Rainfall distribution varies monthly as well as annually. Analysis of rainfall monthly average in the period 2003-2012, as shown by Figure 5.3, reveals that the wettest month was April with 69.6 mm and the driest month was July, with 17.2 mm.

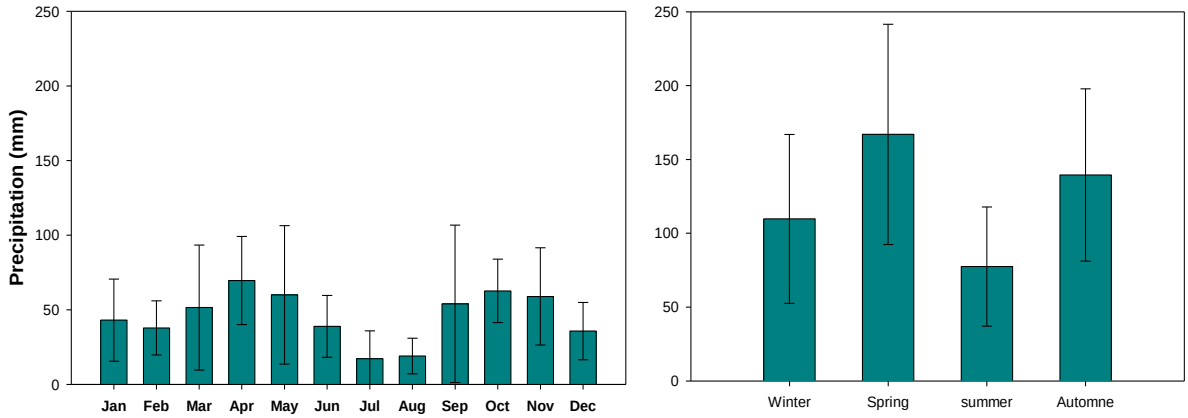

Figure 5. 4: Monthly and seasonal rainfall average in Pitillas (Olite-INTIA metrological station)

5.2.3 Land cover

At the study area, land cover varies according to the geomorphology of the field. The main types of land cover identified include shrubland located essentially at highlands, and areas with high slope gradient, consisting principally of autochthon plants that are tolerant to high soil salinity and adapted to steppe conditions (Figure 5.5).

The study area also includes cropland situated in the lowlands, with moderate slopes. Fields are cultivated with winter cereals (wheat and barley) often with conventional tillage, although recently no tillage practices were introduced. Farmers usually sow in Autumn (October), after preparing the seedbed with a mouldboard plough or chisel. Common practices include leaving fallow plots and introducing rotations crops (sunflower and leguminous). Average cereal yields are low, approximately 3000 - 4000 kg /ha year, with high inter-annual variability.

Figure 5. 5: General view of the study site (Pitillas Navarre)

5.3. Selection of observed EGs and identification of corresponding CTIc1 and CTIc2 values

CTI Calculation

CTI values are computed by following several steps. Firstly, the study area data is converted from Digital Elevation Model (DEM) into a raster GRID format,by TOpographicPAramateriZation (TOPAZ), driving and measuring the slope and accumulated upstream drainage area in each raster grid. The Planform curvature is computed by an internal curvature function of ArcView, using a moving 3×3 altitude sub-matrix to determine the curvature of the terrain at individual raster grid cells from digital elevation grids. A full quadratic polynomial equation is utilizes to account for elevation values at the nine individual raster grid cells considered (Zevenbergen and Thorne, 1987) (Figure 5. 6).

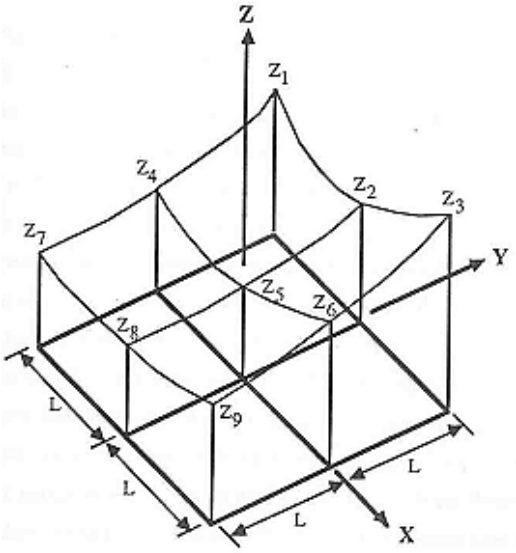

Figure 5. 6: Altitude sub-matrix used to determine topographic parameters from digital elevation grids (Source: (Parker et al., 2007).

CTI values for each raster grid cell are then obtained by multiplying the three topographic parameters: upstream drainage area, local slope, and planform curvature. Only positive CTI values (indicating swales) are considered as possible locations for gully formation. Negative CTI values indicating a concave surface (ridge) are overwritten to CTI = -1 (or no valid data). At the end of the process, two new datasets are obtained: a table and a raster grid. The table document contains the CTI values, number of raster grid cells with CTI values, and the cumulative count and percentile associated with each CTI. The raster grid graphically represents CTI values in categories of cumulative percentage values, where only those cells with cumulative percentage values over 90% are displayed (Figure 5.7).

Definition of the location of observed EGs within cultivated fields required long term monitoring, which was carried out from eight orthophotos (1:5000) with 0.5 m x 0.5 m resolution, taken in 2003 (17 Apr-20 Sep), 2006 (28 May), 2008 (19 Jun), 2010 (5-21 Jun), 2011 (25 Sep), 2012 (23 Jun), 2013 (24 Jul) and 2014 (17 Aug). The position of small channels was digitized, with identification of downstream and upstream ends, which were also georeferenced and measured (length). All photos were taken approximately at the same time of the year, usually in Summer. We can assume that most of the aerial survey dates (see above) had been carried out before obliteration of EGs by conventional tillage.

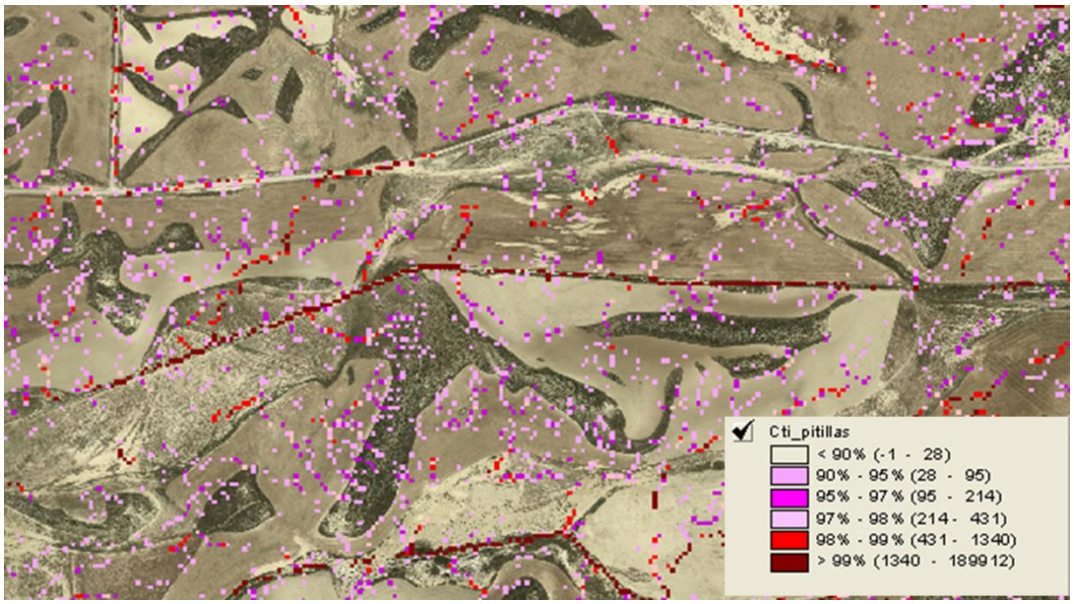

Figure 5. 7: Example of raster grid dataset containing CTI values

The high resolution of the orthophotos along with knowledge of the land simplified the identification of gullies in the orthophotos. These are public domain orthophotomaps (http://www.navarra.es/appsext/tiendacartografia/seleccion_hoja.aspx?idp=21).

Determination of the location of EGs from orthophotos was based mainly on previous knowledge of EG sites within the study area, and also on the identification of color changes between EG channels and the remaining plot. Along the EG flow path, generally the cultivated crop is eliminated due to concentrated flow action, and therefore there is evident contrast of colors between cultivated and non cultivated areas. This facilitates detection of EGs within cultivated fields (Figure 5.8). Momm et al. (2012) used field inspection and historic aerial photograph interpretation to compare generated EGs locations with observed ones.

Using a GIS interface, the visible EG downstream in the orthophoto was designated as an EG mouth, corresponding to CTIc1. Upstream or at the end of the observed EG, the headcut corresponding to CTIc2 was identified. EG paths were manually located, digitized, and gully lengths were measured. After EG location, drainage areas for each EG were determined using both 2m and 5 m DEMs resolutions, followed by classification into classical or drainage EGs. Classical EGs, considered as the prototype EG, are formed by concentrated runoff flows within the same field where runoff started (drainage area is homogeneous in term of soil and land cover). Drainage EGs "are created by concentrated flows draining areas upstream of the field" (Casalí et al., 1999) (Figure 5.1).

Only classical EGs were studied (drainage EGs were excluded) as the CTI approach was designed to simulate only classical EGs. The CTI of the study area was calculated using 2m and 5m DEMs within a raster grid to determine $CTIc_1$ and $CTIc_2$ values. Using an GIS interface, the CTI values for each EG start and end were determined by superimposing the layers containing the CTI values (raster grid) with the layer containing EGs start and end points. CTIc1 and CTIc2 were then determined for each (Figure 5.9). As the resolution of DEMs and orthophotos were different, there could be an error embedded in the definition of grid cells that correspond to CTI in addition to user inaccuracy in the designation of EG start and end points of EG. Then two buffers, 2m and 5 m (DEM pixel dimension), were applied along the EG channel at the 2 m

and 5m DEMs, respectively, to minimize the embedded errors and maximize the conversion of collected points to CTI values.

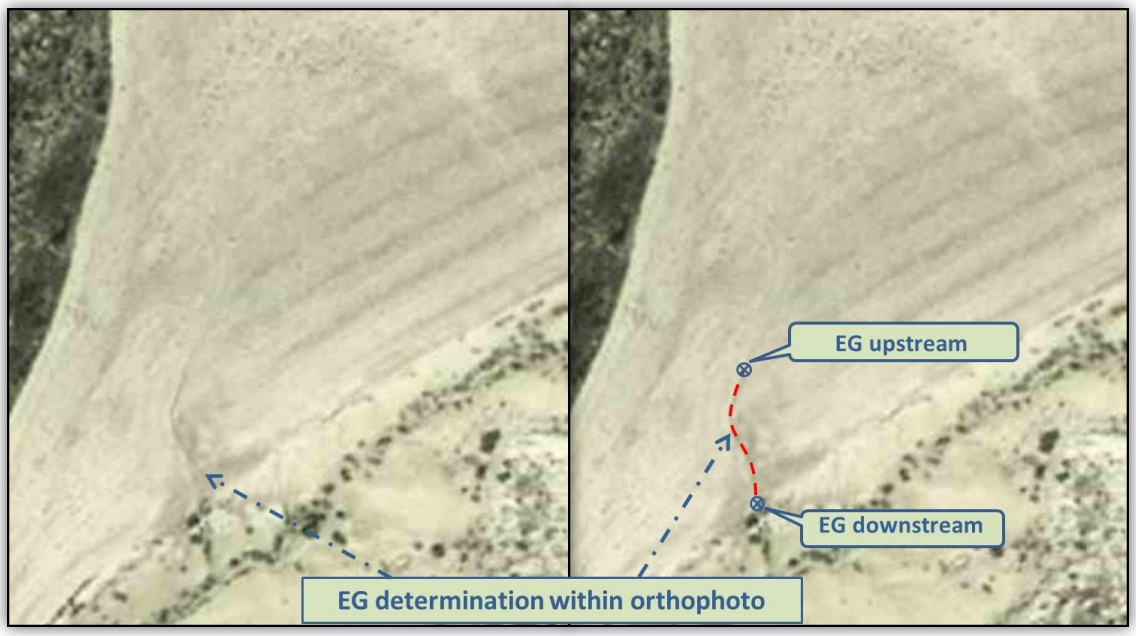

Figure 5. 8: Determination of EG location on an orthophoto (year 2014)

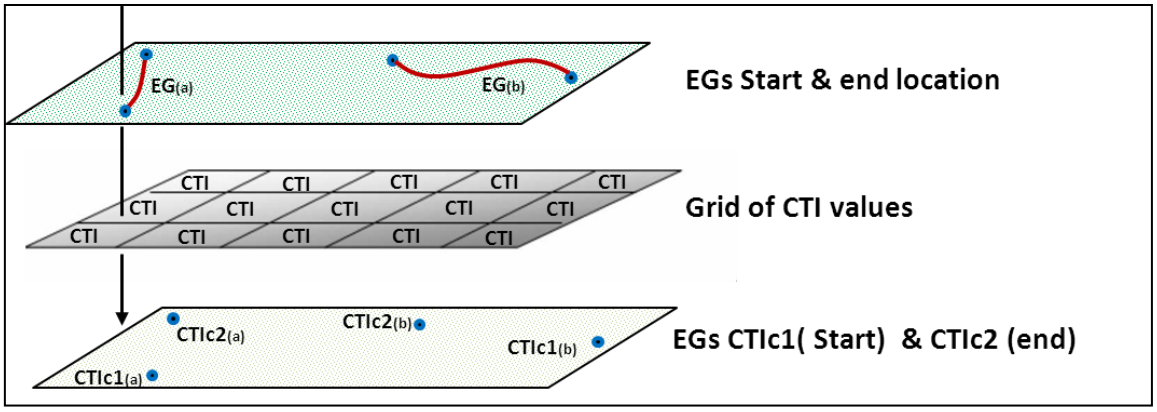

Figure 5. 9: CTI and EG layer superimposing

5.4. Spatiotemporal variability of CTIc1, CTIc2 and their applicability

Throughout the studied years, 58 small watersheds affected by EGs were identified. However, most gullies appeared only once, during the entire study period; these were excluded from this study due to unrepresentativeness. An EG should appears at least twice throughout the study period to be considered representative - those appearing only once were considered exceptional or unpredictable cases, and therefore not considered. After application of the representativeness criterion, 17 EGs were finally considered (Table 5.1).

Repetitiveness of EGs presented high inter-annual variability; e.g., EG nº15 appeared seven times throughout the eight years observed. Of the 58 EGs observed, 41 appeared only once, five EGs appeared twice, six EGs appeared three times, two EGs appeared four and five times, and one EG appeared six times (Table 5.1).

Inter-annual variation was also observed for the positions and trajectories of EGs within the same EG watershed, showing flow paths, trajectories, lengths, starting and ending locations throughout the years (Figure 5.10). This could be due to the type and direction of tillage, other anthropic factors, or characteristics of rainfall events for each year. 2011 data were excluded from the analysis because the orthophoto was taken at the end of September, when the study area was probably tilled (causing EGs to refill). An unusually low number of observed EGs (only one) strongly supports this assumption. Therefore it is not possible to know the real number of EGs that appeared in this area. The 2003 orthophotos were multiple from mid-April to late on September, with a realistic number of observed EGs in relation to rainfall events, and therefore these data were valid.

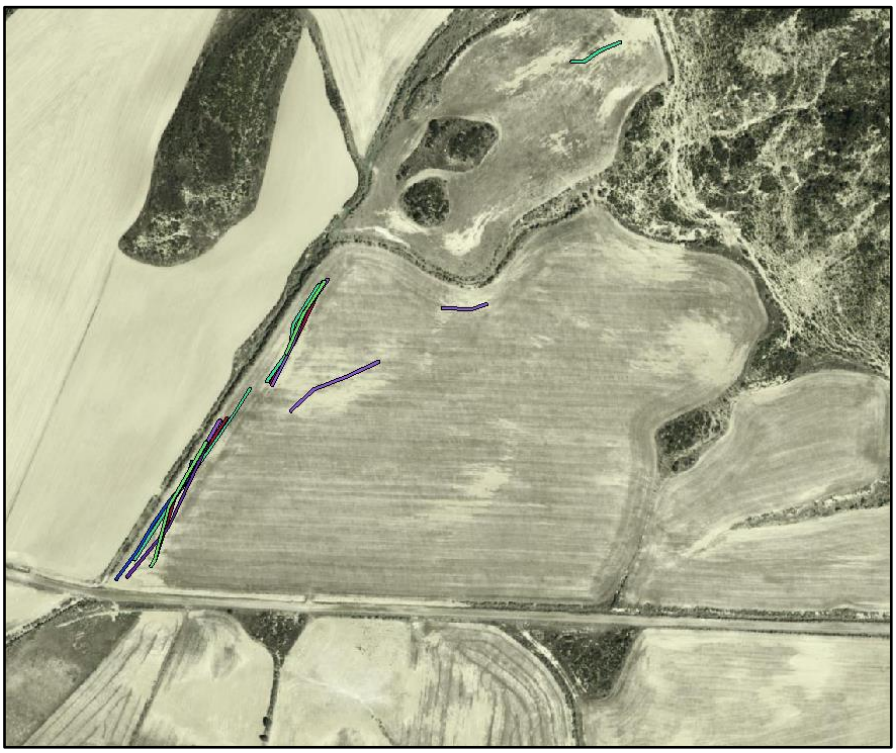

Figure 5. 10: Illustration of development of the same EGs in different years (colors) with different flow paths and start (downstream mouth) and end (upstream headcut) points

Length of EGs varied from 15.7 m to 181 m (maximum), which corroborates with the values reported by Casalí et al. (1999) and De Santisteban et al. (2006). A positive correlation was observed between the total precipitation during the agricultural year and total annual length of EGs, with a determination coefficient $R^2 = 0.85$ ($p\ 0.003 < 0.05$) (Figures 5.11 and 5.12).

Table 5. 1. Observed EGs during the study period, occurrence and classification (classical or drainage EGs) according to DEM resolutions 2m and 5m

EGs ID &	EGs lengths (m)	EGs	EGs classification

(number of times appeared)	2003	2006	2008	2010	2012	2013	2014	classification using 2m DEM & EG drainage area (ha)	using 5m DEM & EG drainage area (ha)
15 (7)		87.2	99.8	97.4	89.7	131.1	102.8	Drainage (11.0.8)	Drainage (26.58)
5 (6)		17.2	15.8	22.7	26.2	37.6	27.5	Classical (1.41)	Classical (1.26)
3(5)		59.9	139.5	101.6		180.4	73.5	Classical (0.68)	Classical (0.07)
16 (5)		52.1	76.3	68.9		70.9	72.1	Classical (0.26)	Drainage (20.56)
17 (4)		25.6		44.0		54.3	32.2	Drainage (3.91)	Classical (0.41)
23 (4)		33.6	34.4		123.9		112.9	Classical (0.44)	Drainage (161.21)
9 (3)			17.5			23.3	32.4	Classical (0.02)	Classical (0.19)
12 (3)	181.6	37.1					26.5	Classical (0.49)	Drainage (0.05)
14 (3)		82.2				45.1	75.6	Classical (0.77)	Drainage (16.10)
30 (3)			84.4	83.7		99.4		Classical (1.68)	Drainage (318.09)
35 (3)	110.1	37.5			24.3			Drainage (0.33)	Drainage (0.30)
38 (3)	111.6		55.4	98.8				Classical (1.09)	Drainage (3.78)
6 (2)						39.3	44.8	Classical (0.70)	Classical (0.62)
37 (2)				68.0	72.2			Classical (0.23)	Classical (0.07)
53 (2)	91.7	139.9						Classical (0.90)	Classical (0.08)
56 (2)	60.7	127.7						Drainage (1.23)	Classical (0.06)
57 (2)	131.8	76.7						Drainage (1.8)	Drainage (1.64)
4 (1)					82.5				
21 (1)					102.0				
32 (1)					44.4				
7 (1)							70.9		
8(1)							51.4		
11 (1)							32.5		
13 (1)							27.2		
18 (1)						97.1			
19 (1)						34.1			
20 (1)						86.0			
22 (1)						58.5			
24 (1)						67.3			
25 (1)						37.7			
26 (1)						30.8			
EGs ID & (number of times appeared)	EGs lengths (m)							EGs classification using 2m DEM & EG drainage area (ha)	EGs classification using 5m DEM & EG drainage area (ha)
	2003	2006	2008	2010	2012	2013	2014		

27 (1)						39.1			
28 (1)						89.0			
31 (1)						36.2			
33 (1)					64.2				
36 (1)				34.5					
40 (1)			8.8						
41 (1)			20.8						
42 (1)			21.7						
43 (1)			38.3						
44 (1)			17.4						
45 (1)			22.5						
46 (1)			51.0						
47 (1)			21.3						
48 (1)			49.1						
49 (1)			65.0						
50 (1)			28.6						
51 (1)		97.0							
52 (1)		44.5							
54 (1)		55.7							
58 (1)		151.6							
59 (1)	27.5								
60 (1)	35.9								
10 (1)	145.1								
29 (1)	91.9								
34 (1)	40.5								
39 (1)	74.0								
55 (1)	90.7								
Annual EGs number	13	16	19	9	9	19	14		

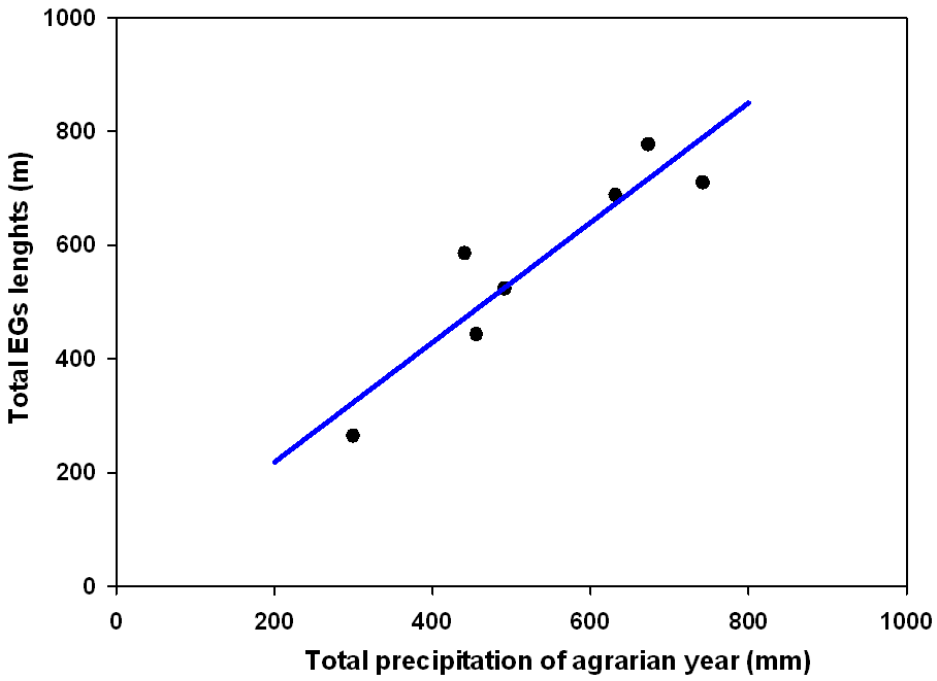

Figure 5. 11: Total precipitation of agrarian year (mm) vs. total EG lengths (m) throughout the studied years for EGs that appears more than 1 time

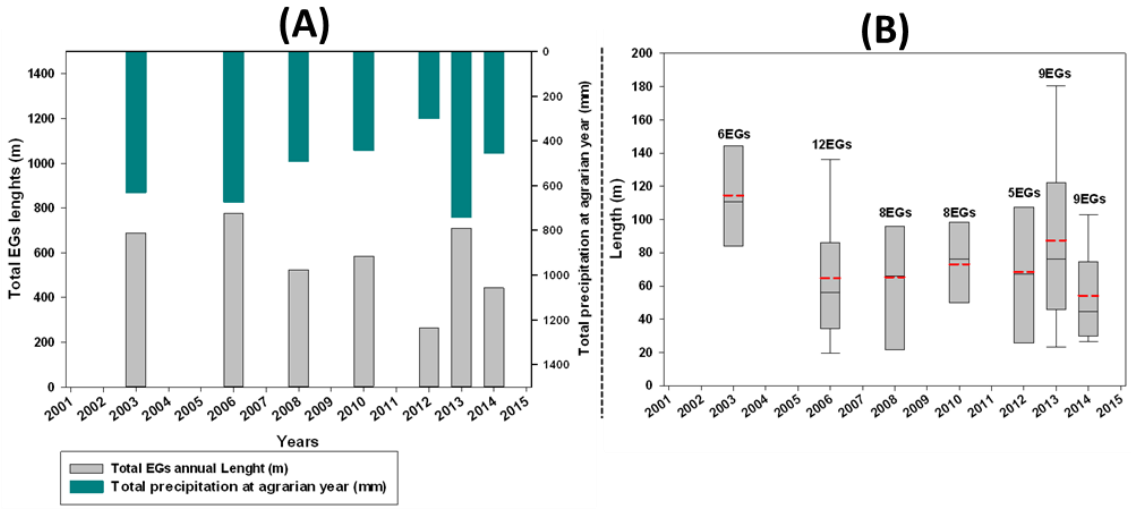

Figure 5. 12: Total EG lengths vs. total precipitation of agrarian year (A) and variation of EG lengths (B) throughout the studied years

The agrarian year considered herein ranged from October to September (from sowing to tillage). Such high correlation between total precipitation and total EG lengths P and L is remarkable, as generally for this type of climate it is assumed that rainfall characteristics (*i.e.*, intensity of relevant events) are more important than total annual rainfall. As no measurements of total eroded volume were available, EG lengths have been considered as a substitute for EG volume (Figure 5.13). The relationship between EG lengths and volumes was established in accordance with previous studies (Casalí et al., 1999, De Santisteban et al., 2006) that monitored the same study area (and its EGs) throughout several years. Figure 5.13 illustrates the high correlation between EG volume (V) and length (L), with R^2= 0.84. It should be noted that the coefficient of determination and the representative equation were

determined excluding outlier data, which represented measurements of a single EG formed in 2000 that presented a very unusual shape (very wide) (De Santisteban, 2003).

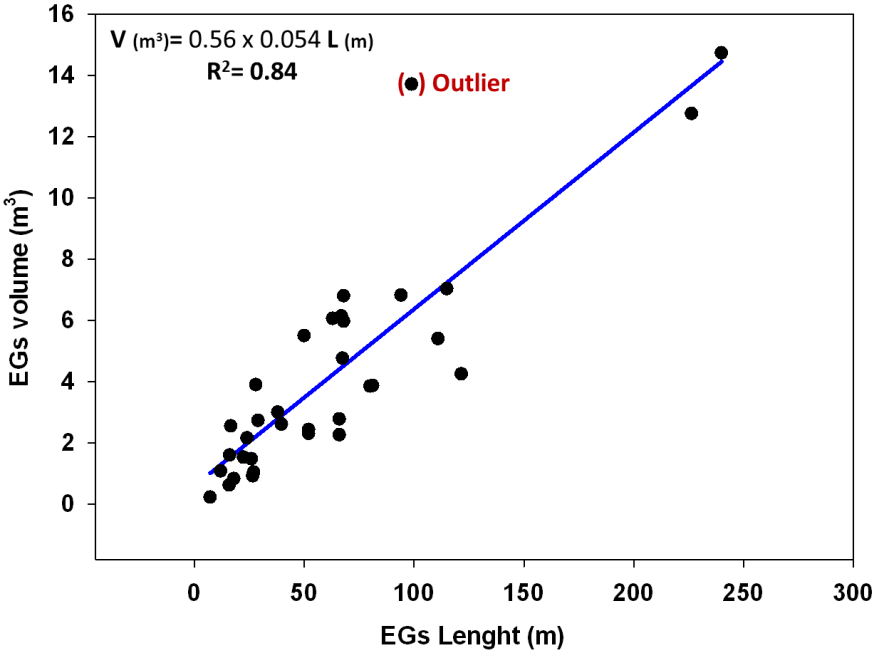

Figure 5. 13: Relationship between EG volume and length at the Pitilla region (Source : De Santisteban et al., 2006)

Using the 7 years available orthophotos it is possible to obtain convenient estimation of EG erosion wihin studied area once the relationship length-volume of the study is found (Chahor et al., 2017). This approximation has been previously explored (Nachtergaele and Poesen, 1999). Therefore, using the obtained equation between measured EGs length and volume (figure 5.13); it is possible to estimate the annual eroded volume within the study area (figure 5.14) considering only the agricultural field areas the average total soil losses during the seven studied years was 2.9 10^{-5} kg m^{-2} $year^{-1}$. Comparing to other studies obtained average soil losses can be considered as very low, for instance Grissinger and Murphey (1989) found that the average of EG soil losses for 2 years in watershed in northern Mississippi was about 2.1 kg m^{-2} $year^{-1}$. Lentz et al. (1993) report losses due to ephemeral gullies ranging between 0.08 and 1.6 kg m^{-2} $year^{-1}$ for three watersheds in Minnesota after 3 years.

After classification of selected EGs, 12 were finally classified as classical EGs using a 2m DEM, and only five were identified when the 5m DEM were used. The remaining EGs were categorized as drainage EGs. This difference in the amount of classical EG (11 *vs.* 5) can be mainly explained by the fact that the lower the DEM resolution, the higher the possibility of overestimating the drainage area of the EG and therefore, of including areas with different characteristics (defining unrealistic classical EGs instead of drainage EGs). By increasing DEM resolution, EGs that were initially classified as drainage are re-classified as classical. By increasing the details of topographic information, watersheds are more precisely determined, becoming generally (much) smaller (Table 5.1).

As a consequence, the uncultivated area that was initially classified as drainage EG was not located within the EG watershed, being re-classified as classical EG. Momm et al. (2013) indicated that DEMs generated at higher raster grid sizes have a limited ability to detect topographic variations that are smaller than the raster grid cell size.

For instance, at a low DEM resolution (5m) it is not possible to detect small streams, drainage channels, or other small forms. EG drainage areas are then frequently overestimated, and so are CTI values (Figure 5.15).

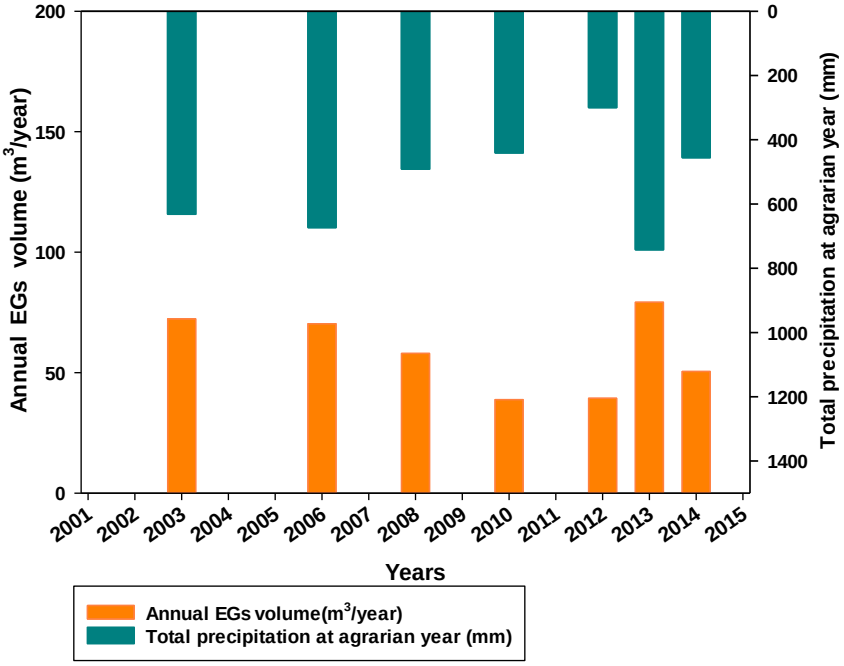

Figure 5. 14: Total EG volumes vs. total precipitation of agrarian year for all observed EGs during the 7 years of survey

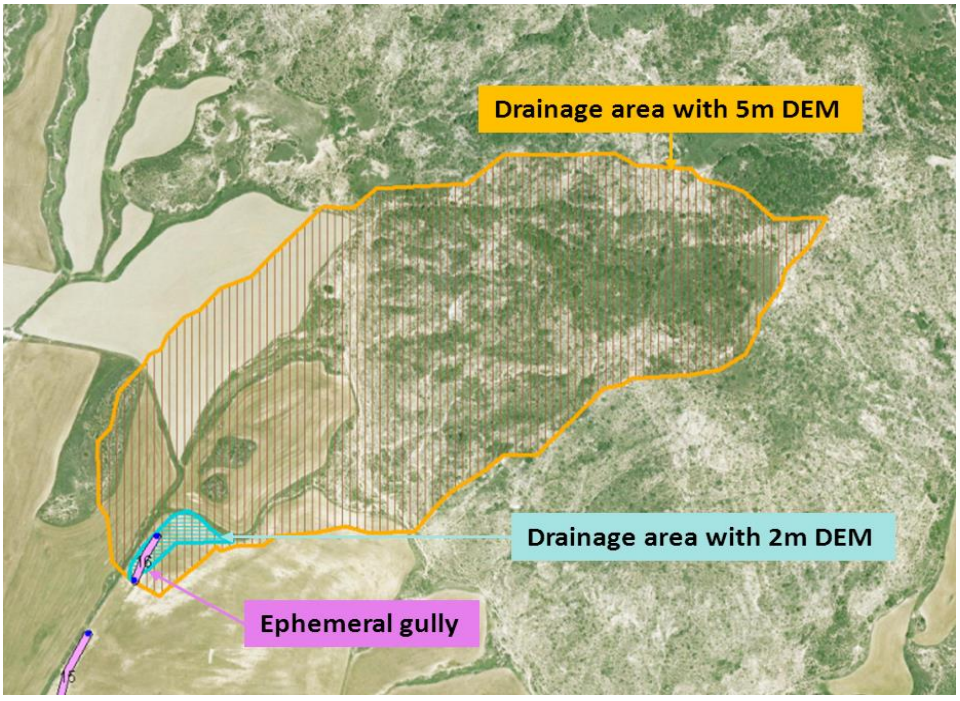

Figure 5. 15: Illustration of EG drainage area delimitation, for the same EG, using 2m and 5m DEM resolutions for EG classification.

$CTIc_1$ and $CTIc_2$ were determined for classical EGs using 2 m DEM resolution; values obtained with 5 m DEM were not taken in consideration due to the low number of classical EGs identified (5).

The values for $CTIc_1$ ranged from 0 to 1690; $CTIc_1 = 0$ was registered for EG nº 30, which appeared three times in a flat field. The maximum value, $CTIc_1 = 1690$, was registered in EG nº 5 which was the most frequent EG, occurring in six out of the eight study years and presenting the highest slope gradient. CTIc2 values were lower, ranging from 0 to 490. The global average values for CTIc1 and CTIc2 were, respectively, 505 and 77 (Figure 5.16).

When classical EGs were considered, $CTIc_1$ and $CTIc_2$ values for each year presented considerable variability, despite the small size of the study area and the supposedly homogeneous soil, land management and meteorological conditions (Figure 5.17). However, CTIc1 annual average values were not statistically different from year to year, which was also true for CTIc2.

CTI variability can be explained by the existence of slightly different soil uses and managements in the different EGs; also, the existence of different processes involved in EG formation are a possibility, other than topographic factor such as subsurface flow (exfiltration of seepage), preferential flow paths (tunnel collapse), etc.(Bernard et al., 2010). According to Vandekerckhove et al. (1998), Poesen et al. (2011) these types of erosion can alter the topographic index threshold for gully head initiation. Another factor that could affect CTIc values is tillage on the same direction as the dominate slope, which promotes the development of EGs even with lower CTIc values.

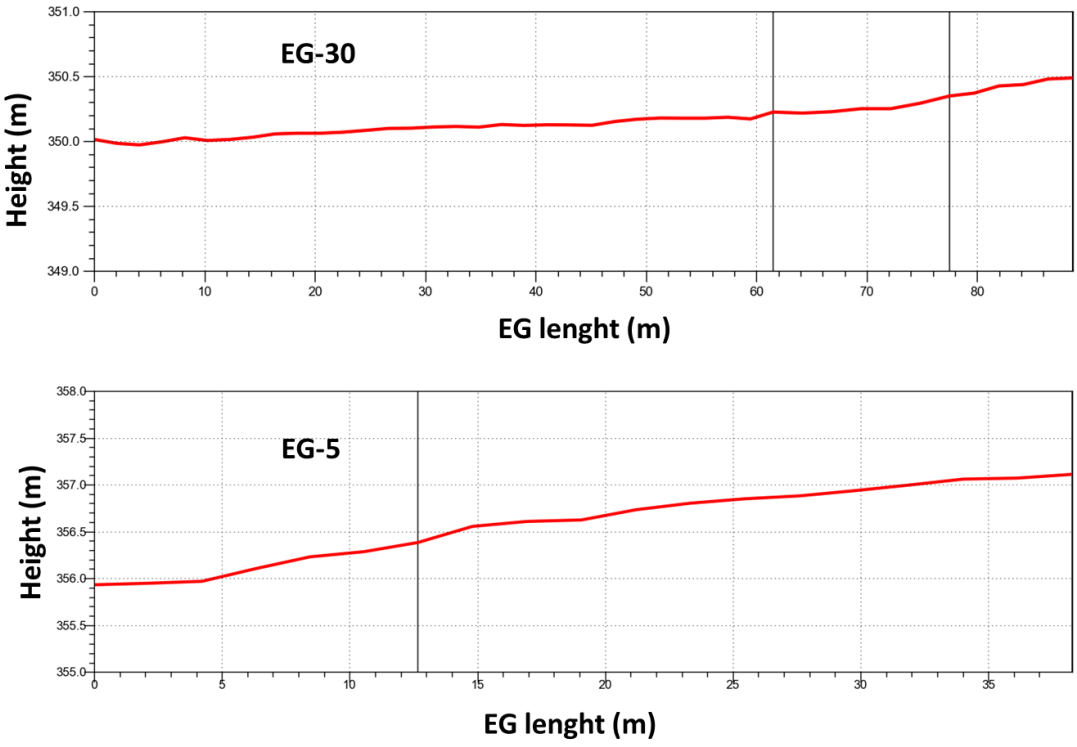

Figure 5. 16: Profiles of EGs nº30 and EG nº5

Overall $CTIc_2$ values were lower than $CTIc_1$. This could mean that the intensity of concentrated overland flow necessary to create an EG nickpoint or EG initiation, represented by $CTIc_1$, is higher than the intensity of concentrated overland flow necessary for headcut migration, represented by $CTIc_2$. This was corroborated by Bennett (personal communication, (2006), who mentioned that the hypothesis that the intensity of concentrated overland flow necessary to create an EG nickpoint is greater than the intensity necessary for headcut migration was reasonable.

The CTIc values observed herein were much higher than those obtained elsewhere, e.g., the Mississippi area, with CTIc maximum of 62 as shown by Parker and Bingner (2007) using 10 m and 30 m DEM resolutions. This difference can be partially explained by the high variation in rainfall rates: approximately 500 mm in study area and approximately 2000 mm in Mississippi. In addition, soil type and land use and management are different as well as field topography. The study area utilized herein is characterized by rugged terrain and small cultivated plots, while the studied fields in Mississippi were large and flat.

Different DEM resolutions could cause lower CTIc values. CTIc values resulting from 2m DEM were higher than those obtained from 5m DEM (with very low global averages of $CTIc_1$ and $CTIc_2$ corresponding to 76.2 and 1.8, respectively). Momm et al. (2012) found that the CTI threshold value decreased exponentially with higher DEM resolution. According to Kienzle (2004) and Zhang and Montgomery (1994), decreases in raster grid resolution lead to decreases in local average slope and planform curvature values - as DEM resolution increases, higher values of local slope are obtained causing higher values of CTIc.

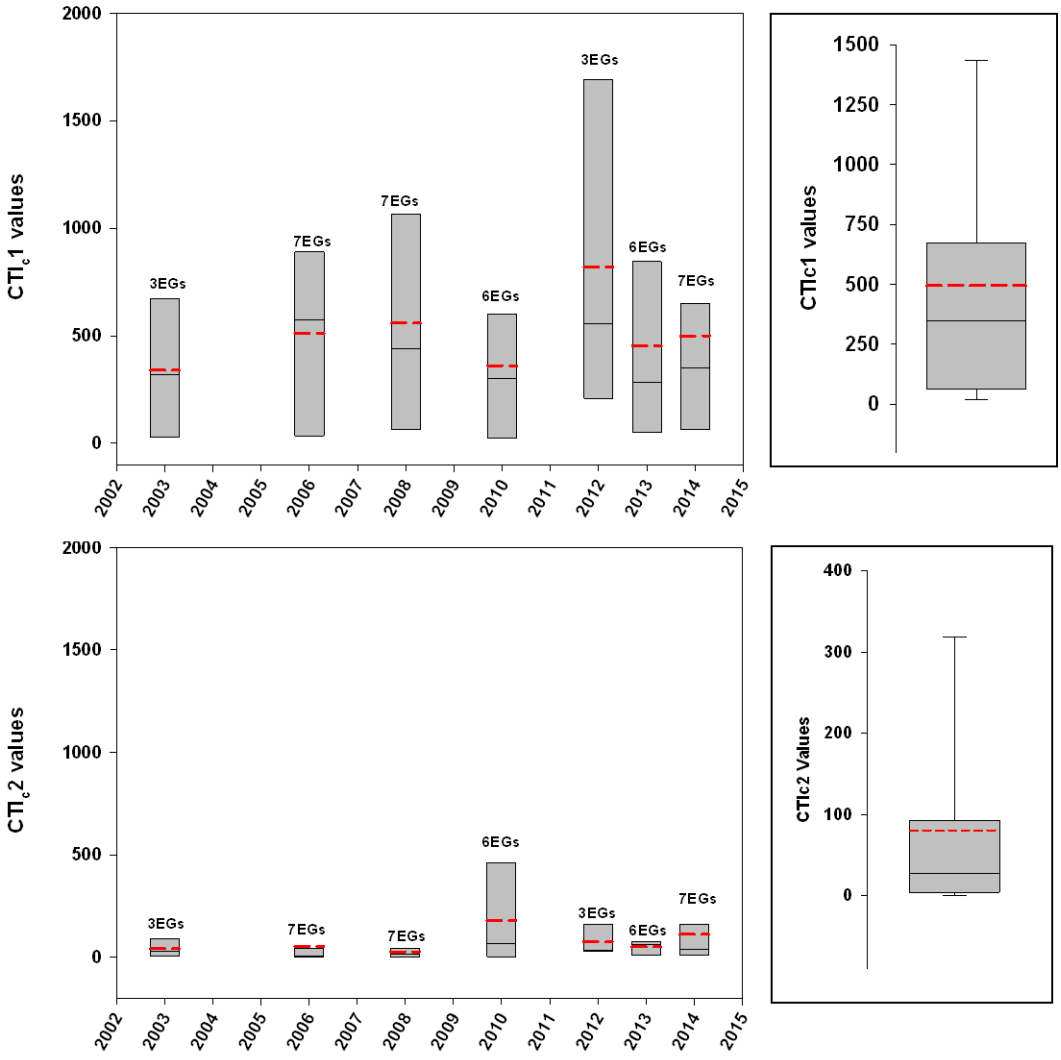

Figure 5. 17: Annual and general variations of CTIc1 and CTIc2 for classical EGs that appeared at least twice throughout the study period, using 2m DEM resolution

Chapter6: Evaluation of the AnnAGNPS model to predict ephemeral gully erosion

6.1 Introduction and objectives

The Tillage-Induced Ephemeral Gully Erosion Model (TIEGEM) was incorporated into the Annualized Agricultural Non-Point Source (AnnAGNPS) model, in which EG initiation, growth, and associated soil losses are simulated. An evaluation of the EG erosion predicted by AnnAGNPS is required to confirm the capability of the model to reproduce the EGs processes in Navarrese settings. In this context, several studies have been carried out to evaluate the performance of the AnnAGNPS model for the simulation of sheet and rill erosion processes (Chapters 4 and 5). However, limited efforts have been devoted to the assessment of the AnnAGNPS model in the prediction of EG erosion processes, to quantify the contribution of EG to soil erosion. Gordon et al. (2007) used historical precipitation data to simulate the effect of management on cumulative soil losses due to EG erosion over long term EG growth. It was verified that, over a 10-year period, erosion rates could be 250%-450% higher when EGs were tilled and reactivated annually ,than in no-till conditions. Taguas et al. (2012) used AnnAGNPS to simulate the possible contribution of EGs under different agricultural management practices (conventional tillage and spontaneous grass cover) to erosion. It was reported that the application of gully control measures could significantly reduce soil losses: 46% and 19%, respectively, for spontaneous grass cover and conventional tillage. Li et al.(2016) tested the capabilities of AnnAGNPS to estimate EG formation and sediment yield caused by EG erosion in three small EG watersheds at the Neal Smith National Wildlife Refuge (Iowa, U.S.A.). After a sensitivity analysis was carried out, the AnnAGNPS model was calibrated and validated to predict runoff and sediment yield, including EG erosion from 2008 to 2013. Simulations of EG volume were underestimated by 32%, 60% and 58% for the three watersheds. Gastesi (2014) calibrated AnnAGNPS to predict sediment yield EGs at mouths, using observed data from eight EGs of the LaTejeria watershed (Navarra) in the period January-September 2004. Gastesi (2014) verified that model prediction was enhanced when the calibration factor input was adjusted for each observed EG.

Chapter 5 addressed the prediction of EG location with AnnAGNPS. This Chapter considers that the location of EGs is known *a priori*. Then, focus is set only on the specific AnnAGNPS module utilized to predict EG parameters (Width, length, depth, volume, etc.). As AnnAGNPS can only simulate classical EGs, this evaluation was carried out using data from four classical EGs that were monitored throughout several years. This part of the study focuses only on the TIEGEM evaluation, as the PEG tool for the prediction of EG location has already been extensively discussed previously. To this end, the downstream points of observed EGs were considered as initial headcut points.

The main objective of this chapter is to evaluate the capability of the AnnAGNPS EG module (TIEGEM) to estimate the EG size (width, length and volume). This using data collected by current and past members of our research group at the Public University of Navarre.

6.2 Description of observed EG areas used for model evaluation

This study was carried out in the same zone aforedescribed in Chapter 5. The availability of a comprehensive database of monitored EGs and corresponding formation conditions (meteorological parameters, land cover and management data) is paramount for the evaluation of the EG erosion predicted by the AnnAGNPS model.

Between October 1995 and October 2001, field studies were conducted to monitor the appearance and evolution of ephemeral gullies in the Pitillas region (Casalí et al., 1999, De Santisteban et al., 2006). A dataset was built including four EGs, which was utilized to evaluate the AnnAGNPS . Selected EGs were monitored throughout the entire study period and were formed as described herein. Required input data for model operation were adequately gathered and prepared (daily climate, soil properties, land cover and management of plots where EGs were formed). The selected EGs were LaMatea1, LaMatea2, La Abejera0 and Cobaza1, which are described next.

6.2.1 La Matea 1 and La Matea2

La Matea1 and La Matea2 are separated EGs that occurred in the same plot (nº 164-Polygon 8 in Pitillas). Both EGs were classified as classical EGs.

a. Topography

These EGs are characterized by a relative small contributing area with high slope gradients that averaged 9.4% and 9.1% for La Matea 1 and La Matea2, respectively. Figure 6.1 shows the La Matea catchments where it can be observed that the upstream area presents a high slope gradient (reaching 14.5%). The downstream part presents an alluvial fan form with an average 3% slope that ends at an uncultivated land depression.

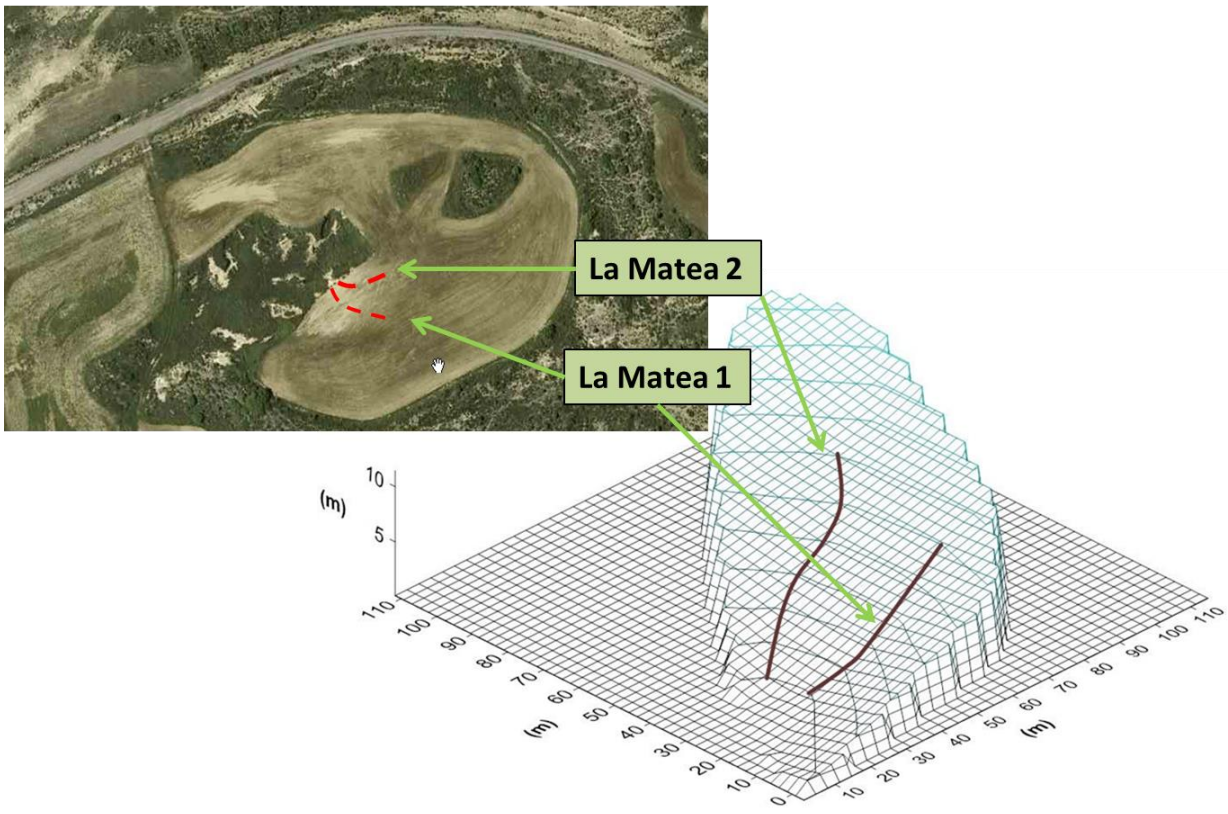

Figure 6. 1: Location of LaMatea 1 and LaMatea2 and topography of catchments

b. Soil

According to the USDA soil texture classification, the La Matea catchment is mainly silty clay in texture. The sand, loam and clay content of this soil are 16.7%, 42.1% and 41.2%, respectively (Table 6.1).

Table 6. 1. Soil properties of the EG drainage areas

Ephemeral gully	Soil texture	Sand (%)	Silt (%)	Clay (%)	Organic Matter (%)	Electrical conductivity (dS/m)	Saturated hydraulic conductivity (mm/hr)	Bulk Density (g/cm3)
La Matea 1&2	Silty Clay	16.7	42.1	41.2	-	-	4.3	1.5
La Abejera 0	Silty Loam	20.1	52.9	27.0	1.0	9.5 - 53.9	0.8	1.6
Cobaza 1	Silty Loam	34.4	59.9	8.7	1.8	0.4	-	1.4

c. Land use and management

In addition to winter cereal, sunflower was also cultivated in the plot where the La Matea EGs occurred. Conventional management techniques were applied during the entire cultivated period. Table 6.2 summarizes the different land uses and management practices during the study period.

Table 6. 2. Land use and management practices in LaMatea 1 and LaMatea2 during the study period

Year	Date	Crop	Management operation	Equipment utilized	Comments
1995	1st week October	Cereal	Plowing and sowing	Chisel	Contour plowing
1996	June		Harvesting		Crop residues were maintained
1996	1st week October	Cereal	Plowing and sowing	Chisel	Towards the maximum slope
1997	June		Harvesting		Crop residues were maintained
1998	March	Sunflower	Plowing and sowing	Chisel	Contour plowing
1998	July		Harvesting		Crop residues were maintained
1999	Summer		Tillage	Chisel	Contour plowing (bare soil)
1999	End of October	Cereal	Plowing and sowing	Chisel	Contour plowing
2000	June		Harvesting		Crop residues were maintained
2000	1st week October	Cereal	Plowing and sowing	Chisel	Contour plowing
2001	June		Harvesting		Crop residues were maintained

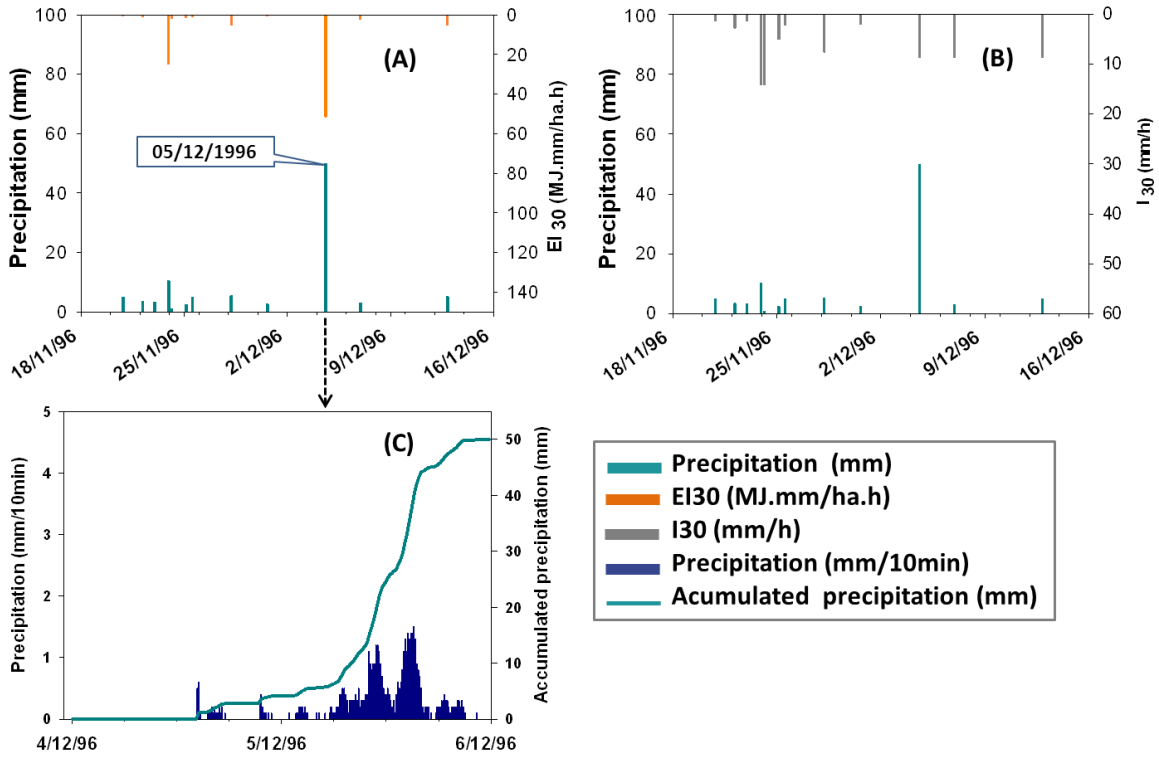

Figure 6. 2: Daily precipitation for the period around the event that caused Eg erosion for La Matea 1 & 2 and the corresponding (A) maximum intensity in 30 minutes I30, (B) kinetic energy EI30 and (C) instantaneous (10min) and accumulated histograms for the event occurred on December 4th and 5th , 1996.

In December, 1998, La Matea 1 and 2 were measured for the third time, approximately nine months after the plot was sowed with sunflower. The plot was then left fallow until the measurement date. The formation of these gullies could be attributed to the rainfall events recorded between seeding and measurement dates. The rainfall amount registered by the pluviograph located in the study area reached 300 mm. Rainfall amounts ranged between - 1mm to 50mm, with intensity I30 ranging between 0.8 and 30 mm.h^{-1} and kinetic energy EI30 varying from 0.17 to 276.5 MJ.mm.ha^{-1}.h^{-1} (Figure 6.3).

During this period, most of the rainfall events were recorded between April and June. The highest I30 and EI30 values were recorded on May 19th, 1998 (26.3 mm.h-1 and 120 MJ.mm.ha-1.h-1, respectively) and during June 4th and 5th,1998 with 51 mm precipitation, I30 =29.8 mm. h^{-1} and EI30 = 276.5 MJ.mm.ha^{-1}.h^{-1}. According to De Santisteban (2003), the event that originated the gullies cannot be clearly identified.

On September 21st, 1999, La Matea 1 and 2 were measured again after having been plowed during summer of the same year. No important events were recorded by the local pluviograph. However, De Santisteban (2003) reported that on September 13th, 1999, an important rainfall storm caused an overflow of the Cidacos River that crosses Pitillas. The accumulated rainfall was 56.8 mm, recorded by the Olite station that is approximately 5 km from the study area. According to De Santisteban (2003), this precipitation event was responsible for the formation of EGs La Matea 1 and La Matea2.

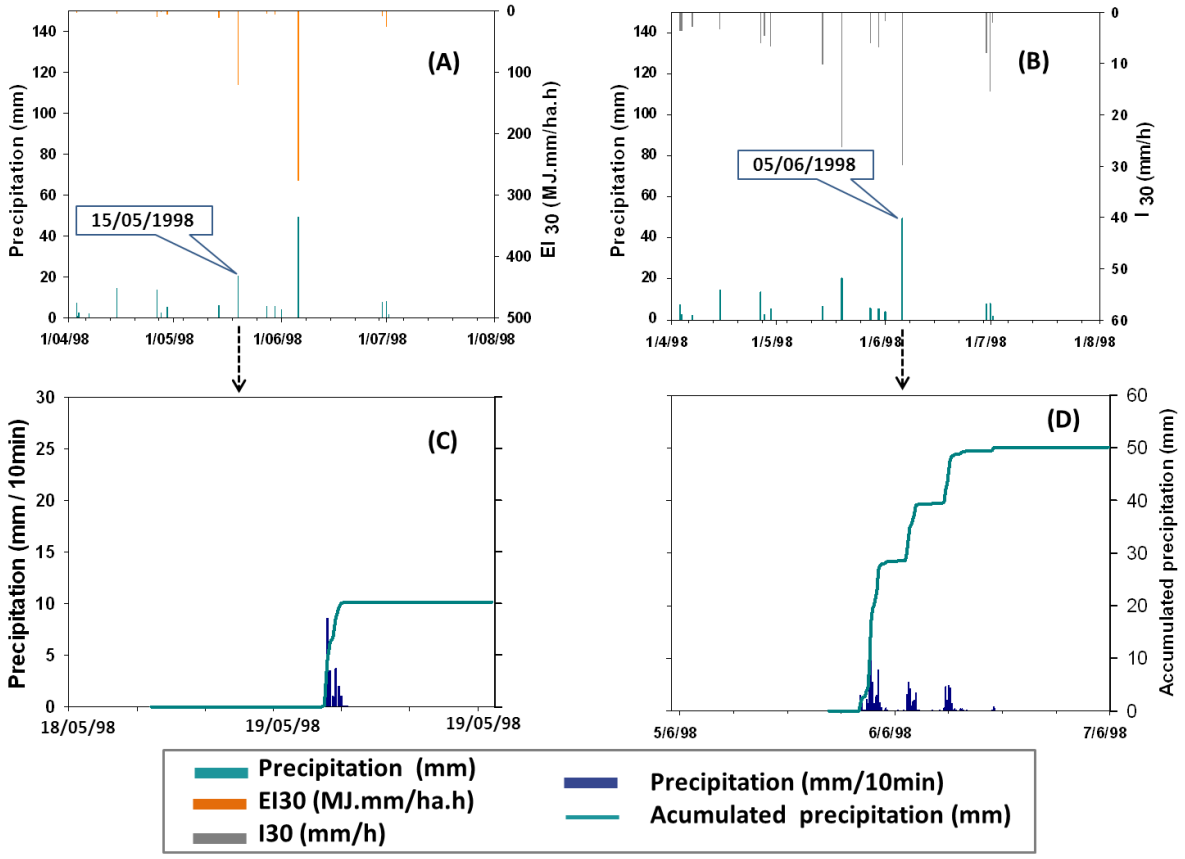

Figure 6. 3: Daily precipitation for the period around the event that caused La Matea 1 & 2 EG erosion and the corresponding (A) intensity I30, (B) kinetic energy EI30 and (C) instantaneous (10min) and accumulated histograms for the events occurred on (D) May 19th 1998and (d) June 5th, 1996.

6.2.2 La Abejera 0

La Abejera0 can be classified as a classical EG (Casalí et al., 1999) located in plot nº 291 - Polygon Nº 8 of Pitillas, presenting an irregular form and slope.

a. Topography

Casali (1997) described the La Abejera0 EG after its appearance on January 1996, and the EG was divided into different reaches according to slope gradient. The first reach was located at the downstream end, with 0.9% average slope where significant sedimentation occurred, presenting mainly an alluvial fan form. The first reach was followed by a high slope gradient reach (7.7%), where the gully presents the greatest width and depth. The next reach was 40m long, with 3.7% average slope and lower erosion. The last reach is the longest part of the EG, where the slope gradient is again significantly high (7.7 %). The EG drainage area presents an elongated shape covering an area of 1.6 ha (Figure 6.4).

a. Soil

The soil of the EG catchment is Silty Loamy in texture with sand, silt and clay contents of 20.1%, 52.9% and 27%, respectively (Table 6.1). According to Casali (1997), in the downstream part of EG, soil is characterized by high saturated conductivity and sodium adsorption ratios (1.3mm.hr-1 and 32.5, respectively) indicating the existence of salinity and alkalinity problems (Table 6. 1). These

conditions render the soil unable to form stable aggregates and to lose its structure in wet conditions, making it more vulnerable to hydraulic erosion (Benito et al., 1993).

a. Land use and management

During the study period, the La Abejera0 EG was usually cultivated with winter cereal, using conventional tillage. Table 6.3 summarizes the different land uses and management operations during the studied period. As the plot shape is elongated, tillage was usually carried out in the direction of the maximum slope.

a. Development and assessment of the La Abejera0 EG

From 1996 to 2001, La Abejera0 was monitored five times (the most monitored EG). In 1996, La Abejera0 was monitored twice, in January and December. Before that, the plot was plowed with moldboard and sown in the first week of October, 1994, following conventional techniques and left fallow after harvesting on June 1995. Casalí et al. (1999) suspected that La Abejera0 was formed in January, 1996, when a significant rainfall event occurred, with a total depth of 17 mm and peak rate of 54 mm h^{-1}. La Abejera0 was erased by tillage in October, 1996, and reappeared due to the precipitation events of December 4th and 5th, 1996, which had a total depth of 51 mm and a peak rate of 12 mm h^{-1}. In addition to the high precipitation amounts recorded during this event, the soil moisture content was already high due to precedent precipitation: 43.4 mm were recorded during the 15 days before the major event (Casali, 1997, Casalí et al., 1999).

Table 6. 3. Land use and management used of La Abejera 0 during the study period

Year	Date	Crop	Management operation	Used equipment	Comments
1994	1st week October	Cereal	Plowing and sowing	Moldboard	Towards the maximum slope
1995	June		Harvesting		
1995	June				After harvesting, plot was left fallow with crop residues
1996	Beginning of October	Cereal	Plowing and sowing	Moldboard	Towards the maximum slope
1999	After 21 September	Cereal	Plowing and sowing	Moldboard	Towards the maximum slope
2000	June		Harvesting		Crop residues were maintained
2000	18- August		Plowing	Moldboard	Towards the maximum slope
	31 - August	Cereal	Plowing and sowing	Moldboard	Towards the maximum slope
2001	June		Harvesting		Crop residues were maintained
	End of August		Plowing	Moldboard	Towards the maximum slope

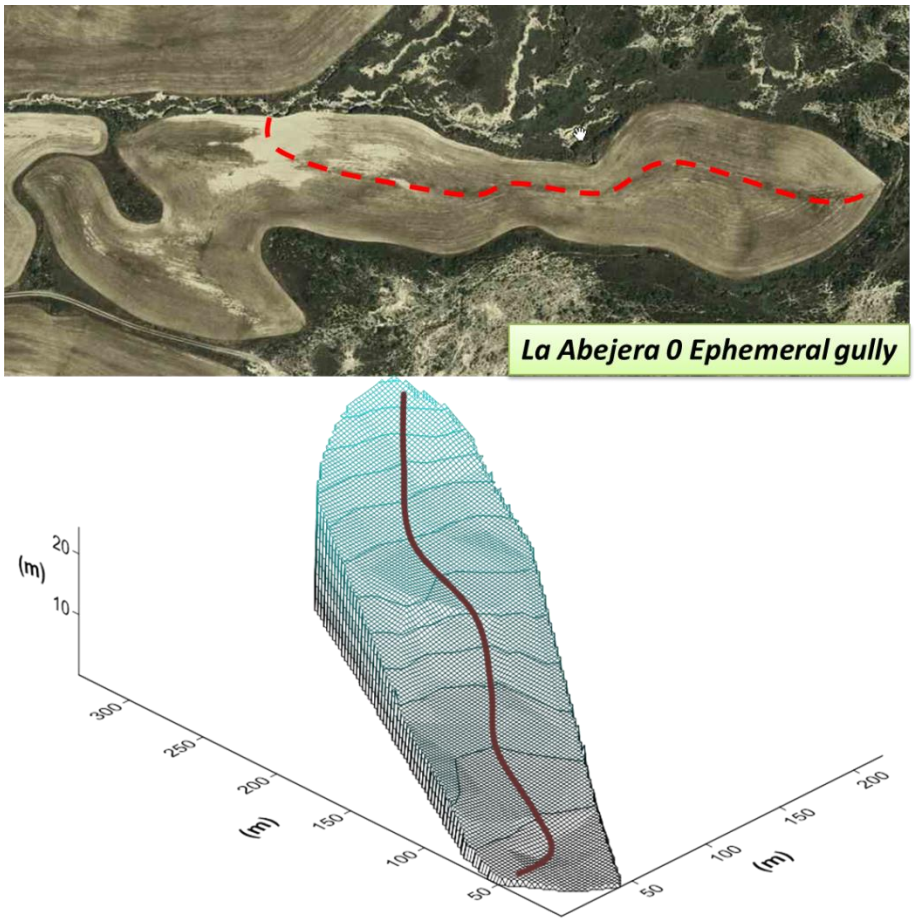

Figure 6. 4: Location of the Abejera 0 EG and the topography of the catchment

On September 21st, 1999, La Abejera0 was assessed for the third time, after the rainfall event occurred on September 13th, 1999 (De Santisteban, 2003). The plot was tilled in the direction of maximum slope and leaved unprotected (De Santisteban et al., 2006).

The fourth measurement was carried out on October 7th, 2000, after the plot was plowed twice on August 18th and 31st, 2000. After the first plowing, precisely on August 29th, 2000, a precipitation event was registered by the local pluviograph (24 mm; I30 = 43.8 mm.h^{-1} and EI30 = 270.4 MJ.mm.ha^{-1}.h^{-1}) causing the apparition La Abejera0 (Figure 6. 5). The EG was not sufficiently well-defined for measurement, and only the EG pathway was detected. At the end of August, 2000, the plot was plowed again in the direction of maximum slope. No changes were observed until September 26th, 2000, when 17.3 mm of rainfall was recorded with I30 = 33.8 mm.h^{-1} and EI20 =254.8 MJ.mm.ha^{-1}.h^{-1} (Figure 6.5). This event caused the formation of the La Abejera0 EG.

The last field measurement was made on October 25th, 2001, after the plot was plowed in the end of August, parallely to the maximum slope. The formation of the La Abejera0 EG occurred as a result of the rainfall event of October 17thand 19th, 2001. Unfortunately, the on-site pluviograph was faulty during this period. The nearest metrological station, Carcastillo Oliva, registered precipitation amounts of 12.7 and 21.8 mm for October 17thand 19th, respectively; the same rainfall quantities were used in the AnnAGNPS model simulation.

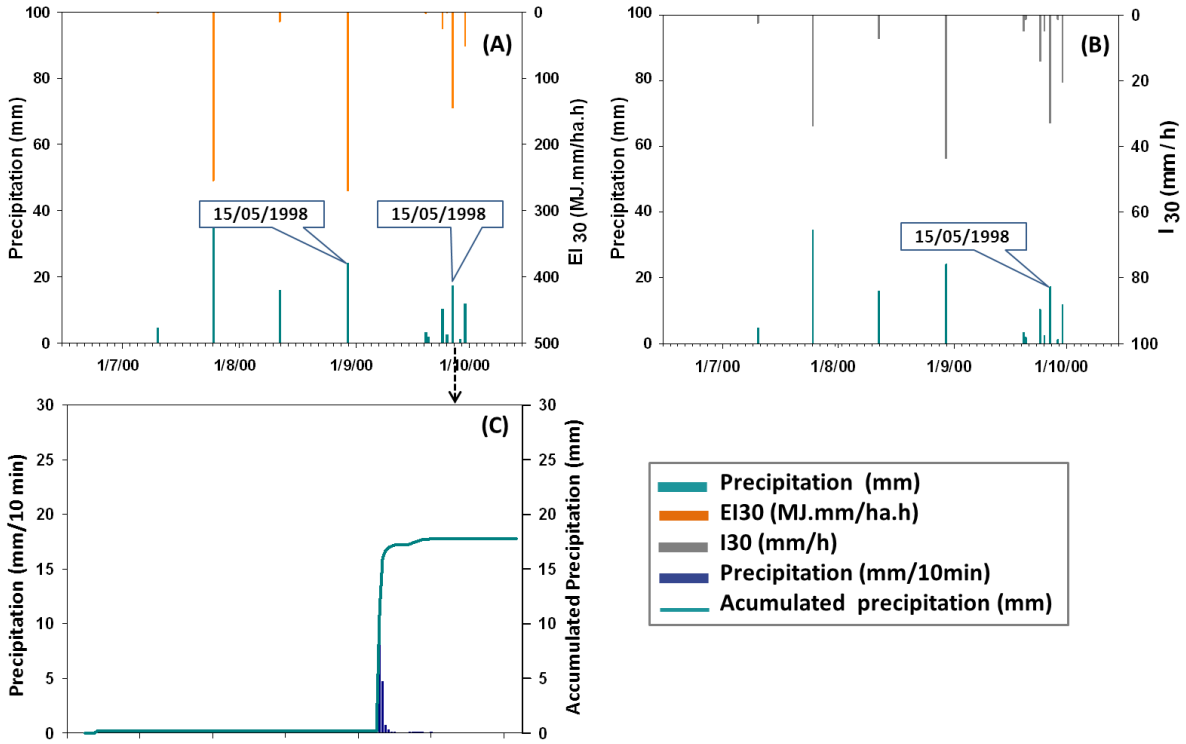

Figure 6. 5: Daily precipitation for the period around the event that caused EG erosion of La Abejera0 and the corresponding (a) intensity I30, (b) kinetic energy EI30 and (c) instantaneous (10min) and accumulated histograms for the event occurred on September26th, 2000

6.2.3 Cobaza 1 EG

Two EGs frequently appear in plot nº 279 - Polygon Nº 8 at Pitillas. The classical EG called Cobaza 1 studied herein is located in the northeastern part of the plot. Cobaza 1 was classified as classical EG because it was formed due to the concentrated flow generated by its own catchments.

a. Topography

Casali (1997) reported that the Cobaza 1 catchment was characterized by its small surface area (0.55 ha), with an average 4.6% slope gradient. According its longitudinal section, the slope of the EG stream can be divided into three parts: starting from the downstream end, the slope increases from 1% to 7%, decreasing to form a plane area, and then increasing its slope until reaching 9% slope gradient at the final part (Figure 6. 6).

a. Soil

The soil texture classification at the Cobaza 1 catchment is Silty Loam, with 34.4%, 56.9% and 8.7% of sand, loam and clay contents, respectively (Table 6.1).

b. Land use and management

Within the Cobaza 1 plot, the monoculture of winter cereal was the dominating land use practice (Table 6.4). Two types of management were carried out throughout the study period: from 1995 to 1996 conventional tillage was practiced, and then no-till farming was adopted. In both cases, operations were performed in the opposite direction of the maximum slope.

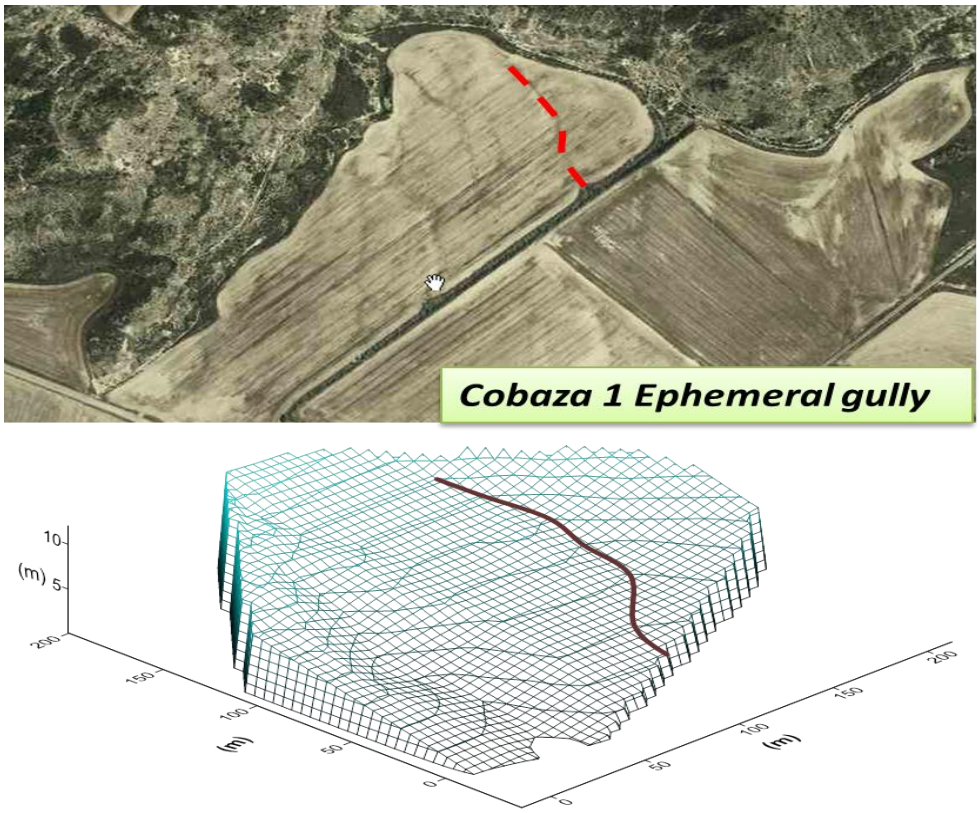

Figure 6. 6: Illustration of the Cobaza 1 EG location and catchment topography.

Table 6. 4. Land use and management utilized at the Cobaza 1 EG plot during the study period

Year	Date	Crop	Management operation	Used equipment	Comments
1995	1st week October	Cereal	Plowing and sowing	moldboard	Contour plowing
1996	June		Harvesting		Crop residues were maintained
1998	1st week October	Cereal	No-till farming	seed drill	Towards the maximum slope
1999	June		Harvesting		Crop residues were maintained

c. Development and assessment of the Cobaza1 EG

During the study period, the Cobaza1 EG was measured only twice. The first measurement was made on January 1996, after plowing in the first week of October, 1995, using moldboard. Similarly to the previous studied EGs, the precipitation event that occurred on January 22nd, 1996, caused the EG formation. The second monitoring was carried out on September 21st, 1999, when the surface of the soil was covered with crop residue. Again, similarly to other EGs formed in this period, the precipitation event that occurred on September 13th, 1999, caused the formation of the Cobaza1 EG. According to De Santisteban et al., (2003), despite the utilization of no-till farming to protect the soil against erosion factors, Cobaza1 was formed due the significant precipitation event (56.8mm).

6.3 General remarks for evaluation of the model

Previous studies (Casali, 1997, De Santisteban, 2003, De Santisteban et al., 2006) provided some of the required input data for the evaluation of EG prediction by the AnnAGNPS model in the Pitillas agricultural fields.

The daily climate AnnAGNPS inputs included recorded precipitation data from a local rainfall gauge in the period January, 1996-July, 2001. Remaining required climate inputs, along with soil, land use and management data, were provided by the Tafalla automatic meteorological station.

The AnnAGNPS model was applied to small watersheds in the Pitillas region, to simulate the development and erosion of EGs. Plots that contained the observed EGs were included in separate AnnAGNPS cells along with specific land use, management and soil type for each plot.

To this end, the AnnAGNPS GIS interface (TOPAGNPS) and 2 m resolution DEM were utilized to establish watershed delimitations including the studied EGs (subdivision into cells) and to calculate representative cell parameters (cell area, slope and length) required for running AnnAGNPS model. The generated watershed covered an area of 414 ha, which was divided into 113 cells using 4 ha and 100 m for CSA and MSCL values, respectively (see chapter 3) (Figure 6.7).

Before evaluating the model, a literature review was conducted to determine the factors affecting EG erosion within AnnAGNPS. Gordon et al. (2007) carried out a sensitivity analysis within AnnAGNPS to examine the effect of critical shear stresses (τ_c) on total ephemeral gully erosion and headcut migration rate (Eq. 2.28). It was concluded that an increase in τ_c along with a decrease in the erodibility coefficient (k_d) reduced the amount of simulated EG erosion. The rate of headcut migration was reduced when the erodibility coefficient was decreased. Headcut migration rate was more dependent on soil erodibility then on runoff magnitude.

Li et al. (2016) used the headcut detachment coefficient (Eq. 2.26) in a sensitivity analysis focused on EG erosion, and verified that the model was highly sensitive to variations in the headcut detachment coefficient. Gastesi (2014) carried out a sensitive analysis where almost every parameter related to EG erosion was analyzed, and classified these parameters according to their impact on the prediction of the annual average sediment yield at the EG mouth. The parameters in decreasing order of relevance were EG erosion calibration factor, width algorithm (8 equations), headcut erodibility coefficient, EG depth of erosion and critical shear stress. EG erosion was very sensitive to k_d variation (K_d is directly related to τ_c as previously shown in Eq. 2.27). The EG depth factor was fixed in advance as stated by Gastesi (2014). In this case, the model could consider by default the tillage depth as the EG depth. The model can be applied to other agricultural areas where there is no data from observed EG, but there is information on land use and management (required for model operation).

Calibrations and validations were carried out at two separated periods to evaluate the model. The more complete and ample dataset was used for calibration, which was carried out between January 1st, 1998 and December 31st, 2001. Observed data were obtained from De Santisteban et al. (2006) and De Santisteban, (2003). Validation was carried out between January 1st, 1995 and December 31st, 1996. Observed data were obtained from Casali (1997) and Casali et al. (1999). 1994 and 1995 climate data were used in a warm-up period to reduce the influence of initial condition errors in model predictions. Rainfall data before 1996 were obtained from the Tafalla automatic meteorological station.

2m resolution DEM was used to create the CTI raster grid for the study area. Drainage area and slope were determined with the AnnAGNPS GIS interface, using the observed location points and mouths of the observed EGs.

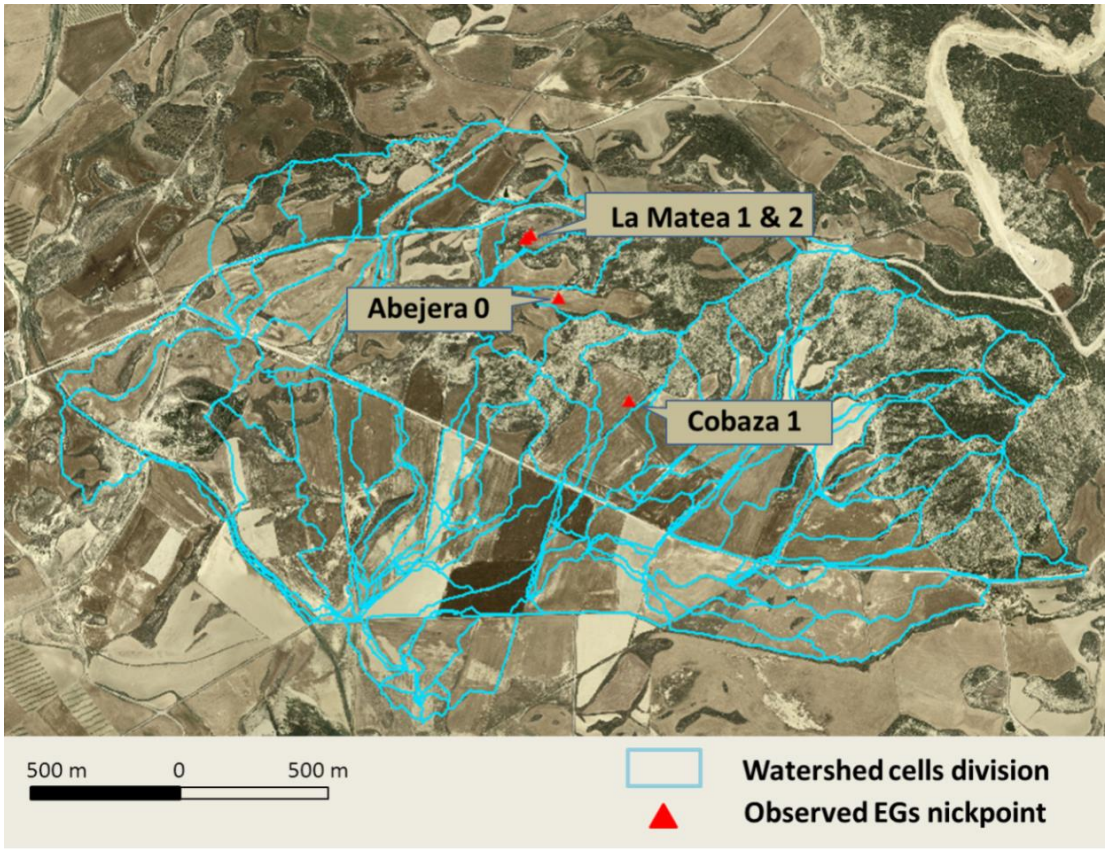

Figure 6. 7: AnnAGNPS watershed cell division and location of observed EGs within cells

Statistical and graphical comparison methods were used in the calibration and validation steps of the assessment of AnnAGNPS performance in the prediction of EG erosion, Due to limited data availability, the percentage error was used to evaluate the capability of the model to reproduce the EG erosion occurred. Graphical comparison was based on the equivalent prismatic gully (EGP) approach, developed by Casali et al. (2015), where it was suggested that the geometry of a gully could be characterized through its mean equivalent width (W_{me}) and mean equivalent depth (D_{me}), which, together with its length (L), define EPG (Figure 6.8).

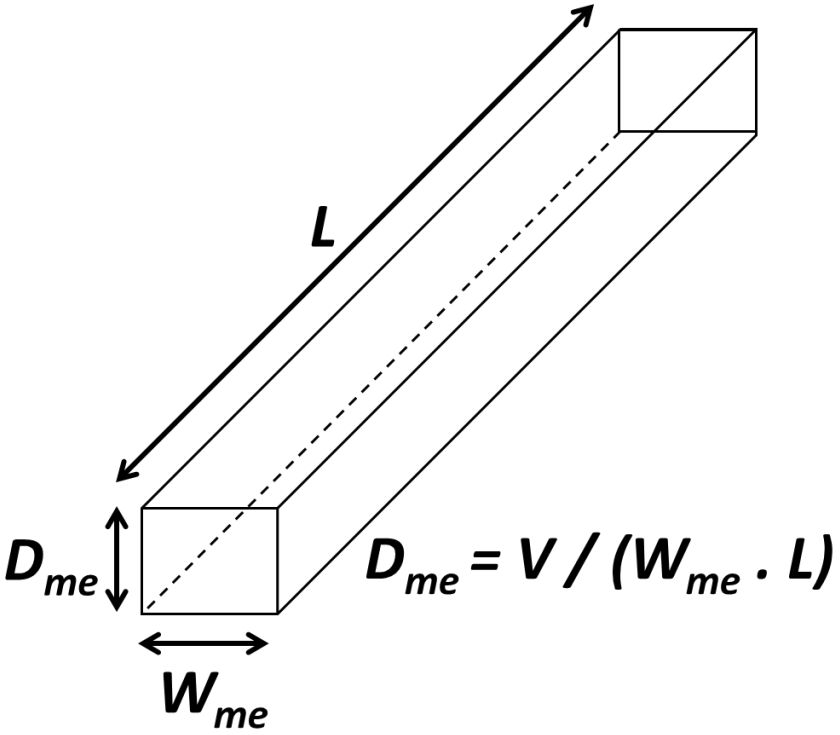

Figure 6. 8: Equivalent prismatic gully (EPG). Source: (Casali et al., 2015)

W_{me} corresponds to the average width along the EG channel. D_{me} was determined by the expression shown in Figure 6.18, along with knowledge of EG volume V and W_{me}. After determination of the simulated and observed dimensions, the EPGs of selected EGs were drawn and compared.

6.4 Evaluation of algorithms to estimate EG width

Integration and transformation of EGEM to REGEM, and then to TIEGEM within AnnAGNPS, has enabled the identification of several model limitations as there is limited information on several critical components (Bingner et al., 2012). One of the most important limiting components is the identification of EG width, and the AnnAGNPS model provided users with six different algorithms to identify EG width.

This part of study does not include sensitivity analyses, as other studies have already carried out exhaustive sensitivity analyses, including all parameters that influenced EG erosion (Gordon et al., 2007, Gastesi, 2014). Also, it seems appropriate to study the effect of specific, selected algorithms on the determination of EG width, as there is limited information on the utilization of width algorithms within AnnAGNPs. Width algorithms have important contribution to the eroded volume of EGs.

In this context, six algorithms were tested to select the most suitable for local conditions, by comparing simulated widths with measured average widths for each EG. To this end, one simulation was carried out for each of the six available algorithms within AnnAGNPS. Figure 6.9 shows the EG section widths generated by the six AnnAGNPS algorithms of the four selected EGs, in addition to the measured widths of the EGs sections. The EG simulated widths ranged from less than 4 cm to more than 3 m, with great variation depending on the selected algorithm. The lowest and highest width values were given by the "Non-submerging Tailwater" and Wells (Wells et al., 2013) algorithms, respectively. The widths of observed EGs ranged from 0.4 m to 1 m, with similar averages: 0.83, 0.84, 0.84 and 0.85 m for Abejera0, Cobaza1,

La Matea1 and La Matea2, respectively. No statistically significant difference was identified between the four EG widths ($P = 0.686 > 0.05$).

Comparison of the simulated and measured widths (Figure 6.9), revealed that EG widths generated by Woodward's (1999) Ultimate were the closest to measured widths, and more realistic than the remaining algorithms. Therefore EG widths were simulated by Woodward's (1999) Ultimate algorithm.

6.5 Model calibration

Usually a step taken *a priori* is calibration of the model for surface runoff prediction, under study area conditions. However the absence of a gauging station at the study area prevented this calibration.

Considering that the curve number is a key factor affecting runoff generation, and with the objective of determining the parameters required to predict runoff, sheet and rill erosion, the methodology utilized in Chapter 3 is herein applied. The methodology considered seasonal CN variation, taking into account the spatial variation between the study area and the Latxaga watershed, as well as differences in cereal management schedules. Thus, for the same phenological states, the CN values of the Latxaga basin were utilized for Pitillas, but applied at different times given the different conditions of the locations.

After EGEM was revised and incorporated into AnnAGNPS, few works have been carried out to evaluate the capability of the model to prodict EGs. Li et al. (2016) calibrated EG processes by varying the headcut detachment coefficient, which influenced EG development and the annual sediment yield. Gastesi (2014) calibrated the model for EG prediction by varying the EG erosion calibration factor within the EG input editor window. A good agreement between simulated and observed sediment yields at EG mouths was observed after calibration.

Gordon et al. (2008) used the AnnAGNPS model to simulate long term EG growth, development, and evolution in four different environments. The objective was to demonstrate the effect of management on cumulative soil losses due to EG erosion over long time periods (10 years). However, no direct comparisons were made between simulated and observed EG dimensions and erosion rates due to the lack of complete field datasets. It was concluded that erosion rates in those four geographic regions could be 250% to 450% higher when gullies were tilled and reactivated annually, in opposition to no-till conditions.

Sensitivity analyses carried out by previous works showed that critical shear stress (τc) and the soil erodibility coefficient (kd) are the two main parameters affecting EG erosion, by conditioning initial gully incision and EG migration (Alonso et al., 2002, Gordon et al., 2007, Gastesi, 2014). Therefore, herein model calibration was performed by considering only τ_c, since k_d is a function of τ_c, as shown by the k_d equation (Chapter 2) developed by Hanson and Simon (2001) and validated by Alonso et al. (2002). As AnnAGNPS is long-term simulation model, EG simulations were carried out continuously throughout the calibration period. A single τ_c value was assigned to each EG during each simulation, which varied during the calibration process. Calibration was accomplished with manual variation of the τ_c value within the AnnAGNPS input editor. Initial τ_c values were internally calculated by the model, from soil texture characteristics. The trial-and-error approach was used to determine the appropriate τ_c value, targeting the lowest error between simulated and observed EG eroded volumes. Another criterion was considered in this calibration, which was the formation date of EGs. Simulated and observed EG formation dates must coincide for model simulation

to be considered valid. For instance, for a specific τ_c value, if the model predicted that the EG was formed after or before the actual (real) formation date of the observed EG, the τc value was not representative of the field conditions when the EG was formed.

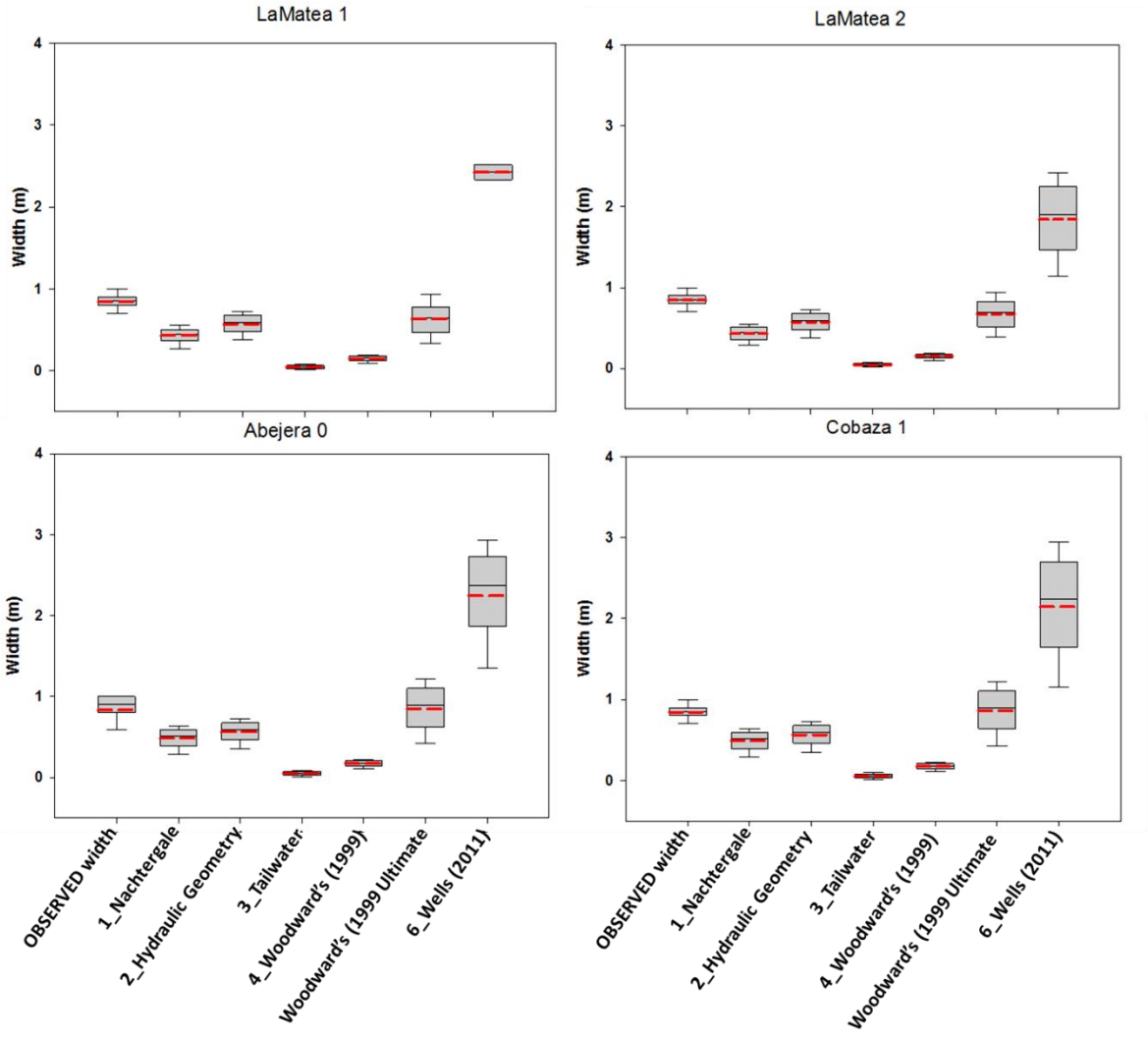

Figure 6. 9: Variation of EG width simulation using six algorithms within AnnAGNPS, with variation of observed EG widths for the four studied EGs (observed EG sections shown for comparison purposes).

6.5.1 The LaMatea1 and La Matea2 EGs

During the calibration period, LaMatea1 and 2 were measured twice. The first monitoring was carried out in December, 1998. The exact formation date was unknown, but AnnAGNPS simulations before calibration attributed EG formations to the rainfall event occurred on May 19, 1998 (20.3mm precipitation, 7.83 mm surface runoff, and 1.6 $mm.hr^{-1}$ peak discharge at EG nickpoint). According to simulations, both EGs grew due to the rainfall event recorded on June 5th, 1998 (50.3 mm precipitation depth, 29 mm surface runoff, and 7 $mm.hr^{-1}$ peak discharge at EGs nickpoint - Figure 6.10). EG lengths reached their maximums at formation time (according to Eq. 2.30, which only depends on EG drainage area) and later events progressively caused EG widening.

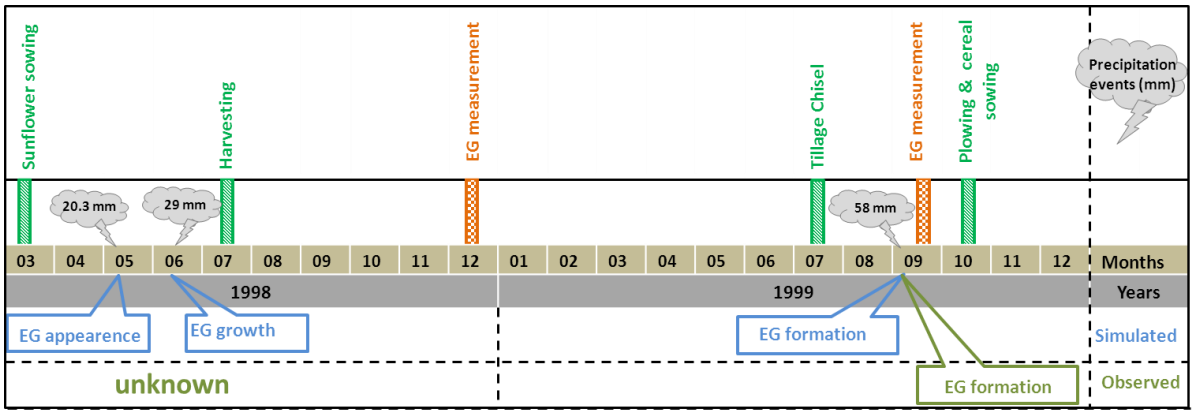

Figure 6. 10: Timeline of La Matea 1 and 2, from 1998 to 1999, including applied management practices and measurement dates.

Table 6.5 shows the results obtained using the internally calculated $\tau_{c\ value}$ before calibration (τ_c = 7.5N.m^{-2}, corresponding to k_d = 3.6(10^{-6}) m^3.s^{-1}.N^{-1}). Simulations before calibration showed an overestimation of 385% and 197% in EG volumes for La Matea 1 and 2, respectively (Table 6.5), mainly due to length overestimation, which reached 261% and 284% for LaMatea 1 and 2 ,respectively (Figure 6.11).

Table 6. 5. Measured and simulated EG characteristics for Matea1 and 2 EGs, before calibration.

	December 1998					
	La Matea1			**La Matea2**		
	Measured	**Simulated**	**Error (%)**	**Measured**	**Simulated**	**Error (%)**
Length (m)	16.10	74.10	361.80	16.60	63.86	284.70
Width (m)	0.88	0.54	38.80	0.80	0.62	22.50
Depth (m)	0.11	0.20	77.70	0.19	0.20	4.10
Volume (m³)	1.60	7.76	385.00	2.55	10.00	197.20
	September 21, 1999					
	La Matea1			**La Matea2**		
	Measured	**Simulated**	**Error (%)**	**Measured**	**Simulated**	**Error (%)**
Length (m)	24.00	74.36	209.80	28.00	63.86	128.00
Width (m)	0.81	0.71	11.94	0.81	0.70	13.80
Depth (m)	0.11	0.20	79.17	0.17	0.20	16.60
Volume (m³)	2.16	7.58	362.90	3.90	8.83	126.40

After having been filled by tillage in the Summer of 1999, according to AnnAGNPS simulations, La Matea 1 and 2 reappeared due to the rainfall event of September 13, 1999 (precipitation depth = 58 mm, generating 27.7 mm and 6.3 mm.hr^{-1} peak discharges at LaMatea 1 and 2 nickpoints, respectively). When observed and simulated EG dimensions were compared, the same response was observed, with an overestimation of 362% and 126% in EG volumes for LaMatea 1 and 2, respectively (Figure 6.11). However, these errors were lower than for the previous time period, mainly due to decreases in estimated EG lengths.

Thus, to improve model performance, model calibration was carried out by adjusting the τ_c values, bringing closer together the observed and simulated volumes.

Gordon et al. (2007) found that higher critical shear stress not only limited the time for soil detachment, but also reduces the rate of headcut migration. This derives from

the headcut migration equation (Eq. 2.28), in which k_d is an inverse function of τ_c. The internal calculated τ_c was increased, to decrease the estimated EG erosion rate.

Application of the trial and error approach finally provided the lowest errors between simulated and observed EG total eroded volumes; these were obtained increasing τ_c by 60% and 114.6%, for La Matea1 and La Matea 2, respectively (Table 6.6). These τ_c values were the highest ones enabling AnnAGNPS simulation of EG appearance on the same dates as observed.

Table 6. 6. Critical shear stress (τ_c) with its corresponding soil erodibility coefficient (k_d) used within model simulations, before and after calibration

	Before Calibration		**After calibration**	
	τ_c (N.m^{-2})	**k_d (m^3.s^{-1}.N^{-1})**	**τ_c (N.m^{-2})**	**k_d (m^3.s^{-1}.N^{-1})**
La Matea 1	7.50	3.63 10^{-6}	12.00	2.88 10^{-6}
La Matea 2	7.50	3.63 10^{-6}	16.10	2.49 10^{-6}
La Abejera 0	5.05	4.45 10^{-6}	8.15	3.50 10^{-6}
Cobaza 1	1.75	7.63 10^{-6}	1.75	7.63 10^{-6}

After AnnAGNPS simulations provided calibration results for LaMatea 1 and 2, the values for volumes and dimensions were improved. However, overestimation of EG volumes is still considerable, mainly due to the significant differences between observed and simulated EG lengths, as shown in Table 6.7 (Figure 6.12).

Table 6. 7. Measured and simulated EG characteristics for the La Matea 1 and 2 EGs, after calibration

	December 1998					
	La Matea1			**La Matea2**		
	Measured	**Simulated**	**Error (%)**	**Measured**	**Simulated**	**Error (%)**
Length (m)	16.10	53.00	229.30	16.60	63.86	284.70
Width (m)	0.88	0.50	44.60	0.80	0.45	43.80
Depth (m)	0.11	0.20	77.70	0.19	0.20	4.60
Volume (m^3)	1.60	5.20	223.20	2.55	5.40	113.80
	September 21, 1999					
	La Matea1			**La Matea2**		
	Measured	**Simulated**	**Error (%)**	**Measured**	**Simulated**	**Error (%)**
Length (m)	24.00	42.00	76.80	28.00	44.00	57.40
Width (m)	0.81	0.66	18.20	0.81	0.64	21.00
Depth (m)	0.11	0.20	79.10	0.17	0.20	16.60
Volume (m^3)	2.16	5.60	159.50	3.90	5.50	42.80

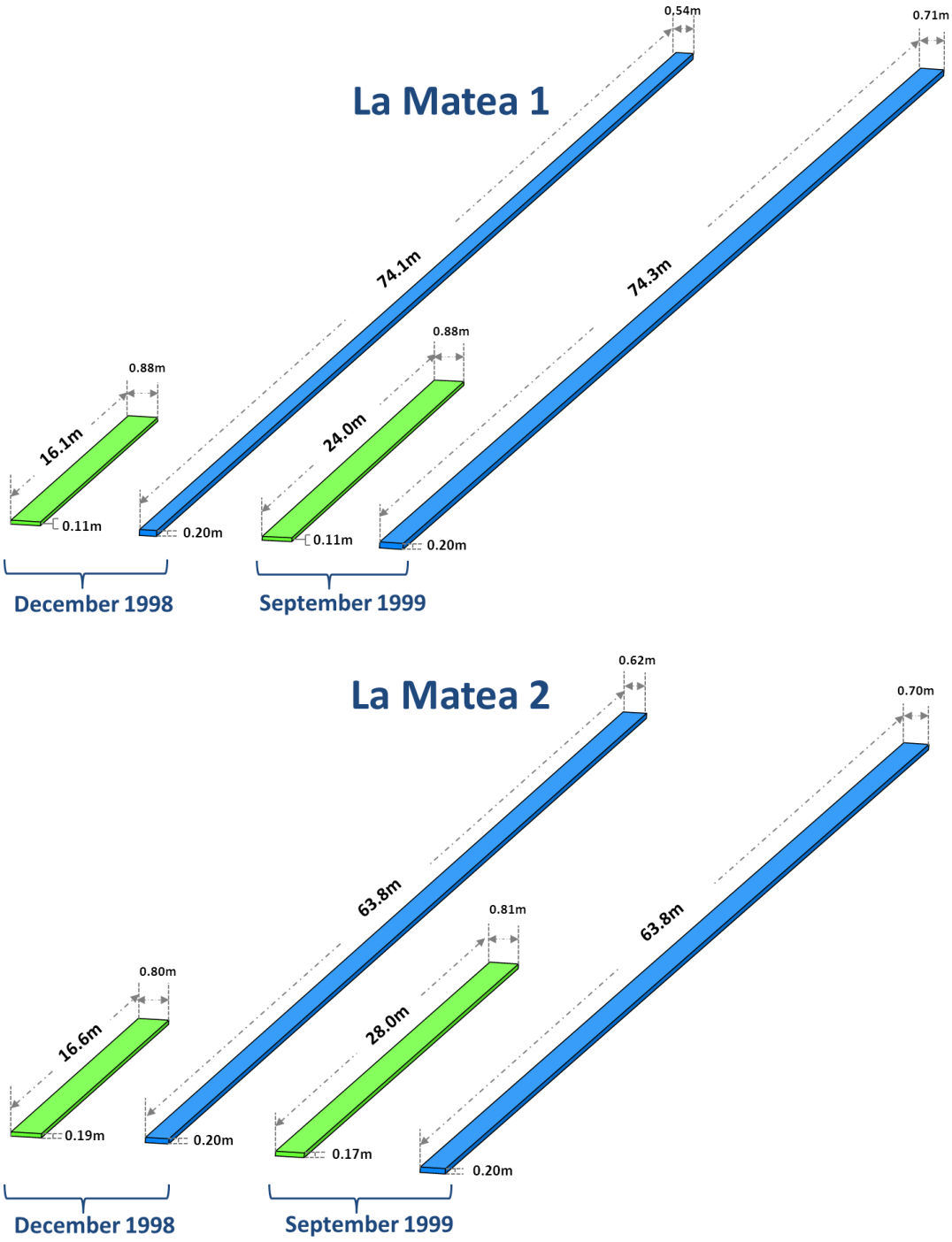

Figure 6. 11: Comparison between observed (green) and simulated (blue) EPGs for La Matea 1(top) and La Matea 2 (bottom), before calibration

6.5.2 La Abejera0 EG

The LaAbejera0 EG was assessed three times during the calibration period. EG measurements were compared to predicted data for the corresponding date before and after τ_c adjustments (internally calculated τ_c based on soil texture was 5.05 $N.m^{-2}$).

Before calibration, the model was able to predict the formation of La Abejera0 EG and its development during the rainfall event of September 13, 1999. According to De Santisteban (2003), the same event was responsible for the appearance of EGs in the field. It was an important rainfall event, with 58mm of precipitation depth that

generated 30.3 mm and 7.5 mm.hr^{-1} of discharge and peak discharges, respectively, which caused the formation of the La Abejera0 EG (Figure 6.13). Simulated EG volume was overestimated by 233.5%, due to high differences in EG depths (Table 6.8 and Figure 6.14). The average depth of the observed EG did not reach tillage depth, however along the EG there were some sections where tillage depth was reached.

Table 6. 8. Measured and simulated EG characteristics for the La Abejera0 EG, before calibration

	La Abejera0					
	September 21, 1999			October 07, 2000		
	Measured	Simulated	Error (%)	Measured	Simulated	Error (%)
Length (m)	67.50	95.18	41.00	39.70	95.18	139.70
Width (m)	0.82	0.86	5.47	0.94	0.86	8.51
Depth (m)	0.09	0.20	131.20	0.07	0.20	185.90
Volume (m^3)	4.76	15.40	223.50	2061.00	15.40	490.00
	October 21, 2001					
	Measured		Simulated		Error (%)	
Length (m)	226.40		95.18		57.90	
Width (m)	0.69		0.82		19.20	
Depth (m)	0.08		0.20		144.10	
Volume (m^3)	12.75		15.10		18.40	

During the agricultural year 1999/2000, De Santisteban (2003) reported that after cereal harvesting in June, 2000, no EG erosion was observed. However, the AnnAGNPS model simulated that the La Abejera0 EG appeared after plowing operations in September, 1999. More precisely, EG initiation was caused by the rainfall event of October 23th, 1999 (11.8 mm), then the EG grew and reached its maximum size after the rainfall event of July 26, 2000 (34.6 mm precipitation). The plot was then plowed on August 18th, 2000. De Santisteban (2003) reported that the rainfall events of August 29th, 2000 (24 mm) only caused the formation of the EG pathway. The EG was not sufficiently well-defined to be measured. The presence of abundant crop residues when the rainfall event occurred prevented EG formation - the model, however, simulated a complete EG formation.

On August 31st, 2000, the EG was refilled by plowing operations. The model predicted the formation of La Abejera0 due to the rainfall event of September 26th, 2000. In this case, the La Abejera0 EG was in fact formed due to the aforementioned rainfall event (17.3 mm precipitation, I30 = 33.8 mm.h^{-1}, and EI30 = 254.8 MJ.mm.ha^{-1}.h^{-1}). There was a 490% overestimation (Table 6.8) between measured and simulated EG volumes, mainly due to the high differences in EG lengths and depths (139.7% and 185.9%, respectively).

On October 25, 2001 the EG was monitored for the third time. In August, 2001, the plot was tilled, and the EG that existed at that time was eliminated. La Abejera0 re-appeared and re-developed as a result of the rainfall events of October 17th and 19th, 2001, with precipitation depths of 12 mm and 20 mm, respectively (De Santisteban, 2003). According to model simulations, the rainfall event of September 22, 2001 (22 mm) was responsible for the formation of La Abejera0, progressively developing with the two succeeding rainfall events of October 17th and 19th, 2001. Comparison between observed and simulated EG volumes show overestimation of EG volumes by 17%. In this case, LaAbejera0 reached an excessive length (276m) in comparison to previous years - it was 137% longer than simulated length (Table 6.8 and Figure 6.14).

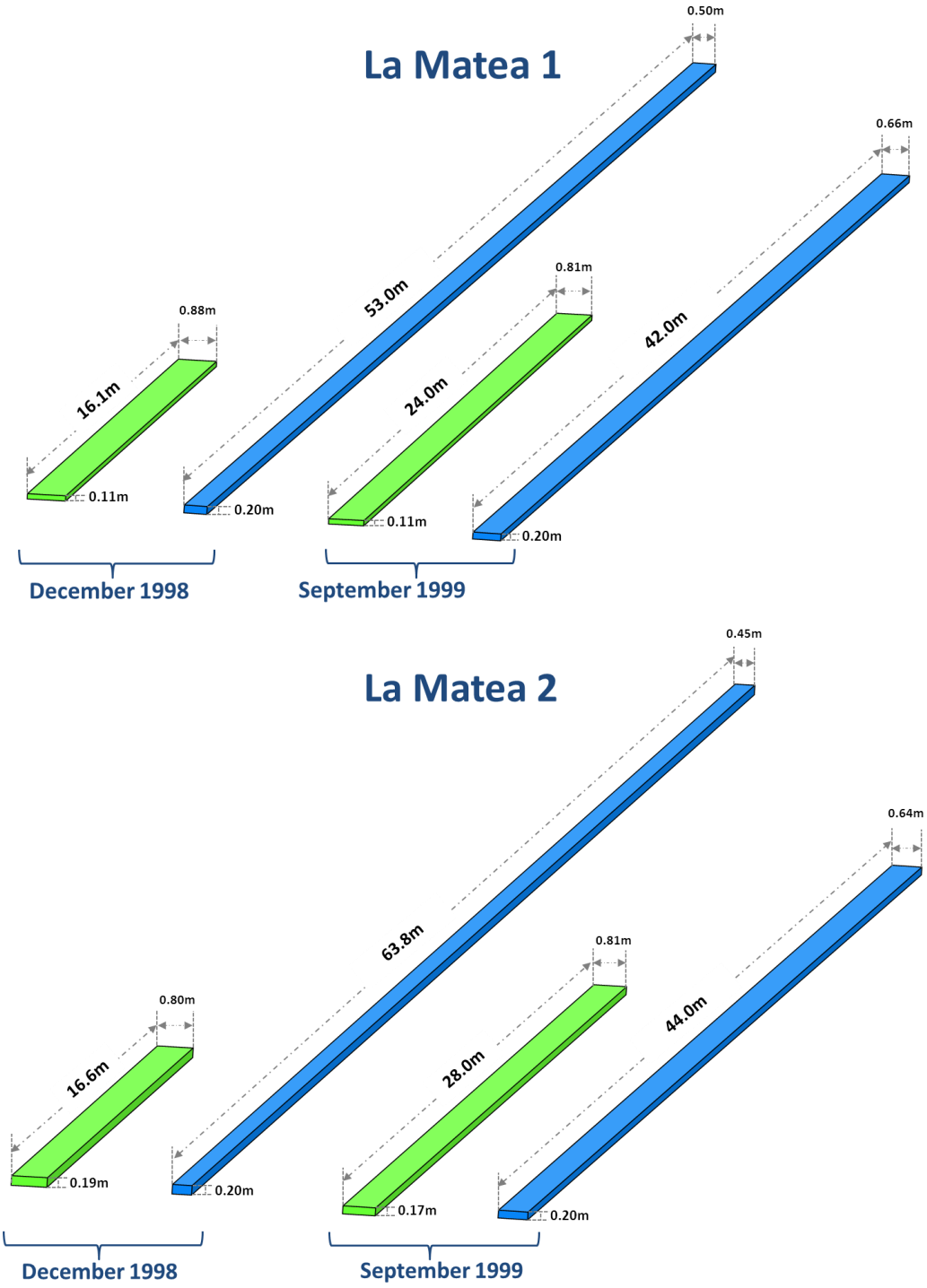

Figure 6. 12: Comparison between observed (green) and simulated (blue) EPGs for La Matea 1 (top) and La Matea 2 (bottom), after calibration

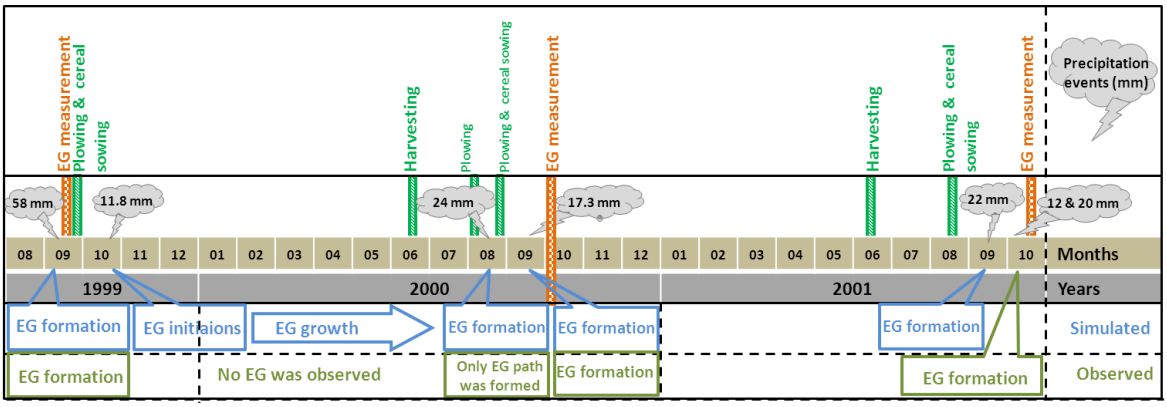

Figure 6. 13: Timeline of La Abejera0, from 1999 to 2001, including applied management practices and measurement dates

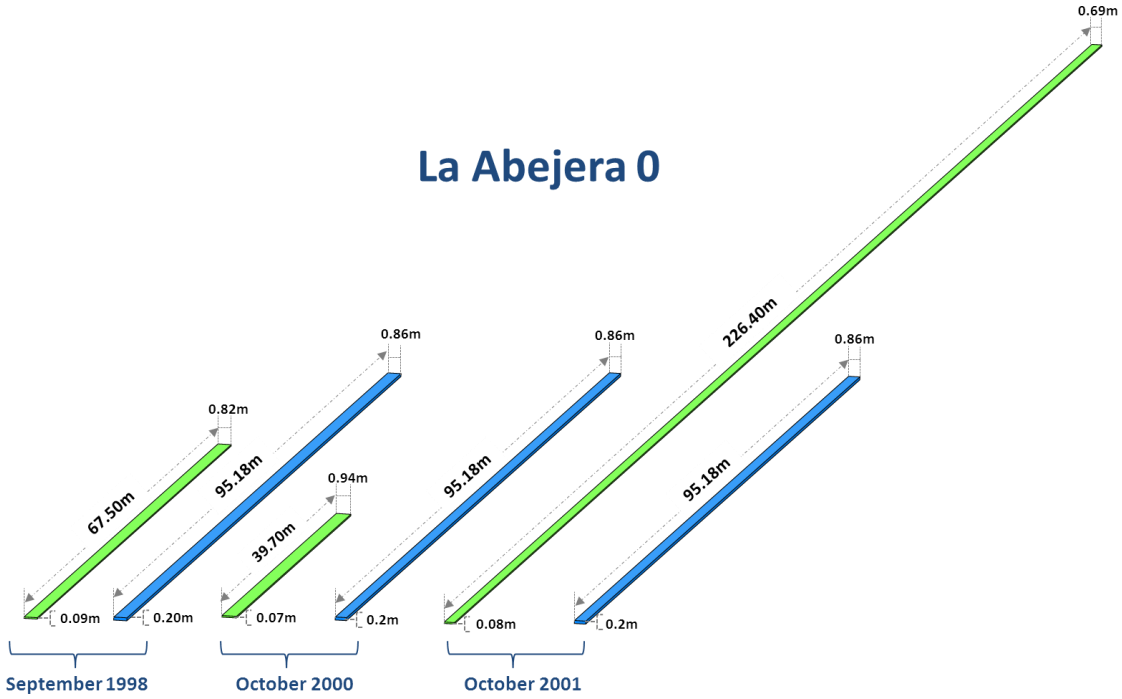

Figure 6. 14: Comparison between observed (green) and simulated (bleu) equivalent prisms for the La Abejera0 EG, before calibration.

Model predictions for the La Abejera0 EG show an overestimation of EG volumes in the three compared situations. Thus, for calibration, τ_c was increased from 5 $N.m^{-2}$ to 8.16 $N.m^{-2}$ (Table 6.6). Despite the decreases in the differences between observed and simulated values, during the first and second measurements the model still overestimated EG volumes by 144.3% and 361.7% for years 1999 and 2000, respectively. In 2001, difference was minimum (3.6%) although difference in lengths was still quite significant (Table 6.8 and Figure 6.14). For the La Abejera0 EG, this important discrepancy between measured and simulated lengths could be due to the elongate shape of its drainage area that enabled a very long EG channel. However, in this case Equation 2.30 (Chapter 2) used by AnnAGNPS to determine the maximum length (Lmax) was not suitable for a precise prediction of LaAbejera 0's length.

When τc was higher than 8.16, the model stopped simulating EG formation on September 26, 2000 - for this reason, during calibration process τc increase was limited to 8.16.

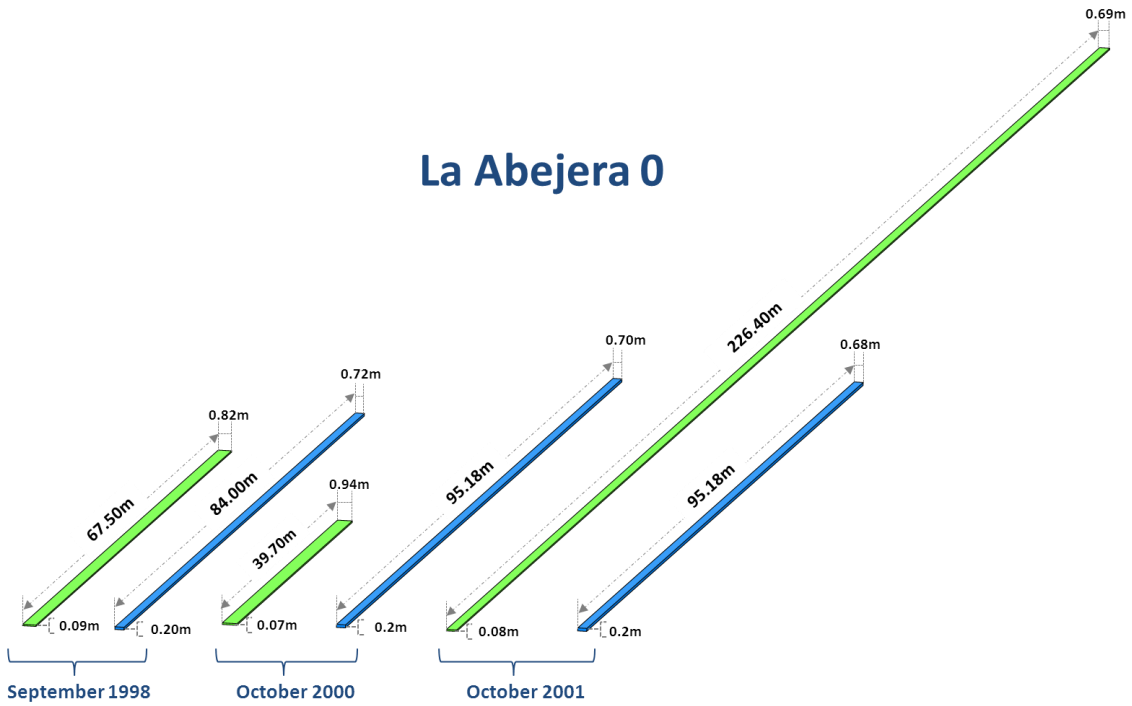

Figure 6. 15: Comparison between observed and simulated equivalent prisms for the La Abejera0 EG after calibration

Table 6. 9. Measured and simulated EG characteristics of the La Abejera 0 EG, after calibration

	La Abejera0					
	September 21, 1999			October 07, 2000		
	Measured	Simulated	Error (%)	Measured	Simulated	Error (%)
Length (m)	67.50	84.00	24.50	39.70	95.18	139.75
Width (m)	0.82	0.72	11.80	0.94	0.70	26.10
Depth (m)	0.09	0.20	131.20	0.07	0.20	185.90
Volume (m^3)	4.76	11.60	144.30	2061.00	12.00	361.70
	October 21, 2001					
	Measured		Simulated		Error (%)	
Length (m)	226.40		95.18		57.90	
Width (m)	0.69		0.68		1.00	
Depth (m)	0.08		0.20		144.10	
Volume (m^3)	12.75		12.28		3.60	

6.5.3 Cobaza1

Unlike the precedent EGs, no-till farming was the soil management selected by the farmers of Cobaza1, which led to a reduction in tillage depth (to seeding depth, 10cm). The Cobaza1 EG was monitored only once after the important rainfall event of September 13th, 1999. Using the specific critical shear stress value internally calculated by the model, τ_c= 1.75 $N.m^{-2}$ (Table 6.6), AnnAGNPS attributed EG formation to the same actual rainfall event during which Cobaza1 was formed. Predicted EG volume

was overestimated by 69.6%. Even when simulated EG length reached its maximum, the model underestimated length by 40% (Table 6.10). Although average EG widths were very similar, the difference between simulated and observed volumes was mainly due to differences in EG depth (59%) (Figure 6.16).

As the simulated length reached its maximum, there is no way to increase simulated length within the calibration process. Then τc variation will affect only EG width, and therefore the initial τc value remained unchanged in the case of the Cobaza 1 EG.

The AnnAGPS model presented the best performance in the prediction of EG erosion at Cobaza1, in comparison with the other EGs. Unsatisfactory results were obtained with La Matea 1, 2 and La Abejera 0 EGs where La Matea 1 and 2 presented very small drainage areas and high slope gradients, while La Abejera 0 presented an elongated drainage area and irregular slope gradient.

The model experiences difficulties to predict EG length when working with complicated situations in term of topographic features (irregular slopes and drainage area shapes). However the model performed well for Cobaza1, characterized by regular drainage area and shape, and a moderate and homogenous slope.

Table 6. 10. Measured and simulated EG characteristics for the Cobaza 1 EG before calibration

Cobaza1 - September, 1998			
	Measured	**Simulated**	**Error (%)**
Length (m)	121.60	86.90	39.90
Width (m)	0.86	0.86	0.50
Depth (m)	0.04	0.10	59.10
Volume (m^3)	4.25	6.90	38.40

6.6 Model validation

After calibration, model validation was carried out using the same inputs considered for calibration and the final values of τ_c. Characteristics of validation period, such as land use and management, were included. The same EGs were monitored between January and December 1996 (Casali, 1997, Casalí et al., 1999), providing observed data that were compared to simulated EG data for model validation. The first assessments were carried out on January, 1996, and included all selected EGs. However, the second measurements were made on December, 1996, only at the La Abejera 0 and LaMatea2 EGs.

6.6.1 LaMatea1 and LaMatea2 EGs

As shown in Table 6.4, the LaMatea plot was seeded with winter cereals in the beginning of October, 1996, and assessment was carried out on January, 1996. During this period, the study area received 220 mm of precipitation, of which 55% was recorded on December, 1995. The same precipitation records were used to simulate EG erosion within validation of the AnnAGNPS.

Casali et al. (1999) and Casali (1997) could not ascertain the formation date of La Matea1 and 2 EGs, although the authors suspected the EGs could have been formed during the rainfall event of January 22nd, 1996 (total precipitation depth 17 mm). The elevated moisture content of the soil at that moment could have facilitated runoff, in addition to bare soil surface conditions. However, the AnnAGNPS model simulated the formation of La Matea 2 due to the rainfall event of December 25th, 1995 (precipitation amount 22.5 mm, which generated 8.2 mm of runoff depth and

1.6mm.hr^{-1} of peak discharge). According to the AnnAGNPS simulations, La Matea 2 developed with following rainfall events, reaching its maximum dimensions at the end of December, 1995. The model did not simulate the formation of La Matea1 during this period, but after monitoring, the date coincided precisely with the event of March 14, 1996 (27mm precipitation depth) (Figure 6.17).

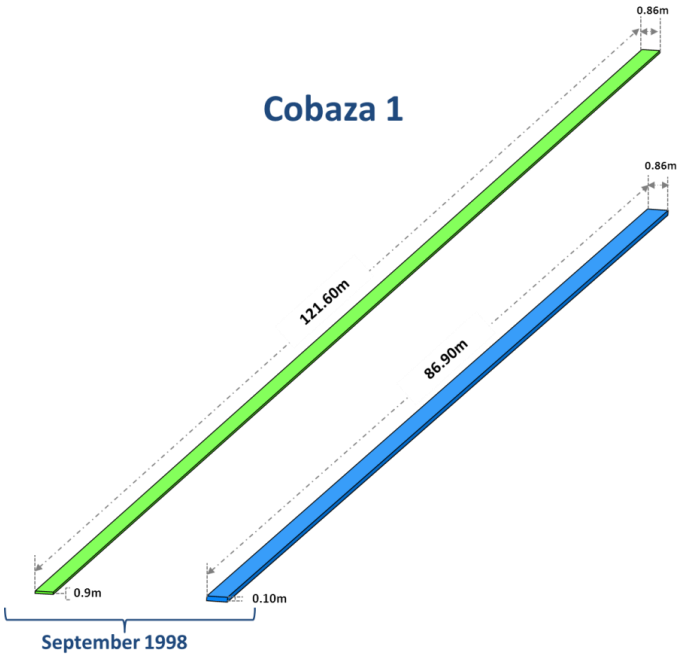

Figure 6. 16: Comparison between observed (green) and simulated (bleu) equivalent prisms for the Cobaza1 EG

The comparison between simulated and measured data revealed an overestimation of LaMatea2 volumes by 95% (table 6.11), mainly due to the excessive overestimation of EG lengths (Table 6.13 and Figure 6.18). The discrepancy between model simulation and real observation regarding the event that formed the EG could be the origin of the differences.

The second monitoring was carried out in December, 1996, when only LaMatea 2 was formed as a consequence of the rainfall events of December,4th and 5th (Casali, 1997, Casalí et al., 1999). The AnnAGNPS model only predicted the initiation of the EG with these events, which was probably due to the atypical characteristics of the rainfall event responsible for the EG appearance. Rainfall was prolonged in time, with constant, low intensity, accumulating more than 50mm. Also, the observed LaMatea 2 length (7.2 m) was very small compared to other years. In addition, the high value of τc assigned to La Matea 2 could have limited the EG migration.

Table 6. 11. Measured and simulated EG characteristics of the La Matea 2 EG, for validation

La Matea2 - January, 1996			
	Measured	**Simulated**	**Error (%)**
Length (m)	29.00	63.86	120.21
Width (m)	0.90	0.44	51.11
Depth (m)	0.10	0.20	91.21
Volume (m^3)	2.73	5.32	94.87

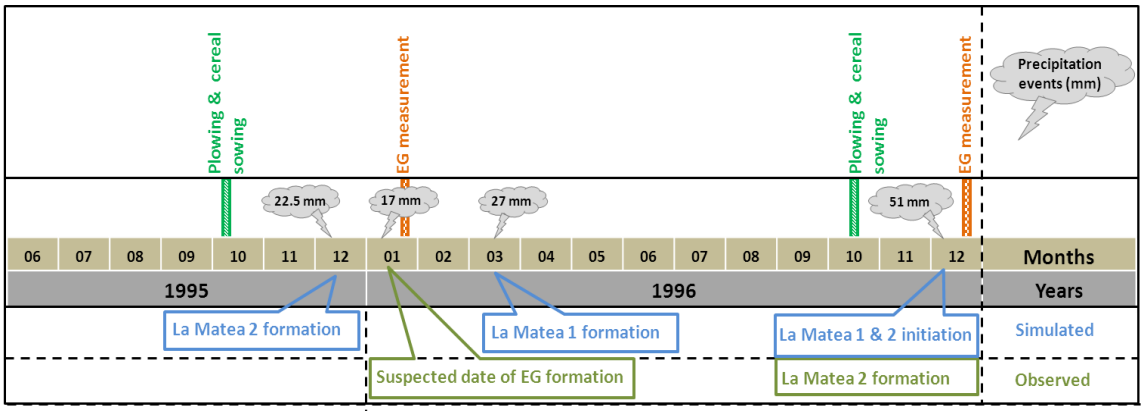

Figure 6. 17: Timeline of La Matea 1 & 2, from 1995 to 1996, including applied management practices and measurement dates

6.6.2 La Abejera0 EG

La Abejera0 was also monitored twice: first monitoring was carried out on January, 1996. Since October, 1994, the plot remained fallow and received 550mm during the entire period. Because of the extended time period between the plowing operations and assessment, it was difficult to identify an exact rainfall event responsible for EG formation. Casali, (1997) suspected that it was highly probable that La Abejera0 was formed in December, 1994, or January, 1995, when a significant rainfall event occurred. AnnAGNPS attributed EG formation to the rainfall event of January 6th, 1995, when 32.5 mm was registered, generating 13.9 mm of runoff and 3.2 mm.hr^{-1} of peak discharge at the EG nickpoint. According to AnnAGNPS, La Abejera0 reached its maximum growth after the rainfall event of December 12th, 1995.

The second monitoring was carried out after the rainfall events of December 4th and 5th, 1996, responsible for the re-appearance of La Abejera0 EG after the plot was plowed and seeded in *beginning of October, 1996* (Casali, 1997, Casalí et al., 1999).Concerning AnnAGNPS simulations, the same rainfall event caused EG formation, with a 51 mm rainfall depth, generating 21.3 mm and 5 mm.hr^{-1}of runoff and peak discharge, respectively (Figure 6.19).

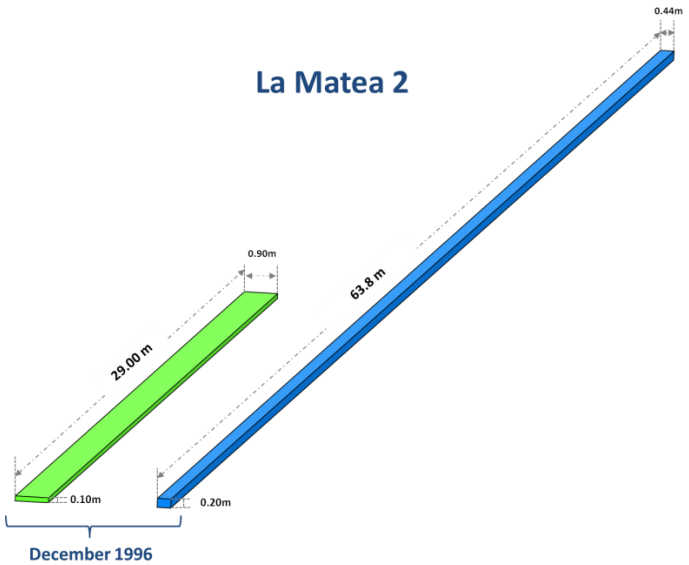

Figure 6. 18: Comparison between observed (green) and simulated (blue) equivalent prisms for the La Matea 2 EG, for validation

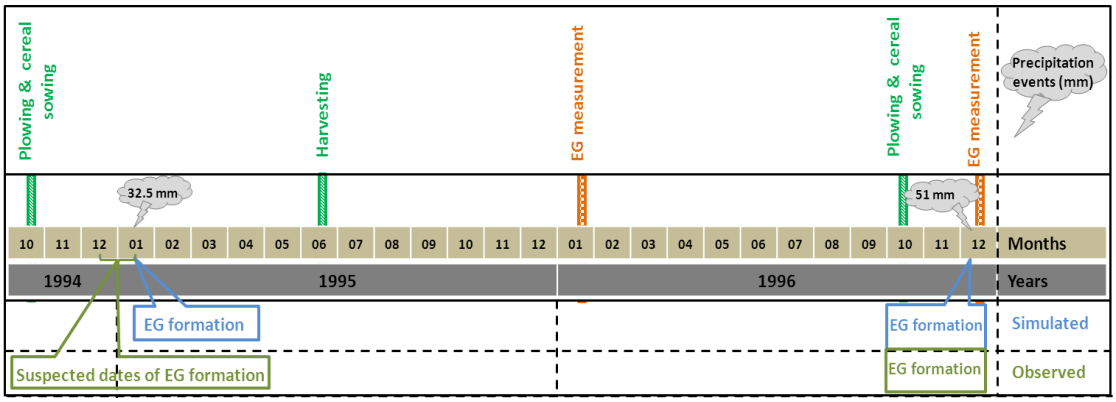

Figure 6. 19: Timeline of the La Abejera0 EG, from 1995 to 1996, including applied management practices and measurement dates.

Comparison of simulated and measured data of the first and second measurements revealed that simulated EG volumes were overestimated by 38.3% and 4123%, respectively (Table 6.12). This occurred because of great differences between measured and simulated lengths in both cases (Figure 6.20). In addition, in December, 1996, the depth of La Abejera 0 was very shallow, leading to great differences between observed and simulated erosions.

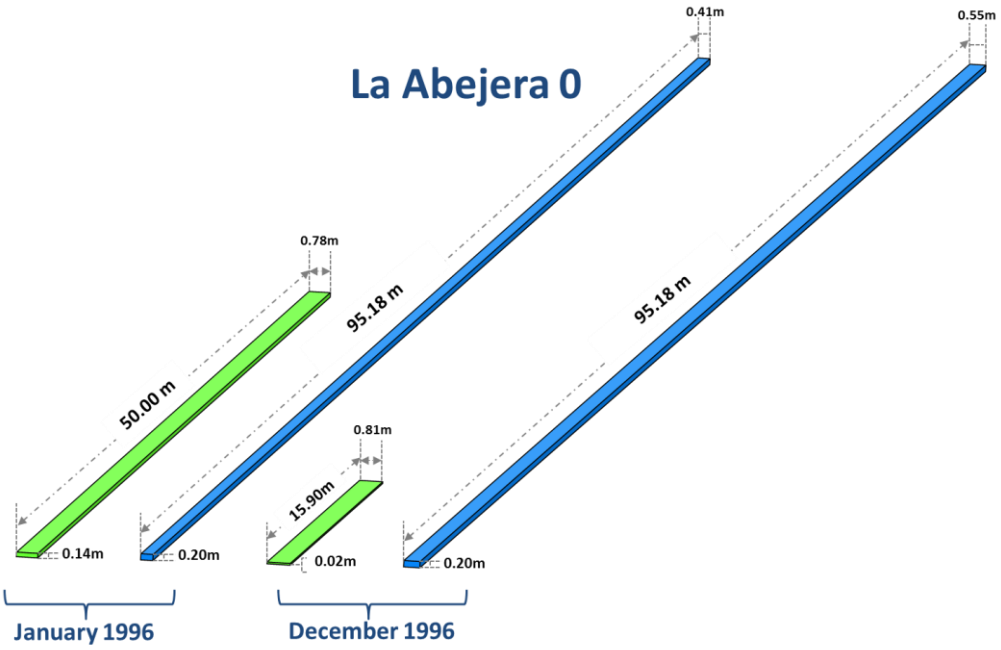

Figure 6. 20: Comparison between observed (green) and simulated (bleu) equivalent prisms the of La Abejera 0 EG, for validation

Table 6. 12. Measured and simulated EG characteristics of the La Abejera 0 EG, for validation

	La Abejera0					
	January 1996			December 1996		
	Measured	Simulated	Error (%)	Measured	Simulated	Error (%)
Length (m)	50.00	95.20	90.36	15.90	95.18	498.62
Width (m)	0.78	0.41	47.44	0.81	0.55	32.10
Depth (m)	0.14	0.20	41.82	0.02	0.20	1029.74
Volume (m^3)	5.50	7.61	38.36	0.22	9.63	4123.68

6.6.3 Cobaza1 EG

As aforementioned, the Cobaza1 EG was only assessed in January 1996. Similarly to previous EGs, the rainfall event of January 22, 1996, caused EG formation. However, the AnnAGNPS model simulation attributes the formation of Cobaza1 to the rainfall event of December 7th, 1995, when 19.5mm were recorded and generated 4 mm of runoff and 0.45 $mm.hr^{-1}$ at the EG nickpoint.

According to the AnnAGNPS simulations, two different rainfall events in 1995 were responsible for the formation of Cabaza1 and La Matea2: December 7th with 19.5 mm and December 25th with 22.5 mm, respectively. Cobaza1 was formed before La Matea 2, and was caused by a less-intensive rainfall event (lower precipitation amounts), and therefore assigned a lower τc value. The La Matea 2 τc value was higher, therefore indicating the necessity of more precipitation to be formed.

According to AnnAGNPS, the development of Cobaza1 reached its maximum at the end of December, 1995. Comparison of simulated and measured results provided the best results rather than calibration, with a 7.5% error in EG volumes, which was the best results obtained within model evaluation (Table 6.15 and Figure 6.21).

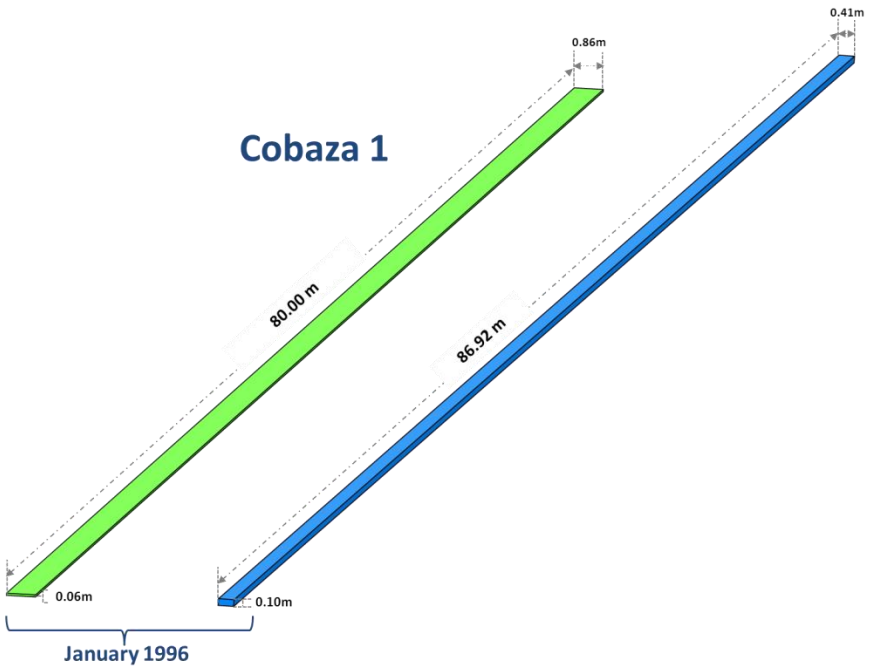

Figure 6. 21: Comparison between observed and simulated equivalent prisms for the Cobaza 1 EG, for validation

Table 6. 13. Measured and simulated EG characteristics of the Cobaza 1 EG, for validation

Cobaza 1 - January, 1996			
	Measured	**Simulated**	**Error (%)**
Length (m)	80	86.9	8.66
Width (m)	0.86	0.41	52
Depth (m)	0.06	0.1	77
Volume (m^3)	3.85	3.56	7.5

Chapter 7: Conclusions

This Chapter summarizes the results and main conclusions of the thesis, followed by a discussion of contributions to current knowledge and future directions.

At the small Latxaga watershed, adequate calibration and validation were achieved for runoff, only modifying the CN values. The response has been satisfactory at monthly level and also at seasonal and annual levels. A precise monthly and seasonal simulation of runoff is particularly relevant as it is a conditioning factor for erosion and sediment exports. Moreover, a satisfactory simulation of sediment exports cannot be considered if runoff, a key parameter in the process, is not appropriately simulated, especially in the moments during which the watershed is most susceptible. Therefore, time-scaled calibration, aimed at an adequate monthly simulation, seems to be an appropriate procedure when compared to calibration aimed at annual adjustments. This last focus can be sufficient from the viewpoint of, for example, planning of hydric resources; however, it results challenging to obtain adequate adjustment of erosion. Event-based calibration could be explored, although herein it has been timelier to select monthly calibration, which is in principle more close to nature and the objectives of the model, which considers long periods.

Calibration consisted of adjusting the initial CN values, as well as adding new CN values during Winter and Spring. Nevertheless, it was necessary to utilize CN values that were less realistic, which could raise questions on the validity of the model.

On one hand, this could be due to the need to adjust the elevated infiltration observed in the zone in dry periods, through CN adjustments. These infiltration levels are much higher that what would be expected for the soil texture. It was observed that, at the beginning of Autumn, simulated runoff was (much) higher than what was observed. This could be due to the presence of preferential flow, verified in the zone. During the experiments of rainfall simulation at the Latxaga watershed, very high infiltration intensities were observed due to the abundance of cracks. These intensities were much higher than those expected. Recent experiments (Iturria et al., 2017a, Iturria et al., 2017b) have demonstrated and accounted for the existence of preferential flows in soils of the Pamplona basin. The calibration exercise carried out by Gastesi (2014) reached similar conclusions, and the same can be said about the behavior observed during runoff calibration in the Cemborain watershed, also carried out within the framework of this thesis.

On the other hand, during the adjustment of simulated runoff in Winter and Spring the opposite has occurred (although less pronounced): it was necessary to increase CN values, as a consequence of the effect transmitted by the very low CN values at the beginning of Autumn and decrease of infiltration by preferential flow paths due to the expansion of the soil. The latter was a consequence of the increased soil humidity during Winter.

This behavior seems to evidence the own limitations of the CN method for small watersheds, where local or peculiar phenomena can present great transcendence and not be adequately simulated. Nevertheless, in large watersheds such effects could be diluted and amortized. Therefore, in this case the necessity of considering continuous temporal adjustments arises, in addition to the temporal adjustment already carried out by the model, as accomplished herein.

This justifies therefore the consistent solution adopted herein, as previously indicated, to adjust the initial CN value as well as reassign new CN values in Winter and Spring, although these final parameter values could be less realistic. However, it

was not possible to calibrate the model for adequate temporal simulation of runoff without this procedure.

It is necessary, nevertheless, to determine and justify more precisely the moments in which to proceed with the adjustment, and attempt to relate these with objective criteria such as the phonological state of the crop or hydrological behavior.

After verification of preferential flow in the zone and of its apparently great transcendence in runoff simulation, there is a clear necessity of characterization of its occurrence, at least in Navarre, and of a more adequate estimation of its influence on infiltration.

Despite the generalized use of the AnnAGNPS model worldwide, a complete sensibility analysis of the model still remains unexplored, using advanced techniques such as

Sobol and Morris (Loizu et al., 2016) and the consequent application of optimization strategies, such as Powell's algorithm (Loizu et al., 2016) or genetic algorithms (Srivastava et al., 2003, Maringanti et al., 2009). Possibly after these are carried out, simulations will acquire more consistence. The calibration strategy of the model through CN, regarding its temporal dynamics, could benefit from a better definition. In this sense, the information available from the Network of Experimental Agrarian Watersheds of Navarre, especially for those watersheds with homogeneous soil use (Latxaga, Oskotz Forestal and La Tejería), is of great value to estimate CN values and its temporal evolution, which is a considerable contribution.

Although carried out in a small watershed with homogeneous soil use, simulation of sediment exports was less satisfactory than runoff, corroborating other similar studies. This can be explained by the high complexity of the phenomenon to the studied, with a great diversity of associated, interrelated processes that also occur at the small Latxaga watershed. In this watershed, relief and channel vegetation seem to play an important role in the dynamics of sediments - this hypothesis was already considered and analyzed by Casalí et al. (2008). These dynamics occur in a specific complex context where erosion occurs in hillsides with very pronounced slopes and sedimentation occurs in the channels, where slopes are less inclined but present the development of dense vegetation subjected to high variability throughout the year. This leads to the conclusion that it is necessary to introduce more detailed topographic information in the simulations, especially on the longitudinal profile of the main channels.

The use of stream networks and corridor models, already implemented within the system of computer models that make up AnnAGNPS, such as CONCEPTS (Conservational Channel Evolution and Pollutant Transport System) (Langendoen, 2000) seem to be necessary for a more precise explanation of sediment yield and load at event, seasonal and monthly scales, even for small watersheds. These models include more detailed science on channel hydraulics, morphology, detachment of soil and transport and deposition of sediments.

The best results regarding the simulation of sediment exports have been obtained for the annual simulation, which was not unexpected, as calibration was directly aimed at this objective, given the impossibility of achieving adequate calibrations at monthly or seasonal levels. At an annual level, the model was capable of predicting the total sediment yield with a difference of less than 1% between measured and simulated values after calibration, and with a difference of 7% for validation. These apparently good values are misleading as, although the annual average value for the period is

adequate, the annual simulation was not correct. Monthly and seasonal simulations were not satisfactory either.

However, it must be highlighted that the model has not been formulated for a detailed estimation of event-based or short-term processes, but for the detection of trends at the long term - which is where its utility is. In this sense, the simple scenario analysis proposed herein results especially illustrative, providing interesting and illustrating information.

As for runoff, a complete sensibility analysis for the model remains unexplored, utilizing advanced techniques such as those aforementioned.

Evaluation of the model for runoff at a larger watershed than Latxaga, much more complex, with different, contrasting characteristics (climate, soil, and topography) and more varied soil use entails, firstly, great complexity in parameterization and in the estimation of fundamental variables. If calibration with variable CN and homogeneous soil use is already complex, this is obviously incremented when multiple soil uses are considered, along with variable crops. The use of Landsat 5 TM and SPOT5 satellite images seems to be a good procedure to identify, with details, the different soil uses and crops. A calibration support tool also seems necessary as well as a rigorous study of scenario parameterization with spatial and temporal variability.

For those crops where comparison was possible (winter cereal), the final Cn values after calibration were similar to those of Latxaga.

However, those calibration results were better than those obtained herein for Latxaga. Calibration is especially difficult at the beginning of Autumn or Summer, so it was also necessary to adjust CN values, in a similar procedure to that utilized herein for Latxaga.

Good surface runoff prediction performance was obtained after calibration, with Em= 0.89, Es=0.97, Ea= 0.930. Also, statistical significance tests with p-value < α = 0.10 indicated satisfactory goodness-of-fit between observed and simulated surface runoffs. However, during validation, the model overestimated surface runoff with PBIAS= 30.7%. The model was not able to reproduce the same results as in calibration, with Em = 0.43 and Ea=-2.09. Better results were obtained at a seasonal time scale, with Es=0.71. During the validation exercise, the model revealed limitations in predicting snowmelt correctly by overestimating the predicted surface runoff after a snow event, producing outlier results at a monthly scale, which affected the statistical results of validation.

The low annual sediment exports estimated for Cemborain (50 kg ha year) must be highlighted. Although 3/4 of the surface is occupied by forest and brushland, the remaining 1/3 (approximately 1200 ha) is cultivated (cereals, olive groves, vineyards). An entirely forest watershed such as Oskotz registered, in less than one decade (2202-2008), more than 700 kg ha year. These elevated registries were mainly due to uncontrolled felling, rather than soil use per se. Assuming that at Cemborain these operations are carried out correctly, the sediments are almost exclusively originated from the cultivated surface (1200 ha). As the 50 kg ha year have been calculated considering the total surface of the watershed (50 km^2), the real rate would be approximately 200 kg ha year. Still, the value is lower than what was registered at Latxaga (approximately 350 kg ha year), especially if taking into account the fact that in vineyards and olive groves, erosion rates are usually higher than those registered for cereal crops. In Cemborain, the agrarian area is close to the watershed outlet, and therefore it is expected that most of the eroded material is evacuated, and soil erosion would not be underestimated.

The availability of orthophotos repeatedly taken at the same zone, for the same times of the year, can provide very valuable information on ephemeral gully erosion. The methodology proposed herein results promising in this sense. From orthophotos, it was possible to locate the upstream and downstream extremes, the main channel, its length, etc, for several years. The location of the gully extremes enabled determination of CTIc values.

The APEGT model within AnnGNPS is, up to now, the main tool available at a user level for the location of gully-susceptible zones and headcuts. Numerous improvements must still be implemented, which should be explored in details. Therefore, this thesis has carried out the most extensive documented evaluation up to the date of CTI (Compound Topographic Index) application for the location of headcuts. Twelve gullies have been analyzed throughout seven years.

The results obtained herein demonstrated that the DEM raster grid cell size affected the determination of critical CTI values. The 5 m resolution DEM prevented the detection of small topographic variations (small streams or drainage channels), which influenced the determination of the real EG drainage area and critical CTI value. Thus, considering the complexity of the topographic nature within the study area, DEM with a raster grid cell size of 2 m or less is essential for the development of automated techniques to locate gully initiation points.

Adequate comprehension of CTI in its application for the location of EGs requires the inclusion of CTIc values: CTIc1 and CTIc2. The first value reflects the critical conditions for the starting of a headcut, and the second value, for its migration. Given that CTI only considers topographic parameters, this technique does not allow for the prediction of headcuts for events or concrete circumstances. For homogeneous zones regarding climate, soil use and management, it would be possible to identify average representative values for CTIc that would be useful to characterize gully headcuts. Given the complexity of the challenge, an approximation is a considerable advance, and agrees with the last objective of AnnAGNPS, which is to support environmental management of agrarian zones at medium- and long- term. This affirmation is supported by the relatively low inter-annual variability of CTIc values, especially CTIc2. Anyway, inter-annual variability within the same year is considerable and highlights the existence of other variables and processes to explain the formation of ephemeral gullies (considering equal climatic, edaphic, and soil use and management conditions), different from excess of shear stress such as subsurface flows (exfiltration of seepage), preferential flow paths, soil humidity regime conditions, which in turn are influenced by position within the environment, etc. For the study area, a threshold CTI for EG initiation is approximately 500. However, the erratic characteristics of Mediterranean climate require more monitoring years to obtain a more accurate and reliable value that is representative of the entire area. The corresponding CTI for EG migration is approximately 90. This is a more reliable threshold value than the former one (for CTIc1) as its variability was much lower.

For the identification of headcuts, it would be desirable to incorporate within topographic criteria (such as CTIc) elements that considered, at least in part, the remaining controlling factors, as for example the factors connected with edaphic characteristics, such as those proposed by Ollobarren et al. (2016).

It was observed that classical EGs of the study zone were not the majority, and the gullies baptized by Casalí et al. (1999) as drainage EGs were also very frequent.

Considering that AnnAGNPS, and in general all available analysis tools, only consider classical EGs, it is clear that most EG erosion cannot be modeled. This is,

without doubts, one of the most important challenges for future work. This limitation includes the location of the initial headcut as well as the development of the gully, which can be in turn analyzed in classical EGs.

The repetitive apparition of EGs has not been elevated in the study zone. This could indicate, complementing what was previously indicated regarding the high variability observed in CTIc values, that the processes implicated in the apparition of EGs are more numerous and complicated than they appear to be.

Through orthophotos it is possible to obtain a fast and convenient estimation of EG erosion in extensive areas during long periods of time (once the relationship length-volume of the study zone itself, as with this method it is only possible to correctly estimate length). This approximation has been previously explored (Nachtergaele and Poesen, 1999). Nevertheless, this thesis improves and completes the approach, including series of photos throughout several.

The erosion intensities obtained are comparable to those measured in situ at the zone by direct methods (Casalí et al., 1999, De Santisteban et al., 2006). Although for a more truthful verification, the areas of small hydrographic watersheds of each gully must be measured to refer the obtained erosion to a surface unit. In addition to the topographic features, a positive correlation was observed between the total precipitation during the agricultural year and the total annual EG lengths.

This thesis has carried out the most actual, extensive documentation of module AnnAGNPS for the estimation of EG erosion (TIEGEM). Calibration has been carried out considering only the main parameter of the model, which is critical shear stress τ_c.

There were two main criteria fundamental for calibration. Firstly, adequate simulation of the moment of EG occurrence/apparition. Secondly, adequate simulation of the gully's volume, which obviously implies in adequate simulation of the gully's dimensions. In the calibration phase, the AnnAGPS model was able to adequately simulate the appearance of EGs. However in the validation phase, the results obtained demonstrated the model was not successful in the simulation of EG formation dates.

The model was capable of satisfactorily predicting EG whenever the topography of the watershed where the gully developed was more or less homogeneous. For example, drainage areas with very irregular borders or with longitudinal and transversal axels very asymmetrical and/or with abrupt changes in slopes, result in important errors in the estimation of the geometry of the gully by the algorithms within the model. The main error was observed in the overestimation of the maximum length of the gully; this length is precisely estimated in function of the drainage area. This could be probably solved by using high resolution DEMs, from which it would be possible to delimitate precisely the drainage area. Nevertheless, these types of DEM are not conventional, especially covering wide extensions of terrain. Calibration revealed that τc variation had a clear effect on EG formation and migration, but not sufficient to decrease EG volume overestimation

It is therefore interesting to propose alternative methods for the calculation of maximum length. In this sense, CTIc2 could be proposed to support a new algorithm for calculation of Lmax in EGs.

An essential element of TIEGEM is the equation developed by Alonso et al. (2002) for the estimation of headcut migration and its erosive effects. Although a clear advance, after time has elapsed it seems convenient to carry out modifications in the equation that allow for the consideration of aspects not previously contemplated but that occur in reality. For example, the presence of non homogeneous soil profiles.

However, it seems that avoiding the beginning of headcut migration until tillage is finished does not seem very realistic. Measurements indicate that migration starts before the aforementioned depth is reached, although the maximum depth reached by the gully in reality is conditioned by tillage efforts.

Setting gully depth equal to tillage depth, a mandatory step, significantly conditions simulation. In addition, there is the difficulty in estimating such depth and the necessity of considering that tillage is not always present, at least not with the same intensity.

The proposed scheme for headcut generation from overcoming τ_c and migration etc., is valid for many circumstances. Nevertheless, it has been progressively verified by the scientific community that many other processes play important roles in the apparition and migration of EGs, such as piping, subsurface flow, and the simple overcoming of τ_c in large zones without the necessity of a migrating headcut

References

Abdelwahab, O.M.M., Bingner, R.L., Milillo, F., Gentile, F., 2016. Evaluation of Alternative Management Practices with the AnnAGNPS Model in the Carapelle Watershed. Soil Sci. 181, 293-305.

Abdelwahab, O.M.M., Bingner, R.L., Milillo, F., Gentile, F., 2014. Effectiveness of alternative management scenarios on the sediment load in a Mediterranean agricultural watershed. Journal of Agricultural Engineering 45, 125-136.

Allen, R.G., Pereira, L.S., Raes, D., Smith, M., 1998. Crop evapotranspiration - Guidelines for computing crop water requirements **
**. FAO Irrigation and drainage paper 56 FAO - Food and Agriculture Organization of the United Nations.

Almagro, M., de Vente, J., Boix-Fayos, C., García-Franco, N., Melgares de Aguilar, J., González, D., Solé-Benet, A., Martínez-Mena, M., 2016. Sustainable land management practices as providers of several ecosystem services under rainfed Mediterranean agroecosystems. Mitigation Adapt. Strateg. Global Change 21, 1029-1043.

Alonso, C.V., Bennett, S.J., Stein, O.R., 2002. Predicting head cut erosion and migration in concentrated flows typical of upland areas. Water Resour. Res. 38, 391-3915.

Arnold, J.G., Allen, P.M., Muttiah, R., Bernhardt, G., 1995. Automated Base Flow Separation and Recession Analysis Techniques. Groundwater 33, 1010-1018.

Arnold, J.G., Williams, J.R., Srinivasan, R., King, K.W., 1996. SWAT: Soil and Water Assessment Tool .

Auzet, A.-., Poesen, J., Valentin, C., 2004. Soil surface characteristics: Dynamics and impacts on soil erosion. Earth Surf. Processes Landf. 29, 1063-1064.

Baginska, B., Milne-Home, W., Cornish, P.S., 2003. Modelling nutrient transport in Currency Creek, NSW with AnnAGNPS and PEST. Environmental Modelling and Software 18, 801-808.

Beasley, D.B., Huggins, L.F., Monke, E.J., 1980. ANSWERS: a model for watershed planning. Transactions, American Society of Agricultural Engineers 23, 938-944.

Benito, G., Gutierrez, M., Sancho, C., 1993. The influence of physico-chemical properties on erosion processes in badland areas, Ebro Basin, NE-Spain. Zeitschrift fur Geomorphologie 37, 199-214.

Bennett, S.J., 2006. Personal communication at 7th International Symposium on Gully Erosion, May 23-27 - Purdue University.

Bernard, J., Lemunyon, J., Merkel, B., Theurer, F.D., Bingner, R.L., Dabney, S.M., Langendoen, E., Wells, R., Wilson, G., 2010. Ephemeral gully erosion : a national resource concern : recommendations for the development of technology and tools for prediction and treatment of ephemeral gully erosion. NSL Technical Research Report 69, 67.

Bingner, R.L., Theurer, F.D., 2002. Physics of suspended sediment transport in AnnAGNPS. Proceedings of the 2002 Second Federal Interagency Hydrologic Modeling Conference , Las Vegas, NV, July-August , 12.

Bingner, R.L., Darden, R.W., Theurer, F.D., Garbrecht, J., 1997. GIS-based generation of AGNPS watershed routing and channel parameters. ASAE Paper No.97-2008 .

Bingner, R.L., Theurer, F.D., 2001. Topographic factors for RUSLE in the continuous-simulation, watershed model for predicting agricultural, non-point source pollutants (AnnAGNPS). Soil Erosion for the 21st Century - An International Symposium .

Bingner, R.L., Theurer, F.D., Yuan, Y., 2012. AnnAGNPS TECHNICAL PROCESSES. http://www. ars. usda. gov/Research/docs. htm?docid=5199 .

Boardman, J., Poesen, J., 2006. Soil Erosion in Europe. JohnWiley.

Borah, D.K., Bera, M., 2003. Watershed-scale hydrologic and nonpoint-source pollution models: Review of mathematical bases. Transactions of the American Society of Agricultural Engineers 46, 1553-1566.

Bos, M.G., 1989. Discharge Measurement Structures. International Institute for Land Reclamation and Improvement (ILRI), Wageningen, The Netherlands, 464.

Brown, L.C., Foster, G.R., 1987. STORM EROSIVITY USING IDEALIZED INTENSITY DISTRIBUTIONS. Trans. ASAE 30, 379-386.

Campo, M.A., Álvarez-Mozos, J., Casalí, J., Giménez, R., 2007. Effect of topography on retreat rate of different gully headcuts in Bardenas Reales area (Navarre, Spain). Progress in gully erosion research , 24-25.

Campo-Bescõs, M.A., Flores-Cervantes, J.H., Bras, R.L., Casalí, J., Giráldez, J.V., 2013. Evaluation of a gully headcut retreat model using multitemporal aerial photographs and digital elevation models. J. Geophys. Res. F Earth Surf. 118, 2159-2173.

Casali, J., 1997. Caracterisación y control de la erosión por cárcavas.

Casali, J., Giménez, R., Campo, M.A., 2015. Gully geometry: what are we measuring? Soil 1, 509-513.

Casalí, J., Gastesi, R., Álvarez-Mozos, J., De Santisteban, L.M., Lersundi, J.D.V.d., Giménez, R., Larrañaga, A., Goñi, M., Agirre, U., Campo, M.A., López, J.J., Donézar, M., 2008. Runoff, erosion, and water quality of agricultural watersheds in central Navarre (Spain). Agric. Water Manage. 95, 1111-1128.

Casalí, J., Giménez, R., De Santisteban, L., Álvarez-Mozos, J., Mena, J., Del Valle de Lersundi, J., 2009. Determination of long-term erosion rates in vineyards of Navarre (Spain) using botanical benchmarks. Catena 78, 12-19.

Casalí, J., Giménez, R., Díez, J., Álvarez-Mozos, J., Del Valle de Lersundi, J., Goñi, M., Campo, M.A., Chahor, Y., Gastesi, R., López, J., 2010. Sediment production and water quality of watersheds with contrasting land use in Navarre (Spain). Agric. Water Manage. 97, 1683-1694.

Casalí, J., López, J.J., Giráldez, J.V., 1999. Ephemeral gully erosion in southern Navarra (Spain). Catena 36, 65-84.

Chahor, Y., Antoñanzas, C., Loizu, J., Casalí, J., Campo-Bescós, M.A., Giménez, R., 2011. Evaluation of the AnnAGNPS model for predicting runoff in large agricultural watershed in Navarre (Spain). EGU General Assembly .

Chahor, Y., Casalí, J., Giménez, R., Campo, M.A., 2016. Evaluation of the Compound Topographic Index (CTI) for predicting ephemeral gully erosion in Navarre. 7 th International Symposium on Gully Erosion Purdue University West Lafayette, Indiana, USA May 23 - 27, 2016.

Chahor, Y., Casalí, J., Giménez, R., Campo-Bescós, M.A., 2017. Long term characterization of ephemeral gully erosion from orthophotographs. EGU General Assembly Vol. 19, 5433.

Chahor, Y., Casalí, J., Giménez, R., Bingner, R.L., Campo, M.A., Goñi, M., 2014. Evaluation of the AnnAGNPS model for predicting runoff and sediment yield in a small Mediterranean agricultural watershed in Navarre (Spain). Agric. Water Manage. 134, 24-37.

Chow, V.T., Maidment, D.R., Mays, L.W., 1988. Applied Hydrology .

Christiaens, K., Feyen, J., 2002. Use of sensitivity and uncertainty measures in distributed hydrological modeling with an application to the MIKE-SHE model. Water Resour. Res. 38, 81-815.

Cronshey, R.G., Theure, F.D., 1998. AnnAGNPS—Non-Point Pollutant Loading Model. In Proceedings First Federal Interagency Hydrologic Modeling Conference 19-23 April, Las Vegas, 9-16.

Daggupati, P., Douglas-Mankin, K.R., Sheshukov, A.Y., 2013. Predicting ephemeral gully location and length using topographic index models. Trans. ASABE 56, 1427-1440.

Das, S., Rudra, R.P., Gharabaghi, B., Gebremeskel, S., Goel, P.K., Dickinson, W.T., 2008. Applicability of ann AGNPS for Ontario conditions. Canadian Biosystems Engineering / Le Genie des biosystems au Canada 50, 1.1-1.11.

De Roo, A.P.J., Offermans, R.J.E., Cremers, N.H.D.T., 1996. LISEM: a single-event, physically based hydrological and soil erosion model for drainage basins. II: sensitivity analysis, validation and application. Hydrol Processes 10, 1119-1126.

De Santisteban, L.M., 2003. Análisis de factores topográficos para predecir la erosión por cárcavas efímeras.

De Santisteban, L.M., Casalí, J., López, J.J., 2006. Assessing soil erosion rates in cultivated areas of Navarre (Spain). Earth Surf. Processes Landf. 31, 487-506.

Desmet, P.J.J., Poesen, J., Govers, G., Vandaele, K., 1999. Importance of slope gradient and contributing area for optimal prediction of the initiation and trajectory of ephemeral gullies. Catena 37, 377-392.

Donézar, M., Del Valle de Lersundi, J., 2001. Red de cuencas experimentales agrarias de Navarra.

Donézar, M., Illarregui, M., Del Valle de Lersundi, J., 1990. *Erosión actual en Navarra.* Gobierno de Navarra, Ministerio de Comercio y Turismo .

Donigian, A.S., 2002. Watershed model calibration and validation: the HSPF experience. Water Environment Federation National TMDL Science and Policy Speciality Conference .

Eckhardt, K., 2005. How to construct recursive digital filters for baseflow separation. Hydrol. Process. 19, 507-515.

EEA, 2003. Assessment and Reporting on Soil Erosion. European Environment Agency Technical Report 94.

Efron, B., 1979. Bootstrap methods: another look at the jackknife. Ann. Stat 7, 1-26.

Efron, B., Tibshirani, R.J., 1993. An Introduction to the Bootstrap. Chapman & Hall, New York.

Famiglietti, J.S., Wood, E.F., 1994. Multiscale modeling of spatially variable water and energy balance processes. Water Resour. Res. 30, 3061-3078.

FAO, 2004.
The ethics of sustainable agricultural intensification FAO Ethics Series 3.

Foster, G.R., 1986. Understanding ephemeral gully erosion. National Research Council, Board on Agriculture, Soil Conservation: Assessing the National Research Inventory 2National Academy Press, Washington, 90-118.

Foster, G.R., Lane, L.J., 1983. Erosion by concentrated flow in farm fields. In Proceedings of the D. B. Simons Symposium on Erosion and Sedimentation. Colorado State University: Ft. Collins , 9.65-9.82.

Foster, G.R., 1982. Modeling the erosion process. Hydrologic Modeling of Small Watersheds , 297-380.

Frey, H.C., Mokhtari, A., Danish, T., 2003. Evaluation of Selected Sensitivity Analysis Methods Based Upon Applications to Two Food Safety Process Risk Models. Office of Risk Assessment and Cost-Benefit Analysis. U. S. Department of Agriculture, Washington, DC.

Gan, T.Y., Dlamini, E.M., Biftu, G.F., 1997. Effects of model complexity and structure, data quality, and objective functions on hydrologic modeling. Journal of Hydrology 192, 81-103.

Garbrecht, J., Martz, L.W., 2004. TOPAZ. Version 3.2. An Automated digital landscape analysis tool for topographic evaluation. Drainage identification, watershed segmentation and subcatchment parameterization. Overview manual. Publication Nº. GRL 04-1, Grazinglands Research Laboratory, USDA, Agricultural Research Service, 7207 West Cheyenne St., El Reno, Oklahoma.

García Ruiz, J.M., López Bermúdez, F., 2009. La erosión del sueloen España. Sociedad Española de Geomorfología , 441.

García-Ruiz, J.M., 2010. The effects of land uses on soil erosion in Spain: A review. Catena 81, 1-11.

Gastesi, R., 2014. Efectos de la actividad agraria sobre los recursos hídricos y la erosión del suelo. Análisis y modelado en cuencas experimentales de la Zona Media de Navarra.

Giménez, R., Casalí, J., Chahor, Y., 2012. Computer tools for agricultural land management: Potentials of the AnnAGNPS model in Navarra. Cuadernos de Investigacion Geografica 38, 107-121.

Goñi, J., Irañeta, I., Sexmilo, J.R., Lafarga, A., 2008. La Colza En Navarra. Navarra Agraria.

Gordon, L.M., Bennett, S.J., Bingner, R.L., Theurer, F.D., Alonso, C.V., 2007. Simulating ephemeral gully erosion in AnnAGNPS. Trans. ASABE 50, 857-866.

Grissinger, E.H., Murphey, J.B., 1989. Ephemeral gully erosion in the loess uplands, Goodwin Creek watershed, northern Mississippi, USA. Final Proc.Int.Conf.River Sedimentation , 51-58.

Gupta, H.V., Sorooshian, S., Yapo, P.O., 1999. Status of automatic calibration for hydrologic models: Comparison with multilevel expert calibration. J. Hydrol. Eng. 4, 135-143.

Hall, G.F., Logan, T.J., Young, K.K., 1985. Criteria for determining tolerable erosion rates. Soil Erosion and Crop Productivity , 173-188.

Hamby, D.M., 1994. A review of techniques for parameter sensitivity analysis of environmental models. Environ. Monit. Assess. 32, 135-154.

Hanson, G.J., Simon, A., 2001. Erodibility of cohesive streambeds in the loess area of the Midwestern USA. Hydrol. Processes 15, 23-38.

Horton, R.E., 1945. Erosional development of streams and their drainage basins; Hydrophysical approach to quantitative morphology. Bull. Geol. Soc. Am. 56, 275-370.

Iñiguez, J., Munilla, C., Sanchez-carpintero, I., Val, R.M., Romero, A., 1982 - 1992. Mapa de Suelos de Navarra, escala 1: 50.000. Publicaciones del Departamento de Edafologia de la Universidad de Navarra.

INTIA, 2017. Agronomic management, farmers face-to-face inquiries, database. Proyecto LIFE Nitratos (LIFE+10 ENV/ES/478). (Instituto Navarro de Tecnologías e Infraestructuras Agroalimentarias) .

Isidoro, D., Quílez, D., Aragüés, R., 2003. Sampling strategies for the estimation of salt and nitrate loads in irrigation return flows: La Violada Gully (Spain) as a case study. Journal of Hydrology 271, 39-51.

Iturria, I., Campo-Bescós, M.A., Zubieta, E., Giménez, R., 2017a. Dinámica del flujo preferente en suelos agrícolas de Navarra: una aproximación experimental. XIII Jornadas de la Zona no saturada En revision.

Iturria, I., Zubieta, E., Giménez, R., Campo-Bescós, M.A., 2017b. Preferential flow dynamics in agricultural soils in Navarre (Spain): an experimental approach to gain insight into water connectivity. Geophysical Research Abstracts, EGU General Assembly Vol. 19.

Kim, S.M., Benham, B.L., Brannan, K.M., Zeckoski, R.W., Doherty, J., 2007. Comparison of hydrologic calibration of HSPF using automatic and manual methods. Water Resour. Res. 43.

Knapen, A., Poesen, J., Govers, G., Gyssels, G., Nachtergaele, J., 2007. Resistance of soils to concentrated flow erosion: A review. Earth Sci. Rev. 80, 75-109.

Knisel, W.G., 1980. *CREAMS: A Field-Scale Model for Chemicals, Runoff, and Erosion from Agricultural Management Systems.* Conservation Res Report No. 26. Washington D.C.: USDA Science and Education Administration.

Krause, P., Boyle, D.P., Bäse, F., 2005. Comparison of different efficiency criteria for hydrological model assessment. Advances in Geosciences 5, 89-97.

Laflen, J.M., Elliot, W.J., Simanton, J.R., Holzhey, C.S., Kohl, K.D., 1991. WEPP: soil erodibility experiments for rangeland and cropland soils. Journal of Soil & Water Conservation 46, 39-44.

Lal, R., 2003. Soil erosion and the global carbon budget. Environ. Int. 29, 437-450.

Lal, R., Reicosky, D.C., Hanson, J.D., 2007. Evolution of the plow over 10,000 years and the rationale for no-till farming. Soil Tillage Res. 93, 1-12.

Lane, L.J., Renard, K.G., Foster, G.R., Laflen, J.M., 1992. Development and application of modern soil erosion prediction technology — the usda experience. Aust. J. Soil Res. 30, 893-912.

Langendoen, E.J., 2000. CONCEPTS – Conservational channel evolution and pollutant transport system: Stream corridor version 1.0. US Department of Agriculture, Agricultural Research Service, National Sedimentation Laboratory, Oxford, MS Research Report No. 16.

Lasanta, T., Garcia-Ruiz, J.M., Beguería, S., 2006. Geomorphic and hydrological effects of traditional shifting agriculture in a Mediterranean mountain area, central Spanish Pyrenees. Mountain Research and Development 26, 146-152.

Legates, D.R., McCabe Jr., G.J., 1999. Evaluating the use of 'goodness-of-fit' measures in hydrologic and hydroclimatic model validation. Water Resour. Res. 35, 233-241.

Lenhart, T., Eckhardt, K., Fohrer, N., Frede, H.-., 2002. Comparison of two different approaches of sensitivity analysis. Phys. Chem. Earth 27, 645-654.

Lentz, R.D., Dowdy, R.H., Rust, R.H., 1993. Soil property patterns and topographic measures associated with ephemeral gully erosion. J. Soil Water Conserv. 48, 355-361.

Léonard, J., Richard, G., 2004. Estimation of runoff critical shear stress for soil erosion from soil shear strength. Catena 57, 233-249.

Leopold, L.B., Wolman, M.G., Miller, J.P., 1964. Fluvial Processes in Geomorphology. W. H. Freeman and Company, San Francisco.

Lezaun, J.A., Armesto, A.P., Lafarga, A., Goñi, J., 2004. Girasol. Navarra Agraria Marzo - Abril, http://www.navarraagraria.com/n143/argira4.pdf.

Li, H., Cruse, R.M., Bingner, R.L., Gesch, K.R., Zhang, X., 2016. Evaluating ephemeral gully erosion impact on Zea mays L. yield and economics using AnnAGNPS. Soil Tillage Res. 155, 157-165.

Licciardello, F., Zema, D.A., Zimbone, S.M., Bingner, R.L., 2007. Runoff and soil erosion evaluation by the AnnAGNPS model in a small Mediterranean watershed. Transactions of the ASABE 50, 1585-1593.

Loizu, J., Álvarez-Mozos, J., Casalí, J., Goñi, M., 2016. Evaluation of TOPLATS on three Mediterranean catchments. J. Hydrol. 539, 141-161.

Mäder, P., Fließbach, A., Dubois, D., Gunst, L., Fried, P., Niggli, U., 2002. Soil fertility and biodiversity in organic farming. Science 296, 1694-1697.

Maringanti, C., Chaubey, I., Popp, J., 2009. Development of a multiobjective optimization tool for the selection and placement of best management practices for nonpoint source pollution control. Water Resour. Res. 45.

Matson, P.A., Parton, W.J., Power, A.G., Swift, M.J., 1997. Agricultural intensification and ecosystem properties. Science 277, 504-509.

Merritt, W.S., Letcher, R.A., Jakeman, A.J., 2003. A review of erosion and sediment transport models. Environmental Modelling & Software 18, 761-799.

Ministerio de Agricultura Pesca y Alimentación, 1986. Caracterización agroclimática de Navarra. Dirección General de la Producción Agraria, Madrid. Dpto. de Agricultura, Ganadería y Montes del Gobierno de Navarra, Instituto Navarro del suelo .

Mockus, 1972. Estimation of directe runoff from storm rainfall. Washington D.C.

Momm, H.G., Bingner, R.L., Wells, R.R., Dabney, S.M., 2011. Application of ground-based lidar for gully investigation in agricultural landscapes. Am. Soc. Photogramm. Remote Sens. Annu. Conf. , 331-340.

Momm, H.G., Bingner, R.L., Wells, R.R., Rigby, J.R., Dabney, S.M., 2013. Effect of topographic characteristics on compound topographic index for identification of gully channel initiation locations. Trans. ASABE 56, 523-537.

Momm, H.G., Bingner, R.L., Wells, R.R., Wilcox, D., 2012. Agnps GIS-based tool for watershed-scale identification and mapping of cropland potential ephemeral gullies. Appl. Eng. Agric. 28, 17-29.

Moore, I.D., Burch, G.J., Mackenzie, D.H., 1988. Topographic effects on the distribution of surface soil water and the location of ephemeral gullies. Transactions of the ASEA 31(4), 1098-1107.

Morgan, R.P.C., Quinton, J.N., Smith, R.E., Govers, G., Poesen, J.W.A., Auerswald, K., Chisci, G., Torri, D., Styczen, M.E., 1998. The European soil erosion model (EUROSEM): a dynamic approach for predicting sediment transport from fields and small catchments. Earth Surf. Proc. Landf. 23, 527-544.

Moriasi, D.N., Arnold, J.G., Van Liew, M.W., Bingner, R.L., Harmel, R.D., Veith, T.L., 2007. Model evaluation guidelines for systematic quantification of accuracy in watershed simulations. Transactions of the ASABE 50, 885-900.

Nachtergaele, J., Poesen, J., 1999. Assessment of soil losses by ephemeral gully erosion using high-altitude (stereo) aerial photographs. Earth Surf. Processes Landf. 24, 693-706.

Nachtergaele, J., Poesen, J., Sidorchuk, A., Torri, D., 2002. Prediction of concentrated flow width in ephemeral gully channels. Hydrol. Processes 16, 1935-1953.

Nachtergaele, J., Poesen, J., Vandekerckhove, L., Oostwoud Wijdenes, D., Roxo, M., 2001. Testing the Ephemeral Gully Erosion Model (EGEM) for two Mediterranean environments. Earth Surf. Process. Landforms 26, 17-30.

Nash, J.E., Sutcliffe, J.V., 1970. River flow forecasting through conceptual models part I - A discussion of principles. Journal of Hydrology 10, 282-290.

Ollobarren, P., Giménez, R., Campo-Bescós, M.A, Casalí, J, 2016. Soil factors controlling gully erosion: an experimental approach. 7th International Symposium on Gully Erosion .

Panagos, P., Borrelli, P., Poesen, J., Ballabio, C., Lugato, E., Meusburger, K., Montanarella, L., Alewell, C., 2015. The new assessment of soil loss by water erosion in Europe. Environ. Sci. Policy 54, 438-447.

Parajuli, P.B., Nelson, N.O., Frees, L.D., Mankin, K.R., 2009. Comparison of AnnAGNPS and SWAT model simulation results in USDA-CEAP agricultural watersheds in south-central Kansas. Hydrol. Process. 23, 748-763.

Parker, C., Thorne, C., Bingner, R.L., Wells, R.R., Wilcox, D.L., 2007. Automated mapping of potential for ephemeral gully formation in agricultural watersheds. NSL Technical Research Report 56.

Parker, C., Thorne, C., Bingner, R., Wells, R., Wilcox, D., 2010. AUTOMATED MAPPING OF THE POTENTIAL FOR EPHEMERAL GULLY FORMATION IN AGRICULTURAL WATERSHEDS. 2nd Joint Federal Interagency Conference, Las Vegas, NV, June 27 - July 1, 2010 .

Patton, P.C., Schumm, S.A., 1975. Gully erosion, Northwestern Colorado: A threshold phenomenon. Geology 3, 88-90.

Penman, H.L., 1948. Natural Evaporation from Open Water, Bare Soil and grass <*br* />. Proc. Roy. Soc, London.

Pimentel, D., Harvey, C., Resosudarmo, P., Sinclair, K., Kurz, D., McNair, M., Crist, S., Shpritz, L., Fitton, L., Saffouri, R., Blair, R., 1995. Environmental and economic costs of soil erosion and conservation benefits. Science 267, 1117-1123.

Poesen, J.W.A., Torri, D.B., Van Walleghem, T., 2011. Ch19 - Gully Erosion: Procedures to Adopt When Modelling Soil Erosion in Landscapes Affected by Gullying, in Morgan, R.P.C., Nearing, M.A. (Eds.), Handbook of Erosion Modelling, 2011 ed. Blackwell-Wiley, Oxford, U.K., pp. 360-386.

Poesen, J., Nachtergaele, J., Verstraeten, G., Valentin, C., 2003. Gully erosion and environmental change: importance and research needs. Catena 50, 91-133.

Poesen, J.W., Vandaele, K., Van Wesemael, B., 1996. Contribution of gully erosion to sediment production on cultivated lands and rangelands. IAHS-AISH Publ. 236, 251-266.

Politis, D.N., Romano, J.P., 1994. The stationary bootstrap. J. Amer. Statist. Assoc 89, 1303-1313.

Polyakov, V., Fares, A., Kubo, D., Jacobi, J., Smith, C., 2007. Evaluation of a non-point source pollution model, AnnAGNPS, in a tropical watershed. Environmental Modelling and Software 22, 1617-1627.

Quinton, J.N., Govers, G., Van Oost, K., Bardgett, R.D., 2010. The impact of agricultural soil erosion on biogeochemical cycling. Nat. Geosci. 3, 311-314.

Rawls, W.J., Brakensiek, D.L., 1989. Estimation of soil water retention and hydraulic properties. Unsaturated Flow in Hydrologic Modeling: Theory and Practice , 275-300.

Renard, K.G., Foster, G.R., Weesies, G.A., McCool, D.K., Yoder, D.C., 1997. Predicting soil erosion by water: A guide to conservation planning with the revised universal soil loss equation (RUSLE). USDA Agriculture Handbook No.703 .

Ritter, A., Muñoz-Carpena, R., 2013. Performance evaluation of hydrological models: Statistical significance for reducing subjectivity in goodness-of-fit assessments. Journal of Hydrology 480, 33-45.

Rorabacher, D.B., 1991. Statistical treatment for rejection of deviant values: Critical values of Dixon's "O" parameter and related subrange ratios at the 95 % confidence level. Anal. Chem. 63, 139-146.

Sarangi, A., Cox, C.A., Madramootoo, C.A., 2007. Evaluation of the AnnAGNPS Model for prediction of runoff and sediment yields in St Lucia watersheds. Biosystems Engineering 97, 241-256.

Saxton, K.E., Rawls, W.J., 2006. Soil water characteristic estimates by texture and organic matter for hydrologic solutions. Soil Sci. Soc. Am. J. 70, 1569-1578.

Schaffner, M., Bader, H.-., Scheidegger, R., 2011. Modeling non-point source pollution from rice farming in the Thachin River Basin. Environ. Dev. Sustainability 13, 403-422.

SCS, 1986. Technical release 55: Urban hydrology for small watersheds. United States Department of Agriculture, Natural Resources Conservation Service, Conservation Engineering Division.

Serrano-Muela, M.P., Lana-Renault, N., Nadal-Romero, E., Regüés, D., Latron, J., Martí-Bono, C., García-Ruíz, J., 2008. Forests and their hydrological effects in mediterranean mountains: The case of the Central Spanish Pyrenees. Mt. Res. Dev. 28, 279-285.

Shamshad, A., Leow, C.S., Ramlah, A., Wan Hussin, W.M.A., Mohd. Sanusi, S.A., 2008. Applications of AnnAGNPS model for soil loss estimation and nutrient loading for Malaysian conditions. International Journal of Applied Earth Observation and Geoinformation 10, 239-252.

Shirmohammadi, A., Chaubey, I., Harmel, R.D., Bosch, D.D., Muñoz-Carpena, R., Dharmasri, C., Sexton, A.M., Arabi, M., Wolfe, M.L., Frankenberger, J., Graff, C., Sohrabi, T.M., 2006. Uncertainty in TMDL models. Transactions of the ASABE 49, 1033-1049.

Shrestha, S., Babel, M.S., Das Gupta, A., Kazama, F., 2006. Evaluation of annualized agricultural nonpoint source model for a watershed in the Siwalik Hills of Nepal. Environmental Modelling and Software 21, 961-975.

Smith, L., 1993. Investigation of Ephemeral Gullies in Loessial Soils in Mississippi. Technical Report . Vicksburg, Miss. :U. S. Army Corps of Engineers, Waterways Experiment Station GL-93-11.

Souchère, V., Cerdan, O., Ludwig, B., Le Bissonnais, Y., Couturier, A., Papy, F., 2003. Modelling ephemeral gully erosion in small cultivated catchments. Catena 50, 489-505.

Srivastava, P., Hamlett, J.M., Robillard, P.D., 2003. Watershed optimization of agricultural best management practices: Continuous simulation versus design storms. J. Am. Water Resour. Assoc. 39, 1043-1054.

Taguas, E., Yuan, Y., Peña, A., Ayuso, J.L., 2010. Prediction of ephemeral gullies by using the combined topographical index in a micro-catchment of olive groves in Andalucia, Spain. Agrociencia 44, 409-426.

Taguas, E.V., Ayuso, J.L., Peña, A., Yuan, Y., Pérez, R., 2009. Evaluating and modelling the hydrological and erosive behaviour of an olive orchard microcatchment under no-tillage with bare soil in Spain. Earth Surf. Process. Landforms 34, 736-751.

Taguas, E.V., Yuan, Y., Bingner, R.L., Gómez, J.A., 2012. Modeling the contribution of ephemeral gully erosion under different soil managements: A case study in an olive orchard microcatchment using the AnnAGNPS model. Catena 98, 1-16.

Theurer, F.D., Clarke, C.D., 1991. Wash load component for sediment yield modeling. In Proceedings of the fifth federal interagency sedimentation conference, March 18-21 , 7-1-7-8.

Theurer, F.D., Comer, G.H., 1992. Classification and Evaluation of Models in Support of the SCS 5 year Water Quality & Quantity Plan of Operations. USDA, SCS, Engineering Division, Washington, DC , 2-100.

Thorne, C.R., Zevenbergen, L.W., Grissenger, E.H., Murphey, J.B., 1986. Ephemeral Gullies as Sources of Sediment. Proceedings of the Fourth Federal Inter-Agency edimentation Conference , 3152-3161.

Thorne, C.R., 1984. Prediction of soil loss due to ephemeral gullies in arable fields. Report CER83-84CRT. Ft. Collins, Colo. :Colorado State University.

Thorne, C.R., Zevenbergen, L.W., 1990. Prediction of ephemeral gully erosion on cropland in the southeastern United States. Soil erosion on agricultural land , 447-460.

Tsou, M.-., Zhan, X.-., 2004. Estimation of runoff and sediment yield in the Redrock Creek watershed using AnnAGNPS and GIS. Journal of Environmental Sciences 16, 865-867.

USDA SOIL Taxonomy, 1998. Keys to Soil Taxonomy by Soil Survey Staff, Eighth Edition., Eighth Edition ed. United States Department of Agriculture, Washington, D.C.

Van Liew, M.W., Arnold, J.G., Garbrecht, J.D., 2003. Hydrologic simulation on agricultural watersheds: Choosing between two models. Transactions of the American Society of Agricultural Engineers 46, 1539-1551.

Van Mullem, J.A., 1989.
Applications of the Green-Ampt infiltration model to watersheds in Montana and Wyoming. Montana State University, Bozeman, Montana .

Vandaele, K., Poesen, J., Govers, G., Van Wesemael, B., 1996. Geomorphic threshold conditions for ephemeral gully incision. Geomorphology 16, 161-173.

Vandekerckhove, L., Poesen, J., Oostwoud Wijdenes, D., De Figueiredo, T., 1998. Topographical thresholds for ephemeral gully initiation in intensively cultivated areas of the Mediterranean. Catena 33, 271-292.

Vázquez, R.F., Willems, P., Feyen, J., 2008. Improving the predictions of a MIKE SHE catchment-scale application by using a multi-criteria approach. Hydrol. Process. 22, 2159-2179.

Vieira, D.A.N., Dabney, S.M., Yoder, D.C., 2014. Distributed soil loss estimation system including ephemeral gully development and tillage erosion. IAHS-AISH Publ. 367, 80-86.

Walton, R., Hunter, H., 1996. Modeling water quality and nutrient fl uxes in the Johnstone River catchment, North Queensland. 23rd Hydrology and Resources Symposium .

Watson, D.A., Laflen, J.M., Franti, T.G., 1986. ESTIMATING EPHEMERAL GULLY EROSION. Paper - American Society of Agricultural Engineers .

Wells, R.R., Momm, H.G., Rigby, J.R., Bennett, S.J., Bingner, R.L., Dabney, S.M., 2013. An empirical investigation of gully widening rates in upland concentrated flows. Catena 101, 114-121.

Williams, J.R., Nicks, A.D., Arnold, J.G., 1985. Simulator for water resources in rural basins. Journal of Hydraulic Engineering - ASCE 111, 970-986.

Wischmeier, W.H., Smith, D.D., 1978. Predicting rainfall erosion losses. Agricultural Handbook No. 537. USDA, Washington, DC.

Woodward, D.E., 1999. Method to predict cropland ephemeral gully erosion. Catena 37, 393-399.

Woolhiser, D.A., Smith, R.E., Goodrich, D.C., 1990. KINEROS, A Kinematic Runoff and Erosion Model: Documentation and user manual. U. S. Departement of Agriculture, Agricultural Research Service ARS -77.

Young, R.A., Onstad, C.A., Bosch, D.D., Anderson, W.P., 1989. AGNPS: A nonpoint-source pollution model for evaluating agricultural watersheds. J.SOIL WATER CONSERVAT. 44, 168-173.

Yuan, Y., Bingner, R.L., Rebich, R.A., 2001. Evaluation of AnnAGNPS on Mississippi Delta MSEA Watersheds. Transactions of the American Society of Agricultural Engineers 44, 1183-1190.

Yuan, Y., Locke, M.A., Bingner, R.L., 2008. Annualized Agricultural Non-Point Source model application for Mississippi Delta Beasley Lake watershed conservation practices assessment. J. Soil Water Conserv. 63, 542-551.

Zevenbergen, L.W., Thorne, C.R., 1987. Quantitative analysis of land surface topography. Earth Surface Processes & Landforms 12, 47-56.